Comparison of topical quercetin nanoformulations for skin protection

Taher Hatahet

THÈSE

Pour obtenir le grade de

Docteur

Délivré par **Université de Montpellier**

Préparée au sein de l'école doctorale Sciences Chimiques Balard

Et de l'unité de recherche Institut Charles Gerhardt

Spécialité : **sciences physico-chimiques et ingénierie appliquée à la santé**

Présentée par **Taher HATAHET**

Comparison of topical quercetin nanoformulations for skin protection

Soutenue le 15/09/2016 devant le jury composé de

Mme Sylvie BEGU, MCU, UMR5253 ICGM	Directeur de thèse
Mme Marie MORILLE, MCU, UMR5253 ICGM	Examinateur
M Jean-Pierre BENOIT, Professeur, UMR1066 MINT	Rapporteur
M Didier BETBEDER, Professeur, UMR995 LIRIC	Rapporteur
M Francisco VEAS, Professeur, IRD, UMR-MD3	Examinateur
M Aiman HOMMOSS, Docteur, Freie Universität Berlin	Examinateur

I would like to express my deepest and sincere gratitude to my thesis advisor, Dr. Sylvie BEGU, for her enlightening guidance and inspiring instruction in the development and completion of this study. Dr. BEGU stimulated my interest in the field of discourse analysis and improved my ability in writing. In the process of meeting and discussion, Dr. BEGU not only provided prudent and pointed guidance but also gave me warm and sincere support.

I would like to pass my infinite thanks to the great Dr. Marie MORILLE. You are the best supervisor and advisor ever. Your comments, corrections, questions were the light for my studies. I know cell culture because of you. And I am here at the end of my thesis because of your support and help.

I am delighted of your presence and your acceptance to review my work. Prof. BENOIT, it was one of my dreams to accept to review my work. You are one of the leading scientist in the field and also one of the most successful researchers. My dream is to be like you one day. Prof. BETDEDER, your remarks will be the rose to add for this work, I am more than dreaming to have my work between your hands and beautiful mind.

Aiman, the Syrian mind, many thanks for you since 2011 till the moment, five years of friendship and great advises in life before research. It is the time to thank you for everything. Prof. Müller, it was dream to work with you since 2012 and I am now submitting my thesis after the great collaboration with you and your kind team. One paper already published and more to come in the future.

Prof. VEAS, I would like to thank you not only for being member of the jury and examine my work. But the thanks start from the day you welcomed me in your laboratory. Without knowing me before, you supported me with your smile, help, advice and science. You are a true idol for a young man.

I would like to thank Prof. Jean-Marie DEVOISSELLE, the director of Institut Charles Gerhardt Montpellier and Prof. Didier TICHIT, chef of Matériaux Avancés pour la Catalyse et la Santé research team and Prof. Joël CHOPINEAU our team director for welcoming me in their laboratories and accepting me as a part of their successful team.

I would like to pass my endless acknowledgments for ERAMUS MUDUS AVEMPACE 2 project team for the financial support and great company during my thesis.

I also want to thank Dr. Anne AUBERT, for her reviewing of my writing and offering opinions about the project. I am so pleased to have you for that successful scientific support Dr. Corine TOURNÉ-PÉTEILH and M. Christophe DORANDEU especially HPLC. Also, I would like to thank Dr Muriel GOLZIO for the beautiful confocal images and the help with small animal skin penetration. Special thanks go to Mr. Pradial PERALTA for his warm company, help and jokes.

I am appreciative of the members of the great MACS, ICGM, Sophie RAISIN, Estelle RASCOL Gilamary GALLON and Mohammed ZAYED, for their support and encouragement during the tough times.

إاليك أنا اليوم أكتب , وبك وحدك أبدأ ولك الفضل كل الفضل فيما أقدم , أمي لو لم تكوني لما كنت. ماما شفاء يا حبيبتي يا تاج رأسي اذا انا لح صير دكتور فلأني ابنك مو لأني عم قدم رسالة الدكتوراه.

بابا غسان يا عزتي وشرفي . بدعواتك وصلت وبرضاك قدرت أوصل لهون , يا رب يقدرني عرد فضلك . بتتذكر لما كنت تقلي قوم صلي من وقتا تعملت الحياة وتعلمت الهداية . انت علمتني الأخرة اللي هي ألف مرة أهم.

حبيبتي راما , أنت الملاك الأبيض اللي الله سبحانه وتعالى بعتها لتنور دربي وتهدي سري و توقف معي بهالسنين. يا رب يتيسر الشغل والرزق الحلال من الله و نتجوز ونكمل العمر سوا لأخرو. بحبك

طروقة, بزمانك قلتلي ليش قدمت عالدكتوراه بدون ماستر . و نسيت أني أخوك المتربي عإيدك . يعني بالعربي الفصيح فرخ البط عوام. يا رب نرجع نلعب فيفا سوا و تجيبني من دار الفرح و تطعميني رز ولبن. بحبببببك يا قدوتي . يا رب تشوف ولادك متلك و أحسن.

طلطول معقول ما قلك اني بحبك باهم لحظة بحياتي الدراسية. معقول ما قللك شكرا عسندويش الشيش والشاورما والفراريج اللي كنت تنتعا معك مشاني. يا رب تفرح بولادك و يربو بعزك .

ماما صفاء وبابا جمال. كل الشكر لأنكن عطيتوني جوهرة من جواهركن. الله يقدرني على إسعادا ونضل عطول عيلة وحدة وأهل وربي يخليكم باقي الجواهر وزواجن و تفروحو فين كلن كلن.

حما ابن الخال الغالي والقدوة أبوك للعيلة كلا. عمورة شريك مونبليه و باريس والشق الفرنسي من العيلة . يزوون و كروووم و خالتي رجوءة و عليتا شكرا لانكم استقبلتوني بالاردن مشان الفيزا و دعمتوني. خالو حسان وولادو ربي يرزقكم و يسر قلبكن و خاطركن. الى الباقي بقلوبنا و عقولنا خالو ابو الفوز الى جنان الخلد يا من علمنتنا الرجولة.

عمتي نازك الله يديمك عمة ثروت و الأغا و كل آل حتاحت ربي يعز اصلكن و يحقق كل امانيكم.

أب زهير أب غسان أبو الريم الفنان غروب السوررين بمونبليه أنتو أهلي بالغربة و أخواتي من غير قرابة. كمولة و وزة و مرضي و ميزو و أبو صلاح أنتو الأهل اللي من غير بلد بس نفس الروح ونفس لبحكاية. أحلاصحاب و أجدع رجالة.

اهم شي واخر شي سورياااااااا الله يرجعك النا ويستر عليك و عاهلك و يفرج الكرب ويزيل البلاء يا منارتنا ويا وجعنا. هالعمل الى ارواح شهداءك الأبرار.

Table of Contents

Table of figures

Résumé de thèse

Part I: Bibliography38

Flavonoids and quercetin

Table of tables

Table of abbreviations

Blank-Lipo	Blank liposomes
Blank-LNC 20	Blank lipid nanocapsules 20 nm
Blank-LNC 50	Quercetin lipid nanocapsules 20 nm
CAA	Cellular antioxidant activity assay
CT	Combinative techniques
CTAB	Cetyl trimethylammonium bromide
DCFDA	2',7' –dichlorofluorescin diacetate
DMSO	Dimethyl sulfoxide
DPPH	2,2-diphenyl-1-picrylhydrazyl
GSH	Glutathione
GSSG	Glutathione disulfide
HPH	High-pressure homogenization
Lab	Labrasol®
MMP-9	Matrix metallopeptidase 9
MPO	Myeloperoxidase
MTT	3-(4,5-dimethylthiazol-2-yl)-2,5 diphenyltetrazolium bromide
NF-κB	Nuclear factor-kappa B

NH_2-MSN	Aminopropyl functionalized mesoporous silica nanoparticles
NLC	Nanostructured lipid carriers
PDI	Polydispersity index
PEG	Polyethylene glycol
PEV	Penetration Enhancer-containing Vesicles
PG	Propylene glycol
Que-Lipo	Quercetin liposomes
Que-LNC 20	Blank lipid nanocapsules 50 nm
Que-LNC50	Quercetin lipid nanocapsules 50 nm
Que-SC	Quercetin smartCrystals®
QM	Quercetin 3,5,7,30,40-pentamethylether
ROS	Reactive oxygen species
SLN	Solid lipid nanoparticles
TBARS	Thiobarbituric acid reactive species
TPA	Tetradecanoylphorbol 13-acetate
TPGS	D-alpha tocopheryl polyethylene glycol 1000 succinate
TNF-α	Tumor necrosis factor alpha
Trc	Transcutol® P
TWEL	Transepidermal water loss

XTT	2,3-Bis-(2-Methoxy-4-Nitro-5-Sulfophenyl)-2H-Tetrazolium-5-Carboxanilide

Résumé de thèse

1. Les flavonoïdes : la quercétine et la peau

Les flavonoïdes sont des pigments d'origine naturelle conférant leurs couleurs aux fleurs et aux fruits, ils sont identifiés dans plus de quatre milles espèces [1-3]. Les flavonoïdes sont classés selon leur structure chimique de base formée par deux cycles aromatiques reliés par trois carbones : C6-C3-C6, chaîne souvent fermée en un hétérocycle oxygéné hexa- ou pentagonal [4]. Les flavonoïdes présentent des propriétés qui leurs permettent d'être utilisés en tant que médicaments [5-7] telle que la capacité à piéger les radicaux libres [8, 9]. A ce jour, les études sur les flavonoïdes ont fait l'objet de nombreux articles de revue [10-12] démontrant l'intérêt de ces molécules.

Parmi les flavonoïdes, la quercétine est la molécule la plus présente dans la nature avec une activité très importante dans la lutte contre les radicaux libres et aussi une bonne activité antiinflammatoire comparativement à d'autres molécules de la même famille [6, 13]. En général, les flavonoïdes présentent une solubilité très limitée dans l'eau et cette limitation bloque leur absorption/pénétration et donc leur efficacité [14]. En tant que membre de cette famille de composés, la quercétine est ainsi également limitée par sa faible solubilité dans l'eau [6, 15].

Sachant que la peau est entre les organes les plus importants du corps humain (2 m^2) et le plus exposé au stress oxydant lié aux radiations UV et aux produits corrosifs et irritants [16], la quercétine est donc une molécule antioxydante de choix pour application topique.

Le premier objectif de thèse a été de développer plusieurs formulations nanométriques de quercétine afin d'augmenter sa solubilité dans l'eau et d'améliorer ses propriétés physicochimiques. Nous avons choisi de développer la quercétine sous forme nanocristalline, mais également dans des formulations de type nanocapsules lipidiques et liposomes de plus en plus utilisées dans le développement des PA peu solubles dans l'eau. Ces formulations seront comparées à la quercétine non formulée que nous appellerons "quercétine initiale".

Le deuxième objectif a été de comparer ces formulations en terme de capacité de chargement de quercétine, de toxicité vis à vis des cellules HaCaT (kératinocytes) THP-1 (monocytes) et Vero (épithéliales), et enfin au niveau du maintien de l'activité anti-oxydante de la quercétine sur les cellules *in vitro,* pour mettre *in fine* en évidence une augmentation de la pénétration cutanée la quercétine *in vivo.*

2. Les formulations de quercétine et leurs caractérisations physicochimiques

2.1.Nanocristaux de quercétine (smartCrystals®)

La première approche de formulation de la quercétine a été faite sous forme de nanocristaux (smartCrystals®). Dans cette approche, la molécule active est mise en suspension avec un stabilisant puis des équipements avec un fort apport énergétique (homogénéisateur haute pression, broyeur à billes en milieu humide,...) sont utilisés pour diminuer la taille des particules à l'échelle nanométrique. La production de nanocristaux de quercetine de première génération était basée sur une étape de 60 minutes avec un broyeur à billes ou de 15 à 20 cycles avec l'homogénéisation à haute pression (1500 bars) [17]. Dans le procédé de seconde génération utilisé dans notre étude, nous avons combiné les deux techniques avec un temps plus court de broyage à billes et pas plus de 2 cycles d'homogénéisation à haute pression (300 bars) [18] (Fig.1 et 4 a). Les particules formées sont homogènes en taille et présentent une stabilité physique prolongée.

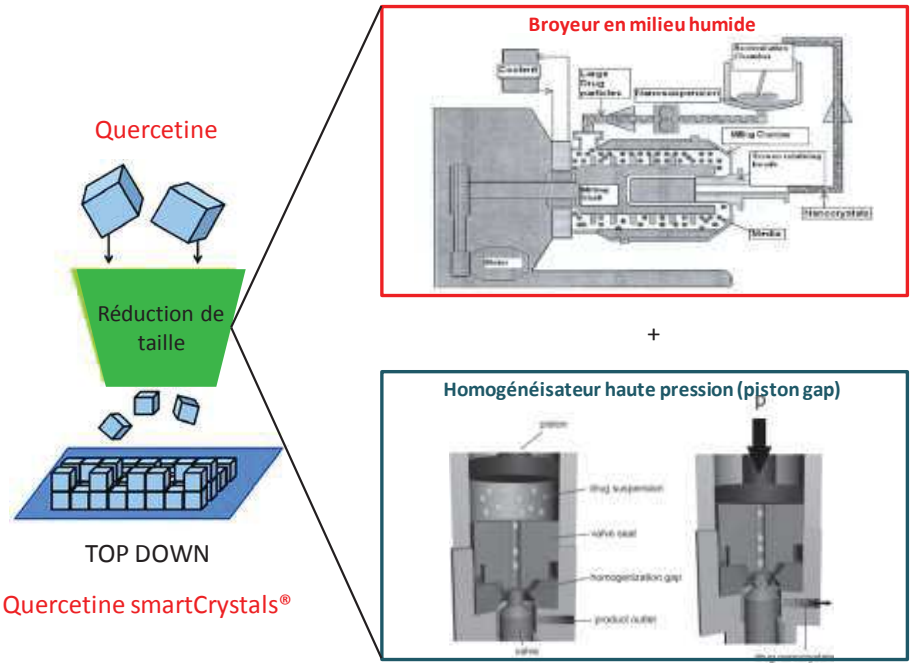

Fig. 1 : représentation schématique de la stratégie utilisée pour former des nanocristaux de quercetine

Résumé de thèse

Dans cette étude, cinq stabilisants sont comparés entre eux en termes de taille des cristaux et du procédé de production le plus court possible avec le broyeur à billes puis l'homogénéisation à haute pression. Tween®80 et D-α-Tocopherol polyethylene glycol 1000 succinate (TPGS) se sont révélés être les meilleurs stabilisants des suspensions avec des distributions de taille centrées à 295 nm (PDI 0.25) avec le Tween® 80 et 203 nm (PDI 0.24) avec le TPGS. Dans cette approche, la solubilité de la quercétine a été augmentée par 5 et la vitesse de dissolution par 7. La cinétique de solubilisation de la quercétine sous forme smartCrystals® est rapide avec un plateau atteint en 60 minutes alors que dans le même temps, seulement 15% est solubilisé avec la quercétine initiale.
La toxicité cellulaire des smartCrystals® a été testée sur les cellules épithéliales (Vero) jusqu'à 50 µg/ml de quercétine et comparée avec la quercétine initiale. Le choix de cellules Vero est basé sur leurs utilisation fréquente dans les études toxicologiques des produits de santé afin de permettre une comparaison avec d'autres principes actifs étudiés dans la littérature comme par exemple le quinocetone, le carbadox et l'olaquindox [19] ou des mises en formes particulières comme par exemple les Quantum Dots [20]. Les cellules traitées avec les smartCrystals® de quercétine formulés avec du TPGS présentent des viabilités cellulaires proches du contrôle pour des concentrations entre 5 à 50 µg/ml.
L'activité de la quercétine sous forme smartCrystals® (que-SC) et de la quercétine initiale sur la capacité de protection des cellules VERO suite à stress oxydant provoqué par un traitement à l'eau oxygénée a ensuite été évalué. Dans le cas de la quercétine initiale, nous observons une activité protectrice des cellules contre l'oxydation et les résultats de viabilité sont proches de ceux obtenus avec les cellules non traitées (contrôle négatif) ($P<0.05$). Avec la quercétine smartCrystals®, nous avons aussi démontré une activité protectrice sur les cellules Vero. La viabilité cellulaire est passée de 45 % en contrôle positif avec l'eau oxygénée à 68 % pour les cellules qui ont été prétraitées avec la quercétine smartCrystals®.
Finalement, l'incorporation de la quercétine smartCrystals® dans des gels non ioniques a été réalisée et la stabilité des cristaux dans les gels a été observée durant 3 mois à 3 températures (4, 25 et 40 degrés Celsius). La quercétine smartCrystals® stabilisée avec du TPGS a montré un meilleur résultat en taille et PDI comparé à celle formulée avec de Tween® 80. Le TPGS sera donc utilisé comme stabilisant pour les formulations de smartCrystals® d'autant plus que la présence de vitamine E dans sa composition représente une autre avantage pour la pénétration cutanée.

2.1.Nanocapsules lipidiques chargées en quercétine

Les nanocapsules lipidiques sont des nanoparticules sphériques formées d'un cœur lipidique (triglycérides), d'une coque phosphatidylcholine (et d'une couronne de chaines d'hydroxystéarates de poly (éthylène glycol) (PEG) et de PEG libre (Fig. 2) [21].

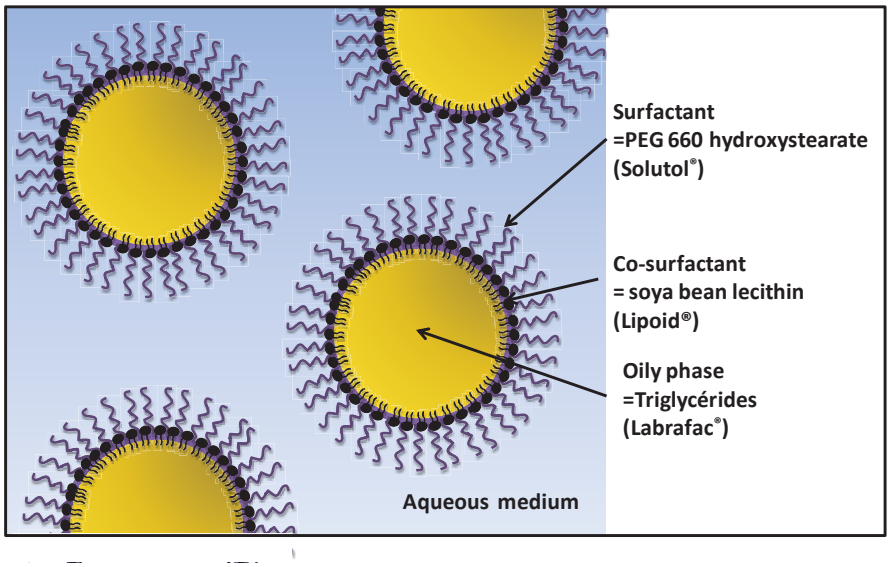

Fig. 2 : Représentation schématique de la structure des nanocapsules lipidiques (LNC). Les LNC, dispersées dans un solvant aqueux, sont composées d'un cœur de triglycérides entouré d'une coque de surfactants (hydroxystéarates de PEG) et de co-surfactants (lécithine de soja, 37% de phosphatidyl choline).

Elles sont de taille variable en fonction de la proportion d'excipients utilisés dans la préparation mais de distribution homogène avec un PDI inferieur à 0.2 [22]. Le processus de préparation est basé sur l'inversion de phase d'une émulsion eau dans huile vers une émulsion huile dans eau, grâce à l'utilisation d'un surfactant à base d'unité éthylène glycol (HS-PEG) dont la balance hydrophile/lipophile (HLB) va évoluer en fonction de la température. En effet, à faible température, ce surfactant sera plutôt hydrophile (HLB est supérieur à 10), alors qu'au-dessus d'une température nommé température d'inversion de phase (TIP), les chaines de PEG seront déshydratées (de manière réversible), induisant un profil plutôt lipophile, et aboutissant donc à un changement de sens de l'émulsion. Après trois cycles de chauffage et de refroidissement, et donc plusieurs passage au niveau de la zone d'inversion de phase (ZIP), un choc thermique/volumique (ajout d'un fort volume d'eau à 4°C) va stabiliser la microémulsion formée au niveau de la ZIP et

aboutir à la formation des nanoparticules (Fig. 3 et 4 b). Le choix de formuler la quercétine dans les nanocapsules lipidiques est basé sur leur nature lipidique qui pourrait leur conférer une affinité importante vis-à-vis des lipides de la peau, sur leur capacité de protéger les PA [23] contrairement à la stratégie de formulation smartCrystals®.

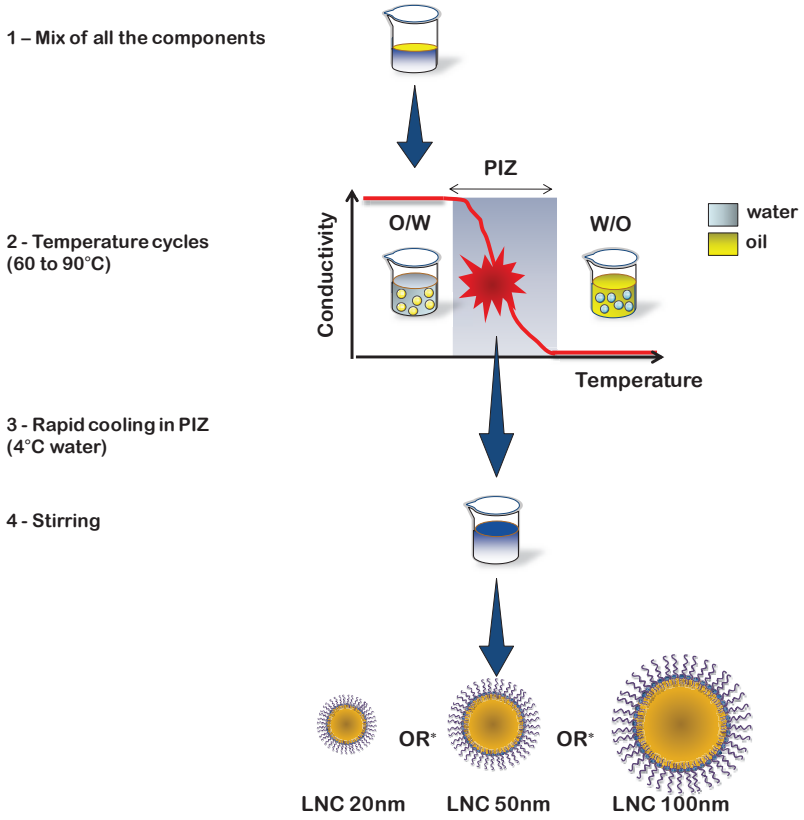

Fig. 3 : Représentation schématique de la préparation de nanocapsules lipidiques de quercétine par la méthode de l'inversion de phase.

Deux formulations de nanocapsules lipidiques avec des distributions de taille autour de 20 et 50 nm ont été préparées après avoir mis au point des modifications au niveau (i) de la composition initiale des nanocapsules lipidiques avec l'ajout de Cremophor® EL pour optimiser la solubilisation de quercétine comparativement au Solutol HS® 15 et (ii) du procédé par l'ajout d'éthanol dans le mélange avant les cycles de chauffage/refroidissement [21]. Ces deux modifications ont été réalisées pour optimiser le chargement de la quercétine dans les capsules lipidiques. Les nanoparticules ainsi obtenues exposent une taille de 26 ± 3 nm et 54 ± 3 nm avec des PDI inférieur à 0.2 indiquant leur homogénéité (DLS et microscope électronique). Les

diffractogrammes DRX mettent en évidence l'imperfection de la structure cristalline à cause de la complexité des lipides et la présence de quercétine [24]. L'état cristallin de la quercétine n'a pas pu être défini à cause de sa faible concentration dans le mélange de lipides (< 3%). La cinétique de libération de la quercétine a été étudiée *in vitro* dans PBS pH 7.4 avec Tween® 20 (2%). Elle a mis en évidence la libération prolongée de quercétine encapsulée par rapport au contrôle positif (solution de quercétine dans le propylène glycol).

Les études de toxicité cellulaire et de l'activité de la quercétine dans les nanocapsules lipidiques ont été réalisées sur les cellules THP-1. Les monocytes (THP-1) peuvent être pris comme un exemple de cellules dendritiques de la peau qui sont dérivées de monocytes circulants dans le sang et recrutés dans des conditions inflammatoires. Les cellules ont été traitées avec de concentration de quercetine variant de 0.5 µg/ml et 5 µg/ml durant 72 heures. La viabilité cellulaire des THP-1 avec les nanocapsules lipidiques 20 et 50 est comparée avec celle obtenue après traitement avec la quercétine initiale. Entre 0.5 et 2.5 µg/ml de quercetine, les nanocapsules ont donné des pourcentages de viabilité proches de ceux obtenus avec quercétine initiale et du contrôle négatif (96.2 % et 86.6 % avec les 20 et les 50). La viabilité cellulaire à 5 µg/ml de quercétine était plus grande avec les nanocapsules lipidiques 20 par rapport à celles de 50. Cette observation peut être due à la concentration de Solutol HS® 15 plus importante dans les 50, car il présente une toxicité un plus élevée que le Cremophor® EL sur des kératinocytes [25].

L'activité antioxydante de la quercétine a ensuite été comparée entre la quercétine initiale et les nanocapsules lipidiques avec le test 2',7' –dichlorofluorescin diacetate (DCFDA). Le DCFDA présente une perméabilité cellulaire importante qui lui permet alors d'interagir avec les radicaux libres présents dans les cellules en formant le DCF (molécule fluorescente). Lorsque les cellules sont mises en présence d'eau oxygénée, l'intensité de fluorescence augmente d'un facteur 1.4 suite à l'augmentation des radicaux libres. Le prétraitement des cellules avec la quercétine initiale ou formulée dans les nanocapsules lipidiques permet alors de diminuer l'intensité de fluorescence d'un facteur 2.9 par rapport au contrôle positif ($P<0.05$) démontrant ainsi que la quercétine est capable de neutraliser les radicaux libres.

2.2. Liposomes chargés en quercétine

La troisième approche est la formulation de la quercétine dans des liposomes. Les liposomes sont utilisés pour encapsuler des actifs depuis les années 70 avec le travail de Gregoriadis *et al*[26].

Jusqu'en 2014, 13 médicaments à base de liposomes ont été approuvés par la FDA. Le domaine de la cosmétique s'est aussi beaucoup intéressé à ces formulations, la première et plus connue est Capture de Dior et ensuite Niosomes (L'Oréal) mis sur le marché en 1987. La formulation de quercétine dans des liposomes que nous avons développée est simple, elle contient du dipalmitoylphosphatidylcholine (DPPC) et du Cremophor® EL (Fig. 4 c). Les liposomes présentent une distribution de taille centrée autour de 179 nm avec un PDI 0.06. Le taux de chargement de quercétine dans les liposomes reste faible par rapport à celui obtenu avec les nanocapsules lipidiques (0.56 µg/ml vs. 10.80 mg/ml). La libération de quercétine formulée dans les liposomes a été étudiée comme précédemment dans les boudins de dialyse et elles sont montrées une libération retardée par rapport au contrôle positif (solution de quercétine dans le propylène glycol) ($P < 0.05$). La quercétine a été détectée dans le récepteur après 5 minutes et les liposomes ont continué à la libérer pendant 2 heures. À la fin de l'étude à 24h, les liposomes avaient libéré la même quantité de quercétine que celui du contrôle positif (35 %).

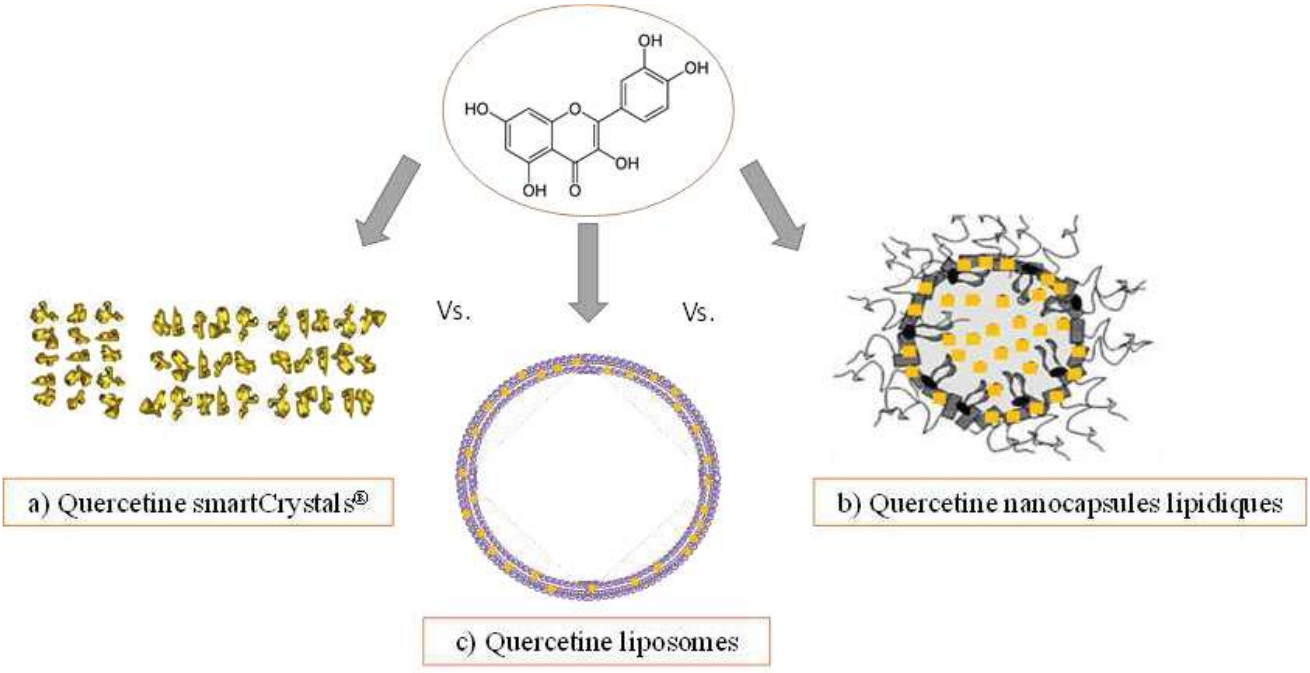

Fig. 4 : Représentation schématique des formulations de quercétine a) quercétine smartCrystals®, b) quercétine nanocapsules lipidiques et c) quercétine liposomes. La couleur jaune représente la quercétine.

Pour résumer la première partie de projet, les résultats de distribution de taille, PDI et de concentration de quercétine et d'efficacité antioxydante dans les trois approches (cinq formulations) ont été regroupés dans le tableau 1.

Nanoformulation de Quercetine	Que-SC Tween® 80	Que-SC TPGS	Que-LNC 20	Que-LNC 50	Que-lipo
Taille (nm)	295 ± 9	203 ± 3	26 ± 3	54 ± 3	179 ± 15
PDI	0.25 ± 0.03	0.24 ± 0.01	0.06 ± 0.001	0.17 ± 0.002	0.06 ± 0.02
Concentration de quercetine (mg/ml)	14.10 ± 3.4	14.40 ± 0.27	10.80 ± 0.78	6.00 ± 0.70	0.56 ± 0.05

Tableau 1 : Caractérisation des formulations en termes de taille, PDI et concentration de quercétine dans les formulations que-SC avec le Tween® 80 et TPGS, les formulations LNC 20 et 50 (que-LNC) et dans les liposomes (que-lipo).

Les formulations étant correctement caractérisées, nous les avons ensuite comparées en termes de toxicité et d'efficacité au niveau cellulaire et ensuite cutané.

3. Etude comparative entre quercétine smartCrystals®, nanocapsules lipidiques de quercétine et liposomes de quercétine sur les cellules *in vitro*

Dans la deuxième partie de projet de thèse, les cinq nanoformulations (quercétine SmartCrystals® stabilisés avec Tween® 80, quercétine SmartCrystals® stabilisés avec TPGS, LNC quercétine 20 nm, LNC quercétine 50 nm, et liposomes de quercétine) sont comparées *in vitro* au niveau de leur toxicité et activité cellulaire. Pour cela, deux lignées cellulaires ont été utilisées : les cellules HaCaT et les cellules THP-1. La sélection des cellules HaCaT permet d'évaluer les conditions d'application cutanée car les HaCaT sont une lignée cellulaire de kératinocytes [27]. La toxicité cellulaire ainsi que l'activité protectrice de la quercétine initiale et formulée ont été évaluées avec

le MTT : test de viabilité cellulaire et le DCFDA : test pour la quantification des radicaux libres intracellulaires.

Afin d'évaluer l'activité de la quercétine sur les cellules immunitaires qui se trouvent dans l'épiderme (spécialement les cellules dendritiques d'origine de monocytes circulant dans le sang), les THP-1 ont été repris comme modèle cellulaire. De la même façon que pour les tests sur les HaCaT, la viabilité cellulaire et l'activité protectrice de la quercétine soit en quercétine initiale soit formulée dans les nanoformulations ont été évaluées (MTT et DCFA).

3.1. Influence des nanoformulations sur la viabilité des cellules HaCaT

La Fig. 5 représente les résultats de viabilité entre 5 et 100 µg/ml de quercétine sur les cellules HaCaT. La quercétine initiale montre une viabilité cellulaire proche de celle obtenue avec le contrôle négatif (cellules sans traitement) avec 97,9 % et 101,7 % respectivement à 5 µg/ml et 25 µg/ml ($P > 0.05$). Ces résultats montrent l'absence de toxicité à ces concentrations. Pour les concentrations plus élevées, entre 50 et 100 µg/ml, les viabilités cellulaires augmentent à 108,5 % et 113,0 %. Ceci peut être expliqué par la solubilité limitée de la quercétine initiale dans le milieu de culture (DMEM) ce qui empêche son internalisation à ces concentrations. Lorsque la quercétine est formulée, l'augmentation de concentration des SmartCrystals® stabilisés avec Tween® 80 a bien entrainé dans ce cas une diminution de la viabilité cellulaire de 78,3 % à 54,6 % entre 5 µg/ml et 25 µg/ml. Ces résultats peuvent être dus à une interaction supérieure des nanocristaux avec les cellules, contrairement à la quercetine initiale, peu soluble qui forme de gros agrégats et n'interagit que très peu. Ces résultats peuvent être liés à la bonne solubilité de la que-SC dans le milieu de culture permettant ainsi une internalisation à forte concentration et donc une toxicité plus importante.

Dans le cas des que-SC stabilisés avec TPGS, nous avons montré le même comportement avec des viabilités qui diminuent en augmentant la concentration de quercétine sur les cellules. Les contrôles de Tween® 80 et TPGS montrent des viabilités cellulaires proches des cellules non traitées ($P < 0.05$). Les que-LNC 20 et 50 sont les formulations les moins toxiques avec des viabilités de 77,6 % et 93,8 % à 50 µg/ml respectivement. Par contre, la viabilité cellulaire à 100 µg/ml était plus faible pour les que-LNC 50 que les que-LNC 20 (60,5 % et 77,4 %), .Cette légère différence peut s'expliquer par une quantité plus importante de surfactants présente dans la formulation des LNC 20 (33,5 % vs. 20,0 % pour les LNC 50)[25].

Enfin, les liposomes de quercétine ont provoqué une diminution de viabilité cellulaire plus importante entre 5 et 25 µg/ml (67,5 % et 77,3 %) qu'à 50 µg/ml et 100 µg/ml (117,8 % et 126,3), cette observation a été aussi faite avec les liposomes non chargés. La toxicité semble donc plus liée aux excipients des liposomes qu'à la quercétine encapsulée.

Pour résumé l'influence de ces différents nanovecteur sur la viabilité des cellules HaCaT, la concentration de 5 µg/ml est la plus adaptée avec des viabilités cellulaires proches de 100 % avec la quercétine initiale et les LNC 50 et 20, et elle sera donc retenue pour la suite des études.

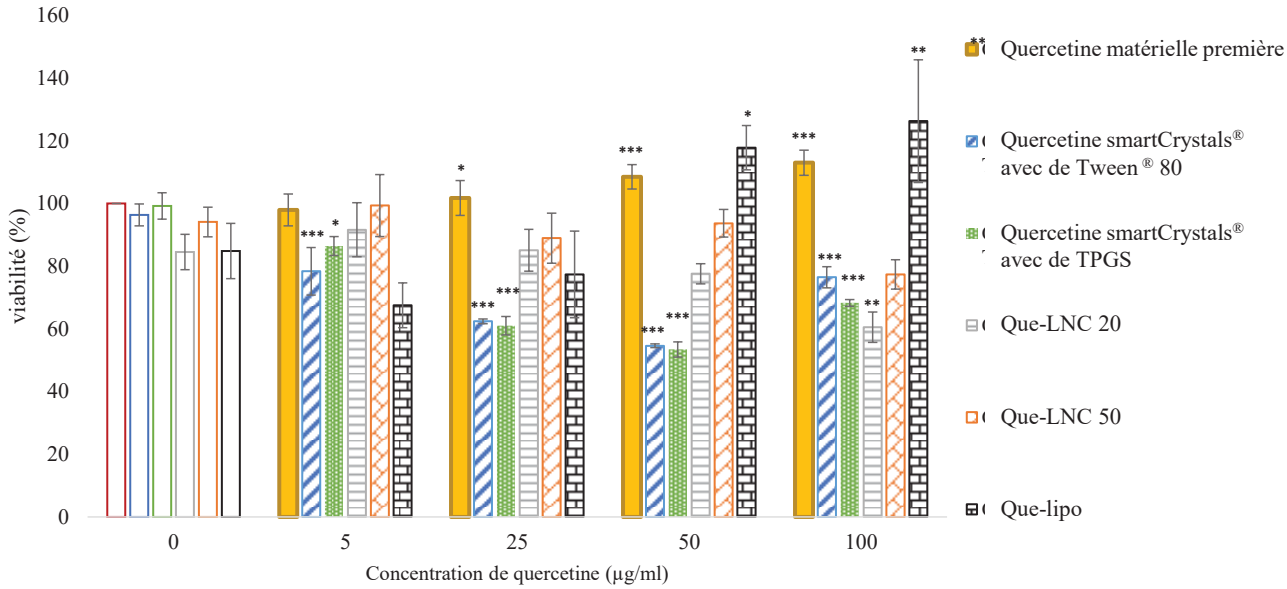

Fig. 5 : Etude de viabilité cellulaire sur HaCaT après traitement avec quercétine initiale, quercétine smartCrystals® formulée avec le Tween® 80 ou TPGS (que-SC), les nanocapsules lipidiques 20 et 50 (que-LNC) et les liposomes (que-lipo). Temps de traitement de 24 heures avec des doses appliquées de 5, 25, 50 et 100 µg/ml. Les études statistiques sont faites entre les formulations de quercétine et leurs blancs respectivement. Le P représente la valeur de signification où le * = P < 0.05, ** = P < 0.01 et *** = P < 0.005 respectivement.

3.2. Activité anti-radicalaire des différentes formulations sur les cellules HaCaT

La seconde partie de l'étude d'interaction avec les cellules HaCaT a permis d'évaluer l'efficacité antiradicalaire de la quercétine. Pour cela, les cellules HaCaT ont été traitées avec du DCFDA, puis traitées avec la quercétine initiale ou ses formulations avant d'être exposées à de l'eau oxygénée pour initier le stress oxydatif. Les résultats de l'intensité relative des ROS générée par

rapport au contrôle positif sont présentés dans la Fig. 6. Le traitement des cellules avec l'eau oxygénée (contrôle positif) augmente l'intensité relative des ROS intracellulaires par 2. Le traitement avec la quercétine formulée ou non limite l'augmentation des ROS grâce à son activité antioxydante. La quercétine initiale a donné des résultats proches du contrôle négatif, ce qui prouve son activité neutralisante sur les ROS. Les formulations que-LNC et que-lipo ont montré une meilleure efficacité avec des intensités relatives de ROS plus faibles que les que-SC. La concentration de 5 µg/ml de quercétine est donc une concentration active sur les cellules HaCaT.

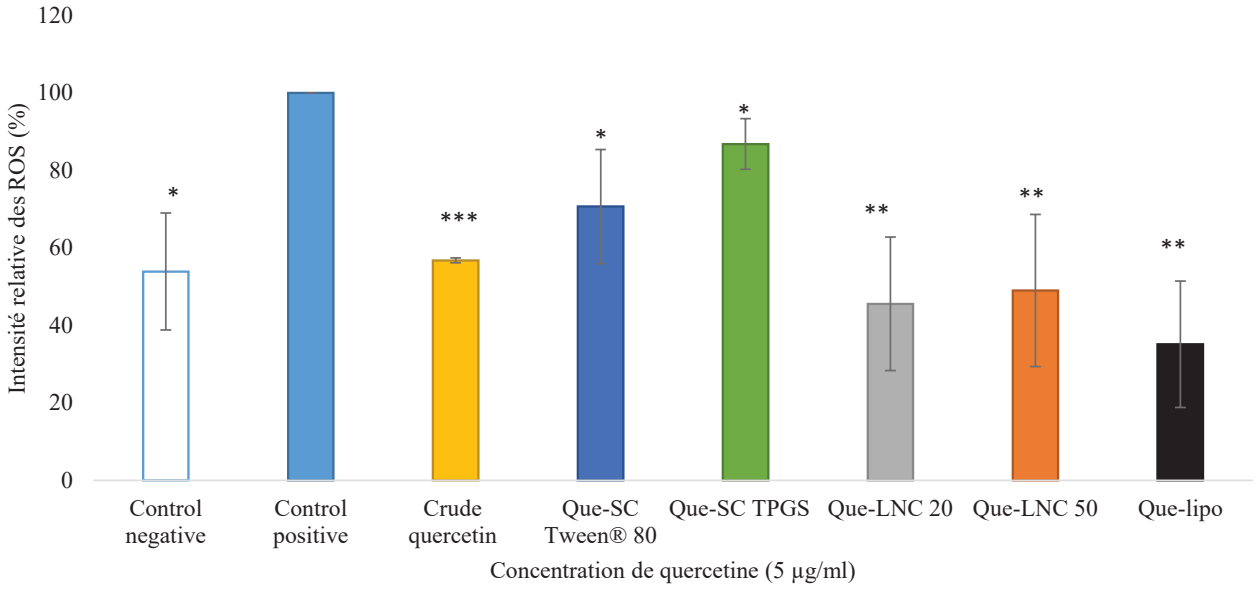

Fig. 6 : Evolution de l'intensité relative des ROS générés dans les cellules HaCaT après le traitement avec quercétine initiale, quercétine smartCrystals® avec le Tween® 80 ou TPGS (que-SC), les nanocapsules lipidiques 20 et 50 (que-LNC) et les liposomes (que-lipo) suivi par contact avec H_2O_2. Temps de traitement de 24 heures et dose appliquée de 5 µg/ml. Les études statistiques sont faites entre les formulations de quercétine et le contrôle positif. Le P représente la valeur de signification où le * = P < 0.05, ** = P < 0.01 et *** = P < 0.005 respectivement.

3.3. Influence des nanoformulations sur la viabilité des cellules THP1

Pour compléter l'étude sur l'interaction de la quercétine et de ses formulations avec les autres types cellulaires de la peau, les cellules THP-1 ont été utilisées comme modèle cellulaire pour savoir si la quercétine pourrait être un bon candidat pour le traitement des maladies inflammatoires de la peau comme par exemple le psoriasis [28]. Sur la base des résultats de toxicité cellulaire sur les HaCaT et l'activité protectrice montrée en Fig. 6, la concentration de 5 µg/ml est à nouveau

appliquée sur les cellules THP-1 pendant 24h. La Fig. 7 représente les pourcentages de viabilité de THP-1 après le traitement avec la quercétine initiale et ses formulations. Le traitement avec la quercétine ou ses formulations à 5 µg/ml n'avait pas présenté de toxicité cellulaire. La viabilité cellulaire obtenue avec quercétine initiale, que-LNC 20, que-LNC 50 ainsi que que-lipo est de plus de 100 % (122,5 %, 110,5 %, 116,9 et 135,9 %). Ceci peut montrer un effet positif de la quercétine sur la prolifération des cellules de THP-1 comme cela avait été observé sur un autre type cellulaire(cellules A549) avec de faibles concentrations de quercétine (5 µM) [29].

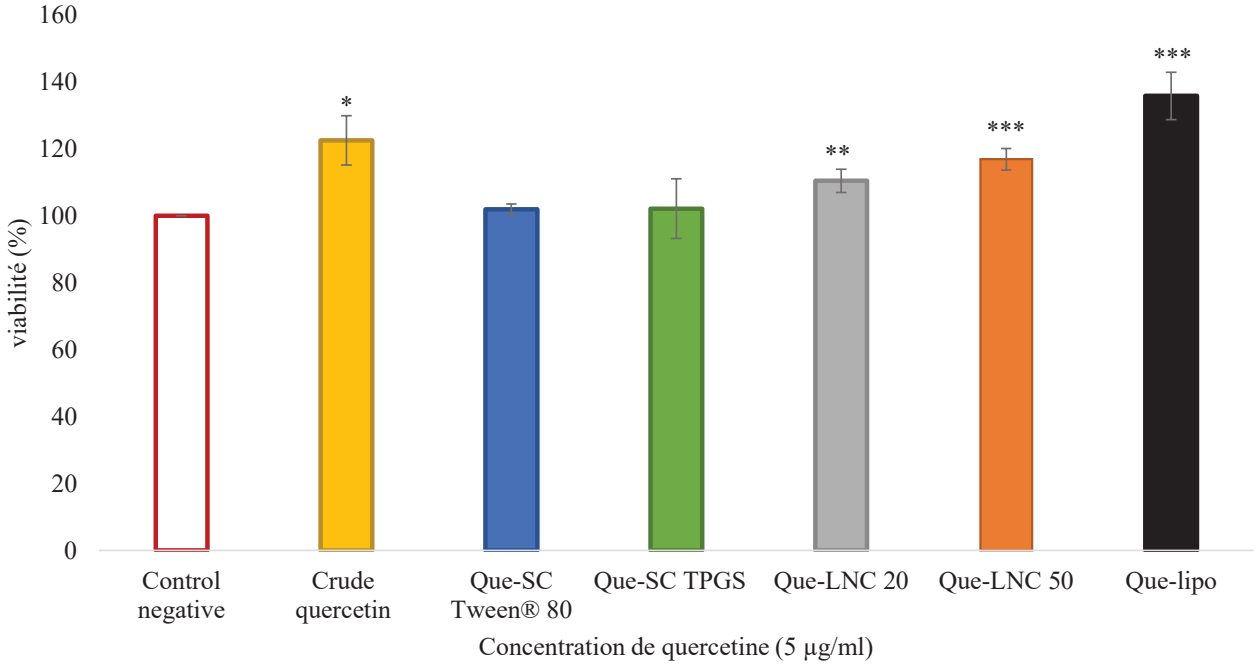

Fig. 7 : Suivi de la viabilité cellulaire de cellules THP-1 après le traitement avec quercétine initiale, quercétine smartCrystals® avec le Tween® 80 et TPGS (que-SC), les nanocapsules lipidiques 20 et 50 (que-LNC) et les liposomes (que-lipo). Temps de traitement est de 24 heures et la dose appliquée est de 5 µg/ml. Les études statistiques sont faites entre les formulations de quercétine et le contrôle négatif. Le P représente la valeur de signification où le * = P < 0.05, ** = P < 0.01 et *** = P < 0.005 respectivement.

3.4. Activité anti-radicalaire des différentes formulations sur les cellules THP1

Suite aux tests de toxicité cellulaire sur les THP-1, l'activité de la quercétine contre les radicaux libres a été testée de la même façon qu'avec les HaCaT. La Fig. 8 présente les résultats des intensités relatives de ROS intracellulaire par rapport au contrôle positif. Le traitement des cellules avec l'eau oxygénée augmente les ROS générés dans les cellules par 1.4 (contrôle positif) par

rapport au contrôle négatif (cellules sans traitement). Le traitement des cellules avec la quercétine initiale ou dans les formulations a neutralisé les radicaux libres dans les THP-1 et réduit l'intensité des ROS de 2.9 par rapport au contrôle positif. Les intensités des ROS sont même plus faibles dans les cellules traitées avec la quercétine que dans le groupe des cellules de contrôle négatif ce qui démontre l'activité puissante de la quercétine.

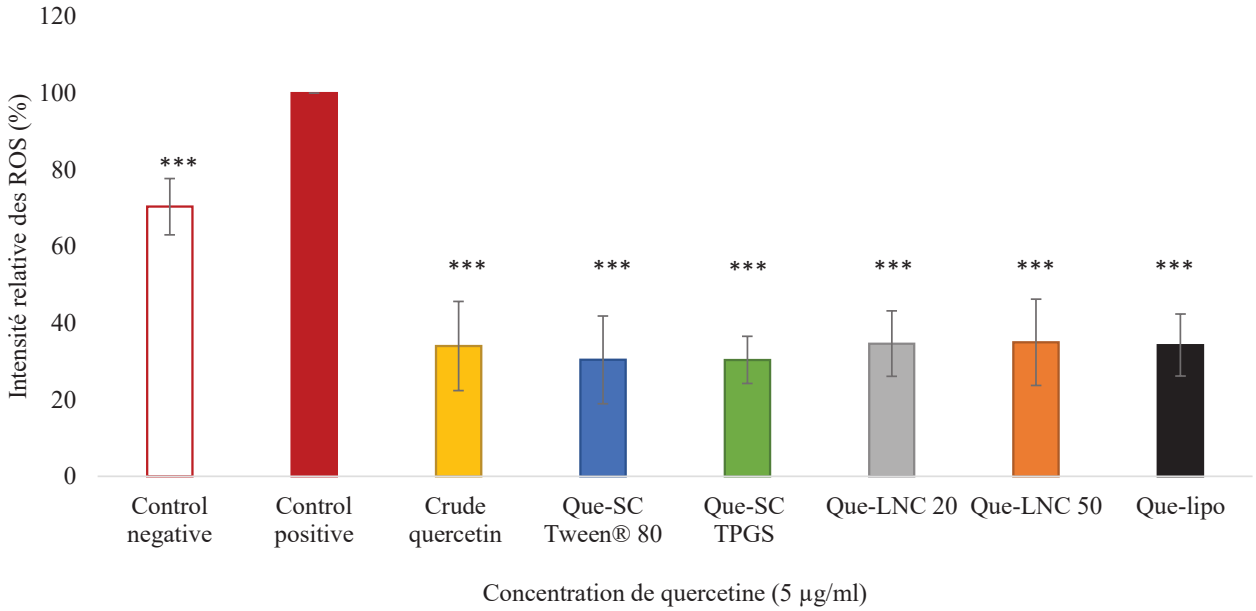

Fig. 8 : Suivi de l'intensité relative des ROS générés dans les cellules THP-1 après le traitement avec quercétine initiale, quercétine smartCrystals® avec le Tween® 80 et TPGS (que-SC), les nanocapsules lipidiques 20 et 50 (que-LNC) et les liposomes (que-lipo) suivi par H_2O_2. Contrôle positif : traitement avec H_2O_2. Contrôle négatif : cellules sans traitement. Temps de traitement est 24 heures et la dose appliquée est 5 µg/ml. Les études statistiques sont faites entre les formulations de quercétine et le contrôle positive. Le P représente la valeur de signification où le * = P < 0.05, ** = P < 0.01 et *** = P < 0.005 respectivement.

En conclusion de cette étude cellulaire, la quercétine formulée a montré une activité protectrice sur deux lignées cellulaires, les HaCaT, représentative des cellules constitutives de l'épiderme, les kératinocytes et les THP1, représentatives des cellules sentinelles immunitaires.

4. Etude *in vivo* de la pénétration cutanée de la quercétine sous forme smartCrystals® et formulée dans les nanocapsules lipidiques

La dernière partie du projet de thèse a concerné l'étude de la pénétration cutanée après application des deux meilleures formulations de quercétine. La pénétration cutanée est l'étape la plus importante et la plus significative de la réussite des stratégies des formulations utilisées dans ce

projet de thèse. Pour avoir la meilleure corrélation avec la réalité, nous avons fait les tests de pénétration cutanée *in vivo* chez l'homme.

Nous avons sélectionné les meilleures formulations en se basant sur 3 critères : (i) la taille, (ii) la concentration en quercétine et (iii) l'activité au niveau cellulaire. Pour la taille, il nous faut avoir la distribution de taille la plus petite et la plus étroite (PDI le plus petit), car les tailles les plus petites permettent de former un film homogène léger favorisant l'hydratation, ce qui, par effet de concentration, peut améliorer la pénétration cutanée de la quercétine vers l'épiderme [23]. Dans le cas des smartCrystals®, la que-SC formulée avec le TPGS a montré la taille la plus petite à 203 nm (PDI 0,24) par rapport à celle obtenue avec Tween® 80 à 293 nm (PDI 0,25) (Tableau 1). Ensuite, que-SC TPGS a permis d'obtenir la concentration la plus élevée de quercétine par ml de formulation (14,4 mg/ml) par rapport au Tween® 80 (14,1 mg/ml), tout en étant moins toxique sur les HaCaT (86,4 % vs. 78,4 %) avec une activité protectrice identique ($P > 0,05$). Au vue de ces résultats, la formulation de que-SC avec le TPGS a été sélectionnée pour l'étude de pénétration *in vivo*.

Dans le cas des formulations de nanocapsules lipidiques, la que-LNC 20 (26 nm PDI 0,06) a permis d'obtenir la concentration la plus élevée de quercétine par ml de formulation (10,8 mg/ml) en comparaison avec que-LNC 50 (54 nm PDI 0,17 et 6,0 mg/ml) (Tableau 1). Les résultats de toxicité et d'activité protectrice sur les HaCaT entre les LNC 20 et 50 étaient proches avec respectivement 91,6 % vs. 99,3 % en viabilité et 45,5 % vs. 46,0 % en intensité des ROS ($P > 0,05$). Sur les THP-1, les résultats de toxicité et d'activité protectrice étaient aussi proches entre les LNC 20 et 50 : 110,5 % vs. 116,9 % en viabilité respectivement et 34,6 % vs. 35,0 % en intensité des ROS ($P > 0,05$). Pour cette raison, la formulation que-LNC 20 a été sélectionnée pour l'étude de pénétration *in vivo*.

La formulation liposomale n'a pas été retenue compte tenue de la faible concentration de quercétine (0.56 mg/ml) et des résultats peu convaincants obtenus avec les cellules HaCaT et THP-1.

La Fig. 9 représente les résultats de pénétration cutanée *in vivo* de que-SC avec de TPGS et que-LNC 20 sir 8 volontaires. La procédure de cette étude est basée sur la publication de Scalia *et al* [30]. Dans le cas de que-SC, 94,6 % de la dose appliquée de quercétine a été détectée dans les strips. Les strips sont des bandes collantes normalisées appliquées sur la peau et ensuite arrachées conduisant à l'arrachement du stratum cornéum. La quercétine a été dosée dans chaque bande par

HPLC. Les résultats ont montré que moins de 6 % de la quercétine appliquée avait pénétré dans les couches inférieures de l'épiderme. Ce résultat nous conduit à proposer la formulation smartCrystals® de quercétine pour une action protectrice contre les UV en cosmétique soit dans des crèmes de jour soit dans des produits solaires.

Avec les formulations de que-LNC, 27,1 % de la dose appliquée de quercétine a été détectée dans les strips, ce qui indique cette fois que plus de 70 % à pénétrer profondément dans les couches de l'épiderme de la peau. Ce résultat nous permet de proposer les formulations de nanocapsules lipidiques de quercétine pour l'application antiinflammatoire dans les maladies comme psoriasis.

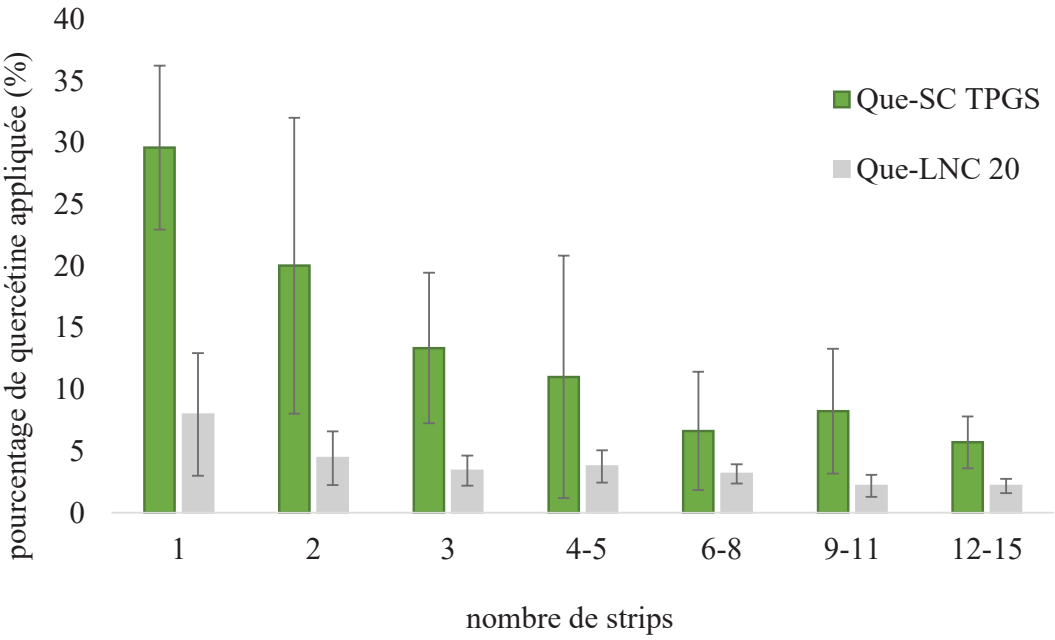

Fig. 9 : Etude de la pénétration cutanée *in vivo* après le traitement avec quercétine smartCrystals® avec le TPGS (que-SC), les nanocapsules lipidiques 20 (que-LNC). Temps de traitement est 1 heure.

5. Conclusion

Dans ce projet, trois approches de formulations nanométriques (smartCrystals, nanocapsules lipidiques et liposomes) ont été testées pour améliorer la solubilité de quercétine. Les formulations ont été optimisées en termes de procédé de préparation (transposition industrielle) et de composition des excipients pour augmenter la quantité de quercétine formulée. Les formulations ont été caractérisées en termes de taille, PDI, taux de chargement en quercétine, état cristallin et

cinétique de libération de quercétine *in vitro*. Ensuite, les formulations ont été comparées entre elles sur les cellules HaCaT et THP-1 avec détermination de leur toxicité et activité protectrice. Enfin, deux formulations (quercétine smartCrystals® avec le TPHS et quercétine LNC 20) ont été sélectionnées et comparées *in vivo* pour évaluer l'amélioration de la pénétration cutanée de quercétine.

Ce projet propose une solution pour formuler la quercétine d'une façon pertinente et efficace qui pourra être extrapolée au niveau industriel pour des applications cutanées de molécules peu solubles dont l'efficacité est limitée par leur faible pénétration cutanée.

Références

[1] R. Slimestad, T. Fossen, I.M. Vagen, Onions: a source of unique dietary flavonoids, J Agric Food Chem, 55 (2007) 10067-10080.

[2] S. Veeriah, T. Kautenburger, N. Habermann, J. Sauer, H. Dietrich, F. Will, B.L. Pool-Zobel, Apple flavonoids inhibit growth of HT29 human colon cancer cells and modulate expression of genes involved in the biotransformation of xenobiotics, Mol Carcinog, 45 (2006) 164-174.

[3] T.L. Wadsworth, D.R. Koop, Effects of the wine polyphenolics quercetin and resveratrol on pro-inflammatory cytokine expression in RAW 264.7 macrophages, Biochemical Pharmacology, 57 (1999) 941-949.

[4] K.E. Heim, A.R. Tagliaferro, D.J. Bobilya, Flavonoid antioxidants: chemistry, metabolism and structure-activity relationships, The Journal of Nutritional Biochemistry, 13 (2002) 572-584.

[5] J. Baumann, F. v. Bruchhausen, G. Wurm, Flavonoids and related compounds as inhibitors of arachidonic acid peroxidation, Prostaglandins, 20 (1980) 627-639.

[6] F. Bonina, M. Lanza, L. Montenegro, C. Puglisi, A. Tomaino, D. Trombetta, F. Castelli, A. Saija, Flavonoids as potential protective agents against photo-oxidative skin damage, International Journal of Pharmaceutics, 145 (1996) 87-94.

[7] Y. Cai, Q. Luo, M. Sun, H. Corke, Antioxidant activity and phenolic compounds of 112 traditional Chinese medicinal plants associated with anticancer, Life Sciences, 74 (2004) 2157-2184.

[8] J.E. Brown, H. Khodr, R.C. Hider, C.A. Rice-Evans, Structural dependence of flavonoid interactions with Cu2+ ions: implications for their antioxidant properties, Biochem J, 330 (1998) 1173-1178.

[9] S.C. Braca.A, Politi.M, Mendez.J, Antioxidant activity of flavonoids from Licania licaniaeflora, 79 (2002) 379–381.

[10] R.J. Nijveldt, E. van Nood, D.E.C. van Hoorn, P.G. Boelens, K. van Norren, P.A.M. van Leeuwen, Flavonoids: a review of probable mechanisms of action and potential applications, The American Journal of Clinical Nutrition, 74 (2001) 418-425.

[11] G.R. Beecher, Overview of Dietary Flavonoids: Nomenclature, Occurrence and Intake, The Journal of Nutrition, 133 (2003) 3248S-3254S.

[12] T. Walle, Absorption and metabolism of flavonoids, Free Radical Biology and Medicine, 36 (2004) 829-837.

[13] H. Kim, S. Namgoong, H. Kim, Antiinflammatory activity of flavonoids: Mouse ear edema inhibition, Archives of Pharmacal Research, 16 (1993) 18-24.

[14] S.V. Jovanovic, S. Steenken, M. Tosic, B. Marjanovic, M.G. Simic, Flavonoids as Antioxidants, Journal of the American Chemical Society, 116 (1994) 4846-4851.

[15] C.F. Lin, Y.L. Leu, S.A. Al-Suwayeh, M.C. Ku, T.L. Hwang, J.Y. Fang, Anti-inflammatory activity and percutaneous absorption of quercetin and its polymethoxylated compound and glycosides: the relationships to chemical structures, Eur J Pharm Sci, 47 (2012) 857-864.

[16] J. Kanitakis, Anatomy, histology and immunohistochemistry of normal human skin, Eur J Dermatol, 12 (2002) 390-399; quiz 400-391.

[17] M. Kakran, R. Shegokar, N.G. Sahoo, L. Al Shaal, L. Li, R.H. Müller, Fabrication of quercetin nanocrystals: Comparison of different methods, European Journal of Pharmaceutics and Biopharmaceutics, 80 (2012) 113-121.

[18] T. Hatahet, M. Morille, A. Hommoss, C. Dorandeu, R.H. Muller, S. Begu, Dermal quercetin smartCrystals(R): Formulation development, antioxidant activity and cellular safety, Eur J Pharm Biopharm, 102 (2016) 51-63.

[19] Q. Chen, S. Tang, X. Jin, J. Zou, K. Chen, T. Zhang, X. Xiao, Investigation of the genotoxicity of quinocetone, carbadox and olaquindox in vitro using Vero cells, Food and Chemical Toxicology, 47 (2009) 328-334.

[20] A. Shiohara, A. Hoshino, K.-i. Hanaki, K. Suzuki, K. Yamamoto, On the Cyto-Toxicity Caused by Quantum Dots, Microbiology and Immunology, 48 (2004) 669-675.

[21] B.a. Heurtault, P. Saulnier, B. Pech, J.-E. Proust, J.-P. Benoit, A Novel Phase Inversion-Based Process for the Preparation of Lipid Nanocarriers, Pharmaceutical Research, 19 (2002) 875-880.

[22] B.a. Heurtault, P. Saulnier, B. Pech, M.-C. Venier-Julienne, J.-E. Proust, R. Phan-Tan-Luu, J.-P. BenoÄ±Ì‚t, The influence of lipid nanocapsule composition on their size distribution, European Journal of Pharmaceutical Sciences, 18 (2003) 55-61.

[23] R.H. Müller, M. Radtke, S.A. Wissing, Solid lipid nanoparticles (SLN) and nanostructured lipid carriers (NLC) in cosmetic and dermatological preparations, Advanced Drug Delivery Reviews, 54, Supplement (2002) S131-S155.

[24] K. Westesen, B. Siekmann, M.H.J. Koch, Investigations on the physical state of lipid nanoparticles by synchrotron radiation X-ray diffraction, International Journal of Pharmaceutics, 93 (1993) 189-199.

[25] C. Maupas, B. Moulari, A. BÃ©duneau, A. Lamprecht, Y. Pellequer, Surfactant dependent toxicity of lipid nanocapsules in HaCaT cells, International Journal of Pharmaceutics, 411 (2011) 136-141.

[26] G. Gregoriadis, P.D. Leathwood, B.E. Ryman, Enzyme entrapment in liposomes, FEBS Letters, 14 (1971) 95-99.

[27] P. Boukamp, R.T. Petrussevska, D. Breitkreutz, J. Hornung, A. Markham, N.E. Fusenig, Normal keratinization in a spontaneously immortalized aneuploid human keratinocyte cell line, J Cell Biol, 106 (1988) 761-771.

[28] E.A. Hamminga, A.J. van der Lely, H.A.M. Neumann, H.B. Thio, Chronic inflammation in psoriasis and obesity: Implications for therapy, Medical Hypotheses, 67 (2006) 768-773.

[29] A. Robaszkiewicz, A. Balcerczyk, G. Bartosz, Antioxidative and prooxidative effects of quercetin on A549 cells, Cell Biology International, 31 (2007) 1245-1250.

[30] S. Scalia, E. Franceschinis, D. Bertelli, V. Iannuccelli, Comparative evaluation of the effect of permeation enhancers, lipid nanoparticles and colloidal silica on in vivo human skin penetration of quercetin, in: Skin Pharmacol Physiol, Basel., Switzerland, 2013, pp. 57-67.

Part I:

Bibliography

Flavonoids and quercetin

Goals:

1. What are flavonoids?

2. Why flavonoids?

3. Why quercetin?

4. Quercetin problematic in brief

5. Our approach with quercetin and its problematic

6. Our objective(s)

1. What are flavonoids?

Flavonoids are plants pigments derived from benzo-g-pyrone (Fig. 1). Flavonoids can be observed by the naked eye as they form the amazing colors of flower petals. They can be found in apples [1], pears [2], onions [3], red wine [4] and others [5, 6]. An increasing interest in flavonoids is rising in the last few decades in several domains. Botanists started to identify flavonoids and used them in the taxonomical studies. Pharmaceutical industry benefits from the natural pool of medically effective compounds, and searches for new drug candidates from flavonoids and their synthesized derivatives. Considering that flavonoids are present mostly in plants, their consumption by human in diet is between 20 mg and 1 g according to nutritional attitude [7]. Since flavonoids are ***phenolic compounds***, they possess ***oxidation-reduction potential***. They are prone to oxidation to quinones occuring upon ring opening [8]. However, this phenomenon is more susceptible under UV light especially if metals are present such as Cu^{2+}[9].

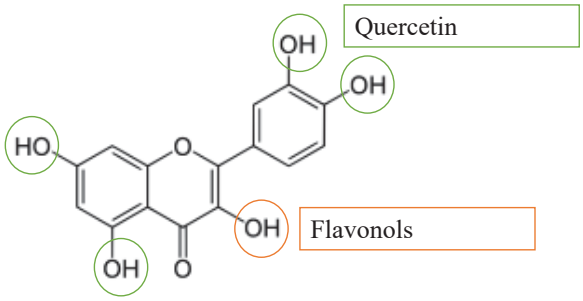

Flavonoids

Fig. 1: Chemical structure of flavonoids, flavonols (orange) and quercetin (green).

At the same time, flavonoids presenting ***hydroxyl groups*** on their structure show antioxidant activity by their ability to donate hydrogen. Consequently a dual functional behavior is observed as flavonoids can be either prooxidant or antioxidant molecules [9]. A lot of doubt and confusing results were found about flavonoids relation to oxidation. Some studies showed that flavonoids consumption within human diet induced lower incidence of coronary heart disease [10] and other studies showed that this correlation is insignificant [11]. Also flavonoids have acid base properties with pKa from 8 to 10.5 and this enables the tautomerism especially in flavonols like quercetin [12].

2. Why flavonoids?

Flavonoids are very promising drug candidates; mainly due to their radicals scavenging ability. We will first define reactive oxygen species and their roles in cells, and then discus in brief about flavonoids free radical scavenging potentials.

Equation 1: $R° + Quercetin \rightarrow R - H^+$

Highly reactive species such as molecular oxygen are generated in the course of many cellular processes like respiratory chain and are catalyzed by oxygenases. Despite to the full reduction of oxygen generating two molecules of water, a partial reduction can occur and thus leads to the formation of the highly toxic superoxide anion $\cdot O^{2-}$. Formed $\cdot O2^{-}$ could be generated for example by macrophages during the immune response against foreign pathogens, but excess amounts must be neutralized before attacking unsaturated lipids and sulfhydryl groups of non-infected cells. Consequently, specific enzymes such as cytochrome oxidase containing metal ions (Fe^{2+} and Cu^{+} ions) entrap reactive molecules in the metal cage region. In case of reactive oxygen species escape from the denaturized enzymes, they start a chain reaction attacking lipid, nucleic acids which causes damage to vital cellular processes. Hydrogen peroxide radicals and peroxynitrite are other forms of reactive species generated by UV radiation [12].

Another cross-linked response to oxidative injury is inflammation [13]. Reactive oxygen species are inducer of proinflammatory cytokines such as the example of macrophages during the immune response, and sometimes the oxidant by itself can activate proinflammatory cytokines such as UV radiation on skin [14]. The continuous exposure to ROS over prolonged periods increases the incidence of DNA mutations and causes the aging phenomenon in weakened tissue and organs [15]. Consequently, chronic inflammation and uncontrolled inflammatory disorders are subsequent to sustained oxidative attack.

Flavonoids are known to scavenge these free radicals [16], to induce the expression of antioxidant enzymes [17, 18] and to protect low density lipoprotein unsaturated moieties from oxidative damages [19]. Flavonoids antiinflammatory actions lay side to side with the antioxidant one. Some explanation for the antiinflammatory mechanism of flavonoids is that they are free radical scavengers, other theories are based on evidences of modulation of the activities of arachidonic

acid metabolism enzymes [20-22], modulation of the production of other proinflammatory molecules [23, 24] and modulation of proinflammatory gene expression [25-27]. This double sword (antioxidant and antiinflammatory activities) can give raise to several therapeutic applications in regards to oxidative damage and inflammation for example in cardiovascular diseases like diabetes [28], hypercholesterolemia [29], hypertension [30], atherosclerosis [19], myocardial ischemia–reperfusion injury [31] and antithrombotic activities in hemorrhage [32]. Also flavonoids proved effectiveness in the protection of different cellular cell lines for example neuronal cells [33], colonocytes [34], pancreatic β-cells [35], hepatic HepG2 cells [36], keratinocytes [37]. Moreover, they are used in different inflammatory disorders like contact dermatitis [26], inflammatory joint disease [38] rheumatoid arthritis [38, 39] and recently psoriasis [40]. All these promising applications and targets make flavonoids as the new trend in drug research. It is worth to note that 4 278 publications dealt with flavonoids in 2016 on ScienceDirect. This reflects the great interest in this family and their possible future indications in the prevention, treatment or co-treatment of oxidative damage related disorders.

3. Why quercetin?

Quercetin is an important member of the flavonoid family, which belongs to a subfamily called flavonols (Fig. 1). Quercetin is present in several fruits and vegetables like red onions, broccolis, sweet potatoes and at least eight berry variants [41]. It is a yellow powder found linked to glycosides in nature for example rutin, which is quercetin-3-O-rutinoside. Quercetin's IUPAC name is 3, 3', 4', 5, 7-pentahydroxy-2-phenylchromen-4-one (figure 1), which indicates the presence of five hydroxyl groups in its structure. This high number of hydroxyl groups makes quercetin as one of the strongest antioxidants among flavonoids [9, 42].

4. Quercetin problematic in brief

Quercetin is a good model drug representing flavonoids with the main structural backbone of flavonoids. This enables quercetin to behave, in the same way as flavonoids, in oxidation-reduction reactions, acid base reactions (pKa = 6.74) [43], optical activity [44], Concerning physicochemical point of view, quercetine exposes polymorphism [45], and unfortunately very low water solubility (0.441 ± 0.0487 μg/mL in PBS buffer at pH 3) [46, 47]. When quercetin is suspended in water, intermolecular hydrogen bonding between quercetin crystals appears and

enables planar configuration [48]. This initiates a starting point of nucleation, agglomeration and precipitation.

From a pharmacologic point of view, quercetin holds many of flavonoids properties, especially antiinflammatory potentials due to its antioxidant power efficiency [49, 50]. While being a good representative of flavonoids family, with low water solubility due to lipophilic cyclic structure with a partition coefficient (log P = 1.82 ± 0.32) [51], Quercetine exposes at the same time several polar head groups. These previously mentioned amphiphilic properties hinder quercetin therapeutic applicability. In parallel, discussion is made about whether quercetin glycoside or aglycone present the higher bioavailability and this is an important point. In fact, quercetin glycosides are mainly taken in human diets, and their absorption is complex and influenced by the presence of other natural compounds. In 1997, Hollman *et al* monitored quercetin plasma concentration after the administration of a large dose of quercetin glycoside from onions and apples. Surprisingly, onions yielded three fold higher plasma concentration of quercetin compared to apples [52]. Scientists believe that quercetin embedded within fruits and vegetables will be more bioavailable than its pure form (pure glycoside or aglycone), furthermore, conjugation of quercetin with glucose enhances its absorption for small gut [52]. Nonetheless, the ingested quantity of fruits and vegetables containing quercetin will confer plasma concentration in the nanomolar range and this cannot be used for therapeutics application [53]. Besides, it was already shown that glycoside forms of quercetin are metabolized by intestinal microflora [54], and even in topical application skin partially metabolizes quercetin glycosides to the free aglycone form [55].

All these remarks should be considered in developing quercetin for therapeutic applications. For this, the enhancement of quercetin bioavailability may be focused on its aglycone form, hence it has stronger antioxidant activity than glycoside counterparts [56] and is the main form of molecule that can be absorbed by passive diffusion.

5. Our approach with quercetin and its problematic

Quercetin as a promising drug candidate is a matter of research with more than 22 000 articles between 1988 and 2016. Quercetin presents antioxidant and antiinflammatory properties useful in different disorders. Most of disorders requires systemic administration such as breast [57], prostate [58], colon [59] and liver [60] cancers or neurodegenerative disorders like Parkinson [61] and Alzheimer [62]. It was also administered to induce the reduction of inflammation related to

rheumatoid arthritis [63], the protection of bronchial epithelial cells from matter-induced damage [64] and cardiac muscle from ischemic injuries [65]. Quercetin can also be of great value in localized disorders such as wounds [66], skin protection against UV radiation [67] and glaucoma [68] (Fig. 2).

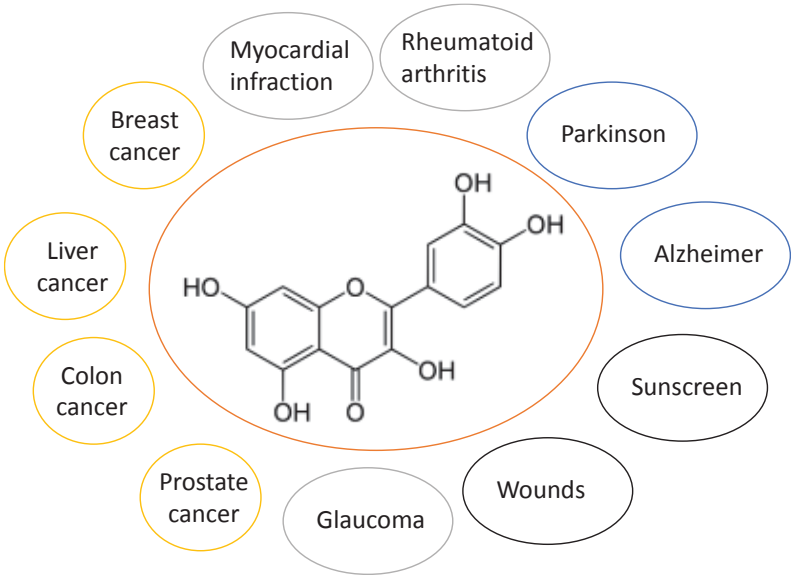

Fig. 2: Quercetin applications under research.

Despite this promising applicabilities of quercetin, still much of this research is on *in vitro* cellular and molecular bases, with quercetine dissolved in organic solvents such as DMSO. Few transferred these successful results to the *in vivo*, probably because quercetin solubility issues [69, 70]. Indeed, when diluted in DMSO, quercetin presents very low bioavailability *in vivo* [71]. Others increased quercetin dose in order to get a sufficient drug concentration in blood or at the active site, consequently, the ingested dose was toxic to other vital organs, probably because quercetin starts to show pro-oxidant rather than antioxidant actions [72].

Nanotechnology is a novel and successful approach to deliver drug to human body and to overcome drug solubility problems, to improve drug physicochemical properties and to enhance its *in vivo* bioavailability. Morever and under some situations, drugs produced at the nanometric scale are more powerful than their macro counterpart is, thus a rational drug use can be concluded. This is very useful even on drugs found already in market, especially, antibiotics that are susceptible to bacterial resistance if used frequently or in high doses. Nanotechnology is a general terms where several practical approaches can be followed to obtain drugs in the nanometric range.

Drugs can be obtained at the nanometric range (nanonization) alone or can be encapsulated in nanovectors (nanoformulation) (Fig. 3).

Drug nanocrystals are suspension of the drug with a stabilizer (particle size is less than 1 μm), produced by two methods: top down and bottom up. Top down when particles size starts to decrease in the course of the process such as in the high-pressure homogenization or bead mill. On the other hand, bottom up techniques involve the transfer of drug molecules for solvent to non-solvent phase with subsequent precipitation and increase in size to not more than 1000 nm like in evaporative precipitation [74]. In the second generation of drug nanocrystals, methods increase drug physical stability, as well as an optimization of process times and yields mainly by combining first generation process [75, 76]. Several drugs formulated using the nanocrystals technology are introduced to the market mention here **Rapamune®** sirolimus (Wyeth Pharmaceuticals, Madison, NJ), **Emend®** aprepitant (Merck, Winehouse Station, NJ), **Tricor®** fenofibrate (Abbott Laboratories) and **Megace ES®** megestrol acetate (Pharmaceutical Companies, Inc. Spring Valley, NY)

Nanovectors are drug carriers at the nanometric scale, where drug is formulated with other excipients, this technique can be used to improve the drug targeted [77] or to increase the systemic circulation of drugs suffering from short half-lives [78]. By contrast to the formation of nanocrystals, the drug is there associated to other excipients to form a nanoparticles, it is “a part” of the system. The use of nanovectors can be of benefit in protecting sensitive drugs from oxidation by oxygen in air and light and in reducing drug side effects by targeted delivery systems. Nanovectors can be liposomes [79], lipid nanocapsules [80], polymeric nanocapsules [81], solid lipid nanoparticles (SLN) or nanostructured lipid carriers (NLC) [82]...

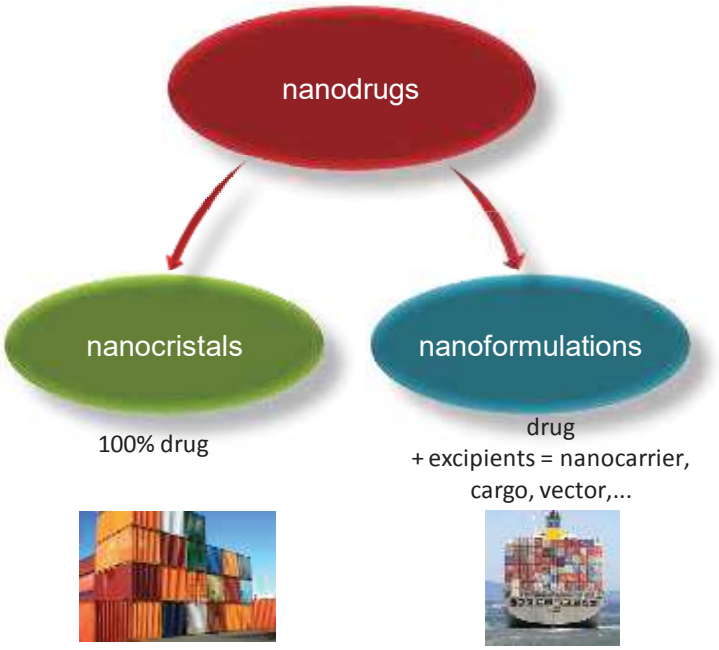

Fig. 3: Schematic two main strategies used to form nanodrugs

From the previous; we can summarize our objectives in the thesis into three points:

1. The use of a "paradigmatic drug" for water insoluble, lipophilic and polar molecule such as quercetin in order to attend an acceptable water solubility for pharmaceutical topic administration. By applying nanotechnology on quercetin, we facilitate drug formulation afterwards and this can be useful considering that 40% of the drugs in the pipelines have solubility problems [83]. Moreover, literature states that about 60% of all drugs coming directly from synthesis are nowadays poorly soluble [84].
2. Testing nanometric quercetin for one of its applications and compare its activity to the crude form. We are focusing on topical protective potentials of quercetin against free radicals generation and inflammation of skin upon UV exposure.
3. The comparative study between the three nano-approaches selected to formulate quercetin (nanocrystals, liposomes and lipid nanocapsules). The comparison is based on the aspects of quercetin loading within each formulation, the formulation process, the possibility to industrialize, the physical stability upon storage, the functional stability of quercetin, the cellular activity, the lowest effective dose and the skin penetration capacity.

In the following chapters, an introduction to quercetin activity on skin will be presented in details under the form of a review article entitled **"Quercetin topical application, from conventional dosage forms to nanodosage forms"**. Then quercetin formulations developed and fully characterized will be presented as research articles: quercetin second generation nanocrystals and quercetin lipid nanocapsules development **"Dermal quercetin smartCrystals®: Formulation development, antioxidant activity and cellular safety"** and **"Dermal quercetin lipid nanocapsules: influence of the formulation on antioxidant activity and cellular protection against hydrogen peroxide"** (published in European journal of pharmaceutics and biopharmaceutics, doi:10.1016/j.ejpb.2016.03.004 and under review at journal of controlled release respectively). Then, a third article will present quercetin formulations into liposomes and will put the three formulations in comparison on cellular level and in terms of skin penetration capacity **"Liposomes, lipid nanocapsules and smartCrystals®: a comparative study for an effective quercetin delivery to skin"**. Afterwards, a general discussion of the thesis project will cover the possibility to industrialization and will give general remarks about the performed studies. Finally, a general conclusion will be presented.

References

[1] A. Schieber, P. Hilt, J. Conrad, U. Beifuss, R. Carle, Elution order of quercetin glycosides from apple pomace extracts on a new HPLC stationary phase with hydrophilic endcapping, Journal of Separation Science, 25 (2002) 361-364.

[2] G.A. Spanos, R.E. Wrolstad, Phenolics of apple, pear, and white grape juices and their changes with processing and storage. A review, Journal of Agricultural and Food Chemistry, 40 (1992) 1478-1487.

[3] M.-J. Ko, C.-I. Cheigh, S.-W. Cho, M.-S. Chung, Subcritical water extraction of flavonol quercetin from onion skin, Journal of Food Engineering, 102 (2011) 327-333.

[4] A. Kumar, A.K. Malik, D.K. Tewary, A new method for determination of myricetin and quercetin using solid phase microextraction–high performance liquid chromatography–ultra violet/visible system in grapes, vegetables and red wine samples, Analytica Chimica Acta, 631 (2009) 177-181.

[5] M.G.L. Hertog, P.C.H. Hollman, M.B. Katan, Content of potentially anticarcinogenic flavonoids of 28 vegetables and 9 fruits commonly consumed in the Netherlands, Journal of Agricultural and Food Chemistry, 40 (1992) 2379-2383.

[6] Y. Cai, Q. Luo, M. Sun, H. Corke, Antioxidant activity and phenolic compounds of 112 traditional Chinese medicinal plants associated with anticancer, Life Sciences, 74 (2004) 2157-2184.

[7] M.G. Hertog, E.J. Feskens, P.C. Hollman, M.B. Katan, D. Kromhout, Dietary antioxidant flavonoids and risk of coronary heart disease: the Zutphen Elderly Study, Lancet, 342 (1993) 1007-1011.

[8] D. Metodiewa, A.K. Jaiswal, N. Cenas, E. Dickancaité, J. Segura-Aguilar, Quercetin may act as a cytotoxic prooxidant after its metabolic activation to semiquinone and quinoidal product, Free Radical Biology and Medicine, 26 (1999) 107-116.

[9] G. Cao, E. Sofic, R.L. Prior, Antioxidant and Prooxidant Behavior of Flavonoids: Structure-Activity Relationships, Free Radical Biology and Medicine, 22 (1997) 749-760.

[10] R.R. Huxley, H.A.W. Neil, The relation between dietary flavonol intake and coronary heart disease mortality: a meta-analysis of prospective cohort studies, Eur J Clin Nutr, 57 (0000) 904-908.

[11] M.G. Hertog, D. Kromhout, C. Aravanis, H. Blackburn, R. Buzina, F. Fidanza, S. Giampaoli, A. Jansen, A. Menotti, S. Nedeljkovic, et al., Flavonoid intake and long-term risk of coronary heart disease and cancer in the seven countries study, Arch Intern Med, 155 (1995) 381-386.

[12] B.H. Havsteen, The biochemistry and medical significance of the flavonoids, Pharmacology & Therapeutics, 96 (2002) 67-202.

[13] S. Reuter, S.C. Gupta, M.M. Chaturvedi, B.B. Aggarwal, Oxidative stress, inflammation, and cancer: How are they linked?, Free Radical Biology and Medicine, 49 (2010) 1603-1616.

[14] C.-F. Hung, C.-L. Fang, S.A. Al-Suwayeh, S.-Y. Yang, J.-Y. Fang, Evaluation of drug and sunscreen permeation via skin irradiated with UVA and UVB: Comparisons of normal skin and chronologically aged skin, Journal of Dermatological Science, 68 (2012) 135-148.

[15] T. Finkel, N.J. Holbrook, Oxidants, oxidative stress and the biology of ageing, Nature, 408 (2000) 239-247.

[16] G.R.M.M. Haenen, J.B.G. Paquay, R.E.M. Korthouwer, A. Bast, Peroxynitrite Scavenging by Flavonoids, Biochemical and Biophysical Research Communications, 236 (1997) 591-593.

[17] Y.-C. Yang, C.-K. Lii, A.-H. Lin, Y.-W. Yeh, H.-T. Yao, C.-C. Li, K.-L. Liu, H.-W. Chen, Induction of glutathione synthesis and heme oxygenase 1 by the flavonoids butein and phloretin is mediated through the ERK/Nrf2 pathway and protects against oxidative stress, Free Radical Biology and Medicine, 51 (2011) 2073-2081.

[18] P. Yao, A. Nussler, L. Liu, L. Hao, F. Song, A. Schirmeier, N. Nussler, Quercetin protects human hepatocytes from ethanol-derived oxidative stress by inducing heme oxygenase-1 via the MAPK/Nrf2 pathways, Journal of Hepatology, 47 (2007) 253-261.

[19] B. Fuhrman, M. Aviram, Flavonoids protect LDL from oxidation and attenuate atherosclerosis, Current Opinion in Lipidology, 12 (2001).

[20] J. Baumann, F. v. Bruchhausen, G. Wurm, Flavonoids and related compounds as inhibitors of arachidonic acid peroxidation, Prostaglandins, 20 (1980) 627-639.

[21] M. Lindahl, C. Tagesson, Flavonoids as Phospholipase A2 Inhibitors: Importance of Their Structure for Selective Inhibition of Group II Phospholipase A2, Inflammation, 21 (1997) 347-356.

[22] G.M. Raso, R. Meli, G. Di Carlo, M. Pacilio, R. Di Carlo, Inhibition of inducible nitric oxide synthase and cyclooxygenase-2 expression by flavonoids in macrophage J774A.1, Life Sciences, 68 (2001) 921-931.

[23] H.-H. Park, S. Lee, H.-Y. Son, S.-B. Park, M.-S. Kim, E.-J. Choi, T.K. Singh, J.-H. Ha, M.-G. Lee, J.-E. Kim, M. Hyun, T. Kwon, Y. Kim, S.-H. Kim, Flavonoids inhibit histamine release and expression of proinflammatory cytokines in mast cells, Archives of Pharmacal Research, 31 (2008) 1303-1311.

[24] S. Hooshmand, D.Y. Soung, E.A. Lucas, S.V. Madihally, C.W. Levenson, B.H. Arjmandi, Genistein reduces the production of proinflammatory molecules in human chondrocytes, The Journal of Nutritional Biochemistry, 18 (2007) 609-614.

[25] M.P. Nair, S. Mahajan, J.L. Reynolds, R. Aalinkeel, H. Nair, S.A. Schwartz, C. Kandaswami, The Flavonoid Quercetin Inhibits Proinflammatory Cytokine (Tumor Necrosis Factor Alpha) Gene Expression in Normal Peripheral Blood Mononuclear Cells via Modulation of the NF-κβ System, Clinical and Vaccine Immunology, 13 (2006) 319-328.

[26] H. Lim, H. Park, H. Kim, Inhibition of contact dermatitis in animal models and suppression of proinflammatory gene expression by topically applied Flavonoid, Wogonin, Archives of Pharmacal Research, 27 (2004) 442-448.

[27] F.T. Vicentini, T. He, Y. Shao, M.J. Fonseca, W.A. Verri, Jr., G.J. Fisher, Y. Xu, Quercetin inhibits UV irradiation-induced inflammatory cytokine production in primary human keratinocytes by suppressing NF-kappaB pathway, in: J Dermatol Sci, 2011 Japanese Society for Investigative Dermatology. Published by Elsevier Ireland Ltd, Netherlands, 2011, pp. 162-168.

[28] B. Sharma, G. Viswanath, R. Salunke, P. Roy, Effects of flavonoid-rich extract from seeds of Eugenia jambolana (L.) on carbohydrate and lipid metabolism in diabetic mice, Food Chemistry, 110 (2008) 697-705.

[29] S. Sudheesh, G. Presannakumar, S. Vijayakumar, N.R. Vijayalakshmi, Hypolipidemic effect of flavonoids from Solanum melongena, Plant Foods for Human Nutrition, 51 (1997) 321-330.

[30] L. Guerrero, J. Castillo, M. Quiñones, S. Garcia-Vallvé, L. Arola, G. Pujadas, B. Muguerza, Inhibition of Angiotensin-Converting Enzyme Activity by Flavonoids: Structure-Activity Relationship Studies, PLoS ONE, 7 (2012) e49493.

[31] M. Akhlaghi, B. Bandy, Mechanisms of flavonoid protection against myocardial ischemia–reperfusion injury, Journal of Molecular and Cellular Cardiology, 46 (2009) 309-317.

[32] R.J. Gryglewski, R. Korbut, J. Robak, J. Święs, On the mechanism of antithrombotic action of flavonoids, Biochemical Pharmacology, 36 (1987) 317-322.

[33] K. Ishige, D. Schubert, Y. Sagara, Flavonoids protect neuronal cells from oxidative stress by three distinct mechanisms, Free Radical Biology and Medicine, 30 (2001) 433-446.

[34] S.J. Duthie, V.L. Dobson, Dietary flavonoids protect human colonocyte DNA from oxidative attack in vitro, European Journal of Nutrition, 38 (1999) 28-34.

[35] O. Coskun, M. Kanter, A. Korkmaz, S. Oter, Quercetin, a flavonoid antioxidant, prevents and protects streptozotocin-induced oxidative stress and β-cell damage in rat pancreas, Pharmacological Research, 51 (2005) 117-123.

[36] C.F. Lima, M. Fernandes-Ferreira, C. Pereira-Wilson, Phenolic compounds protect HepG2 cells from oxidative damage: Relevance of glutathione levels, Life Sciences, 79 (2006) 2056-2068.

[37] M.L. Manca, I. Castangia, C. Caddeo, D. Pando, E. Escribano, D. Valenti, S. Lampis, M. Zaru, A.M. Fadda, M. Manconi, Improvement of quercetin protective effect against oxidative stress skin damages by incorporation in nanovesicles, Colloids and Surfaces B: Biointerfaces, 123 (2014) 566-574.

[38] P.J. Moulton, Inflammatory joint disease: the role of cytokines, cyclooxygenases and reactive oxygen species, Br J Biomed Sci, 53 (1996) 317-324.

[39] K.A. Gelderman, M. Hultqvist, L.M. Olsson, K. Bauer, A. Pizzolla, P. Olofsson, R. Holmdahl, Rheumatoid arthritis: the role of reactive oxygen species in disease development and therapeutic strategies, Antioxid Redox Signal, 9 (2007) 1541-1567.

[40] A. Vijayalakshmi, G. Madhira, Anti-psoriatic activity of flavonoids from Cassia tora leaves using the rat ultraviolet B ray photodermatitis model, Revista Brasileira de Farmacognosia, 24 (2014) 322-329.

[41] S. Bhagwat, D.B. Haytowitz, J.M. Holden, USDA Database for the Flavonoid Content of Selected Foods Release 3.1, (2013).

[42] A. Saija, M. Scalese, M. Lanza, D. Marzullo, F. Bonina, F. Castelli, Flavonoids as antioxidant agents: Importance of their interaction with biomembranes, Free Radical Biology and Medicine, 19 (1995) 481-486.

[43] N. Arshad, N.K. Janjua, S. Ahmed, A.Y. Khan, L.H. Skibsted, Electrochemical investigations of antioxidant interactions with radical anion and dianion of 1,3-dinitrobenzene, Electrochimica Acta, 54 (2009) 6184-6189.

[44] F. Zsila, Z. Bikádi, M. Simonyi, Probing the binding of the flavonoid, quercetin to human serum albumin by circular dichroism, electronic absorption spectroscopy and molecular modelling methods, Biochemical Pharmacology, 65 (2003) 447-456.

[45] G.S. Borghetti, I.M. Costa, P.R. Petrovick, V.P. Pereira, V.L. Bassani, Characterization of different samples of quercetin in solid-state: indication of polymorphism occurrence, Pharmazie, 61 (2006) 802-804.

[46] F. Bonina, M. Lanza, L. Montenegro, C. Puglisi, A. Tomaino, D. Trombetta, F. Castelli, A. Saija, Flavonoids as potential protective agents against photo-oxidative skin damage, International Journal of Pharmaceutics, 145 (1996) 87-94.

[47] Y. Zheng, I.S. Haworth, Z. Zuo, M.S.S. Chow, A.H.L. Chow, Physicochemical and structural characterization of Quercetin-β-Cyclodextrin Complexes, Journal of Pharmaceutical Sciences, 94 (2005) 1079-1089.

[48] M. Rossi, L.F. Rickles, W.A. Halpin, The crystal and molecular structure of quercetin: A biologically active and naturally occurring flavonoid, Bioorganic Chemistry, 14 (1986) 55-69.

[49] T.-H. Wu, F.-L. Yen, L.-T. Lin, T.-R. Tsai, C.-C. Lin, T.-M. Cham, Preparation, physicochemical characterization, and antioxidant effects of quercetin nanoparticles, International Journal of Pharmaceutics, 346 (2008) 160-168.

[50] P.A. Ruiz, A. Braune, G. Holzlwimmer, L. Quintanilla-Fend, D. Haller, Quercetin inhibits TNF-induced NF-kappaB transcription factor recruitment to proinflammatory gene promoters in murine intestinal epithelial cells, in: J Nutr, United States, 2007, pp. 1208-1215.

[51] J.A. Rothwell, A.J. Day, M.R. Morgan, Experimental determination of octanol-water partition coefficients of quercetin and related flavonoids, J Agric Food Chem, 53 (2005) 4355-4360.

[52] P.C.H. Hollman, J.M.P. van Trijp, M.N.C.P. Buysman, M.S. v.d. Gaag, M.J.B. Mengelers, J.H.M. de Vries, M.B. Katan, Relative bioavailability of the antioxidant flavonoid quercetin from various foods in man, FEBS Letters, 418 (1997) 152-156.

[53] M. Russo, C. Spagnuolo, I. Tedesco, S. Bilotto, G.L. Russo, The flavonoid quercetin in disease prevention and therapy: Facts and fancies, Biochemical Pharmacology, 83 (2012) 6-15.

[54] Y. Guo, R.S. Bruno, Endogenous and exogenous mediators of quercetin bioavailability, J Nutr Biochem, 26 (2015) 201-210.

[55] C.-F. Lin, Y.-L. Leu, S.A. Al-Suwayeh, M.-C. Ku, T.-L. Hwang, J.-Y. Fang, Anti-inflammatory activity and percutaneous absorption of quercetin and its polymethoxylated compound and glycosides: The relationships to chemical structures, European Journal of Pharmaceutical Sciences, 47 (2012) 857-864.

[56] L. Montenegro, C. Carbone, C. Maniscalco, D. Lambusta, G. Nicolosi, C.A. Ventura, G. Puglisi, In vitro evaluation of quercetin-3-O-acyl esters as topical prodrugs, International Journal of Pharmaceutics, 336 (2007) 257-262.

[57] M. Sun, S. Nie, X. Pan, R. Zhang, Z. Fan, S. Wang, Quercetin-nanostructured lipid carriers: characteristics and anti-breast cancer activities in vitro, Colloids Surf B Biointerfaces, 113 (2014) 15-24.

[58] G. Sharmila, F.A. Bhat, R. Arunkumar, P. Elumalai, P. Raja Singh, K. Senthilkumar, J. Arunakaran, Chemopreventive effect of quercetin, a natural dietary flavonoid on prostate cancer in in vivo model, Clinical Nutrition, 33 (2014) 718-726.

[59] H. Zhang, M. Zhang, L. Yu, Y. Zhao, N. He, X. Yang, Antitumor activities of quercetin and quercetin-5′,8-disulfonate in human colon and breast cancer cell lines, Food and Chemical Toxicology, 50 (2012) 1589-1599.

[60] M.-T. Sung, Y.-C. Chen, C.-W. Chi, Chapter 22 - Quercetin's Potential to Prevent and Inhibit Oxidative Stress-Induced Liver Cancer, in: V. Preedy (Ed.) Cancer, Academic Press, San Diego, 2014, pp. 231-239.

[61] S.S. Karuppagounder, S.K. Madathil, M. Pandey, R. Haobam, U. Rajamma, K.P. Mohanakumar, Quercetin up-regulates mitochondrial complex-I activity to protect against programmed cell death in rotenone model of Parkinson's disease in rats, Neuroscience, 236 (2013) 136-148.

[62] A.M. Sabogal-Guáqueta, J.I. Muñoz-Manco, J.R. Ramírez-Pineda, M. Lamprea-Rodriguez, E. Osorio, G.P. Cardona-Gómez, The flavonoid quercetin ameliorates Alzheimer's disease

pathology and protects cognitive and emotional function in aged triple transgenic Alzheimer's disease model mice, Neuropharmacology, 93 (2015) 134-145.

[63] C. Gardi, K. Bauerova, B. Stringa, V. Kuncirova, L. Slovak, S. Ponist, F. Drafi, L. Bezakova, I. Tedesco, A. Acquaviva, S. Bilotto, G.L. Russo, Quercetin reduced inflammation and increased antioxidant defense in rat adjuvant arthritis, Archives of Biochemistry and Biophysics, 583 (2015) 150-157.

[64] X. Jin, R. Su, R. Li, L. Song, M. Chen, L. Cheng, Z. Li, Amelioration of particulate matter-induced oxidative damage by vitamin c and quercetin in human bronchial epithelial cells, Chemosphere, 144 (2016) 459-466.

[65] H. Liu, X. Guo, Y. Chu, S. Lu, Heart protective effects and mechanism of quercetin preconditioning on anti-myocardial ischemia reperfusion (IR) injuries in rats, Gene, 545 (2014) 149-155.

[66] K. Gomathi, D. Gopinath, M. Rafiuddin Ahmed, R. Jayakumar, Quercetin incorporated collagen matrices for dermal wound healing processes in rat, Biomaterials, 24 (2003) 2767-2772.

[67] R. Casagrande, S.R. Georgetti, W.A. Verri Jr, D.J. Dorta, A.C. dos Santos, M.J.V. Fonseca, Protective effect of topical formulations containing quercetin against UVB-induced oxidative stress in hairless mice, Journal of Photochemistry and Photobiology B: Biology, 84 (2006) 21-27.

[68] N. Miyamoto, H. Izumi, A. Tawara, K. Kohno, Chapter 10 - Quercetin and Glaucoma, in: V.R. Preedy (Ed.) Handbook of Nutrition, Diet and the Eye, Academic Press, San Diego, 2014, pp. 97-103.

[69] D. Bądziul, J. Jakubowicz-Gil, E. Langner, W. Rzeski, K. Głowniak, A. Gawron, The effect of quercetin and imperatorin on programmed cell death induction in T98G cells in vitro, Pharmacological Reports, 66 (2014) 292-300.

[70] P. Ramyaa, R. krishnaswamy, V.V. Padma, Quercetin modulates OTA-induced oxidative stress and redox signalling in HepG2 cells — up regulation of Nrf2 expression and down regulation of NF-κB and COX-2, Biochimica et Biophysica Acta (BBA) - General Subjects, 1840 (2014) 681-692.

[71] E.U. Graefe, J. Wittig, S. Mueller, A.-K. Riethling, B. Uehleke, B. Drewelow, H. Pforte, G. Jacobasch, H. Derendorf, M. Veit, Pharmacokinetics and Bioavailability of Quercetin Glycosides in Humans, The Journal of Clinical Pharmacology, 41 (2001) 492-499.

[72] A. Robaszkiewicz, A. Balcerczyk, G. Bartosz, Antioxidative and prooxidative effects of quercetin on A549 cells, Cell Biology International, 31 (2007) 1245-1250.

[73] M. Morille, T. Montier, P. Legras, N. Carmoy, P. Brodin, B. Pitard, J.-P. Benoît, C. Passirani, Long-circulating DNA lipid nanocapsules as new vector for passive tumor targeting, Biomaterials, 31 (2010) 321-329.

[74] X. Chen, T.J. Young, M. Sarkari, R.O. Williams, 3rd, K.P. Johnston, Preparation of cyclosporine A nanoparticles by evaporative precipitation into aqueous solution, Int J Pharm, 242 (2002) 3-14.

[75] J. Junghanns, R.H. Muller, Nanocrystal technology, drug delivery and clinical applications, in: Int J Nanomedicine, 2008, pp. 295-310.

[76] R.H. Müller, C.M. Keck, Second generation of drug nanocrystals for delivery of poorly soluble drugs: smartCrystal technology, European Journal of Pharmaceutical Sciences, 34 (2008) S20-S21.

[77] S. Hirsjarvi, C. Belloche, F. Hindre, E. Garcion, J.P. Benoit, Tumour targeting of lipid nanocapsules grafted with cRGD peptides, Eur J Pharm Biopharm, 87 (2014) 152-159.

[78] M. Khalid, P. Simard, D. Hoarau, A. Dragomir, J.-C. Leroux, Long Circulating Poly(Ethylene Glycol)-Decorated Lipid Nanocapsules Deliver Docetaxel to Solid Tumors, Pharmaceutical Research, 23 (2006) 752-758.

[79] V.P. Torchilin, Recent advances with liposomes as pharmaceutical carriers, Nat Rev Drug Discov, 4 (2005) 145-160.

[80] B. Heurtault, P. Saulnier, J.P. Benoit, J.E. Proust, B. Pech, J. Richard, Lipid nanocapsules, preparation method and use as medicine, in, Google Patents, 2001.

[81] C.E. Mora-Huertas, H. Fessi, A. Elaissari, Polymer-based nanocapsules for drug delivery, International Journal of Pharmaceutics, 385 (2010) 113-142.

[82] J. Pardeike, A. Hommoss, R.H. Müller, Lipid nanoparticles (SLN, NLC) in cosmetic and pharmaceutical dermal products, International Journal of Pharmaceutics, 366 (2009) 170-184.

[83] S. Benita, B.H.L. Böhm, Emulsions and nanosuspensions for the formulation of poorly soluble drugs, CRC Press, 1998.

[84] E. Merisko-Liversidge, G.G. Liversidge, E.R. Cooper, Nanosizing: a formulation approach for poorly-water-soluble compounds, European Journal of Pharmaceutical Sciences, 18 (2003) 113-120

Literature review of quercetin topical application

Goals:

Quercetin physiological activities on the skin

Quercetin antioxidant activity

Quercetin antiinflammatory activity

Quercetin anti-ageing and rejuvenating activity

Quercetin in wound healing

Quercetin conventional dosage forms

Quercetin nanodosage forms

Literature review of quercetin topical application

Preface

In the following chapter, quercetin topical applications will be discussed in two parts. It was submitted as review in European Journal of Pharmaceutics and Biopharmaceutics in May, 2016 (under review).

The first part will present a detailed revision of literature about quercetin potential activities on skin. This section will discuss quercetin antioxidant activity and the experimental determination of this activity *in vitro*, on cellular level and *in vivo* on animals. Then, quercetin antiinflammatory activity with proven mechanism of action on skin. Afterwards, quercetin in wound healing and its beneficial impact for a successful healing of injuries and wounds. Finally, we will discuss on quercetin effects on skin ageing and its potential in rejuvenation of skin tissue.

The second part of this chapter will present quercetin formulations intended for the topical route of administration and gives special emphasis on the skin penetration tests performed on these formulations. The section will cover conventional dosage forms such as emulsions with the results related to quercetin penetration enhancement. Afterwards, a detailed literature revision will present quercetin novel nanoformulations with a discussion of their main physicochemical features along with their skin penetration results. The skin penetration results are grouped in order to facilitate the comparison between nanoformulations. The groups are: skin penetration tests performed on pig skin, on rodent skin and finally on human skin.

Quercetin topical application, from conventional dosage forms to nanodosage forms

T. Hatahet[a], M. Morille[a], A. Hommoss[b], R. H. Müller[b] and S. Bégu[a*]

[a] Institut Charles Gerhardt Montpellier, UMR 5253 CNRS-ENSCM-UM, Equipe Matériaux Avancés pour la Catalyse et la Santé, 8 rue de l'Ecole Normale, 34296 Montpellier Cedex 5, France.

[b] Institute of Pharmacy, Department of Pharmaceutics, Biopharmaceutics and NutriCosmetics, Free University of Berlin, Kelchstr. 31, Berlin 12169, Germany.

[*] Corresponding author.

Research article submitted to the

European Journal of Pharmaceutics and Biopharmaceutics

Volume 108, November 2016, Pages 41–53

doi.org/10.1016/j.ejpb.2016.08.011

Abstract

Skin is a multifunctional organ with activities in protection, metabolism and regulation. Skin is in a continuous exposure to oxidizing agents and inflammogens from the sun and from the contact with the environment. These agents may overload the skin auto-defense capacity. To strengthen skin defense mechanisms against oxidation and inflammation, supplementation of exogenous antioxidants is a promising strategy. Quercetin is a flavonoid with both very pronounced effective antioxidant and antiinflammatory activities, and thus a candidate of first choice for such skin supplementation. Quercetin showed interesting actions in cellular and animal based models, ranging from protecting cells from UV irradiation to support skin regeneration in wound healing. However, due to its poor solubility, quercetin has limited skin penetration ability, and various formulations approaches were taken to increase its dermal penetration. In this article, the quercetin antioxidant and antiinflammatory activities in wound healing and supporting skin against ageing are discussed in detail. In addition, quercetin topical formulations from conventional emulsions to novel nanoformulations in terms of skin penetration enhancement are also presented. This article gives a comprehensive review of quercetin for topical application from biological effects to pharmaceutical formulation design for the last 25 years of research.

Key words

Quercetin, antioxidant activity, antiinflammatory activity, wound healing, skin antiaging, in vitro skin penetration, in vivo skin penetration, Franz cells.

Quercetin topical application

Graphical abstract

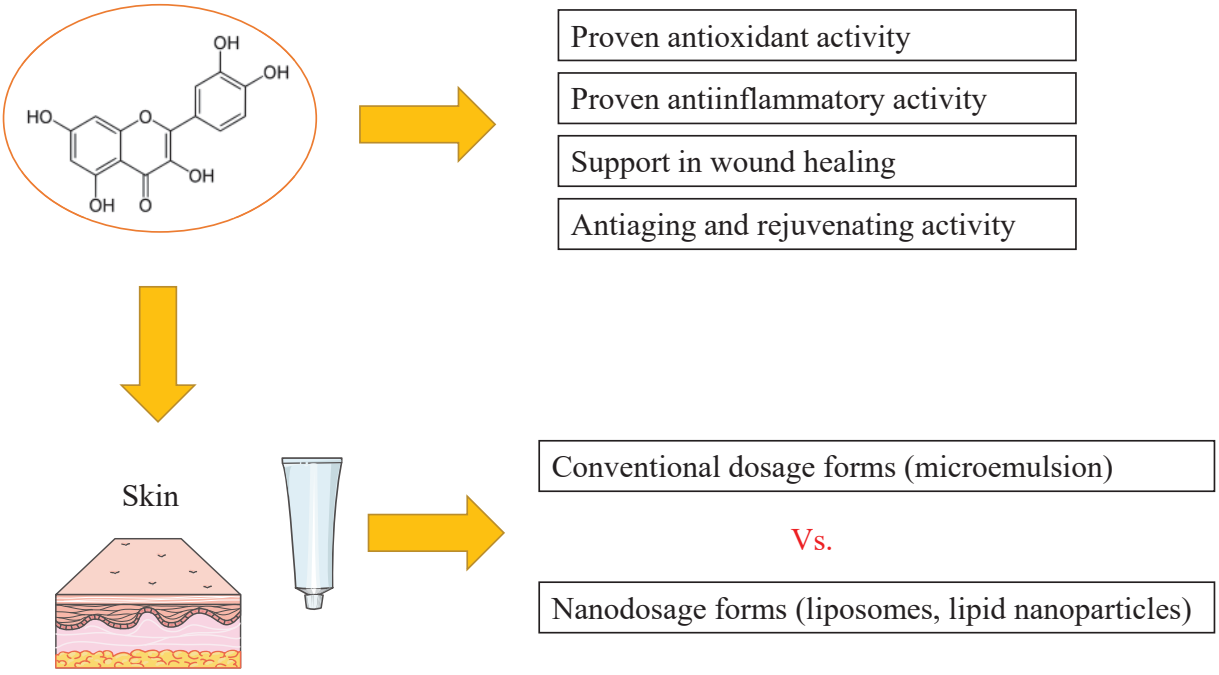

1. Introduction

Skin is the largest organ of the human body, which secures the internal homeostasis and regulates the temperature of the body. Besides that, skin has barrier function, it prevents germs from passing into internal organs, protects human body from exogenous pollutants and oxidizing agents like radiation and corrosive materials. As a result, skin is continuously exposed to oxidants and inflammogens. Even if skin possesses several antioxidative systems to withstand external oxidation sources. However, in case that oxidative stress is superior to the defense mechanism of skin, skin damage can occur [1, 2].

Supporting skin defense mechanisms by exogenous antioxidants is a promising strategy. Antioxidants like Coenzyme Q10 [3, 4], vitamin C [5], ß-carotene [6, 7] and polyphenols [8, 9] were tested to evaluate their benefits on skin. Among them, flavonoids, which are strong polyphenolic antioxidants, are potential good candidates. They are plant pigments found in several fruits and vegetables like apples [10], onions [11] and peas [12]. With the presence of several hydroxyl groups on their structures, quercetin is the strongest antioxidant among flavonoids and the most common in nature [13]. At the same time, quercetin has the broadest antiinflammatory activity compared to apigenin, morin, (-)-epicatechin and biochanin A [14]. In spite of these promising activities, quercetin suffers from poor water solubility and inability to penetrate skin (Table 1) [15]. Quercetin shows water solubility less than 0.5 µg/ml and higher solubility in polar organic solvents (2 mg/ml in ethanol) [16-18]. Quercetin also has a partition coefficient of 1.82 ± 0.32 due to the presence of nonpolar groups in its structure [19]. But despite of this log P, quercetin polar hydroxyl groups hinder its skin penetration capacity [13]. Focusing on topical delivery from formulation approach, the use of nanoformulations with therapeutic agents such as linoleic acid within ethosomes and transfersomes [20], paclitaxel-loaded within ethosomes [21] and asiaticoside in ultradeformable vesicles [22] showed to enhance their topical delivery. This is linked to nanoformulation characteristics such as their lipid nature and their small particle size along with their elasticity that facilitate their deep penetration. The presence of ethanol conferred higher skin penetration for encapsulated molecules compared to liposomes, the rigid nature of liposomal bilayer is fluidized by the ethanol presence that facilities ethosomes penetration.

Quercetin topical application

Consequently, quercetin is also formulated within several nanoformulations in order to enhance topical drug delivery [23, 24].

Quercetin physicochemical properties	**Values**
Chemical structure	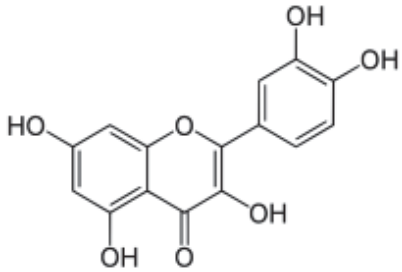
Molecular Formula	$C_{15}H_{10}O_7$
Molecular weight	302.2 g/mol
Chemical name (IUPAC)	2-(3,4-dihydroxyphenyl)-3,5,7-trihydroxychromen-4-one
Solubility in MilliQ water	0.48 ± 0.1 µg/ml [16]/
Solubility in PBS pH 3	0.44 ± 0.1 µg/ml [18]
Solubility in DMSO	30 mg/ml [17]
Solubility in ethanol	2 mg/ml [17]
Partition coefficient (log P)	1.82 ± 0.3 [19]
Polymorphism	Three polymorphic forms [25]

Table 1: Quercetin main physicochemical parameters

Quercetin partition coefficient is determined experimentally.

In this paper, recent studies on quercetin skin activities from *in vitro* models to *in vivo* animal studies will be presented. Then, formulation strategies followed to overcome quercetin limited water solubility and to increase its stability in formulation will be discussed. The effect of formulating quercetin in conventional dosage forms to enhance its skin penetration capacity will be explored. Finally, recent nanoformulations of quercetin and their potential as novel strategy for quercetin skin delivery will be discussed.

2. Quercetin physiological activities on skin

2.1. Quercetin antioxidant activity

Skin is the largest organ in the human body exposed to oxidizing agents from environment such as solar radiation (visible/UV) and chemicals (xenobiotic). These environmental pollutants can induce oxidative stress to skin tissue either directly or indirectly by the generation of reactive oxygen species (ROS). Skin tissue contains several defense mechanisms for the prevention or inception of oxidative stress and for the initiation of cellular repair afterwards. Skin has many mechanisms to prevent the formation of free radicals. For example (i) metallothionein, present in cutaneous tissue, chelates metal ions, has a great importance in controlling free radical generating reactions; (ii) the increase of melanin production upon exposure to UV radiation. For the oxidative damage control, skin also has endogenous mechanisms based on two categories: nonenzymatic and enzymatic. Among nonenzymatic mechanisms, small molecular size antioxidants such as glutathione (GSH), α-tocopherol, carotenoids and oxycarotenoids found in skin cells, are molecules able of both neutralizing free radicals as well as relocalizing radical damaging functions from sensitive targets (as an example from lipid membrane to cytosol). Enzymatic activities depend on molecules such as superoxide dismutase, catalase and glutathione peroxidase. These enzymes serve as a backup for the regeneration of consumed antioxidants, like in the replenishment of GSH by glutathione disulfide (GSSG) reductase, as well as for the elimination of reactive compounds, such as the transfer system for glutathione S-conjugates [26].

Quercetin antioxidant activity will be explored in three parts. The first part will take into consideration all the chemical assays used to determine quercetin activity *in vitro*. Then, a second part will deal with quercetin activities tested at the cellular level, and the molecular mechanism underlining quercetin potentials. Finally, animal-based studies regarding quercetin protection to

cutaneous tissue after its exposure to oxidative stress stimulators such as UV irradiation will be reviewed.

2.1.1. *In vitro* antioxidant activity (chemical tests)

In vitro tests for antioxidant activity provide information about the antioxidant activity of quercetin without the need for complex cellular based assays. They can ensure quercetin activity from batch to batch and can be set as routine analysis. Three aspects can be investigated *in vitro*. (i) Hydrogen donating activity can be measured with 2,2-diphenyl-1-picrylhydrazyl (DPPH assay) [27]. (ii) Superoxide anion formation inhibition and scavenging activity can both be quantified by means of xanthine oxidase and cytochrome C assays [28]. (iii) Metal chelating activity can be determined using metal specific methods [29]. Finally antioxidants can inhibit the peroxidation of unsaturated lipids, thus antilipoperoxidative activity can be analyzed using the colorimetric detection of thiobarbituric acid reactive species (TBARS) by a reaction mediated by Fe^{2+}/Citrate [30]. In 2006 Casagrande *et al.* [31] evaluated iron-chelating activity of 4 µg/ml quercetin solution. Quercetin chelated 65% of total iron within 15 minutes contact time. This is in agreement with the fact that quercetin presents two sites for chelating bivalents metals: 5-OH and 4-oxo group or between the 3′- and 4′-OH groups (Table 1) [32]. On the other hand, Casagrande *et al.* determined the functional stability of crude quercetin and formulated quercetin in emulsions for topical application. Antilipoperoxidative activity was tested during six months at four storage temperatures 4°C, room temperature, 37°C and 45°C. Rat liver mitochondria were used as unsaturated lipid source for the lipid peroxidation assay. Initially crude quercetin presented 65.6% antilipoperoxidative activity, while 0.05 % quercetin loaded within nonionic cream (high lipid content) and anionic gel cream (low lipid content) had 78%, and 70%, respectively. Upon storage, a higher loss of activity was observed in formulation with low lipid content especially at low temperatures. This may be attributed to precipitation of quercetin out from lipidic environment where lipids are in more packed conformation. Keeping in mind the lipophilic nature of quercetin rings, the more lipophilic the environment is for quercetin the better it is stabilized (Table 2). In 2007, the same group studied the antilipoperoxidative activity of quercetin in more detail [33]. The same nonionic cream and anionic gel cream formulations were compared to crude quercetin in terms of antioxidative stability during 6 months storage using DPPH test. Initial activity was 41.6 %, 37.8 %, and 38.5 % for crude quercetin, nonionic cream and anionic gel cream, respectively. The activity was

preserved during the whole storage period. Afterwards skin retention of the formulated quercetin was monitored in terms of antilipoperoxidative activity on pig's skin mounted on Franz cell for 12 hours. Anionic gel cream with lower lipid content showed higher drug release and consequently higher skin retention and antilipoperoxidative activity (25.0 %) at 3 hours interval. While nonionic cream with higher lipid content, showed a gradual release and with slight accumulation in skin and presented highest antilipoperoxidative activity (54.0 %) after 12 hours. This is in agreement with their previous report, that higher lipid content confers higher protection for quercetin activity, this time proven *in vitro* on pig's skin.

Wu *et al.* in 2008 [34] prepared quercetin in polymeric nanoparticles (Table 4). Quercetin was added to polyvinyl alcohol (PVA) and Eudragit® E at a ratio of 1:10:10 respectively. The nanoparticles, prepared by nanoprecipitation, presented a mean diameter of 82 nm with a polydispersity index (PDI) of 0.22; PDI shows how broad the particles size distribution is. Quercetin encapsulation efficiency was 99.9 %. Quercetin nanoparticles were compared to quercetin-DMSO and quercetin-water in terms of DPPH activity, anti-superoxide formation, superoxide anion-scavenging activity and antilipoperoxidative activity. In all tests, quercetin nanoparticles showed scavenging concentration (SC50) and inhibitory concentration (IC50) (the concentration to cause 50 % effect in respect to each test) close to quercetin-DMSO proving the preservation of quercetin activity after formulation (Table 2). Quercetin-water was hundred times less effective than quercetin nanoparticles and quercetin-DMSO. This may be explained by the fact that all the tests request the antioxidant molecules to be soluble in the reaction medium, as a result suspended quercetin in water will be very weak compared to solubilized quercetin in DMSO or to nanoparticles. The second potential explanation may be due to the influence of the surface area of reacting quercetin, which is greater in the nanoparticles than in the larger suspended crude format. This confers higher reactivity for the nanoparticles compared to quercetin-water. Finally, the small size of formulated nanoparticles below 100 nm (82 nm) enabled to retain the activity of quercetin to values close to the solubilized form in DMSO.

2.1.2. *In vitro* antioxidant activity of quercetin (cellular evaluation)

Antioxidant actions are not limited to ROS scavenging abilities but also include the modulation of endogenous (antioxidant, detoxifying) enzymes. The evaluation of antioxidants at cellular level can be done by two different approaches. The first approach is a cellular antioxidant activity assay

(CAA) used to evaluate the antioxidant activity of plant extracts and food supplements. It is based on the detection of ROS (such as hydrogen peroxide) inside the cell by reaction of these reactive species with the redox sensor dihydrodichlorofluorescein ($DCFH_2$). In this reaction, $DCFH_2$ oxidizes to fluorescent dichlorofluorescein (DCF). However, this method lacks the specificity to ROS generated in response to oxidative attacks [35]. The second approach is the evaluation of endogenous enzymes, like the upregulation of the expression of antioxidants enzymes, or the inhibition of prooxidant enzymes. As our main scope is quercetin and its skin penetration in formulation, we keep the more detailed review articles to give further information about antioxidants cellular tests for example in the publication of López-Alarcón *et al.* [36].

All biological investigations on formulated quercetin started from the concept that to test an antioxidative activity, a source of oxidation is required. As quercetin activity is of high interest in skin diseases related to phototoxicity, researchers tested quercetin activity to compensate UV irradiation damage.

Quercetin cellular actions were evaluated as crude material on human fibroblasts and kératinocytes (NHEK) [37] and in formulations on normal human keratinocytes (HaCaT) [23, 38]. The treatment with 50 µM of crude quercetin protected human keratinocytes and human fibroblast from intoxication by 500 µM buthionine sulfoximine. Keratinocytes viability increased by 2.3 fold (Table 2). However, this cytoprotective activity was not related to an increase in the intracellular glutathione (GSH), as quercetin was not able to reestablish the depleted GSH due to cellular intoxication [37]. Quercetin was formulated into liposomes by Liu *et al.* [23] and Manca *et al.*.[38] with different excipients. Liu *et al.* [23] suggested formulation of quercetin deformable liposomes with Tween® 80 as edge activator (Table 4). Cells were irradiated with a UVB dose of 0.02 J/cm^2 and treated with 25 µg/ml quercetin liposomes 16 hours before irradiation and 24 hours or 48 hours post irradiation. Then, cell viability was determined by MTT assay. UVB exposed cells without quercetin treatment decreased in viability from 65.7 ± 7.8 % at 24 h to 42.5 ± 6.5 % at 48 h. While quercetin in both control solution and liposomal formulation was capable of cells protection. Cell viability was 76.2 ± 4.3 % at 24 h and 59.5 ± 3.8 % at 48 h for quercetin in solution and 89.9 ± 4.5 % at 24 h and 78.8 ± 3.2 % at 48 h for liposomal quercetin (Table 2). Furthermore, Liu *et al.* proved that quercetin was able to attenuate ROS generation in cells exposed to UVB and showed the antilipoperoxidative activity of quercetin on cells. Quercetin also decreased the concentration of malondialdehyde from 10.98 nmol/mg protein in non-treated UVB exposed cells to 3.14 nmol/mg

for treated UVB exposed cells (Table 2) [23]. Manca *et al.* [38] tested another quercetin liposomal formulation and compared it to glycerosomes (glycerol containing liposomes) (Table 4) on HaCaT cells with hydrogen peroxide. Quercetin liposomes and glycerosomes were also able to protect keratinocytes in culture from the damaging effect of hydrogen peroxide. Consequently, viable cells increased from 26.0 ± 9.0 % in non-treated H_2O_2 exposed cells to 68.0 ± 4.0 % and 67.0 ± 6.0 % in the liposomes and glycerosomes group, (Table 2). This result was explained by a better cellular uptake with both nanoformulations compared to crude quercetin. The enhanced cellular internalization with liposome may be due to the fusion with plasma membrane or pinocytosis [39]. The pinocytosis of liposomal formulation with the cell membrane enables the release of liposomes contents directly into the cytoplasm avoiding the potential passage by the lysosomal apparatus. In case of liposomal destabilization during the cell membrane fusion [40], the released drug can pass by micropinocytosis.

2.1.3. *In vivo* antioxidant activity assays of quercetin in animals

Referring back to cellular assays (section 2.1.2), the concept of having a source of oxidation is presumed. Hairless mice were exposed to UV irradiation, and then skin health parameters such as Transepidermal water loss (TEWL) and erythema were assessed upon exposure to UV. For further details, Hung *et al.* defined the damaging effect of UV irradiation on mice stratum corneum [41]. Skin histological analysis were then performed and quercetin protective effect on skin was determined. Quercetin activity was demonstrated by quantification of endogenous antioxidant enzymes before and after exposure and without or with quercetin treatment. Two publications investigated the protective effect of quercetin *in vivo* on mice's skin [42, 43]. Both applied UVB to dorsal skin of hairless mice from 20 cm above the table where mice were placed. Quercetin was formulated in emulsions in both publications and applied three times: 60 min and 5 min before irradiation and directly after irradiation.

In 2006, Casagrande *et al.*[42] compared quercetin nonionic emulsion (formulation 1 = high lipid content) and quercetin anionic emulsion (formulation 2 = low lipid content). In this study, reduced glutathione GSH (nmol) per mg of skin homogenate was detected after a dose of 2.46 J/cm^2 by fluorescence assay using o-phthalaldehyde. Quercetin containing formulations were applied topically at a dose of 5 mg. Quercetin showed higher activity in emulsion containing higher lipid content (formulation 1) than in anionic emulsion (formulation 2). Both formulations inhibited the

Quercetin topical application

UVB irradiation-induced depletion of GSH (50 nmol/mg skin in the UV group *vs* 140 nmol/mg formulation 1 and 60 nmol/mg formulation 2). However, only in the formulation 1 treated group the GSH activity returned to non-irradiated control levels (125 nmol/mg). Myeloperoxidase (MPO) activity in irradiated skin can be related to the presence of immune cells (neutrophils) and hence can be a good marker for skin inflammation. Hairless mice were exposed to a dose of 1.23 J/cm^2 then the number of total leukocytes per mg of skin was determined. Again, both formulations inhibited the MPO activity increase and hence the neutrophil migration. However, only formulation 1 was able to reestablish control levels (Table 3). Lastly, qualitative analyses of skin proteinases by substrate-embedded enzymography showed that formulations containing quercetin were capable of inhibition of secretion / activity of proteinase in skin tissue. The results observed by Casagrande *et al.* were further supported by the work of Vicentini *et al.* in 2008 [43]. 3 mg of quercetin were applied topically on the dorsal skin from a water in oil (w/o) microemulsion and 2.87 J/cm^2 UVB dose was used for GSH depletion. Quercetin-loaded w/o microemulsion maintained GSH levels near to the ones in untreated–unexposed controls (90 nmol/mg vs. 100 nmol/mg control) (Table 2). Determination of skin proteinases by SDS–PAGE enzymography showed that quercetin-loaded w/o microemulsion regenerated the inhibition of proteinase secretion/activity increase induced by UVB irradiation. However, quercetin-loaded w/o microemulsion failed to confer protection against UV-induced skin reddening *in vivo*. These *in vivo* studies proved that is promising to apply quercetin topically to skin for antioxidative protective effects. Nonetheless, skin penetration and permeation should be carefully controlled to gain sufficient quercetin protective actions on skin tissue and to avoid its side effects in the systemic circulation.

Quercetin topical application

Test type	*In vitro* chemical assay		*In vitro* cellular assay		*In vivo* animal assay	
	Method	**Result**	**Method**	**Result**	**Method**	**Result**
Antilipoperoxidative activity	Thiobarbituric acid reactive species (TBARS)	65.6% antilipoperoxidative activity [31] IC50 for quercetin 77.17 ± 9.98 g/ml [34]	N-methyl-2-phenylindole (HaCaT cells)	3 fold decrease in MDA concentration [23]	TBARS (mice)	1.6 fold decrease in MDA concentration [44]
Anti-superoxide formation	Xanthine oxidase	IC50 = 5.31 ± 0.12 g/ml [34]	N/A	N/A	N/A	N/A
Superoxide anion-scavenging activity	Cytochrome c	SC50 = 1.59 ± 0.6 g/ml [34]	superoxide dismutase (SOD)-inhibitable reduction of ferricytochrome c (neutrophils	IC50 = 3.82 ± 0.45 µM [45]	O-phthalaldehyde fluorescent assay	3 fold increase in glutathione (mice) [42] 2.5 fold increase in glutathione (mice) [43]
					Superoxide dismutase	6 fold decrease in its concentration (rats) [46]
					Reduced glutathione	1.5 fold increase in concentration (mice) [44]
Hydrogen donating ability	DPPH	SC50 = 4.2 4 ± 0.48 g/ml [34]	Hydrogen peroxide (HaCaT)	2.5 fold increase in cell viability [38]	Catalase content	1,3 fold increase in catalase content (rats) [46]
			buthionine sulfoximine (NHEK)	2.3 fold increase in cell viability [37]		
			UVB irradiation (HaCaT)	1.2 – 1.4 fold increase in cell viability [23]		

Table 2: Tests related to quercetin antioxidant activity.

Quercetin topical application

Three levels of assay can be performed to validate quercetin antioxidant activity:

(i) The *in vitro* chemical assays include thiobarbituric acid reactive species (TBARS) for antilipoperoxidative activity, xanthine oxidase for anti-superoxide formation activity, cytochrome C for superoxide anion-scavenging activity and di(phenyl)-(2,4,6-trinitrophenyl)iminoazanium (DPPH) for hydrogen donating activity.

(ii) The *in vitro* cellular assays include the detection of malondialdehyde (MDA) using n-methyl-2-phenylindole on HaCaT cells. The inhabitable reduction of reduction of ferricytochrome C by superoxide dismutase on neutrophils. Finally, the increase in cellular viability after the intoxication of keratinocytes by hydrogen peroxide.

(iii) The *in vivo* animal assays include the detection of TBARS, superoxide dismutase, glutathione, reduced glutathione and catalase content on mice or rats.

2.2. Quercetin antiinflammatory activity

Inflammation is a protective response to localized injury. It can be due to physical causes such as trauma, chemical by a corrosive substance, and / or biological like stress. Inflammatory response may be also an effect of an autoimmune diseases like psoriasis [47]. As evocated in the last section, inflammation is closely linked to oxidation and hence to UV irradiation. UV exposure causes the initiation and propagation of reactive oxygen species and hence induces oxidative stress damage. Oxidative stress activates several inflammatory associated signal transduction pathways in cells [48]. Among these pathways is nuclear factor-kappa B (NF-κB) [49], known for its ambiguous role in cytokine production and modulation of immune response [50]. Here comes the advantage of using quercetin as inhibitor on this pathway. Quercetin proved to inhibit (i) the recruitment of NF-κB transcription factor to proinflammatory gene promoters by tumor necrosis factor (TNF), (ii) hydrogen peroxide (H_2O_2)-induced NF-κB DNA binding activity and consequently DNA damage [51, 52]. Quercetin inhibitory activity of NF-κB was detected on human hepatoma cells [53] and more recently on primary human keratinocytes [54].

Quercetin antiinflammatory activity was compared to several flavonoids, such as apigenin, morin, (-)-epicatechin and biochanin A and to a non-steroidal antiinflammatory drug (indomethacin). Indeed quercetin was the strongest antiinflammatory flavonoid against mice ear edema [14]. Quercetin was administered orally at a dose of 2 mg/mouse dissolved in 0.5 % Tween® 80 one hour before the topical application of the inflammogens (2 % cotton oil or 2% arachidonic acid) on the ear. For testing a possible activity via topical route 25 µl of 2 mg quercetin dissolved in acetone were applied to ear's skin and 30 minutes later, the same inflammogens were applied. After five hours, ear thickness was measured (inhibition percent of ear's edema was calculated) and compared to the control group treated with vehicle and inflammogens only. For the oral route, control groups ear thicknesses were 0.22 and 0.27 mm with cotton oil and arachidonic acid, respectively, and 0.14 and 0.13 mm with indomethacin treatment. Quercetin was the flavonoid with highest ear edema inhibition capacity with 0.16 and 0.21mm. The same was observed with topical administration of flavonoids. Quercetin diminished edema thickness from 0.25 mm with both inflammogens to 0.19 and 0.12 mm compared to indomethacin 0.14 and 0.05 mm with cotton oil and arachidonic acid, respectively. The skin penetration of crude quercetin here may be attributed to the destruction of barrier function with solvent (acetone). Quercetin proved to possess broad antiinflammatory activities

[14]. Knowing that quercetin presents the lowest skin permeability compared to its polymethoxylated compounds and glycosides, it is the most powerful inhibitor of O_2^- generation (by neutrophils) *in vitro* with an IC50 of 3.82 ± 0.45 μM compared to 5.34 ± 0.28 μM for rutin and 5.80 ± 0.67 μM for quercetin 3,5,7,30,40-pentamethylether (QM) (Table 2). This high antiinflammatory capacity was further confirmed by testing elastase release due to degranulation of azurophilic granules form neutrophils. Quercetin was five times more powerful than its glycoside (rutin) (Table 3). Even though rutin presented 2.5 fold increase in flux through nude mouse skin mounted on Franz cell, rutin showed a degree of skin irritation with higher erythema values over the control group [55].

Vicentini *et al.* investigated the mechanism underling quercetin antiinflammatory actions in 2011 [54]. Quercetin showed 80 % inhibition of interleukin 1β mRNA (IL-1β mRNA) at a dose of 20 μg/ml in methanol when primary human keratinocytes were exposed to UVB (0.05 J/cm^2). Quercetin pretreatment also suppressed induction of IL-6, IL-8, and TNF-α in exposed cells measured by real-time quantitative RT-PCR. Furthermore, quercetin pretreatment inhibited UV irradiation-induced NF-kB DNA binding activity by approximately 80 % (Table 3). This result presents the applicability of quercetin in protection against solar irradiation and the benefit effects of introducing it in novel sunscreens. However, quercetin also inhibited IL-1β activation of NF-kB and induction of cytokine expression. This indicates that quercetin inhibition of cytokine induction is not UV irradiation specific. Therefore, these results highlight other applicability of quercetin in other skin disease like psoriasis [54, 56, 57]. It is worth to note that quercetin activity on the inhibition of NF-kB is cell and stimulation specific for example quercetin did not inhibit TNF-α-induced NF-kB transcriptional activity on murine small intestinal epithelial cell (IEC) line Mode-K [51].

In 2014, Caddeo *et al.* formulated quercetin in liposomes and PEVs (Penetration Enhancer-containing Vesicles) (Table 4). Then, they tested quercetin antiinflammatory activity *in vivo* on the back skin of female mice. The inhibitory effect of vesicular quercetin on 12-ortho tetradecanoylphorbol 13-acetate (TPA)-induced inflammation was evaluated by two biomarkers: edema formation and myeloperoxidase (MPO) activity. Liposomes and PEVs were prepared by thin film hydration method and size homogenization was performed by sonication. In both formulations, soybean lecithin with 70 % phosphatidylcholine (Lipoid® S75) was used as lipid phase. PEVs used either 5 or 10 % PEG 400 in the aqueous phase (PEVs are liposomal formulation where PEG is added to PBS to boost skin penetration capacity of the formulation). Liposomes size was 116 ± 5.3 nm and PEVs 5 % and 10 % presented a size of 152 ± 2.4 nm and 148 ± 3.5 nm respectively. PDI results were ≤ 0.35 with surface charge (−10 mV), due to

the low charge carried by S75. Higher entrapment efficiency was achieved by PEVs than liposomes (52 ± 4.4 % for liposomes vs. 75 ± 3.0 % and 60±0.8 % for 5 % PEG-PEVs and 10 % PEG-PEVs respectively) (Table 4). Quercetin loaded liposomes reduced edema formation from 11.5 mg/g (biopsy/bodyweight) in TPA control group to 7 mg/g. Both quercetin loaded PEVs reduced biopsy weight to 6.2 mg/g (Table 3). MPO reduction was also validated for both liposomal formulation and PEVs. TPA positive control group increased MPO in the skin from 50 ng/ml supernatant in the negative control to 620 ng/ml. Quercetin liposomes reduced MPO concentration to 210 ng/ml and quercetin loaded PEVs to 110 ng/ml and 250 ng/ml for 5 % and 10 % PEG-PEVs, respectively (Table 3). Interestingly, in 2013, the same author tested diclofenac loaded 5 % PEG-PEVs under the same conditions. This study provided evidence that topically applied quercetin, when delivered by 5 % PEG-PEVs, was more effective than diclofenac at the same dose (10 mg/ml). Indeed, a 4.7 fold decrease was achieved by quercetin versus 2.7 fold with diclofenac [58, 59].

	Method	Result
Edema	Ear thickness (mice) topical route Cotton oil Arachidonic acid Back skin weight (mice) 12-otetradecanoylphorbol 13-acetate	Control 0.25 mm, quercetin 0.19 mm Control 0.25 mm, quercetin 0.12 mm [14] 1.7 fold decrease in edema weight [58]
Elastase release	Degranulation of azurophilic granules in (neutrophils	IC50= 6.25 ± 2.58 μM [45]
Myeloperoxidase release	Degranulation of azurophilic granules in (neutrophils) TPA-induced inflammation on mice back skin	3 fold decrease concentration [42] 4.7 fold decrease concentration [58]
Proinflammatory cytokines	Primary human keratinocytes were exposed to UV (0.05 j/cm^2) Il-1β mRNA IL-6 mRNA IL-8 mRNA TNF-α mRNA NF-κB activation	2.5 fold decrease in release 5 fold decrease in release 3 fold decrease in release 2 fold decrease in release 80% inhibition of binding with DNA [54]

Table 3: test performed for the determination of quercetin antiinflammatory activity.

Edema was tested by either the thickness of mice ear or the weight of mice back skin. Elastase and myeloperoxidase release was determined by the degranulation of azurophilic granules in neutrophils. Western blot was used for the determination of proinflammatory cytokines and quantified using a chemifluorescent substrate.

2.3. Quercetin in wound healing

Potent antioxidant and free radical scavenger activities of quercetin along with its strong antiinflammatory activity highlighted the possible application of this flavonoid for wound healing. Wound healing is a complex physiological compensating mechanism [60]. The applicability of quercetin during wound healing is beneficial for suppressing the uncontrolled

inflammation. Inflammation hinders the successful skin regeneration process and may transform an acute wound to a chronic one.

Quercetin ability to support the healing process was investigated in 2003 by Gomathi *et al..in vivo* on male albino Wistar rats. Quercetin was introduced to collagen films at a concentration of 1 mM. Wounds were generated by a mean of a scalp at day 0. Rats were separated in three groups: (i) control group, (ii) application of collagen films or (iii) application of quercetin incorporated collagen films in the rat skin at the wound place. Wound contraction, hydroxyproline, uronic acid, total protein, superoxide dismutase and catalase were tested on the granulation tissue. Quercetin incorporated collagen films showed a significant wound contraction (80 % reduction in wound surface) compared to collagen alone treated group (60 %) and control group (57 %). Quercetin incorporated with collagen increased hydroxproline concentration in the granulation tissue from 0.78 in the control group to 1.84 mg/mg tissue, which indicates that there was an enhanced production of collagen in the granulation tissue. Subsequent to collagen production, a decrease in hyaluronic acid is observed explaining the reduction of uronic acid content in quercetin treated groups. Considering superoxide dismutase, a 6 fold decrease in its concentration was observed with quercetin treated group, which might be related to quercetin antioxidant activity rather its antiinflammatory one. As free radicals are inducers of gene expression of superoxide dismutase, a more efficient free radical scavenging ability with the presence of quercetin resulted in the reduction of superoxide dismutase concentration in the granulation tissue. Quercetin converts the superoxide radical to hydrogen peroxide and hydrogen peroxide stimulates catalase release. This could be linked to an increase of catalase content from 1.91 in the control group to 2.55 unit/g tissue in quercetin treated rats [46]. In summary, quercetin activity in wound healing is a matter of both its antioxidant and antiinflammatory actions. In contrast to skin protection against UV, fibroblasts are the main target for quercetin wound dressings to support the healing process.

2.4. Quercetin and skin ageing

Retardation of skin ageing and wrinkling is of major interest in cosmeceuticals. Skin ageing is a complex process that involves both intrinsic (physiological changes on time) and extrinsic factors (photoageing, lifestyle, pollution). However the target of all antiaging products scope on the extrinsic controllable ones. Skin ageing is manifested by several physiological changes, for example defective barrier function, collagen atrophy, loss of skin elasticity, especially in the face. In addition, a generalized reduction in the vasculature of the dermis is observed, a

factor more pronounced factor in smokers. Vitamin D production is also reduced in elderly people [61-63]. All these changes cooperate to induce skin ageing and wrinkling.

Quercetin is useful in reducing photoageing because of its antioxidant activity. Quercetin protection against UV light and its application in sunscreen are discussed in detail in the quercetin antioxidant activity section (section 2.1). It is also worth to note that quercetin antiinflammatory activity may also contribute to fighting skin ageing. Skin elasticity is directly related to skin hydration state [64], which is linked to proper lipid biosynthesis and configuration. Quercetin as a lipid peroxidation inhibitor can protect skin from dehydration [65]. Quercetin inhibition of matrix metalloproteinase activity may also show a role in protection of skin collagen from destruction during inflammatory response to extrinsic ageing factors [66, 67]. In an *in vivo* study, Joshan *et al.*.[44] tested quercetin protective activity against photoageing on female albino mice. Mice dorsal skin were exposed to a UV dose of 0.036-0.216 J/cm^2 over 12 weeks period, then skin ageing markers like skin moisture, collagen content, thiobarbituric acid reacting substances (TBARS) and reduced glutathione were evaluated. Skin wrinkles and blood vessels were visually scaled and epidermal thickness were determined after the 12 weeks. 1 % Quercetin was applied topically in mixture of ethanol, propylene glycol and water (0.5:1:1 (v/v/v). This application increased skin moisture content (43.0 ± 1.2 %) compared to the UV exposed group (28.2 ± 0.9 %) and reduced TBARS from 20 nM/mg (animal tissue) in the UV exposed group to 12.5 nM/mg in the quercetin group. Moreover, the concentration of reduced glutathione increased by 1.5 fold in quercetin treated group compared to UV exposed group (Table 2). The higher concentration of the reduced form indicates that quercetin was able to neutralize free radicals and to protect cellular antioxidants like glutathione from depletion. As a last consequence after progressive UV exposure, skin wrinkles and superficial blood vessels appear, epidermal thickness is also increased in photosensitivity [68]. Quercetin reduced wrinkles number and depth from several deep wrinkles overall the dorsal region of the UV exposed group to few shallow wrinkles along the back. Regarding to epidermal thickness, the quercetin treated group was more similar to negative control group.

In another study, quercetin was studied on HFL-1 human embryonic fibroblasts and mouse melanocytes (B16F10 cell line) for its antiaging and rejuvenating actions. Chondrogianni *et al.* [69] treated young HFL-1 with 2 µg/ml quercetin in DMSO daily until senescence. β-galactosidase activity was regarded as a marker for senescence [70]. Cells treated with quercetin exhibited a lower percentage of β-galactosidase positive staining (13.7 % for quercetin treated vs. 77 % for DMSO group). On the other hand, quercetin-rejuvenating activity was tested on

middle aged and terminally senescent HFL-1 cells. Quercetin (2 µg/ml) was added to middle aged cells for 5 days after senescence and 2 weeks for terminally senescent cells, then proliferating cells were counted. Interestingly, quercetin increased the number of proliferating cells by 1.3 fold compared to DMSO group for both middle-aged cells and terminally senescent counterparts. After that, quercetin ability to protects HFL-1 from reactive oxygen species ROS was investigated. Cells were treated with 2 µg/ml quercetin and subjected to 300 µM H_2O_2 intoxication for 2.5 hours then a recovery period of 5 days was set. Viable cells were counted at the end of the experiment and the ROS was determined by 2′, 7′-dichlorodihydrofluorescein diacetate H_2DCF-DA. Quercetin had no significant effect on cell survival number while showed a 40 % decrease in ROS compared to the DMSO group. The mechanism underlying quercetin protective activity on HFL-1 was investigated. For this, proteasome that is the main secondary antioxidant system of the cell was studied. Young HFL-1 cells were treated with 2 µg/ml quercetin for 24 h and the CT-L proteasome (chymotrypsin-like proteasome) activity was measured. Quercetin increased both proteasome activity by 2.4 fold and enhanced protein expression levels of representative proteasome subunits.

Finally photoageing and exposure to UV light can induce skin pigmentation by anticipating several cellular pathways. For example, thymine dinucleotides enhance pigmentation of melanocytic cells and stimulate tyrosinase mRNA levels [71]. Tyrosinase is a copper-containing glycoprotein that catalyzes several steps in the melanin pigment biosynthesis and is mainly responsible for the age spots. Tyrosinase is regulated by proteasome activity as it is shown that tyrosinase is a proteasome substrate, proteasome is responsible of the degradation of mutant or structurally aberrant tyrosinase [72]. Mouse melanocytes (B16F10 cell line) were treated with 5 µg/ml quercetin for 3 days, afterwards tyrosinase was extracted from cells and quantified along with proteasome activity. Quercetin was able to increase the proteasome activity by 1.5 fold and reduce tyrosinase by 30 % compared to control cells [69]. These findings propose quercetin as a perfect candidate for a novel rejuvenating product. Quercetin is not only an antioxidant and skin cells protectant, but also presents interesting antiaging properties with whitening activities.

Quercetin presented potent antioxidant activity on three levels: *in vitro* chemical assays proved the increase of quercetin activity after its efficient formulation, on cellular level as quercetin showed cell protective actions on keratinocytes and *in vivo* on animal's skin. These antioxidative effects are also supported by the ability of quercetin to exert antiinflammatory actions such as inhibition of NF-κB and IL-6 induction by UV irradiation. The mixture between both antioxidant and antiinflammatory actions and their crosslinking mechanisms highlighted

quercetin as a novel sunscreen. Furthermore, as quercetin possesses both antioxidant and antiinflammatory activities, it could be beneficial on wound healing, here; fibroblasts are the main targets in contrast to keratinocytes in sunscreen. In addition, quercetin showed promising rejuvenating actions on keratinocytes with supportive whitening effect. This makes quercetin highly suitable as a novel natural molecule for such actions.

Quercetin activities on cellular level that were proven for skin related disorders are presented in Figure 1.

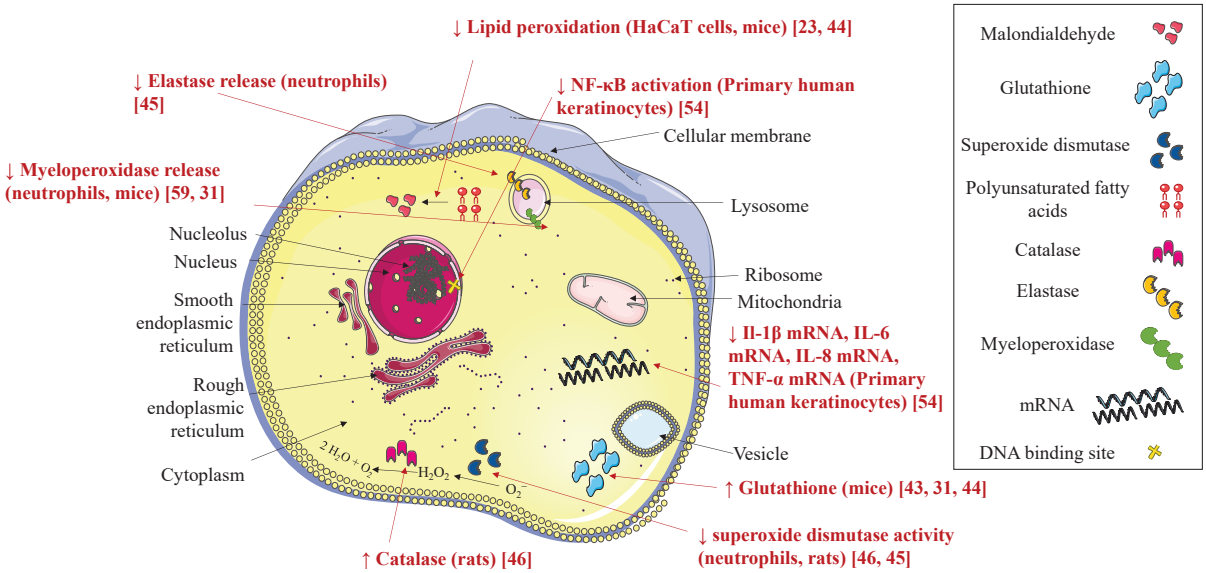

Figure 1: Quercetin activities on cellular level.

Quercetin decreased the release of myeloperoxidase and elastase, also decreased the activity of superoxide dismutase on neutrophils. Quercetin decreased the lipid peroxidation on HaCaT cell line. Quercetin decreased the activation of NF-κB and inhibited the mRNA of IL-1β, IL-6, IL-8 amd TNF-α on primary human keratinocytes.

However, all these desired benefits necessitate quercetin topical application, and this application should be thoroughly studied according to the desired activity (Figure 2). Ideally, quercetin should penetrate skin without reaching systemic circulation in case of cosmetic application for a possible sunscreen or anti-aging cream. At the same time, a satisfactory skin penetration to both stratum spinosum and stratum basale should be planned for quercetin to protect viable keratinocytes from UVA light, or to support in inflammatory skin disorders such as psoriasis. However, if the goal is to prolong fibroblasts survival and proliferation in burned skin and enhance the process of wound healing, a deeper penetration is required, and this point is critical. The targeted fibroblasts are beyond the basement membrane, and then it is challenging to deliver the finite dose of quercetin to these cells without reaching systemic circulation i.e. avoiding the adverse effects by minimizing systemic uptake.

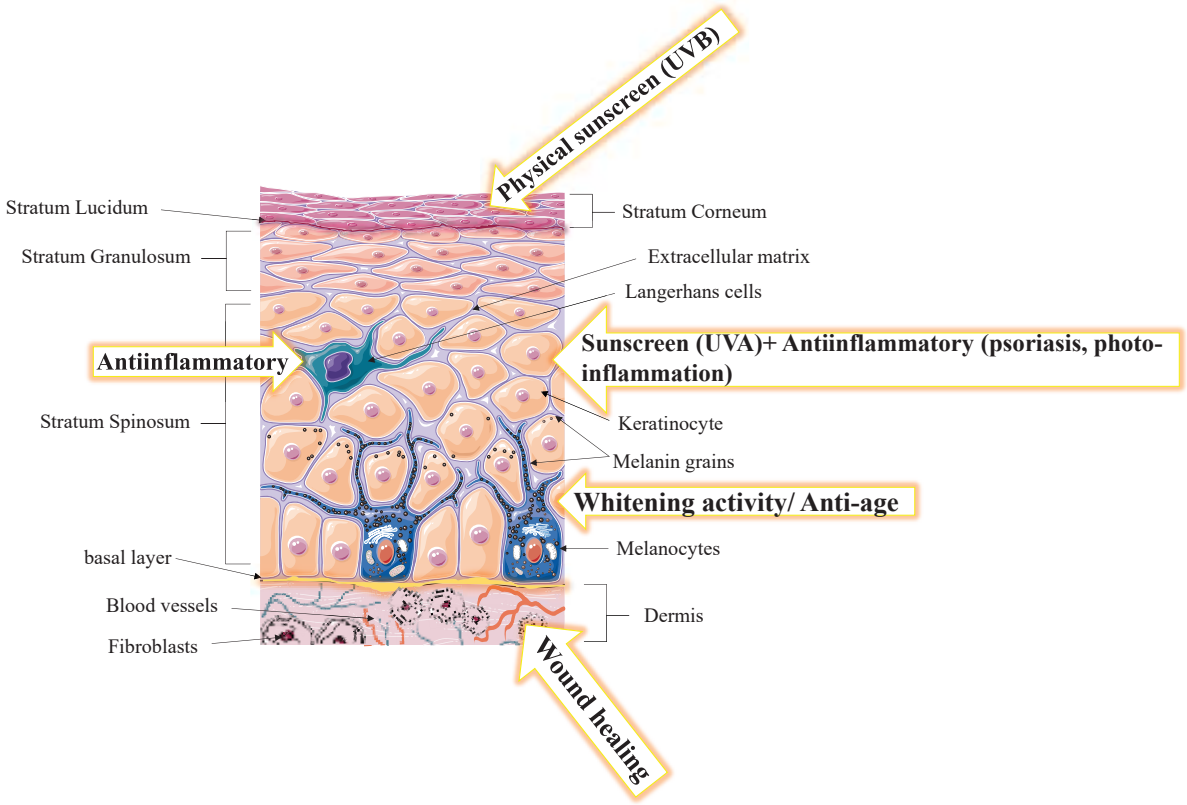

Figure 2: Quercetin properties in function of site of action in different skin layers.
Quercetin possesses a physical protection against UVB over stratum corneum. Within epidermis, quercetin shows a protective effect against UVA irradiation and in several inflammatory disorders like psoriasis. By targeting melanocytes, quercetin shows whitening and anti-aging effects by targeting fibroblasts. Finally, quercetin can support wound healing process in case of sufficient penetration into dermis.

In order to transport quercetin, that is naturally of limited via topical route, to the desired site of action, a suitable delivery system is essential. Conventional dosage forms such as creams, emulsions and gels are the first way to formulate quercetin and to modulate its skin penetration profile. On the other hand, nanodosage forms are promising second way to formulate quercetin at the nanoscale range in order to enhance its dermal activity.

3. Conventional dosage to increase quercetin skin penetration

Conventional dosage forms for dermal application are either aqueous like gels, or oily hydrophobic ointments, or a mixture of both like creams and emulsions. The choice of the external phase of the formulation has a major effect on the drug release. Indeed aqueous gels are known to boost fast release, in contrast to oily formulation that provide a reservoir for a prolonged release kinetics. Quercetin by itself has very limited skin penetration capacity. It is limited by both water insolubility and the lipophilic partition coefficient (log P= 1.82 ± 0.32)

due to the nonpolar groups in its structure [73]. For this end, quercetin dermal delivery is very much dependent on the dosage form. The poor water solubility requires the presence of a lipid phase in order to enhance quercetin solubility in the formulation, On the other hand, quercetin polar heads favor water presence, so quercetin can localize at the interface. Furthermore, water-containing formulations are easier to apply, more friendly to the skin and preferred by patients over viscous lipid formulations and fluid watery ones. For these reasons, quercetin was formulated in emulsions.

Casagrande *et al.* in 2007 [33] formulated quercetin in two emulsions differing in their lipid content. The emulsion with high lipid content (formulation 1) contained 10 % of self-emulsifying wax (Polawax® :cetostearyl alcohol and polyoxyethylene derived of a fatty acid ester of sorbitan 20E) and the emulsion with low lipid content contained 2 % of Polawax® (formulation 2). Both emulsions contained the anionic hydrophilic colloid 0.18 % (carboxypolymethylene, Carbopol® 940) as a stabilizer and triethanolamine 0.20 % as neutralized. Macadamia nut oil 2.50 % and squalene 1.00 % were used emollients, and propylene glycol 6.00 % as moisturizer and solubilizer. A mixture of phenoxyethanol and parabens 0.40 % (Phenova®) were used as preservatives. High lipid content emulsion was superior in delivering quercetin to the skin, proven by higher quercetin antilipoperoxidative activity over the emulsion with low lipid content. However, the exact quantity of penetrated quercetin and its exact deposition within the skin was not determined.

In 2008, Vicentini *et al.*.[43] prepared quercetin in w/o microemulsion. 0.3 % of quercetin were dissolved in 38.25 % of canola oil, 47.75 % of Span® 80 / Tween® 80 (3:1) and 15 % water/propylene glycol mixture (3:1). The microemulsion formed spontaneously after vortexing. *In vitro* skin penetration study was performed on pig ear skin using Franz diffusion cell. In parallel, an *in vivo* penetration study was conducted using HRS/J mice. 100 mg of microemulsion (300 µg quercetin) were applied to 1.77 cm^2 Franz cell mounted with pig ear skin. 150 mM phosphate buffer (pH 7.2) containing Tween® 20 (0.5 %) was selected as receptor medium. At the end of the study, the skin was stripped 15 times. The first strip was discarded and the rest was collected and considered as stratum corneum (SC), while the remaining skin portion was epidermis (E) and dermis (D). Quercetin microemulsion was compared to quercetin propylene glycol solution of same concentration. About 11 % of the applied dose were detected in the SC and 5 % in the E+D after 12 hours of application. On contrary, quercetin from the control formulation was ~2 and 20 times lower than the microemulsion in the SC and E+D, respectively. No transdermal penetration was detected in the tested time. The *in vivo* study on mice was run for 6 hours applying the same amount of formulation to about 2 cm^2 dorsal skin.

Similarly, the microemulsion delivered about ~14 % of the applied dose to the SC and ~8 % to E+D, which was 1.5 and 2 fold greater than the delivered quercetin by the control formulation. Conventional emulsions are a good strategy to improve the delivery of drugs to skin. Further studies are needed to explore more formulations with other lipids that possess better affinity to quercetin. However, quercetin may require a more advanced delivery system that ensures a high loading capacity of this drug and confers greater skin adhesiveness in order to prolong drug / skin contact time.

4. Nanodosage forms to increase quercetin skin penetration

The main objective of formulating quercetin in nanodosage forms is to overcome its topical limit penetration ability related to its poor water solubility and to increase its stability. Quercetin was formulated in several nanodosage forms for example nanoemulsions [74], liposomes [75], lipid nanoparticles [76] nanostructured lipid carriers NLC, solid lipid nanoparticles SLN [77, 78] and mesoporous silica [79]. Quercetin showed no transdermal delivery with novel dosage forms like lipid nanoparticles [76], nanostructured lipid carriers [78], aminopropyl functionalized mesoporous silica nanoparticles [79] and glycerosomes [38]. This phenomenon may be explained by quercetin poor water solubility [13, 80] and selective lipophilicity to certain lipids [81] despite of the barrier function of the stratum corneum (Table 4).

Extrapolation and comparison of skin penetration results is very difficult especially when skin from different sources is used for the tests. Besides this, the use of different methods of quantification of drug, different receptor mediums and variant durations of test make comparison difficult [82]. For this, skin penetration experiments will be divided into three groups. The first group will discuss about studies performed on mice [24] and SD rats [23] *ex vivo* on Franz diffusion cell. The second group will involve experiments performed on pig's skin [38, 74, 75, 79] and the last group will explore tests on full thickness human skin *in vivo* [76] and *ex vivo* on Franz diffusion cell [78].

Quercetin topical application

Formulations	Preparation technique	Excipients	Particles size (nm)	PDI	Surface charge (mV)	Quercetin encapsulation efficiency %	Quercetin practical concentration (mg) per ml of formulation
Quercetin deformable liposomes [23]	Ethanol Injection method	Lecithin Cholesterol Tween 80	132 ± 14	N/A	21.1 ± 0.8	80.4 ± 4.22	N/A
Quercetin polymeric nanoparticles [34]	Nanoprecipitation technique	Polyvinyl alcohol (PVA) Eudragit® E	82 ± 0	0.22 ± 0.01	N/A	99.9 ± 0.59	4.995 ± 0.003 mg/mg powder
Quercetin loaded Liposomes liposomes and glycerosomes [38]	Thin film hydration method	Lecithin Glycerol	102 ± 3 80 ± 3	0,32 0,26	-78.0 ± 2.0 -67.0 ± 3.0	88.0 ± 3.00 81.0 ± 1.00	4,4 ± 0,15 4,1 ± 0,05
Quercetin in liposomes and PEVs (Penetration Enhancer-containing Vesicles) [58]	Thin film hydration method	Soybean lecithin with 70% phosphatidylcholine PEG 5 % or 10 %	116 ± 5 152 ± 3 148 ± 4	0,35 0,34 0,31	−9.0 ± 0.4 −10.0 ± 0.8 −10.0 ± 0.7	52.0 ± 4.40 75.0 ± 3.00 60.0 ± 0.80	5,2 ± 0,44 7,5 ± 0,30 6,0 ± 0,08
Quercetin nanoemulsion [74]	Spontaneous emulsification	Lecithin Octyldodecanol and cetyltrimethylammonium bromide	307 ± 19 188 ± 2	N/A	−27.4 ± 6.0 76.3 ± 2.1	99,5 ± 0,30 99,1 ± 0,60	1.00 ± 0.00 0.99 ± 0.01
Quercetin loaded penetration enhancer vesicles PEV [75]	Thin film hydration method	Lecithin and Transcutol® P or Labrasol® or Propylene glycol or PEG 400	226 ± 5 86 ± 5 83 ± 10 190 ± 4	0.28 0.29 0.35 0.31	–49.0 ± 5.0 –32.0 ± 3.0 –63.0 ± 4.0 –58.0 ± 2.0	59.0 ± 8.00 75.0 ± 9.00 57.0 ± 8.00 48.0 ± 7.00	1,18 ± 0,16 1,50 ± 0,18 1,14 ± 0,16 0,96 ± 0,14

Quercetin topical application

Quercetin lipid nanoparticles [76]	Hot and cold high pressure homogenization	Tristearin Lecithin	527	0,58	N/A	46,5	N/A
Quercetin nanostructured lipid carrier (NLC) [77]	Probe ultrasonication	Compritol 888 Oleic acid	282 ± 3	0,31	-37.0 ± 3.0	0,025 % drug loading	0,25 mg/ml
Quercetin aminopropyl functionalized mesoporous silica nanoparticles (NH2-MSN) [79]	Sol-gel method	N-cetyl-trimethylammonium bromide Tetraethyl orthosilicate	250 ± 50	N/A	+13.6 ± 0.2	8 % mentioned as drug loading %	N/A
Quercetin-loaded lecithin-chitosan nanoparticles [24]	Ethanol Injection method	Lecithin Chitosan TPGS	95	0,44	10.9 ± 0.1	48,5	0,63 mg/ml

Table 4: Formulated quercetin nanodosage forms for topical application.
Comparative table of different nanoformulation with quercetin prepared for topical delivery. The comparison includes the type of nanoformulation, the preparation method, the used excipients and the physicochemical properties of each nanoformulation including the particle size, surface charge, quercetin encapsulation efficiency and quercetin concentration in mg per ml of formulation.

Quercetin topical application

4.1. Rodents skin based penetration tests

Rodents skin is thinner and more permeable than human and pig skins [83]. However, they are less expensive and easier to handle in laboratory practice. Rodents skin showed similar stratum corneum lipids composition [84].Absorption profile of antiinflammatory (ammonium glycyrrhizinate in niosomes) [85] and short chain alcohols [86] were closed to human skin confirming the successful use of murine model for *in vitro / in vivo* correlation with human volunteers. Still hairy rodents have the disadvantage of extremely high density of hair follicles with higher appendage number [87, 88]. For this, mice and rats are shaved prior to skin excision. The last studies with quercetin nanodosage forms were performed on skin of SD rats and kumming mice by Liu [23] and Tan [24], respectively.

Liu *et al.* [23] suggested deformable liposomes for effective skin delivery of quercetin. Tween® 80 was selected as edge activator, while cholesterol and phosphatidylcholine were chosen as lipid phase. Quercetin loaded deformable liposomes were prepared by ethanol injection technique and they presented a particle size of 132 nm and surface charge of -21.1 mV. Quercetin encapsulation efficiency was 80.4 ± 4.2 % (Table 4). Skin penetration was analyzed with shaved skin excised from rats' abdomen using Franz diffusion cells. Experiments were run at 32°C with physiological saline buffer as receptor fluid and a total time of 7 hours before quercetin extraction from skin. About 3.5 % of the applied dose was permeated through skin in case of deformable liposomes compared to less than 1 % in case of quercetin suspension in water. Likewise, a higher quercetin settling in skin with nanodosage form was proven over the control. It is worth to note that the ability of quercetin to permeate the skin especially from the suspension (with keeping in mind the low affinity of quercetin to the receptor fluid is questionable. Indeed, as it was previously proved using vasopressin that shaving of the skin before application increased flux 5 times over the control [89]. This result explains the presence of permeated portion.

In 2011, Tan *et al.* [24] studied lecithin-chitosan nanoparticles for the topical delivery of quercetin. These nanoparticles were also prepared by ethanol injection technique. Particles size was 95 nm (PDI 0.44); zeta potential was +10.9 mV (because of the presence of the polycationic polymer chitosan). Quercetin achieved 48.5 % encapsulation efficiency and 2.5 % drug loading within formulated nanoparticles (Table 4). Skin penetration tests were made both *in vitro* on mice excised skin and *in vivo* on viable animals. In both cases, no skin permeation was detected after 12 hours, whereas quercetin deposition results were comparable between *in vitro* and *in vivo* experiments. Quercetin loaded lecithin-chitosan nanoparticles

showed 2.3 and 1.2 fold increase in drug settling within epidermis and dermis respectively compared to quercetin control solution in propylene glycol.

4.2. Pig skin based penetration tests

The second group of research work covers studies with pig ear skin. Pig ear skin is a very close surrogate for human skin. It shares several anatomical and physiological similarities with human skin [90]. Moreover, pig ear skin is more available and less expensive [91].

In 2009, Fasolo *et al.* [74] developed quercetin containing nanoemulsions. Two types of nanoemulsions were prepared: one with negatively charged droplets composed of octyldodecanol and egg lecithin (surface charge −27.4 mV) and the second with positively charged droplets (surface charge +76.3 mV) by the addition of the cationic surfactant: cetyl trimethylammonium bromide (CTAB). Nanoemulsions were formulated by spontaneous emulsification that corresponds to the injection of organic solvent containing the oily materials into aqueous phase. Then, the evaporation of the organic phase is done under reduced pressure conditions. Nanoemulsions without CTAB possessed a larger particle size compared to nanoemulsions with CTAB (307 ± 19 nm vs. 188 ± 2 nm). Quercetin encapsulation efficacy was over 99 % for both nanoemulsions (Table 4). Penetration assay on Franz cell was performed over 8 hours using 50 % v/v hydroethanol solution as receptor medium. To note, Fasolo *et al.* determined only quercetin permeated and did not provide data about quercetin skin deposition. Quercetin nanoemulsions were applied to skin at a dose of 1000 µg quercetin, only 1.524 µg quercetin were permeated through pig ear skin in case of nanoemulsions without CTAB. In contrast, 4.064 µg quercetin permeated from quercetin nanoemulsions with CTAB. In terms of permeated drug percentage, both formulation showed less than 1 % drug permeation. The higher drug permeation observed with positively charged nanoemulsions of quercetin is in agreement with other publications, where a higher drug permeation is observed with positively charged nanoemulsions having a higher affinity for negatively charged skin [92-94]. At the same time, cationic surfactants are known to be more skin destructive than anionic surfactants and cause higher drugs flux (drug diffusion through a surface unit of membrane per unit of time) [95]. The percentage of permeated quercetin could be potentially attributed to the fact that porcine skin is more permeable than human skin [96, 97]. In addition, the use of a receptor medium that contains alcohol may also cause damage to the barrier function of the utilized skin [98].

Quercetin topical application

In 2011 Chessa *et al*. [75] incorporated quercetin to liposomes using five different penetration enhancers: Transcutol® P (Trc), propylene glycol (PG), polyethylene glycol 400 (PEG) and Labrasol® (Lab). These penetration enhancer containing vesicles were prepared by thin the film hydration method followed by sonication. Particles size, PDI and zeta potential for Trc, PG, PEG and Lab were 226 nm (0.28 PDI, -49.0 mV), 83 nm (0.35 PDI, -63.0 mV), 190 nm (0.31 PDI, -58.0 mV) and 86 nm (0.29 PDI, -32.0 mV) respectively. Quercetin encapsulation efficiency ranged from 48 % with PEG to 75 % with Lab (Table 4). Following vesicles preparation, newborn pig's skin was mounted on Franz diffusion cells and skin penetration was assessed. After 8 hours, the skin was subjected to 10 strips to separate the stratum corneum. Dermis was separated from epidermis using surgical sterile scalpel. PEG containing vesicles yielded the highest skin permeation with 30 % of the applied dose detected in the receptor fluid, as well as the highest deposition in epidermis (55 % of the applied dose). It is worth to note that PEG 400 was tested for its penetration enhancement with several drugs such as naloxone [99], estradiol [100], levonorgestrel [101] and zidovudine [102]. Nonetheless PEG 400 causes skin damage by alteration of skin structure and modulation of the mass flow of water [103].

Manca *et al.* [38] also developed quercetin loaded liposomes and glycerosomes. Similar to Chessa *et al.*, they prepared quercetin nanovesicles using the thin film hydration method followed by sonication. However, instead of using a mixture of penetration enhancer/water to prepare PEVs, they prepared glycerosomes using a 50 % mixture glycerol / water. They used lecithin as a lipid. Liposomes were 102 nm (PDI 0.32) with a surface charge -78.0 mV. The glycerosomes were 80 nm (PDI 0.26) with a surface charge -67.0 mV. Both formulations showed encapsulation efficiency over 80 % (Table 4). Skin penetration tests were performed over 24 hours at 37°C using Franz cells with newborn pig's skin. At the end of the test, skin layers were separated in the same way as in the publication of Chessa *et al*. However, both liposomes and glycerosomes did not promote quercetin permeation, but glycerosomes were more efficient in delivering quercetin to the skin compared to liposomes (over 20 % of the applied dose vs. 10 to 20 % for liposomes). Quercetin deposition order was stratum corneum, epidermis and dermis respectively in both formulations. This seems to be in accordance to the fact that without the use of a strong penetration enhancer as in the example of Chessa *et al.*, no skin permeation would be observed unless skin barrier function is damaged due to a wound or injury.

In 2015, Sapino *et al.* [79] investigated the formulation of quercetin within aminopropyl functionalized mesoporous silica nanoparticles (NH_2-MSN). CTAB was used as structure directing agent and tetraethyl

orthosilicate as silica source. Quercetin was then loaded in NH_2-MSN at a concentration of 8 % and incorporated into a w/o emulsion. At the end of the skin penetration studies no transdermal delivery of quercetin was detected (24 hours), this confirms other reports where quercetin showed no skin permeation in nanodosage forms [76, 78]. However, association of quercetin to silica nanoparticles leads to 2 fold increase in skin deposition compared to free quercetin (10.98 µg/cm^2 vs. 4.77 µg/cm^2),

Respecting the fact that porcine skin is more permeable than human skin, quercetin loaded nanodosage forms showed no evidence for skin permeation except in case of the use of penetration enhancers like CTAB or PEG 400.

4.3. Human skin based penetration tests

Ending by the third group, Scalia *et al.* in 2013 [76] reported *in vivo* skin penetration of quercetin from solid lipid nanoparticles (SLN). Quercetin was encapsulated in tristearin/phosphatidylcholine nanoparticles. For this, quercetin was dissolved in melted tristearin in the pre-emulsion step and then subjected to cold or hot high pressure homogenization. Quercetin encapsulation efficiency within lipid nanoparticles was 46.5 %. Particles size was 527 nm with a PDI of 0.58 for nanoparticles prepared by hot high-pressure homogenization (Table 4). Afterwards lipid nanoparticles were incorporated into an oil-in-water emulsion (0.3 % w/w quercetin). Then the final emulsion was applied on the forearm of a group of 10 healthy volunteers (22-27 years old). Quercetin final emulsion was applied at a dose of 4 mg/cm^2 for 60 minutes, quercetin non-encapsulated in lipid nanoparticles was incorporated in the same emulsion and regarded as control formulation. After the end of the application period, *in vivo* skin penetration assay was performed using 15 stripping tapes of scotch transparent adhesive tape. The first strip tape along with the cotton swab used to remove the remaining formulation was analyzed for unabsorbed quercetin. Then strips were separated into in four groups (group 1: strips 2–4; group 2: strips 5–7; group 3: strips 8–11; group 4: strips 12–15). 66.9 ±11.1 % of quercetin applied dose in the control formulation were recorded on the cotton swab and strip 1 while quercetin loaded lipid nanoparticles was 57.8 ±11.0 %. This very limited improvement by SLN may be attributed to the short duration of drug application, besides the intact barrier function of the stratum corneum (the volunteers were healthy and presented a healthy skin). 21.2 ± 2.9 % of the applied dose was penetrated into the skin for quercetin lipid nanoparticles compared to only 18.1 ± 0.3 % of the dose in the control. Penetration of quercetin from SLN in the strips was as follows: the highest drug portion was in strips 2-4 (approximately 14 %) followed by 5-7 (3.5 %) then 8-11 (3 %) and finally

strips 12-5 (1.5 %). Quercetin in SLN showed higher drug deposition in the upper layers of the stratum corneum and lower percentage in the deeper layers. This observation is in accordance that lipid nanoparticles generate an occlusive effect on the skin, thus increase skin hydration and promote drug delivery to upper skin layers [104]. Meanwhile their relatively large size above 500 nm favors deeper skin penetration via follicular route [105] rather than transepidermal penetration [106].

In 2013, Bose *et al.* [78] developed quercetin in both solid lipid nanoparticles (SLN) and nanostructured lipid carriers (NLC). Compritol® 888 was used as solid lipid for both nanosystems, whereas oleic acid was incorporated into nanostructured lipid carriers as liquid lipid. Both quercetin nanosystems were prepared by the probe ultrasonication method. Quercetin NLC were 282 nm, PDI of 0.31 and zeta potential of -37.0 mV (Table 4). Quercetin exhibited a better physical stability results for 14 weeks at 2-8°C when loaded at 0.0125 % than 0.025 %. Skin penetration studies were performed on full thickness human skin *ex vivo* using 0.64 cm^2 Franz diffusion cell over 24 hours. Bose *et al.* [78] reported the absence of transdermal delivery for quercetin from both nanosystems. This result is in accordance with Scalia *et al.* [76] who confirm that the majority of applied quercetin from nanoparticles was found in the top layers of the skin. This is very important for such antioxidant molecule, considering the main site of action is the skin cells in the upper layers. At the end of the penetration test, Bose *et al.* determined skin quercetin retention without detailing its distribution among skin layers. The percentage of drug skin retention was 19.2 % with NLC according to Bose *et al.* and it falls in the same range that is in the *in vivo* work of Scalia *et al.* who detected 21.2 ± 2.9 %.

In summary, quercetin even when formulated in a lipid nanoparticle vector shows no evidence for transdermal delivery on human skin. Keeping in mind that quercetin as a molecule is a paradigmatic model for a lipophilic drug (octanol−water partition coefficient log P = 1.82) [73] with 5 polar hydroxyl heads and very low water solubility [81], thus quercetin is not the perfect drug candidate for a transdermal delivery system. Quercetin local skin deposition is more valuable than performing a transdermal delivery through skin. Quercetin envisaged dermal applications described above (section 2) are all of local interest and the absence of a systemic absorption is desirable. Nanodosage forms were able to increase quercetin skin retention via their occlusive effect and higher surface area. Transdermal delivery for quercetin nanodosage forms was not achieved without the help of penetration enhancers. The use of penetration enhancers should be taken with caution as these molecules affect skin barrier function and may cause skin damage. However, nanodosage forms are very promising drug delivery systems for targeting skin and

upper layers of epidermis. This is desirable for quercetin to exert its activity in protecting skin tissue from oxidative stress, photoageing and uncontrolled skin inflammation.

Finally, one can compare *in vivo* skin permeation / penetration for quercetin between microemulsion [43] and lecithin-chitosan nanoparticles [24] as in both studies formulations were applied on dorsal skin of mice, quercetin applied quantity was the same (300 µg) and both studies detected quercetin levels in the skin after 6 hours of application. Results are relatively close between nanoparticles and microemulsion. The larger portion of quercetin was detected in the upper skin layers at the SC level, lower concentrations were detected in the dermis. Quercetin showed no transdermal delivery in both studies.

5. Conclusion

Quercetin proves to possess several interesting physiological actions on skin. It has a strong antioxidative activity. It protects keratinocytes for exogenous oxidizing agents and scavenges free radicals, prevents endogenous antioxidant depletion and inhibits lipid peroxidation upon exposure to UV. Quercetin also presents broad antiinflammatory actions. It is stronger than other flavonoids in inhibiting edema after contact with inflammogens. It presents inhibiting actions on NF-κB and on the release of several proinflammatory cytokines. These combined antioxidative/antiinflammatory actions highlight quercetin as a promising molecule for the treatment of chronic wounds. Additionally quercetin shows anti-aging actions on middle-aged keratinocytes and rejuvenating actions on terminally senescent cells. In parallel, quercetin inhibits tyrosinase in melanocytes thus enables a whitening effect on skin. All these possible targets and applications for quercetin require a successful local delivery to skin. Due to quercetin poor water solubility and inability to penetrate skin, researches are conducted on the formulation of a potent delivery system. In this article, the last advances in delivery of quercetin to skin via conventional dosage forms and nanodosage forms were presented and discussed. The variation of formulations in terms of excipients used and the physicochemical characteristics, along with effect of particle size on skin penetration are discussed. Quercetin in both types of formulations presented no transdermal delivery except in case of the use of penetration enhancers. Conventional and nanodosage forms showed higher quercetin deposition in the upper skin layers of the epidermis. Despite of achieving extremely small particle size with nanodosage forms, still the lipid content and the lipid type seem to be the main determinant of the extent of quercetin depth in skin layers. More studies should be performed to get more

insight about the exact depth that a formulation containing quercetin can achieve. At the same time, more research should be made to investigate other possible applications for quercetin in other skin disorders like psoriasis or atopic dermatitis.

Quercetin topical application

References

[1] A.B. Wysocki, Skin anatomy, physiology, and pathophysiology, Nurs Clin North Am, 34 (1999) 777-797, v.

[2] C.S. Sander, H. Chang, S. Salzmann, C.S.L. Muller, S. Ekanayake-Mudiyanselage, P. Elsner, J.J. Thele, Photoaging is Associated with Protein Oxidation in Human Skin In Vivo, 118 (2002) 618-625.

[3] U. Hoppe, J. Bergemann, W. Diembeck, J. Ennen, S. Gohla, I. Harris, J. Jacob, J. Kielholz, W. Mei, D. Pollet, D. Schachtschabel, G. Sauermann, V. Schreiner, F. Stab, F. Steckel, Coenzyme Q10, a cutaneous antioxidant and energizer, Biofactors, 9 (1999) 371-378.

[4] J. Pardeike, K. Schwabe, R.H. Müller, Influence of nanostructured lipid carriers (NLC) on the physical properties of the Cutanova Nanorepair Q10 cream and the in vivo skin hydration effect, Intrnational Journal of Pharmaceutics, 396 (2010) 166-173.

[5] S. Shibuya, H. Nojiri, D. Morikawa, H. Koyama, T. Shimizu, Chapter 14 - Protective Effects of Vitamin C on Age-Related Bone and Skin Phenotypes Caused by Intracellular Reactive Oxygen Species, in: V.R. Preedy (Ed.) Aging, Academic Press, San Diego, 2014, pp. 137-144.

[6] J.V. Freitas, N.P. Lopes, L.R. Gaspar, Photostability evaluation of five UV-filters, trans-resveratrol and beta-carotene in sunscreens, European Journal of Pharmaceutical Sciences, 78 (2015) 79-89.

[7] E.A. Offord, J.-C. Gautier, O. Avanti, C. Scaletta, F. Runge, K. Krämer, L.A. Applegate, Photoprotective potential of lycopene, β-carotene, vitamin E, vitamin C and carnosic acid in UVA-irradiated human skin fibroblasts, Free Radical Biology and Medicine, 32 (2002) 1293-1303.

[8] P.K. Vayalil, A. Mittal, Y. Hara, C.A. Elmets, S.K. Katiyar, Green Tea Polyphenols Prevent Ultraviolet Light-Induced Oxidative Damage and Matrix Metalloproteinases Expression in Mouse Skin, J Investig Dermatol, 122 (2004) 1480-1487.

[9] J. Nichols, S. Katiyar, Skin photoprotection by natural polyphenols: anti-inflammatory, antioxidant and DNA repair mechanisms, Archives of Dermatological Research, 302 (2010) 71-83.

[10] S. Veeriah, T. Kautenburger, N. Habermann, J. Sauer, H. Dietrich, F. Will, B.L. Pool-Zobel, Apple flavonoids inhibit growth of HT29 human colon cancer cells and modulate expression of genes involved in the biotransformation of xenobiotics, Mol Carcinog, 45 (2006) 164-174.

[11] R. Slimestad, T. Fossen, I.M. Vagen, Onions: a source of unique dietary flavonoids, J Agric Food Chem, 55 (2007) 10067-10080.

[12] C. Ewald, S. Fjelkner-Modig, K. Johansson, I. Sjöholm, B. Åkesson, Effect of processing on major flavonoids in processed onions, green beans, and peas, Food Chemistry, 64 (1999) 231-235.

[13] F. Bonina, M. Lanza, L. Montenegro, C. Puglisi, A. Tomaino, D. Trombetta, F. Castelli, A. Saija, Flavonoids as potential protective agents against photo-oxidative skin damage, International Journal of Pharmaceutics, 145 (1996) 87-94.

[14] H. Kim, S. Namgoong, H. Kim, Antiinflammatory activity of flavonoids: Mouse ear edema inhibition, Archives of Pharmacal Research, 16 (1993) 18-24.

[15] A. Saija, A. Tomaino, D. Trombetta, M. Luisa Pellegrino, B. Tita, C. Messina, F.P. Bonina, C. Rocco, G. Nicolosi, F. Castelli, 'In vitro' antioxidant and photoprotective properties and interaction with model membranes of three new quercetin esters, European Journal of Pharmaceutics and Biopharmaceutics, 56 (2003) 167-174.

[16] T. Hatahet, M. Morille, A. Hommoss, C. Dorandeu, R.H. Muller, S. Begu, Dermal quercetin smartCrystals(R): Formulation development, antioxidant activity and cellular safety, Eur J Pharm Biopharm, 102 (2016) 51-63.

[17] Lh, Quercetin | CAS 117-39-5 | Santa Cruz Biotech, in, 2016.

[18] Y. Zheng, I.S. Haworth, Z. Zuo, M.S. Chow, A.H. Chow, Physicochemical and structural characterization of quercetin-beta-cyclodextrin complexes, J Pharm Sci, 94 (2005) 1079-1089.

[19] J.A. Rothwell, A.J. Day, M.R. Morgan, Experimental determination of octanol-water partition coefficients of quercetin and related flavonoids, J Agric Food Chem, 53 (2005) 4355-4360.

[20] C. Celia, F. Cilurzo, E. Trapasso, D. Cosco, M. Fresta, D. Paolino, Ethosomes(R) and transfersomes(R) containing linoleic acid: physicochemical and technological features of topical drug delivery carriers for the potential treatment of melasma disorders, Biomed Microdevices, 14 (2012) 119-130.

[21] D. Paolino, C. Celia, E. Trapasso, F. Cilurzo, M. Fresta, Paclitaxel-loaded ethosomes(R): potential treatment of squamous cell carcinoma, a malignant transformation of actinic keratoses, Eur J Pharm Biopharm, 81 (2012) 102-112.

[22] D. Paolino, D. Cosco, F. Cilurzo, E. Trapasso, V.M. Morittu, C. Celia, M. Fresta, Improved in vitro and in vivo collagen biosynthesis by asiaticoside-loaded ultradeformable vesicles, J Control Release, 162 (2012) 143-151.

[23] D. Liu, H. Hu, Z. Lin, D. Chen, Y. Zhu, S. Hou, X. Shi, Quercetin deformable liposome: Preparation and efficacy against ultraviolet B induced skin damages in vitro and in vivo, Journal of Photochemistry and Photobiology B: Biology, 127 (2013) 8-17.

[24] Q. Tan, W. Liu, C. Guo, G. Zhai, Preparation and evaluation of quercetin-loaded lecithin-chitosan nanoparticles for topical delivery, Int J Nanomedicine, 6 (2011) 1621-1630.

[25] G.S. Borghetti, I.M. Costa, P.R. Petrovick, V.P. Pereira, V.L. Bassani, Characterization of different samples of quercetin in solid-state: indication of polymorphism occurrence, Pharmazie, 61 (2006) 802-804.

[26] H. Sies, Strategies of antioxidant defense, Eur J Biochem, 215 (1993) 213-219.

[27] M.S. Blois, Antioxidant Determinations by the Use of a Stable Free Radical, Nature, 181 (1958) 1199-1200.

[28] I. Fridovich, Quantitative Aspects of the Production of Superoxide Anion Radical by Milk Xanthine Oxidase, Journal of Biological Chemistry, 245 (1970) 4053-4057.

[29] N. Majkic-Singh, M. Koprivica, S. Spasic, M. Stojanov, I. Berkes, Evaluation of bathophenanthroline method for serum iron assay, Clin Chem, 26 (1980) 1360.

[30] G. Lefevre, M. Beljean-Leymarie, F. Beyerle, D. Bonnefont-Rousselot, J.P. Cristol, P. Therond, J. Torreilles, [Evaluation of lipid peroxidation by measuring thiobarbituric acid reactive substances], Ann Biol Clin (Paris), 56 (1998) 305-319.

[31] R. Casagrande, S.R. Georgetti, W.A. Verri, J.R. Jabor, A.C. Santos, M.J.V. Fonseca, Evaluation of functional stability of quercetin as a raw material and in different topical formulations by its antilipoperoxidative activity, in: AAPS PharmSciTech, 2006, pp. E64-71.

[32] K.E. Heim, A.R. Tagliaferro, D.J. Bobilya, Flavonoid antioxidants: chemistry, metabolism and structure-activity relationships, The Journal of Nutritional Biochemistry, 13 (2002) 572-584.

[33] R. Casagrande, S.R. Georgetti, W.A. Verri Jr, M.F. Borin, R.F.V. Lopez, M.J.V. Fonseca, In vitro evaluation of quercetin cutaneous absorption from topical formulations and its functional stability by antioxidant activity, International Journal of Pharmaceutics, 328 (2007) 183-190.

[34] T.-H. Wu, F.-L. Yen, L.-T. Lin, T.-R. Tsai, C.-C. Lin, T.-M. Cham, Preparation, physicochemical characterization, and antioxidant effects of quercetin nanoparticles, International Journal of Pharmaceutics, 346 (2008) 160-168.

[35] K.L. Wolfe, R.H. Liu, Cellular Antioxidant Activity (CAA) Assay for Assessing Antioxidants, Foods, and Dietary Supplements, Journal of Agricultural and Food Chemistry, 55 (2007) 8896-8907.

[36] C. López-Alarcón, A. Denicola, Evaluating the antioxidant capacity of natural products: A review on chemical and cellular-based assays, Analytica Chimica Acta, 763 (2013) 1-10.

[37] S.D. Skaper, M. Fabris, V. Ferrari, M. Dalle Carbonare, A. Leon, Quercetin protects cutaneous tissue-associated cell types including sensory neurons from oxidative stress induced by glutathione depletion: cooperative effects of ascorbic acid, Free Radic Biol Med, 22 (1997) 669-678.

[38] M.L. Manca, I. Castangia, C. Caddeo, D. Pando, E. Escribano, D. Valenti, S. Lampis, M. Zaru, A.M. Fadda, M. Manconi, Improvement of quercetin protective effect against oxidative stress skin damages by incorporation in nanovesicles, Colloids and Surfaces B: Biointerfaces, 123 (2014) 566-574.

[39] N. Düzgüneş, S. Nir, Mechanisms and kinetics of liposome–cell interactions, Advanced Drug Delivery Reviews, 40 (1999) 3-18.

[40] V.P. Torchilin, Recent advances with liposomes as pharmaceutical carriers, Nat Rev Drug Discov, 4 (2005) 145-160.

[41] C.-F. Hung, C.-L. Fang, S.A. Al-Suwayeh, S.-Y. Yang, J.-Y. Fang, Evaluation of drug and sunscreen permeation via skin irradiated with UVA and UVB: Comparisons of normal skin and chronologically aged skin, Journal of Dermatological Science, 68 (2012) 135-148.

[42] R. Casagrande, S.R. Georgetti, W.A. Verri Jr, D.J. Dorta, A.C. dos Santos, M.J.V. Fonseca, Protective effect of topical formulations containing quercetin against UVB-induced oxidative stress in hairless mice, Journal of Photochemistry and Photobiology B: Biology, 84 (2006) 21-27.

[43] F.T.M.C. Vicentini, T.R.M. Simi, J.O. Del Ciampo, N.O. Wolga, D.L. Pitol, M.M. Iyomasa, M.V.L.B. Bentley, M.J.V. Fonseca, Quercetin in w/o microemulsion: In vitro and in vivo skin penetration and efficacy against UVB-induced skin damages evaluated in vivo, European Journal of Pharmaceutics and Biopharmaceutics, 69 (2008) 948-957.

[44] D. Singh Joshan, S.K. Singh, Investigational study of Juglans regia extract and quercetin against photoaging, Biomedicine & Aging Pathology, 3 (2013) 193-200.

[45] C.F. Lin, Y.L. Leu, S.A. Al-Suwayeh, M.C. Ku, T.L. Hwang, J.Y. Fang, Anti-inflammatory activity and percutaneous absorption of quercetin and its polymethoxylated compound and glycosides: the relationships to chemical structures, Eur J Pharm Sci, 47 (2012) 857-864.

[46] K. Gomathi, D. Gopinath, M. Rafiuddin Ahmed, R. Jayakumar, Quercetin incorporated collagen matrices for dermal wound healing processes in rat, Biomaterials, 24 (2003) 2767-2772.

[47] E.A. Hamminga, A.J. van der Lely, H.A.M. Neumann, H.B. Thio, Chronic inflammation in psoriasis and obesity: Implications for therapy, Medical Hypotheses, 67 (2006) 768-773.

[48] D.R. Bickers, M. Athar, Oxidative Stress in the Pathogenesis of Skin Disease, Journal of Investigative Dermatology, 126 (2006) 2565-2575.

[49] S.J. Cooper, G.T. Bowden, Ultraviolet B regulation of transcription factor families: roles of nuclear factor-kappa B (NF-kappaB) and activator protein-1 (AP-1) in UVB-induced skin carcinogenesis, Curr Cancer Drug Targets, 7 (2007) 325-334.

[50] P.P. Tak, G.S. Firestein, NF-κB: a key role in inflammatory diseases, in: J Clin Invest, 2001, pp. 7-11.

[51] P.A. Ruiz, A. Braune, G. Holzlwimmer, L. Quintanilla-Fend, D. Haller, Quercetin inhibits TNF-induced NF-kappaB transcription factor recruitment to proinflammatory gene promoters in murine intestinal epithelial cells, in: J Nutr, United States, 2007, pp. 1208-1215.

[52] C.A. Musonda, J.K. Chipman, Quercetin inhibits hydrogen peroxide (H2O2)-induced NF-kappaB DNA binding activity and DNA damage in HepG2 cells, Carcinogenesis, 19 (1998) 1583-1589.

[53] A.B. Granado-Serrano, M.A. Martin, L. Bravo, L. Goya, S. Ramos, Quercetin modulates NF-kappa B and AP-1/JNK pathways to induce cell death in human hepatoma cells, in: Nutr Cancer, England, 2010, pp. 390-401.

[54] F.T. Vicentini, T. He, Y. Shao, M.J. Fonseca, W.A. Verri, Jr., G.J. Fisher, Y. Xu, Quercetin inhibits UV irradiation-induced inflammatory cytokine production in primary human keratinocytes by suppressing NF-kappaB pathway, in: J Dermatol Sci, 2011 Japanese Society for Investigative Dermatology. Published by Elsevier Ireland Ltd, Netherlands, 2011, pp. 162-168.

[55] C.-F. Lin, Y.-L. Leu, S.A. Al-Suwayeh, M.-C. Ku, T.-L. Hwang, J.-Y. Fang, Anti-inflammatory activity and percutaneous absorption of quercetin and its polymethoxylated compound and glycosides: The relationships to chemical structures, European Journal of Pharmaceutical Sciences, 47 (2012) 857-864.

[56] B. Choquenet, C. Couteau, E. Paparis, L.J.M. Coiffard, Quercetin and Rutin as Potential Sunscreen Agents: Determination of Efficacy by an in Vitro Method, Journal of Natural Products, 71 (2008) 1117-1118.

[57] A. Vijayalakshmi, V. Ravichandiran, V. Malarkodi, S. Nirmala, S. Jayakumari, Screening of flavonoid “quercetin” from the rhizome of Smilax china Linn. for anti-psoriatic activity, in: Asian Pac J Trop Biomed, 2012, pp. 269-275.

[58] C. Caddeo, O. Diez-Sales, R. Pons, X. Fernandez-Busquets, A.M. Fadda, M. Manconi, Topical anti-inflammatory potential of quercetin in lipid-based nanosystems: in vivo and in vitro evaluation, Pharm Res, 31 (2014) 959-968.

[59] C. Caddeo, O.D. Sales, D. Valenti, A.R. Sauri, A.M. Fadda, M. Manconi, Inhibition of skin inflammation in mice by diclofenac in vesicular carriers: liposomes, ethosomes and PEVs, Int J Pharm, 443 (2013) 128-136.

[60] T.K. Hunt, The physiology of wound healing, Annals of Emergency Medicine, 17 (1988) 1265-1273.

[61] D. Cerimele, L. Celleno, F. Serri, Physiological changes in ageing skin, British Journal of Dermatology, 122 (1990) 13-20.

[62] J. Calleja-Agius, Y. Muscat-Baron, M.P. Brincat, Skin ageing, Menopause Int, 13 (2007) 60-64.

[63] M.A. Farage, K.W. Miller, P. Elsner, H.I. Maibach, Intrinsic and extrinsic factors in skin ageing: a review, International Journal of Cosmetic Science, 30 (2008) 87-95.

[64] M. Hara, A.S. Verkman, Glycerol replacement corrects defective skin hydration, elasticity, and barrier function in aquaporin-3-deficient mice, Proceedings of the National Academy of Sciences, 100 (2003) 7360-7365.

[65] J. Terao, M. Piskula, Q. Yao, Protective Effect of Epicatechin, Epicatechin Gallate, and Quercetin on Lipid Peroxidation in Phospholipid Bilayers, Archives of Biochemistry and Biophysics, 308 (1994) 278-284.

[66] J. Majtan, J. Bohova, R. Garcia-Villalba, F. Tomas-Barberan, Z. Madakova, T. Majtan, V. Majtan, J. Klaudiny, Fir honeydew honey flavonoids inhibit TNF-α-induced MMP-9 expression in human keratinocytes: a new action of honey in wound healing, Archives of Dermatological Research, 305 (2013) 619-627.

[67] J.H. Chung, J.Y. Seo, H.R. Choi, M.K. Lee, C.S. Youn, G.-e. Rhie, K.H. Cho, K.H. Kim, K.C. Park, H.C. Eun, Modulation of Skin Collagen Metabolism in Aged and Photoaged Human Skin In Vivo, 117 (2001) 1218-1224.

[68] J. Lock-Andersen, P. Therkildsen, F. de Fine Olivarius, M. Gniadecka, K. Dahlstrom, T. Poulsen, H.C. Wulf, Epidermal thickness, skin pigmentation and constitutive photosensitivity, Photodermatol Photoimmunol Photomed, 13 (1997) 153-158.

[69] N. Chondrogianni, S. Kapeta, I. Chinou, K. Vassilatou, I. Papassideri, E.S. Gonos, Anti-ageing and rejuvenating effects of quercetin, Experimental Gerontology, 45 (2010) 763-771.

[70] F. Debacq-Chainiaux, J.D. Erusalimsky, J. Campisi, O. Toussaint, Protocols to detect senescence-associated beta-galactosidase (SA-[beta]gal) activity, a biomarker of senescent cells in culture and in vivo, Nat. Protocols, 4 (2009) 1798-1806.

[71] N. Agar, A.R. Young, Melanogenesis: a photoprotective response to DNA damage?, Mutation Research/Fundamental and Molecular Mechanisms of Mutagenesis, 571 (2005) 121-132.

[72] H. Ando, H. Kondoh, M. Ichihashi, V.J. Hearing, Approaches to Identify Inhibitors of Melanin Biosynthesis via the Quality Control of Tyrosinase, Journal of Investigative Dermatology, 127 (2007) 751-761.

[73] J.A. Rothwell, A.J. Day, M.R.A. Morgan, Experimental Determination of Octanol−Water Partition Coefficients of Quercetin and Related Flavonoids, Journal of Agricultural and Food Chemistry, 53 (2005) 4355-4360.

[74] D. Fasolo, V.L. Bassani, H.F. Teixeira, Development of topical nanoemulsions containing quercetin and 3-O-methylquercetin, Pharmazie, 64 (2009) 726-730.

[75] M. Chessa, C. Caddeo, D. Valenti, M. Manconi, C. Sinico, A.M. Fadda, Effect of Penetration Enhancer Containing Vesicles on the Percutaneous Delivery of Quercetin through New Born Pig Skin, Pharmaceutics, 3 (2011) 497-509.

[76] S. Scalia, E. Franceschinis, D. Bertelli, V. Iannuccelli, Comparative evaluation of the effect of permeation enhancers, lipid nanoparticles and colloidal silica on in vivo human skin penetration of quercetin, in: Skin Pharmacol Physiol, Basel., Switzerland, 2013, pp. 57-67.

[77] S. Bose, Y. Du, P. Takhistov, B. Michniak-Kohn, Formulation optimization and topical delivery of quercetin from solid lipid based nanosystems, International Journal of Pharmaceutics, 441 (2012) 56-66.

[78] S. Bose, B. Michniak-Kohn, Preparation and characterization of lipid based nanosystems for topical delivery of quercetin, European Journal of Pharmaceutical Sciences, 48 (2013) 442-452.

[79] S. Sapino, E. Ugazio, L. Gastaldi, I. Miletto, G. Berlier, D. Zonari, S. Oliaro-Bosso, Mesoporous silica as topical nanocarriers for quercetin: characterization and in vitro studies, Eur J Pharm Biopharm, 89 (2015) 116-125.

[80] A. Saija, A. Tomaino, D. Trombetta, M. Giacchi, A.D. Pasquale, F. Bonina, Influence of different penetration enhancers on in vitro skin permeation and in vivo photoprotective effect of flavonoids, International Journal of Pharmaceutics, 175 (1998) 85-94.

[81] L. Montenegro, C. Carbone, C. Maniscalco, D. Lambusta, G. Nicolosi, C.A. Ventura, G. Puglisi, In vitro evaluation of quercetin-3-O-acyl esters as topical prodrugs, International Journal of Pharmaceutics, 336 (2007) 257-262.

[82] F.P. Schmook, J.G. Meingassner, A. Billich, Comparison of human skin or epidermis models with human and animal skin in in-vitro percutaneous absorption, International Journal of Pharmaceutics, 215 (2001) 51-56.

[83] R.L. Bronaugh, R.F. Stewart, E.R. Congdon, Methods for in vitro percutaneous absorption studies II. Animal models for human skin, Toxicology and Applied Pharmacology, 62 (1982) 481-488.

[84] D. Chantasart, S.K. Li, N. He, K.S. Warner, S. Prakongpan, W.I. Higuchi, Mechanistic studies of branched-chain alkanols as skin permeation enhancers, Journal of Pharmaceutical Sciences, 93 (2004) 762-779.

[85] C. Marianecci, F. Rinaldi, M. Mastriota, S. Pieretti, E. Trapasso, D. Paolino, M. Carafa, Anti-inflammatory activity of novel ammonium glycyrrhizinate/niosomes delivery system: human and murine models, J Control Release, 164 (2012) 17-25.

[86] H. Durrheim, G.L. Flynn, W.I. Higuchi, C.R. Behl, Permeation of hairless mouse skin I: Experimental methods and comparison with human epidermal permeation by alkanols, J Pharm Sci, 69 (1980) 781-786.

[87] E.C. Jung, H.I. Maibach, Animal models for percutaneous absorption, J Appl Toxicol, 35 (2015) 1-10.

[88] A. Capt, A.P. Luzy, D. Esdaile, O. Blanck, Comparison of the human skin grafted onto nude mouse model with in vivo and in vitro models in the prediction of percutaneous penetration of three lipophilic pesticides, Regul Toxicol Pharmacol, 47 (2007) 274-287.

[89] P.S. Banerjee, W.A. Ritschel, Transdermal permeation of vasopressin. I. Influence of pH, concentration, shaving and surfactant on in vitro permeation, International Journal of Pharmaceutics, 49 (1989) 189-197.

[90] I.P. Dick, R.C. Scott, Pig ear skin as an in-vitro model for human skin permeability, J Pharm Pharmacol, 44 (1992) 640-645.

[91] S. Singh, K. Zhao, J. Singh, IN VITRO PERMEABILITY AND BINDING OF HYDROCARBONS IN PIG EAR AND HUMAN ABDOMINAL SKIN, Drug and Chemical Toxicology, 25 (2002) 83-92.

[92] S. Hoeller, A. Sperger, C. Valenta, Lecithin based nanoemulsions: A comparative study of the influence of non-ionic surfactants and the cationic phytosphingosine on physicochemical behaviour and skin permeation, International Journal of Pharmaceutics, 370 (2009) 181-186.

[93] E. Yilmaz, H.-H. Borchert, Design of a phytosphingosine-containing, positively-charged nanoemulsion as a colloidal carrier system for dermal application of ceramides, European Journal of Pharmaceutics and Biopharmaceutics, 60 (2005) 91-98.

[94] Y. Baspinar, H.-H. Borchert, Penetration and release studies of positively and negatively charged nanoemulsions—Is there a benefit of the positive charge?, International Journal of Pharmaceutics, 430 (2012) 247-252.

[95] E.W. Smith, H.I. Maibach, Percutaneous Penetration Enhancers, Taylor & Francis, 1995.

[96] M.J. Bartek, J.A. Labudde, H.I. Maibach, SKIN PERMEABILITY IN VIVO: COMPARISON IN RAT, RABBIT, PIG AND MAN, J Investig Dermatol, 58 (1972) 114-123.

[97] N.H.P. Cnubben, G.R. Elliott, B.C. Hakkert, W.J.A. Meuling, J.J.M. van de Sandt, Comparative in Vitro–in Vivo Percutaneous Penetration of the Fungicide ortho-Phenylphenol, Regulatory Toxicology and Pharmacology, 35 (2002) 198-208.

[98] D.W. Lachenmeier, Safety evaluation of topical applications of ethanol on the skin and inside the oral cavity, Journal of Occupational Medicine and Toxicology (London, England), 3 (2008) 26-26.

[99] B.J. Aungst, N. J. Rogers, E. Shefter, Enhancement of naloxone penetration through human skin in vitro using fatty acids, fatty alcohols, surfactants, sulfoxides and amides, International Journal of Pharmaceutics, 33 (1986) 225-234.

[100] K.H. Valia, Y.W. Chien, E.C. Shinal, Long-Term Skin Permeation Kinetics of Estradiol (I): Effect of Drug Solubilizer-Polyethylene Glycol 400, Drug Development and Industrial Pharmacy, 10 (1984) 951-981.

[101] P. Catz, D.R. Friend, Transdermal delivery of levonorgestrel. VIII. Effect of enhancers on rat skin, hairless mouse skin, hairless guinea pig skin, and human skin, International Journal of Pharmaceutics, 58 (1990) 93-102.

[102] N. Suwanpidokkul, P. Thongnopnua, K. Umprayn, Transdermal delivery of zidovudine (AZT): The effects of vehicles, enhancers, and polymer membranes on permeation across cadaver pig skin, AAPS PharmSciTech, 5 (2004) 82-89.

[103] P.P. Sarpotdar, J.L. Gaskill, R.P. Giannini, Effect of polyethylene glycol 400 on the penetration of drugs through human cadaver skin in vitro, J Pharm Sci, 75 (1986) 26-28.

[104] J. Pardeike, A. Hommoss, R.H. Müller, Lipid nanoparticles (SLN, NLC) in cosmetic and pharmaceutical dermal products, International Journal of Pharmaceutics, 366 (2009) 170-184.

[105] A. Patzelt, H. Richter, F. Knorr, U. Schäfer, C.-M. Lehr, L. Dähne, W. Sterry, J. Lademann, Selective follicular targeting by modification of the particle sizes, Journal of Controlled Release, 150 (2011) 45-48.

[106] B. Baroli, Penetration of nanoparticles and nanomaterials in the skin: Fiction or reality?, Journal of Pharmaceutical Sciences, 99 (2010) 21-50.

Part II:

Experimental work

Chapter one: Quercetin smartCrystals®

Chapter two: Quercetin lipid nanocapsules

Chapter three: Quercetin liposomes and comparative study

Complementary results

Chapter one: Quercetin smartCrystals®

Goals:

Development of quercetin smartCrystals®

Physicochemical characterization

Kinetic solubility enhancement

Burst dissolution profile

Incorporation to nonionic gel

Cellular safety on VERO cells

Protective activity on VERO cells

Part II:

Experimental work

Chapter one: Quercetin smartCrystals®

Preface

In this chapter, the first approach of quercetin nanocrystals development using the second-generation technology (smartCrystals®) is presented. SmartCrystals® are produced by combing both bead milling with subsequent high pressure homogenization at relatively low pressure (300 bar). This technology enables the use of bead milling with reduced time compared to first generation nanocrystals and the implementation of the high pressure homogenization for only two cycles compared to more than 15 in the one step process. Herein, the superiority of smartCrystals® technology over first generation nanocrystals is discussed in details.

Drug nanocrystals are considered as new chemical entities as drug physicochemical properties and behavior on cells (cellular toxicity) may vary after nanonization [1]. Some drugs such as taxol® and paclitaxel® showed an increase of cellular toxicity when they are produced using nanocrystal technologies. Higher toxicity on MCF-7 human breast cancer cell line is then favored [2]. Others drugs presented the same safe profile or sometimes had lower toxicity allowing them to be produced for pharmaceutical market such as Emend® (Merck) and Tricor® (Abbott). Therefore and for the first time, we evaluated quercetin nanocrystals cellular toxicity and antioxidant activity on cells.

In this study, quercetin smartCrystals® formulations were developed by screening different surfactants for the optimal stabilization of the nanocrystals in suspension: TPGS, Poloxamer® 188, Tween® 80, Plantacare® 810 and Plantacare® 1200. The selection of the surfactants is based on previous studies. Derivatives of vitamin E were previously used for preparation of quercetin nanostructured lipid carriers [3]. The results obtained with quercetin nanostructured lipid carriers using TPGS (a novel stabilizer composed of vitamin E) are interesting to be tested for stabilization of quercetin nanosuspensions. Poloxamer® 188 is a copolymer surfactant known to be used in nanocrystals formulation with good physical stability for 3 months [4, 5]. Plantacare® series are natural, nonionic, polyhydroxy stabilizers, with steric stabilization properties. Plantacare® 810 was

used to stabilize drugs such as lutein [6] and fenofenamic acid [7] loaded within solid lipid nanoparticles (SLN) and nanostructured lipid carriers formulation, allowing steric stabilization next to electrostatic stabilization. Plantacare® 1200 presents a microemulsion stabilization effect with lower temperature dependency [8]. It was also used for dermal application of linoleic acid in microemulsion for the treatment of xerosis [9]. Furthermore, Plantacare® series are considered skin friendly [10]. They showed a slight skin irritating capacity in epicutaneous patch test when compared to other surfactants [11].

References

[1] U.S.F.a.D. Administration, Nanotechnology - Nanotechnology Fact Sheet, in: FDA (Ed.), Office of the Commissioner, USA, 2015.

[2] Z. Lin, W. Gao, H. Hu, K. Ma, B. He, W. Dai, X. Wang, J. Wang, X. Zhang, Q. Zhang, Novel thermo-sensitive hydrogel system with paclitaxel nanocrystals: High drug-loading, sustained drug release and extended local retention guaranteeing better efficacy and lower toxicity, Journal of Controlled Release, 174 (2014) 161-170.

[3] M. Sun, S. Nie, X. Pan, R. Zhang, Z. Fan, S. Wang, Quercetin-nanostructured lipid carriers: characteristics and anti-breast cancer activities in vitro, Colloids Surf B Biointerfaces, 113 (2014) 15-24.

[4] P.R. Mishra, L.A. Shaal, R.H. Müller, C.M. Keck, Production and characterization of Hesperetin nanosuspensions for dermal delivery, International Journal of Pharmaceutics, 371 (2009) 182-189.

[5] B. Morakul, J. Suksiriworapong, J. Leanpolchareanchai, V.B. Junyaprasert, Precipitation-lyophilization-homogenization (PLH) for preparation of clarithromycin nanocrystals: Influencing factors on physicochemical properties and stability, International Journal of Pharmaceutics, 457 (2013) 187-196.

[6] K. Mitri, R. Shegokar, S. Gohla, C. Anselmi, R.H. Müller, Lipid nanocarriers for dermal delivery of lutein: Preparation, characterization, stability and performance, International Journal of Pharmaceutics, 414 (2011) 267-275.

[7] J.C. Schwarz, A. Weixelbaum, E. Pagitsch, M. Löw, G.P. Resch, C. Valenta, Nanocarriers for dermal drug delivery: Influence of preparation method, carrier type and rheological properties, International Journal of Pharmaceutics, 437 (2012) 83-88.

[8] W. von Rybinski, B. Guckenbiehl, H. Tesmann, Influence of co-surfactants on microemulsions with alkyl polyglycosides, Colloids and Surfaces A: Physicochemical and Engineering Aspects, 142 (1998) 333-342.

[9] A.S.B. Goebel, U. Knie, C. Abels, J. Wohlrab, R.H.H. Neubert, Dermal targeting using colloidal carrier systems with linoleic acid, European Journal of Pharmaceutics and Biopharmaceutics, 75 (2010) 162-172.

[10] T.F. Tadros, Surfactants in Personal Care and Cosmetics, in: Applied Surfactants, Wiley-VCH Verlag, 2005, pp. 399-432.

[11] A. Mehling, M. Kleber, H. Hensen, Comparative studies on the ocular and dermal irritation potential of surfactants, Food and Chemical Toxicology, 45 (2007) 747-758.

Dermal quercetin smartCrystals®: formulation development, antioxidant activity and cellular safety

T. Hataheta, M. Morillea, A. Hommossb, C. Dorandeua, R. H. Müllerb and S. Bégua*

[a] Institut Charles Gerhardt Montpellier, UMR 5253 CNRS-ENSCM-UM, Equipe Matériaux Avancés pour la Catalyse et la Santé, 8 rue de l'Ecole Normale, 34296 Montpellier Cedex 5, France.

[b] Institute of Pharmacy, Department of Pharmaceutics, Biopharmaceutics and NutriCosmetics, Free University of Berlin, Kelchstr. 31, Berlin 12169, Germany.

[*] Corresponding author.

Research article published in the

European Journal of Pharmaceutics and Biopharmaceutics

Volume 102, May 2016, Pages 51–63

doi:10.1016/j.ejpb.2016.03.004

Abstract:

Flavonoids are natural plant pigments, which possess high antioxidative and antiradical activities. However, their poor water solubility led to a limited bioavailability. To overcome this major hurdle, quercetin nanocrystals were produced implementing smartCrystals® technology. This process combines bead milling and subsequent high-pressure homogenization at relatively low pressure (300 bar). To test the possibility to develop a dermal formulation from quercetin smartCrystals®, quercetin nanosuspensions were admixed to Lutrol® F127 and hydroxythylcellulose nonionic gels. The physicochemical properties (morphology, size and charge), kinetic solubility, dissolution velocity and the antioxidant properties (DPPH assay) as well as the cellular interaction of the produced quercetin smartCrystals® were studied and compared to crude quercetin powder. Quercetin smartCrystals® showed a strong increase in the kinetic solubility and the dissolution velocity (7.6 fold). SmartCrystals® loaded or not into gels proved to be physically stable over a period of three months at 25°C. Interestingly, *in vitro* DPPH assay confirmed the preservation of quercetin antioxidative properties after nanonization. In parallel, the nanocrystalline form did not display cellular toxicity, even at high concentration (50 µg/ml), as assayed on an epithelial cell line (VERO cells). In addition, the nanocrystalline form confirmed a protective activity for VERO cells against hydrogen peroxide induced toxicity *in vitro.* This new formulation presents a promising approach to deliver quercetin efficiently to skin in well-tolerated formulations.

Key words:

Quercetin, smartCrystals®, nanocrystals, nanosuspensions, flavonoids, antioxidative effect, nonionic gel, cellular toxicity, Hydrogen peroxide induced toxicity

Graphical abstract:

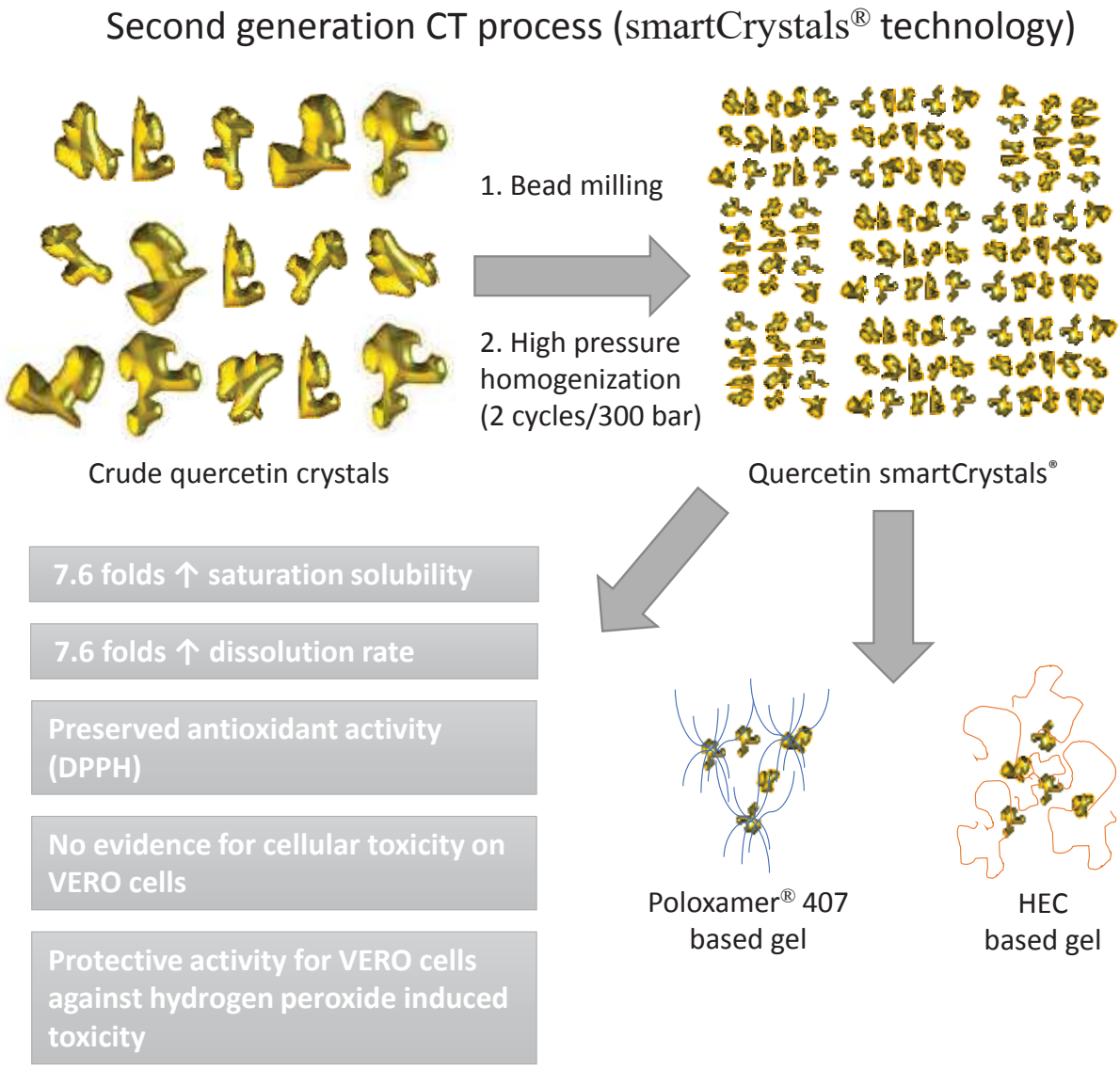

1. Introduction

Antioxidants are of high interest in the prevention of oxidative stress not only for oral administration but also for topical administration. In this context, antioxidants are used to support treatment for diseases that require a higher activity of the immune system (mosquito borne diseases or viral infections) [1-3]. In dermal preparations, products containing antioxidants are useful for protection against UV radiation damage [4, 5] or for prevention of skin cancer [6-8]. Flavonoids are plant pigments found in a wide variety of fruits and vegetables such as apples [9], pears [10], onions [11], and red wine [12]. Many flavonoids like quercetin, rutin, hesperidin and naringenin are potent antioxidants [13]. Quercetin was chosen as an active principle because it is considered as the most powerful antioxidant, and the most distributed in nature [14]. Moreover, it has already been used for its antiinflammatory [15, 16] and anti-tumor activities [17, 18], also for cellular protective properties in brain [19], liver [20], kidney [21] and colon diseases [22]. In order to mimic the topical application, UV irradiation was used to introduce lipid peroxidation on phosphatidylcholine liposomes. Interestingly, in this model, quercetin showed the highest protective activity among various tested flavonoids [14, 23]. This UV protective effect is of high relevance in skin ageing and wrinkling [24] and indicates quercetin as potential active drug for skin protection against photoageing.

Nevertheless, its poor water solubility limits dermal bioavailability leading to a decrease in its potential for topical administration. In this context, nanocrystals proved to be a successful formulation strategy for the increase of dermal bioavailability of poorly soluble actives [25]. Nanocrystals have a simple but effective mechanism of bioavailability enhancement by increasing the kinetic solubility (Cs) and thus increasing the concentration gradient between the application site (e.g. dermal formulation) and the acceptor medium (e.g. skin). In addition, a higher dissolution velocity due to the large surface area occurs. Finally, nanocrystals show high adhesion and prolonged retention times, by adhering firmly to the skin [26]. Nanocrystals can be obtained by different industrial processes. The first-generation of nanocrystals used to be produced by different processes, but generally in a one-step procedure: bottom up such as "Nanomorph®", or top down processes such as wet bead milling developed by Alkermes® [27] and high-pressure homogenization (HPH) developed by R.H. Müller *et al*. from the company DDS Germany [28]. The second-generation of nanocrystals are generally produced thanks to combinative process, such

as association of microprecipitation followed by HPH (Nanoedge or H69 technologies), spray drying and HPH (H42 technology), freeze drying and HPH (H96) and wet bead milling associated to HPH (CT technology) [29]. SmartCrystals® were developed as second-generation technology [30] using combination processes as a "toolbox" for tailor-made nanocrystals specific for different demands. In this study, the combination technology of bead milling and subsequent HPH was performed (known as CT process®) [31]. This yields monodispersed nanocrystals, homogenous in size with increased physical stability [32].

Research groups mainly focused on the preparation of quercetin nanocrystals either by bead milling or by high-pressure homogenization [33, 34] . Others focused on the application of nanotechnology (nanocrystals, solid lipid nanoparticles, etc.…) for expected oral delivery [35, 36]. Up until now, the advantages of formulating quercetin nanocrystals using the second-generation of smartCrystals® for dermal application have not been investigated.

To stabilize these smartCrystals®, five different stabilizers were tested. Two standard nonionic stabilizers: (i) polysorbate 80 (Tween® 80) and (ii) poloxamer 188 (Lutrol® F68), two alkyl polyglucoside "green" stabilizers (iii) caprylyl / capryl glucoside (Plantacare® 810) and (iv) lauryl glucoside (Plantacare® 1200) which were previously used in drug nanocrystals stabilizations [37-39]. Finally, (v) a vitamin E derived surfactant, α-tocopheryl polyethylene glycol 1000 succinate (TPGS) is used as a novel stabilizer for drug nanocrystals. The obtained quercetin smartCrystals® were characterized and compared to crude quercetin regarding physicochemical characteristics (size, charge, shape, kinetic solubility and dissolution velocity) as well as antioxidative properties and cytotoxicity against an epithelial cell line (VERO cells). As a last step, quercetin nanosuspensions were admixed to two different nonionic gels Lutrol® F127 (poloxamer 407) and hydroxythylcellulose (HEC) and the stability of the smartCrystals® in suspension and in dermal non-ionic gels was assessed over a period of three months at three different temperatures (4°C, 25°C and 40°C).

2. Materials and Methods

2.1 Materials

Quercetin aglycone (3, 3', 4', 5, 7-pentahydroxy-2-phenylchromen-4-one), 3-(4, 5-dimethylthiazol-2-yl)-2, 5-diphenyltetrazolium bromide (MTT) and hydroxythylcellulose (HEC) were purchased from Sigma (Sigma Aldrich, France). Tween® 80 (polysorbate 80), TPGS (α tocopheryl polyethylene glycol 1000 succinate), Plantacare® 810 (caprylyl/capryl glucoside), and Plantacare® 1200 (lauryl glycoside) were purchased from Cognis (Ludwigshafen, Germany). Lutrol® F68 (poloxamer188, 1800 g/mol) and Lutrol® F127 (poloxamer407) were kindly provided by BASF (Ludwigshafen, Germany).

2.2 Preparation of quercetin nanosuspensions

Crude quercetin (5%) was suspended in a 0.5% stabilizer solution (Tween® 80, TPGS, Lutrol® F68, Plantacare® 810 or Plantacare® 1200) in milliQ water. Quercetin nanosuspensions were then produced using the smartCrystals® technology [30]. Briefly, 120 ml of primary quercetin suspension were subjected to 30 min milling time using a pearl mill Bùhler PML 2 (Bùhler AG, Uzwil, Switzerland) with 0.2 mm zirconium oxide beads as milling medium. Samples were withdrawn every 5 minutes from the wet bead-milling machine to perform in-process size measurements (section 2.5 and 2.6). Optimal milling time was determined after analyzing the sizes. After milling, the suspension was separated from the beads using a sieve (mesh size 80). The beads were then washed with 120 ml of original 0.5% stabilizer solution to collect any quercetin crystals adhered to the beads. The resulted suspensions were then homogenized using a high-pressure homogenizer (HPH), Micron LAB 40 (APV Gaulin GmbH, Germany) for two cycles at 300 bar [40]. Finally, the selected stabilizers were used to prepare new batches using the concluded optimal milling time.

2.3 Nanosuspensions - Gel formulation

Quercetin nanosuspensions were admixed to two different gel formulations: Lutrol® F127, which is a temperature dependent gelling agent or hydroxythylcellulose (HEC). First, 5% quercetin nanosuspensions were diluted with milliQ water by a mass ratio factor of 1:1.6 then Lutrol® F127 or HEC was added to allow a final concentration of 16.7% and 1.7% respectively [41, 42]. The resulted gels were tested for stability at 4°C, 25°C and 40°C. Size, polydispersity index (PDI) and zeta potential of smartCrystals® were measured at day 0, day 30 and day 90, after a dilution step,

to break the gel and allow measurement by photon correlation spectroscopy (see thereafter, section 2.5 for precise sample preparation).

2.4 Lyophilisation

Quercetin nanosuspensions were frozen to -80°C using Cryonext freezer (Cryonext laboratories, France), then freeze-dried by Heto lyophilizer (PowerDry Laboservices, France) for 24 hours to obtain dry quercetin smartCrystals®.

2.5 Photon correlation spectroscopy and electrophoretic mobility measurements

10 µl of the quercetin nanosuspension was added to 10 ml of MilliQ water, vortexed for 10 seconds and then measured at 25°C to obtain the average size (Z-average) and polydispersity index (PDI) by photon correlation spectroscopy using a Zetasizer Nano ZS (Malvern Instruments, UK). 10 µl of the quercetin nanosuspension was diluted with either 10 ml of 50 µS/cm water (calculated by the addition of NaCl solution to MilliQ water) or 10 ml of original stabilizer solution [43]. 1 ml of this mixture was transferred into a Disposable Capillary Cell (Malvern Instruments, UK) allowing the measurement of the electrophoretic velocity of particles in an electrical field and the determination of zeta potential thanks to Helmholtz–Smoluchowski equation.
For size measurements after gel formulation, 10 µl of the gel formulation was diluted with 10 ml MilliQ water and vortexed for 30 sec, and then 2 ml was transferred to PCS analysis. For zeta potential measurements, 10 µl of the gel formulation was diluted with 10 ml of either 50 µS/cm water or original stabilizer solution, vortexed for 1 min, then 1 ml was transferred to PCS for measurement.

2.6 Laser diffraction (LD)

Size distribution was measured by laser diffraction (Mastersizer 2000 Malvern Instruments, UK) with an agitation speed of 1750 rpm. Sample volume was adjusted according to the concentration indicated by the manufacturer using deionized water. All sizes were analyzed using the

characterization mode of the Mie equation with optical parameters 0.01 for the imaginary refractive index (IRI) and 1.59 for the real refractive index (RI).

2.7 X ray analysis

X-ray diffraction patterns of dry quercetin smartCrystals® were analyzed using a D8 Advance LA Cu 1.5406 Å Bruker axs (Burker, Karlsruhe, Germany) equipped with a generator (40kv 40mA) and a parafocusing geometry circle of Bragg Brentano. The test was performed between angles of 2 to 70 θ at a fixed detection velocity, a solid detector lynx eyes 1D was used for the sample detection.

2.8 Transmission electron microscopy

Transmission electron microscope (TEM) analysis was performed with a TEM Jeol 1200EXII (Jeol Ltd, Japan) with an accelerating voltage of 100 kV and equipped with a 4k/3 kelopixels quemesa Camera (Olympus, Japan). 5 µl of the nanosuspension was left to dry for 30 min at 25°C after being deposited on uncoated carbon TEM grids Type CU formar carbon 3 MMM (Agar Scientific, UK). Images were taken using measure IT software at appropriate magnification.

2.9 HPLC analysis

HPLC was used for the determination of quercetin concentration in the nanosuspensions and the kinetic solubility. The chromatographic analysis of the quercetin nanosuspensions was performed on a LC62010HT **(**Shimadzu, Kyoto, Japan) using a C18 column Prontosil (120-5-C18 H5.0 µm), NC-04 (250 ×4.0 mm) as stationary phase and a mobile phase solution composed of 10% methanol 80% acetonitrile and 10% of phosphoric acid 0.2% at a pH=1.9. The detection was carried by a UV lamp (UV-VIS detector, Shimadzu, Kyoto, Japan) at 368 nm, which is specific for quercetin [44].

Two experiments were developed for the determination of (i) quercetin concentration in the nanosuspension (experiment 1: quercetin is extracted by methanol and then quantified) and (ii) kinetic solubility (experiment 2: quercetin concentration is determined in solution without extraction).

For experiment 1, a fixed flow rate of 1 ml/min during a run time of 15 minutes was set and applied to calculate the quercetin concentration in the final nanosuspension. Standard quercetin solutions prepared in methanol within a range 62.5-500 µg/ml were used as a calibration curve (calibration curve 1 r^2= 0.999 and %RSD is 2.5). The quercetin retention time was 2.3 min. 10 µl of the quercetin nanosuspension was diluted to 1 ml with methanol and then injected (n=3).
Secondly, for experiment 2 (quercetin kinetic solubility measurements), a gradient flow rate was used in a 20 min run time by increasing the acetonitrile concentration from 40% to 80% while the acidified water concentration decreased from 50% to 10%. The gradient flow was performed in order to delay the elution of quercetin from that of Tween® 20. The quercetin retention time was 4.10 min. Serial dilutions of known concentrations of quercetin in 0.5% Tween® 20 PBS buffer pH=7.4 were used to prepare a calibration curve from 0.2 to 4 µg/ml (calibration curve 2 r^2= 0.996 and %RSD is 7.7). Quercetin quantification limit was 0.1 µg/ml. This was performed in order to mimic the situation in an aqueous medium. Then 1 ml of the quercetin nanosuspension, and the quercetin physical dispersion (crude quercetin suspended in milliQ water) were centrifuged at 21,000 gravitational force for 1 h using a Sigma 2k 25 ultracentrifuge (sigma Zentrifugen, GmbH, Germany), to separate the non-solubilized quercetin (bottom of the tube) to the solubilized one (in the supernatant). Centrifugation time is adjusted according to the *Stoke* equation for particles sedimentation. Supernatants were collected and 50 µl of each were injected into HPLC and the water kinetic solubility was calculated according to the method mentioned.

2.10 Dissolution velocity (flow through cells)

Flow through cell USP apparatus 4 equipped with a piston pump Sotax (Sotax AG, Aesch, Switzerland) was used for testing the dissolution velocity. 5 mg of dry quercetin smartCrystals® or crude quercetin were accurately weighed using an OHAUS Discovery balance (OHAUS Corporation, New Jersey, USA) and were placed in the sample chamber. 100 ml of degassed MilliQ water were used as release medium to maintain sink conditions. The flow rate was maintained at 8 ml/min at 32°C (n=3) and 1 ml of the release medium was withdrawn at 5, 10, 15, 30, 60 and 120 minutes, then replaced by 1 ml of fresh medium. Afterwards, the quercetin concentration was determined: 50 µl of withdrawn samples were diluted with 950 µl milliQ water and analyzed using HPLC (section 2.9, experiment 2).

2.11 Hydrogen donating ability *in vitro* by 2, 2-diphenyl-1-picrylhydrazyl (DPPH)

Quercetin showed linear DPPH inhibition in concentrations between 1 and 6 µg/ml. Quercetin nanosuspensions with selected stabilizers were diluted with methanol to fit into linearity concentrations of quercetin. DPPH concentration was adjusted to 400 µM. The volume of DPPH solution to quercetin solution was 1:3 (volume factor). DPPH with methanol was used as a positive control with methanol as a reference. The activity reaction was performed in the dark for 30 min, afterwards the DPPH absorbance was measured at 517 nm using a UV/Vis spectrophotometer (Lambda 35, PerkinElmer, USA). Then the DPPH percentage activity was calculated as efficient concentration 50 (EC50) (the concentration of crude quercetin or quercetin smartCrystals® able to reduce 50 % of the initial DPPH concentration).

2.12 Cell culture and cellular cytotoxicity on Vero cells

Vero cells (CCL81™) were purchased from American Type Culture Collection ATCC (Manassas, Virginia, USA). Cells were cultured using Dulbecco's Modified Eagle's medium (DMEM) (Gibco®) with 10% fetal bovine serum (FBS) purchased from Life technologies™ (Carlsbad, California, USA). To assess the potential cytotoxicity of the formulation, cells were cultured at a concentration of 1×10^5 cells/well in 24 well plates (Corning, New York, USA). Cells were then exposed to 5, 15, 25, 50 µg/ml of crude quercetin, or quercetin smartCrystals® (diluted nanosuspensions) suspended in classic cell culture medium (DMEM + 10% FBS). After 24 hours exposure, cell viability was assessed by the 3-(4, 5-dimethylthiazol-2-yl)-2, 5-diphenyltetrazolium bromide (MTT) assay. The MTT assay evaluates cellular mitochondrial activity by following the cleavage of tetrazolium salts to a soluble formazan dye by succinate-tetrazolium reductase, a mitochondrial enzyme only active in viable cells. MTT (5 mg/ml) was added to each well for 4 hours. Culture media was then aspirated and replaced by 200 µl of acidified isopropanol (0,06N HCl) to dissolve formazan crystals. Finally, 100 µl was transferred to 96 well plates and read at 570 nm and 750 nm using a Multiskan™ GO microplate spectrophotometer (Thermo Scientific™, Waltham, Massachusetts, USA). Non-treated cells were recognized as the positive control and represent the 100% viability.

2.13 Protection against hydrogen peroxide induced cellular toxicity

Cells were cultured at a concentration of 1×10^5 cells/well in 24 well plates and incubated at 37°C, 5% CO_2 for 24 hours. Cells were then exposed to 50 µg/ml of crude quercetin, or quercetin smartCrystals® (diluted nanosuspensions) suspended in classic cell culture medium (DMEM + 10% FBS) for 4 hours. After that, 40 µl of 10 mM of hydrogen peroxide (H_2O_2) were added to each well and incubated for 2 hours. Cells were then washed two times with PBS. Then, 360 µl of DMEM + 10% FBS and 40 µl of MTT were added and let incubated for another 4 hours. Culture media were then aspirated and 200 µl of acidified isopropanol (0,06N HCl) were added. Finally, 100 µl were transferred into 96 well plate and absorbance at 570 nm and 750 nm was determined using a Multiskan™ GO microplate spectrophotometer (Thermo Scientific™, Waltham, Massachusetts, USA) [45].

2.14 Statistical analysis

Statistical analysis of the dissolution velocity and cellular cytotoxicity was run using Stata software (StataCorp, College Station, Texas, USA). A Two-sample t-test with unequal variances was used for the analysis of cellular toxicity results and a two-sample t-test with unequal variances supported with a two-sample Kolmogorov-Smirnov test for equality of distribution functions were used to verify the significant difference of the dissolution profiles. P expresses the significant value where * = $P < 0.05$, ** = $P < 0.01$ and *** = $P < 0.005$ respectively.

3. Results & Discussion

3.1 Optimization of smartCrystals® production process

Optimization of the preparation was performed in two steps: (i) assessing the optimal milling time and (ii) producing the smallest homogenous crystals with each stabilizer (Tween® 80, TPGS, Lutrol® F68, Plantacare® 810 or Plantacare® 1200).

In the first step, the milling time was set for 30 minutes and quercetin size profile was measured every 5 minutes using PCS (Fig. 3.1) and LD (Fig. 3.2). PCS allow the size measurement of

particles from about 3 nm to 3 µm, and LD was therefore used to detect particles larger than 3 µm. LD size results are expressed in terms of the percentage distribution of sizes within the population. Volumes equivalent to the hydrodynamic sphere diameter LD50, LD90, and LD99 diameters are used throughout this article.

By observing the hydrodynamic diameters measured by PCS in Fig. 1, particle size reduction in the nanometer range can be noticed within the first 10 minutes for all the stabilizers. Within 5 min of milling, the sizes were reduced to 329 nm (PDI 0.21), and to 303 nm (PDI 0.24) for quercetin nanosuspensions stabilized with Tween® 80 and TPGS respectively and to 526 nm (PDI 0.3) for quercetin nanosuspensions stabilized with Plantacare® 810. After 10 minutes of milling, the size decreased to reach 502 nm (PDI 0.22) with Lutrol® F68 and 574 nm (PDI 0.22) with Plantacare® 1200 respectively. Nevertheless, after either 5 min (Tween® 80, TPGS and Plantacare® 810 stabilized nanosuspensions) or 10 min milling (Lutrol® F68 and Plantacare® 1200 stabilized nanosuspensions), particles began to agglomerate. Upon this prolonged milling time, the energy used for particles fragmentation is converted into kinetic energy increasing particle adhesion and agglomeration, which could explain this size increase [46].

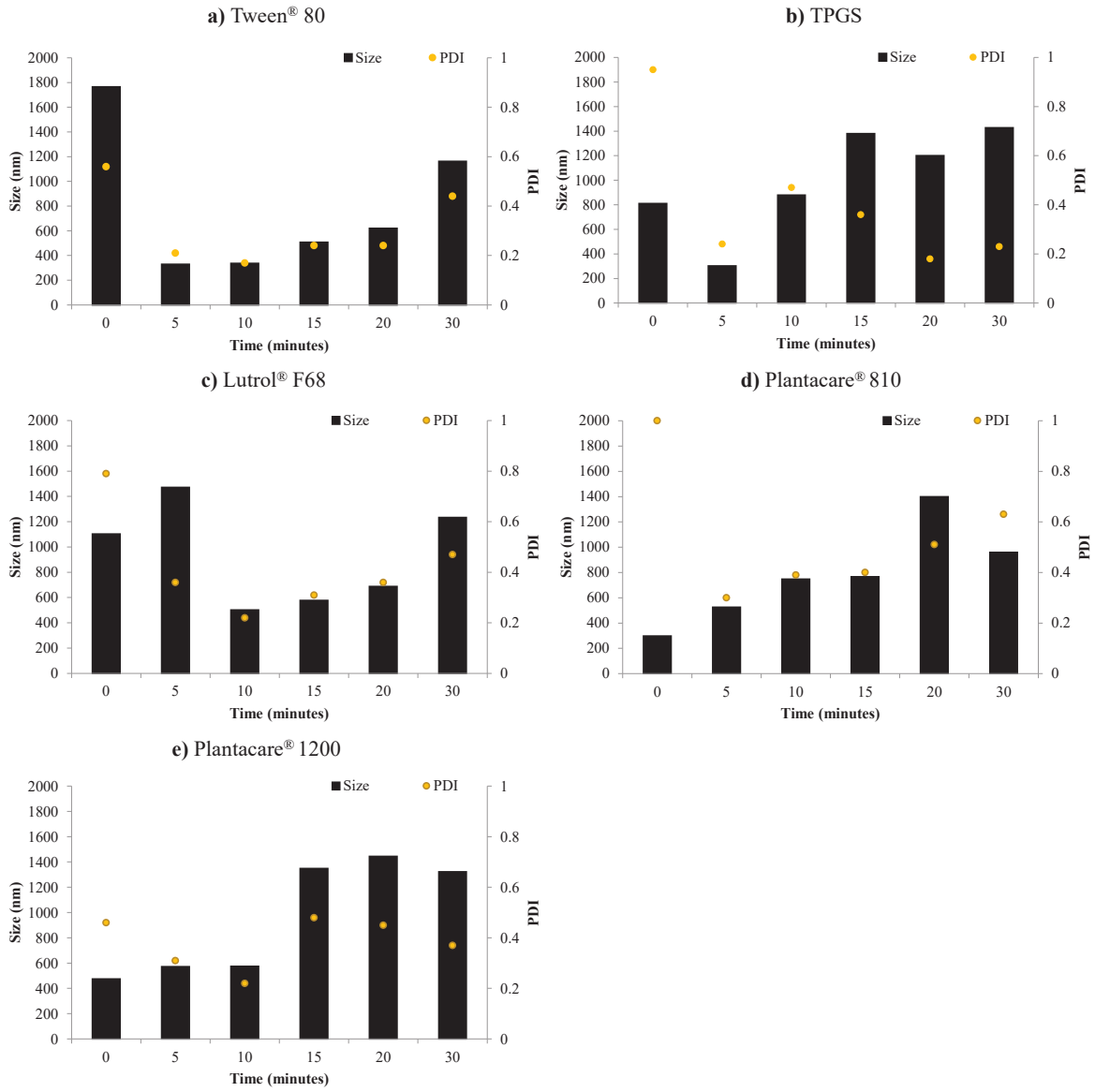

Fig. 1: Quercetin suspensions size and PDI evaluation using PCS

PCS size and polydispersity index (PDI) as a function of milling time in the bead mill of suspensions stabilized with a) Tween® 80, b) TPGS, c) Lutrol® F68, d) Plantacare® 810 and e) Plantacare® 1200.

Fig. 2 shows the LD complementary results for the milling process providing information on larger particles in the suspension. The difference between the value of LD50 and LD99 (which is a diameter sensitive to measure very large particles) gives an indication about particles' aggregation state that cannot be monitored by PCS. Results at time 0 represents the size distribution of quercetin

in the coarse suspension with each stabilizer. Aggregates larger than 3 µm were not observed at 5 minutes milling time with Tween® 80 and Plantacare® 810, but still present with TPGS as LD50 and LD99 5 µm and 32 µm respectively. Looking at Lutrol® F68 and Plantacare® 1200 stabilized nanosuspensions, only Lutrol® F68 at 10 minutes showed aggregation with LD99 equals to 35 µm. Again, by LD upon prolonged milling, particles agglomeration was confirmed with all stabilizers except Tween® 80 and Lutrol® F68. Thus, the best milling time for Tween® 80, TPGS and Plantacare® 810 stabilized nanosuspensions seems to be of 5 minutes whereas for Lutrol® F68 and Plantacare® 1200 stabilized nanosuspensions 10 minutes seems better adapted.

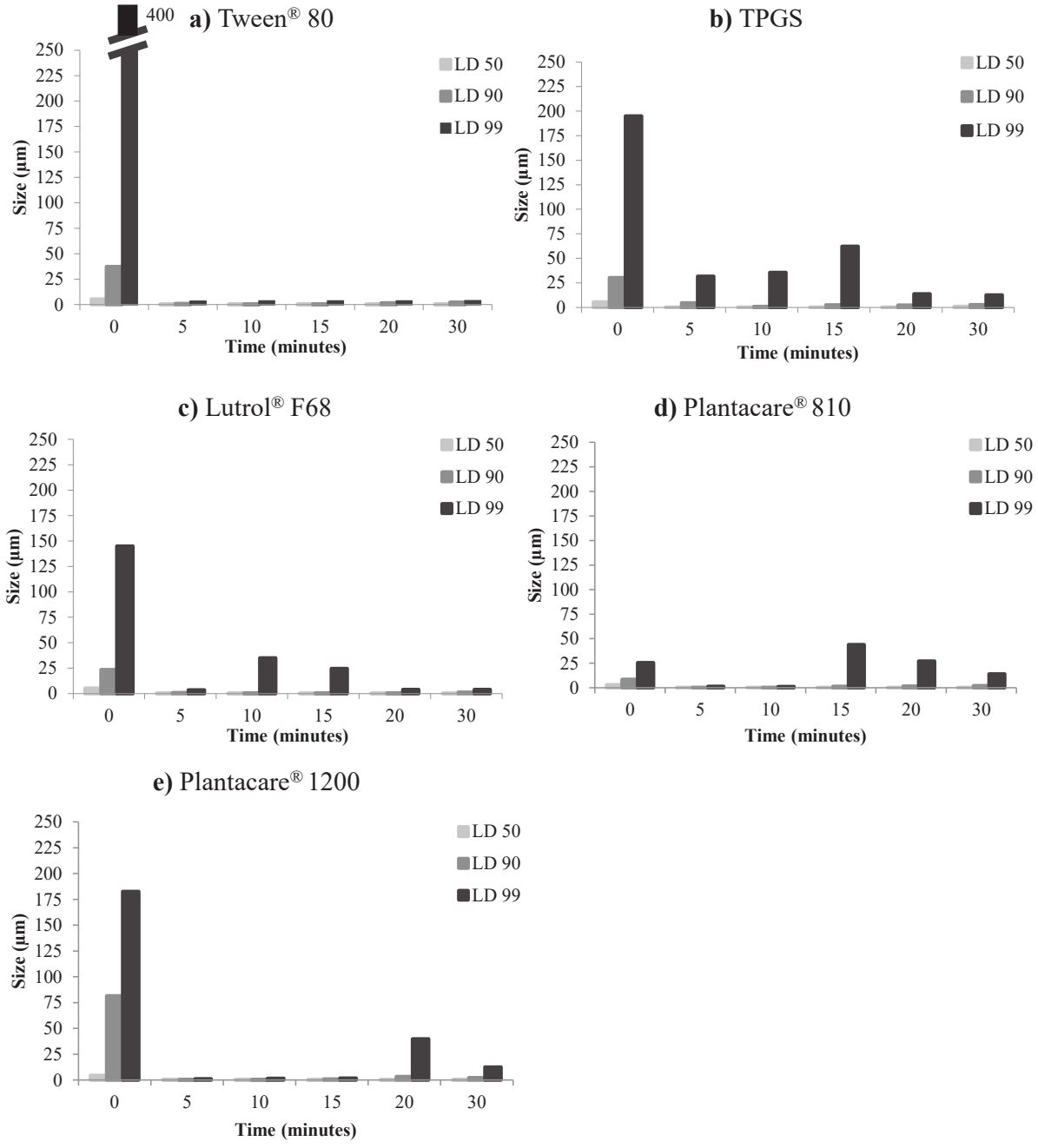

Fig. 2: Quercetin suspensions size distribution evaluation using LD

LD size distribution as a function of milling time in the bead mill of suspensions stabilized with a) Tween® 80, b) TPGS, c) Lutrol® F68, d) Plantacare® 810 and e) Plantacare® 1200.

After the milling step (30 minutes), quercetin nanosuspensions stabilized with the five stabilizers were subjected to the same HPH condition (300 bar, 2 cycles). Fig. 3 presents the PCS and LD

sizes results of the final nanosuspensions. The use of HPH yielded smaller and more homogeneous quercetin nanosuspensions with an average size of 220 nm (PDI 0.19) with Tween® 80, 397 nm (PDI 0.16) with TPGS, 381 nm (PDI 0.24) with Lutrol® F68, 426 nm (PDI 0.38) with Plantacare® 810 and 243 nm (PDI 0.37) with Plantacare® 1200 (Fig. 3, a). LD99 results were all less than 450 nm for all stabilizers confirming the successful disaggregation with HPH (Fig. 3, b). This decrease in particle size and the disappearance of aggregation confirm the advantage of the combinative techniques over one-process techniques. Taking the example of quercetin nanocrystals with Tween® 80 prepared using only bead milling by Kakran's *et al*, quercetin nanocrystals were approximately 340 nm (PDI 0.21)) and the milling time was 60 minutes [34]. By applying the smartCrystals® combinative technique, quercetin smartCrystals® were 220 nm (PDI 019) using only 5 minutes milling followed by HPH.

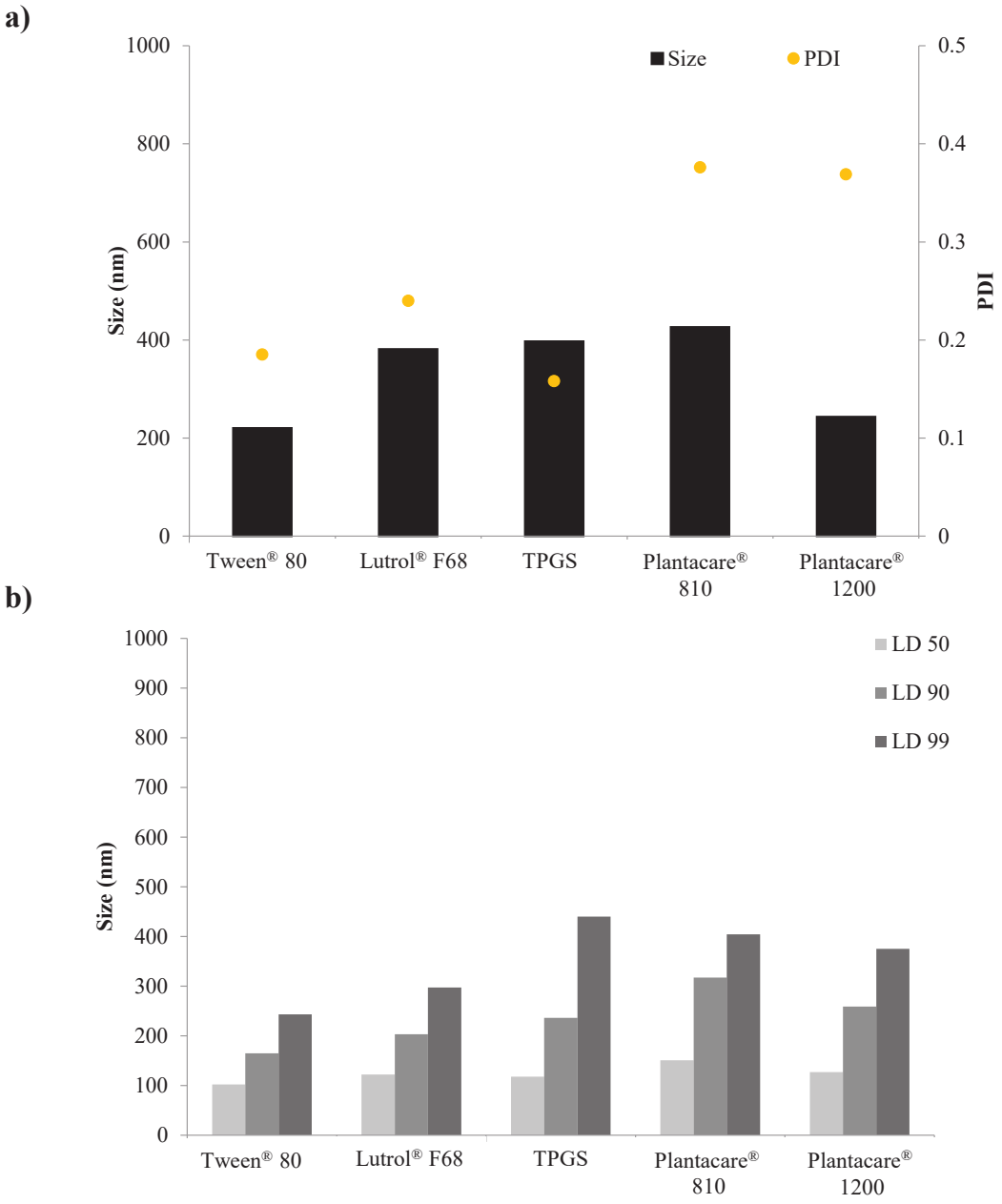

Fig. 3: Final quercetin nanosuspensions size results (PCS/LD).

Size results of the suspensions with 30 min bead milling with the subsequent HPH step (2 cycles at 300 bar). a) PCS size and PDI. b) LD50, LD90 and LD99 of suspensions stabilized with the five different stabilizers.

Taking into account the final suspension size, the smallest average size was obtained with Tween® 80 (220 nm), Plantacare® 1200 (243 nm) and Lutrol® F68 (381 nm) (Fig. 3.3, a). By analyzing PDI data, TPGS was the stabilizer which leads to the lowest polydispersity index of 0.16, followed by Tween® 80 with 0.19 and Lutrol® F68 with 0.24 (Fig. 3.3, a).

From the size, PDI and milling time, it can be concluded that the best two stabilizers for 5% quercetin nanosuspensions prepared by smartCrystals® technology were Tween® 80 and TPGS. SmartCrystals® stabilized with these two stabilizers showed the smallest particles size with homogenous profile in the shortest milling time. As a result, optimized milling conditions with HPH were used to produce new batches of quercetin smartCrystals® stabilized with Tween® 80 and TPGS. The reproduced quercetin nanosuspension was 295 nm (PDI 0.25) with Tween® 80 and 203 nm (PDI 0.24) with TPGS.

Tween® 80 concentration for stabilization of quercetin nanocrystals varied in the literature, from 1 to 2% when 5% quercetin nanosuspensions were prepared by HPH or bead milling. Quercetin nanocrystals prepared only by HPH (20 cycles at 1500 bar) were around 700 nm (PDI 0.17) [47] and quercetin nanocrystals prepared by bead milling alone using 0.2 mm beads were 340 nm (PDI 0.21). By applying the smartCrystals® combination process, a nanometric size of 220 nm (PDI 0.19) was achieved, with two fold lower stabilizers concentration [34].

To resume, small and monodisperse quercetin smartCrystals® were formulated using 2 fold less stabilizer than previously formulated nanocrystals with a shorter production time. This confirms the interest in the use of smartCrystals® combinative technology that allows a reduced milling time, which is very important considering large scale production as long preparation time increases costs and decreases the number of produced batches per day.

3.2 Physicochemical characterizations of quercetin smartCrystals®

3.2.1 Surface charge

To predict the physical stability of quercetin smartCrystals®, zeta potential was measured. The higher the absolute values of the zeta potential, the more stable the particles are expected to be. Results are presented in Fig. 4. The difference between the measurements in the original stabilizer medium (0.5% Tween® 80 or TPGS) and the salted water (50 µS/cm water) provides an indication about the thickness of the diffuse layer, as the diffuse layer is eliminated in the salted water [48]. All zeta potentials of quercetin nanosuspensions were negative, as PEG chains present in the structure of Tween® 80 and TPGS can form negative dipoles that are able to decrease the surface charge proportionally to their concentration [49]. Nanosuspensions stabilized with Tween® 80 compared to TPGS stabilized ones expressed more negative zeta potential in both 50 µS/cm water

(-25.7 compared to -16.1 mV) and in original stabilizer solution (-26.8 mV compared to -22.7 mV) for nanosuspensions with Tween® 80 and TPGS respectively. Both stabilizers sterically stabilize the particles in addition to the electrical repulsive forces they could generate [50]. Indeed, it should be noted that the adsorbed steric stabilizer layer reduces the measured zeta potential, as it shifts the plan of shear to greater distance from the particle surface. Therefore, values around 25 mV observed with Tween® 80 seem sufficient to stabilize the system along with steric stabilization [51]. Regarding TPGS, the difference between values at 50 µS/cm water and original stabilizer solution (-16.1 vs. -22.7 mV) may indicate a thicker adsorbed layer compared to Tween® 80 and hence an increased stability [38].

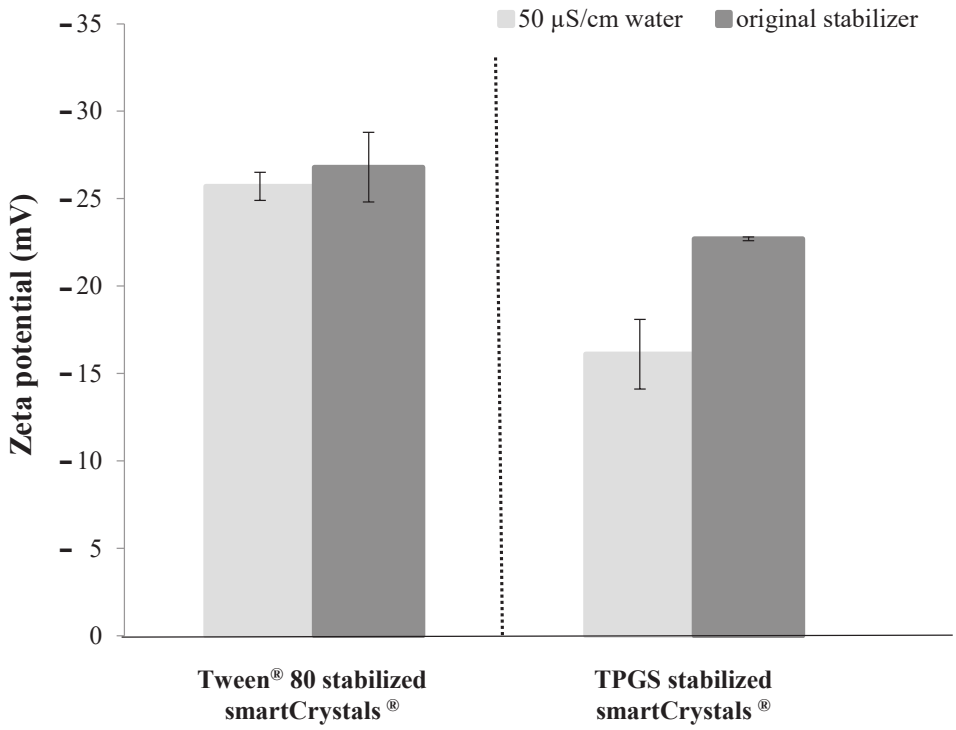

Fig. 4: Zeta potential of quercetin nanosuspensions

Zeta potential of quercetin nanosuspensions with Tween® 80 and TPGS produced by bead milling for 5 minutes followed by 2 cycles of high pressure homogenization at 300 bar. Reacting media 50 µS/cm water and original stabilizer solution.

3.2.2 Quercetin nanosuspensions stability

For all pharmaceutical and cosmetical products, a satisfactory stability profile is desired. Therefore, three months stability tests were performed on quercetin nanosuspensions. Stability tests were conducted at three different temperatures 4°C, 25°C and 40°C. The average PCS size and PDI at day 0, day 30 and day 90 (Fig. 5, a) were used to assess the stability.
The increase in quercetin nanosuspension size from day 0 to day 90 at 25°C was 50 nm (from 295 to 343 nm) with Tween® 80, and 150 nm (from 203 to 340 nm) with TPGS. Interestingly, PDI remained under 0.30 for both formulations (Fig. 5, a). This increase in size has already been observed with lutein nanocrystals when prepared by HPH [52]. In this study, after 90 days of storage at 40°C, quercetin nanosuspension stabilized with Tween® 80 was 381 nm (PDI 0.19), and quercetin nanosuspensions stabilized with TPGS were 389 nm (PDI 0.16).

3.2.3 Lyophilisation and crystallinity determination

To allow X-ray studies, the quercetin nanosuspensions were lyophilized [53]. Therefore, the effect of lyophilisation on particles size was first evaluated. For this, dry quercetin smartCrystals® were rehydrated with the original stabilizer solution after lyophilisation and the sizes and PDI of these nanosuspensions were measured (Fig. 5, b). Before lyophilisation, quercetin nanosuspensions stabilized with Tween® 80 were 366 ± 8 nm, after reconstitution of the suspension the size increased to 403 ± 8 nm. The same increase by about 40 nm in particle size was observed with quercetin nanosuspensions stabilized with TPGS, where particle size increased from 239 ± 8 nm to 290 ± 3 nm. An increase in particles size upon lyophilisation by 200 nm was reported with ascorbyl palmitate nanocrystals in the absence of cryoprotectant [54]. Cryoprotectant was not used in our case and the size increase was 5 times less. At the same time, in the case of the ascorbyl palmitate nanocrystals, the PDI increased from ~0.3 to ~0.4 while the PDI stayed the same (0.25 ± 0.03) before and after lyophilisation for quercetin nanosuspensions stabilized with Tween® 80 and TPGS. Thus, smartCrystals® were lyophilized without cryoprotectant avoiding strong size increase while keeping a good dispersity.

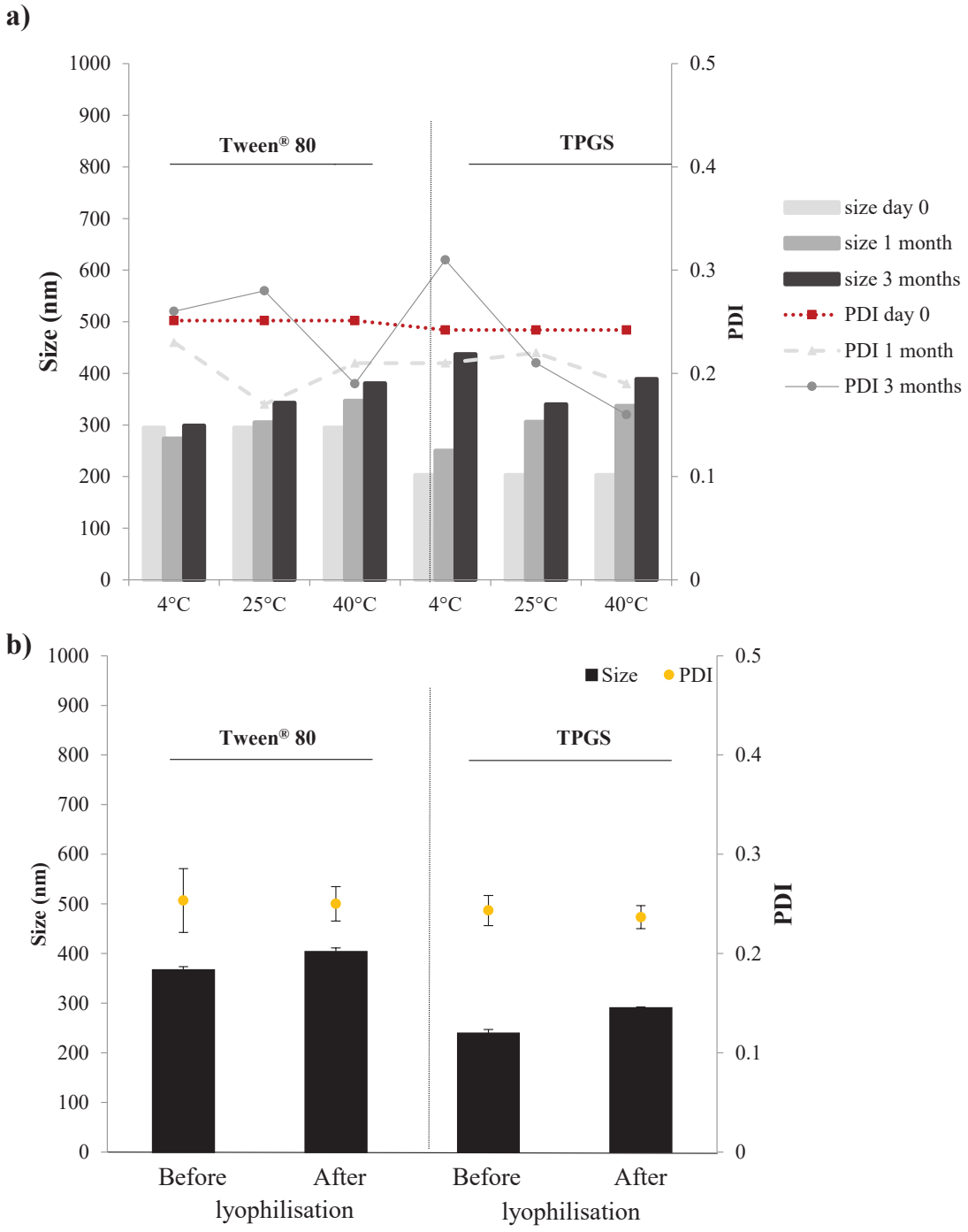

Fig. 5: a) Quercetin nanosuspensions stability at 4°C, 25°C and 40°C b) Effect of lyophilisation on the PCS size and PDI of quercetin nanosuspensions

Results recorded before and after lyophilisation ±SD (n=3)

The X-ray diffraction pattern of coarse quercetin, lyophilized quercetin smartCrystals® stabilized with Tween® 80 and TPGS are given in Fig. 6 (a). Peaks at 2, 10.8, 12.5, 15.8, 27.4 θ observed on crude quercetin diffractogram were still present in both lyophilized smartCrystals® formulations, indicating that quercetin after nanonization process had kept its crystalline nature. However, the absence of some peaks on quercetin smartCrystals® stabilized with Tween® 80 and TPGS like the peaks at 9.5, 10.3, 11.4, 11.9 and the reduced extent of the peak at 10.8 and 12.5 compared to crude quercetin, clearly indicates a change in the polymorphic form of quercetin after the nanonization process. This comes in accordance with previous reports showing the presence of three polymorphic forms for quercetin. Crude quercetin powder was pharmaceutical grade (QGPb), then quercetin in its smartCrystals® form had the pharmaceutical grade (QGPa) [55]. This change in the polymorphic form could have its reflection on the behavior of quercetin in viable system and its interaction with cells.

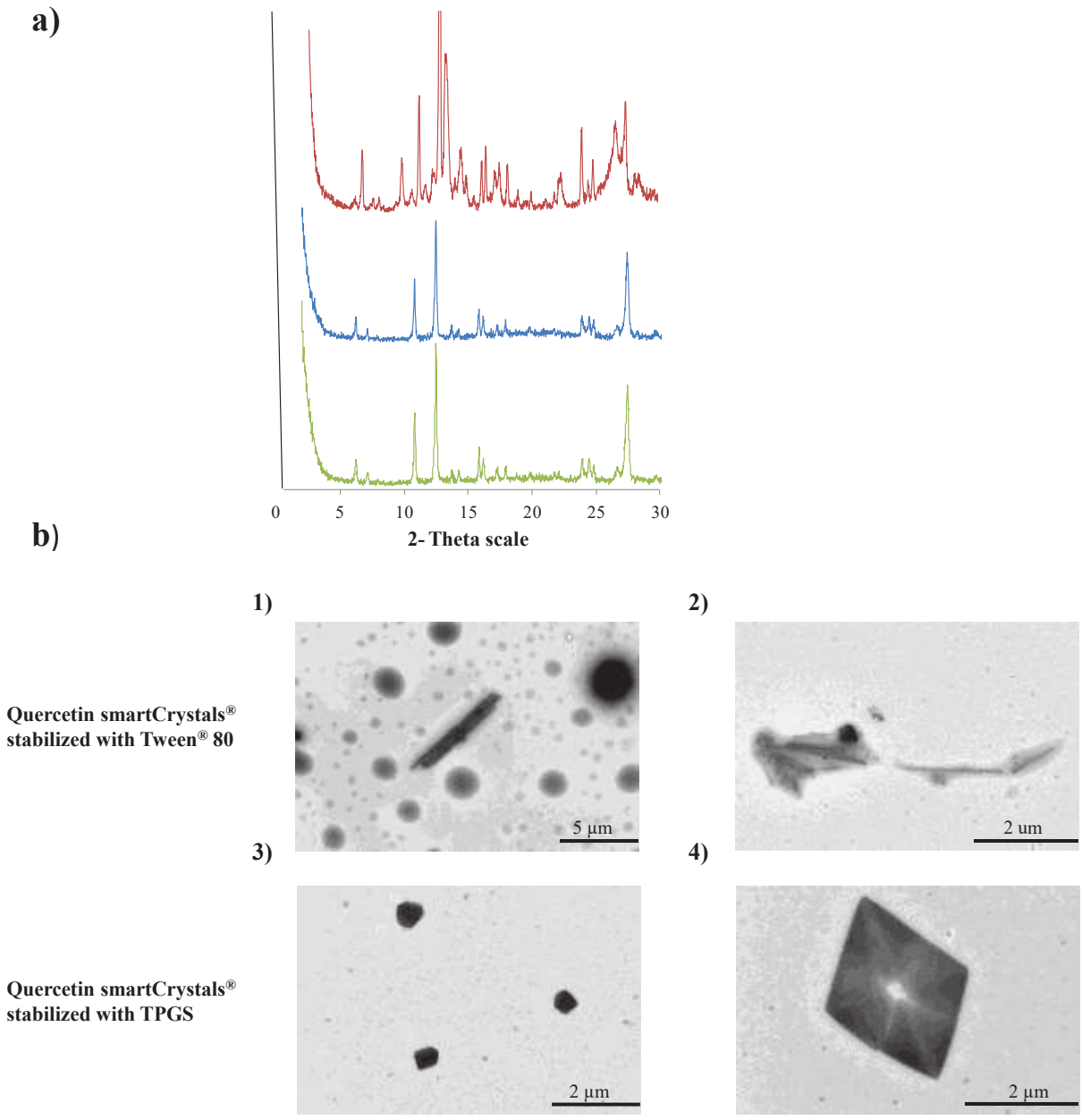

Fig. 6: X ray diffraction pattern and TEM images of crude quercetin and quercetin nanosuspensions

a) The X ray diffraction pattern crude quercetin (upper), lyophilized quercetin smartCrystals® stabilized with Tween® 80 (middle) and TPGS (lower).

b) Images of transmission electron microscopy of quercetin smartCrystals® original stabilizer solution.

1 and 2) with Tween® 80, 3 and 4) with TPGS original stabilizer solution.

3.2.4 Electron microscopic examination

5 µl of quercetin nanosuspensions were deposited and dried on TEM grids. Fig. 6 (b) shows transmission electron microscopy images of quercetin smartCrystals® stabilized with Tween® 80 (Fig. 6, b 1 and 2) and TPGS (Fig. 6, b 3 and 4) diluted with original stabilizer solution (0.5% stabilizer). Images showed the absence of nanocrystals aggregates and liquid droplets around the crystals were hypothesized to be an excess of Tween® 80 (Fig. 6, b 1). SmartCrystals® in presence of Tween® 80 were in a needle-like shape with particle size of about 700 nm to about 2 µm. (Fig. 6, b 2). By contrast, nanocrystals in presence of TPGS behaved differently as a square shape (500 nm) was prevalent in the samples tested (Fig. 6, b 3). In addition, with this last stabilizer, a cubic shape, was observed in smaller numbers (Fig. 6, b 4), which could be linked to the fusion of several nanocrystals together. Particles size in presence of TPGS was in the same range of PCS results observed between 200 and 500 nm. Square nanocrystals shape was already observed on particles stabilized by Lutrol® F68 (and lecithin) prepared by HPH [32] and also with others nanocrystals (Amoitone B, Nur77 receptor agonist) stabilized by Lutrol® F68 prepared by microfluidization [56]. This confirms that crystals shape is mainly determined by the stabilizers and not only by the process used to obtain nanocrystals.

3.3 Kinetic solubility determination

A certain loss of quercetin during milling and in the course of the homogenization step cannot be avoided, thus, quercetin concentration was determined (Table 1). The kinetic solubility was determined using HPLC (Section 2.9) for both crude quercetin and quercetin nanosuspensions. Nanosuspensions were centrifuged to separate nanocrystals from dissolved quercetin. Crude quercetin possessed a kinetic solubility of 0.48 ± 0.12 µg/ml in MilliQ water, while quercetin smartCrystals® had a kinetic solubility of 3.63 ± 0.67 µg/ml and 2.62 ± 0.26 µg/ml when stabilized with Tween® 80 and TPGS, respectively (Table 1). This allowed respectively a 7.56 fold and 5.46 fold increase in kinetic solubility. This is in accordance with the fact that particle size in the nanometer range below 1000 nm leads to increase kinetic solubility [26].

	theoretical concentration	measured concentration	kinetic solubility	saturation solubility increasing factor	DPPH activity
	w/v%	w/v%	µg/ml		EC50 µg/ml
crude quercetin in milliQ water		----	0.48±0.12	1	3.98
quercetin smartCrystals® stabilized with Tween® 80	5.00	1.41±0.34	3.63±0.67	7.56	3.72±0.08
quercetin smartCrystals® stabilized with TPGS	5.00	1.44±0.027	2.62±0.26	5.46	3.41±0.07

Table 1: Quercetin concentration in the nanosuspensions, their kinetic solubilities and DPPH activities ±SD (n=3) upon formulation.

3.4 Dissolution rate study

Topical application is also influenced by the dissolution profile of the applied drug. Indeed, with faster dissolution and higher kinetic solubility, a higher concentration gradient is generated between dermal formulation and skin, hence more dissolved drug will be absorbed (Fick law) [57]. The velocity of dissolution of such water insoluble molecule like quercetin is a limiting step for its absorption. Decreasing particles size to the nanometer range proved to increase water solubility for quercetin nanosuspensions over crude quercetin, favoring an effect on their dissolution kinetics [32]. A faster dissolution profile is required in order to allow a rapid skin penetration of dissolved molecules. Quercetin molecules penetrating into skin should be immediately replaced in the dermal formulation by molecules fast dissolving from the nanocrystals (= depot) [58].

The quercetin smartCrystals® dissolution profile was determined using the flow cell USP apparatus 4 using MilliQ water as dissolution medium. To ensure a temperature near to the skin, dissolution kinetic was performed at 32°C for 120 minutes.

Quercetin in its crude form required 30 min to get its highest dissolved amount of 13 ± 4.7 % (Fig. 7). The quercetin nanosuspension stabilized with Tween® 80 showed approximately a 6 fold increase in the total dissolved amount compared to crude quercetin with faster dissolution profile

with 56.4±3.1 % in 5 min and 79.1 ± 13.7 % in 30 min (P < 0.005). Quercetin nanosuspension stabilized with TPGS showed a dissolution profile with 33.3 ± 2.3 % in 5 min and provided its highest dissolved amount in 2 hours with 94.6 ± 12.6 % (about 7.5 fold increase in dissolution compared to crude quercetin, P < 0.005). No significant difference was observed between quercetin nanosuspensions stabilized with Tween® 80 and quercetin nanosuspensions stabilized with TPGS dissolution profiles.

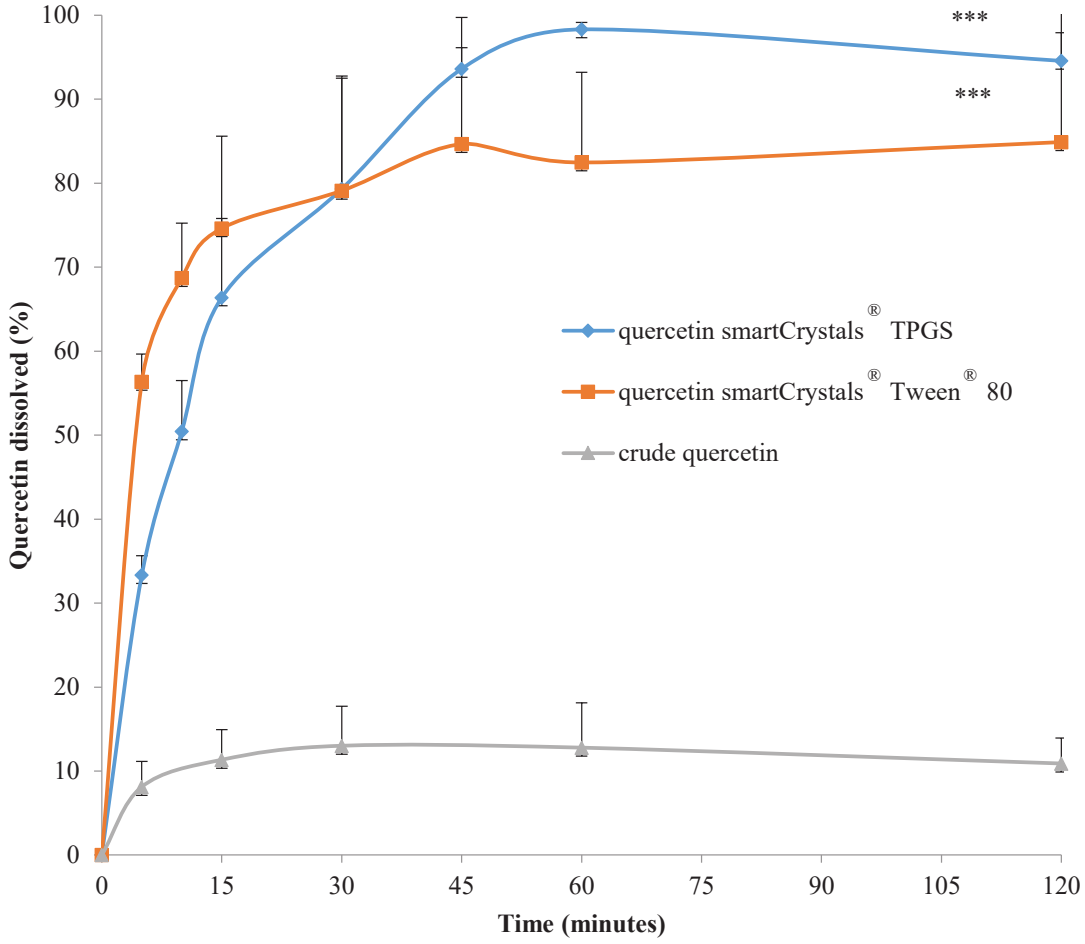

Fig. 7: Dissolution profiles of crude quercetin/quercetin smartCrystals® nanosuspensions stabilized with Tween® 80 and TPGS.

Quercetin dissolved percentage normalized to total quercetin quantity ±SD (n=3), t-test and Kolmogorov-Smirnov test showed significant difference between crude quercetin and quercetin smartCrystals®, * = P < 0.05, ** = P < 0.01 and *** = P < 0.005.

3.7 Hydrogen donating ability *in vitro* by 2, 2-diphenyl-1-picrylhydrazyl (DPPH)

To evaluate the antioxidant activity of quercetin, the *in vitro* antioxidant assay with DPPH was used. This molecule, carrying a free radical on its hydrazine position, allows compounds exposing antioxidative effect to react with [59]. DPPH in its radical form has a strong absorption band at 517 nm. The absorbance at this wavelength will be diminished if the molecule reacts with an antioxidant. When quercetin in methanol was added to DPPH methanolic solution, a linear absorbance decrease was observed from 1 µg/ml to 6 µg/ml and then reached its plateau activity (data not shown). The DPPH test was performed on quercetin nanosuspensions in order to determine its activity and whether the formulation affected quercetin free radical activity. 400 µM DPPH solution was used as positive control representing 100% free radical activity or 0% inhibition. EC50 was compared between crude quercetin and quercetin smartCrystals® stabilized with Tween® 80 and TPGS.

Results of antioxidative activity of quercetin smartCrystals® stabilized with Tween® 80 and TPGS were 3.72 ± 0.08 and 3.41 ± 0.07 µg/ml respectively (Table 1). The EC50 values lower than 3.98 µg/ml (crude quercetin) may be attributed to the larger reacting surface of quercetin smartCrystals® compared to crude quercetin, hence providing a greater quantity of quercetin in the DPPH reaction. This can be also explained by a potentiating effect of quercetin with stabilizers, as controls with just stabilizers were not active [60].

3.8 Cellular cytotoxicity

To assess the safety of quercetin smartCrystals®, a cytotoxicity study on VERO cells was performed. Cells were incubated with quercetin smartCrystals® with increasing concentrations of quercetin (5, 15, 25 and 50 µg/ml). This concentration range was tested before on crude quercetin and proved to protect HaCaT cells from a UVB dose of 10 mJ/cm^2 [5].

After 24 h, a MTT assay was performed to determine the cell viability thanks to the evaluation of the mitochondrial succinate dehydrogenase activity. Interestingly, crude quercetin and quercetin smartCrystals® showed the same cell survival rates as the control of non-treated cells (representing the 100 % of cell viability) (Fig. 8, a). T-test was performed to compare the different formulations

and no statistical difference was observed ($P > 0.05$), except in case of quercetin smartCrystals® stabilized with Tween® 80, where the lowest viability was observed (83 ± 15.5 % viable cells at 50 µg/ml) ($P < 0.05$). To note, the influence of the stabilizers alone was evaluated and revealed no implication of such molecules on cellular viability. In the range of concentrations tested, no apparent toxicity for quercetin smartCrystals® stabilized with TPGS was observed (statistically indifferent from crude quercetin at the same concentration). Based on these results, quercetin smartCrystals® stabilized with TPGS were regarded safe up to 50 µg/ml concentration on Vero cells.

3.9 Protection against hydrogen peroxide induced cellular toxicity

After the determination of the safety of quercetin smartCrystals® stabilized with Tween® 80 and TPGS (Fig. 8 a), the protective effect of quercetin against the cellular viability due to H_2O_2 intoxication was evaluated using MTT (Fig. 8, b). 50 µg/ml of crude quercetin or quercetin smartCrystals® were added to cells 4 hours before the exposure to H_2O_2. The increase of cellular viability with quercetin pretreatment reflects the antioxidant activity of quercetin. Interestingly, H_2O_2 exposure decreased the percentage of viable cells to 45 ± 9.5 %, whereas, the pretreatment with crude quercetin significantly protected the cells form H_2O_2 intoxication (96 ± 11 %) (Fig. 8, b) ($P < 0.005$). At the same level, quercetin smartCrystals® stabilized with Tween® 80 and TPGS were able to show cellular protective actions against H_2O_2 with viable cells percentage of 68 ± 6.8 % and 65 ± 6.3 % respectively (Fig. 8, b). Both results were significantly different from H_2O_2 control cells ($P < 0.05$). The weaker protective ability observed with quercetin smartCrystals® in comparison to crude quercetin may be explained by the change in the polymorphic form of quercetin [55]. Nevertheless, it is important to note that the solubility improvement afforded by quercetin smartCrystals® stabilized allows to overcome this weaker activity.

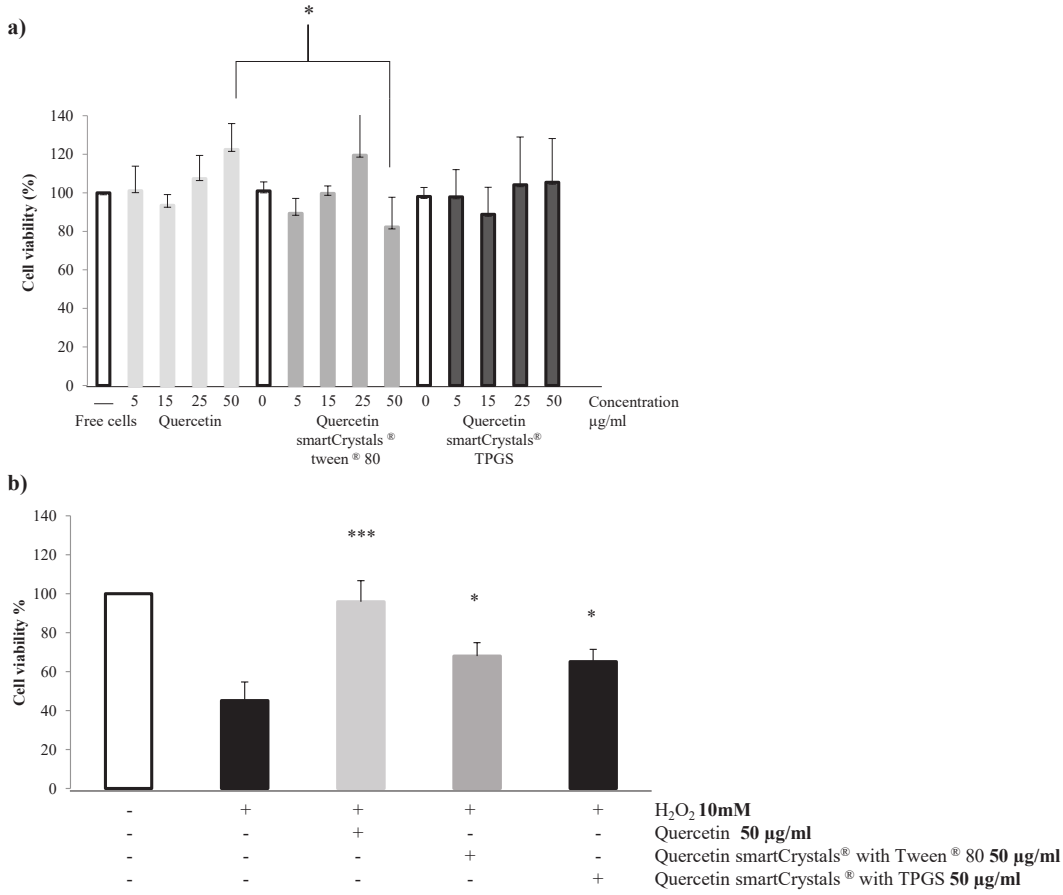

Fig. 8: Cellular toxicity (a) and cellular protective effect on H_2O_2 exposure (b) of quercetin and quercetin smartCrystals®

a) Effect of crude quercetin and quercetin smartCrystals® stabilized with Tween® 80 and TPGS on viability of Vero cells. ±SD (n=3) after 24 hours treatment. b) Protective effect of crude quercetin and quercetin smartCrystals® stabilized with Tween® 80 and TPGS on viability of Vero cells after the exposure to 10 mM of H_2O_2 (T-test P values > 0.05, no statistical difference between the data).

3.10 Quercetin smartCrystals® incorporation into nonionic gels and their stability in gel formulation

With the final goal of a topical application, Quercetin smartCrystals® stabilized with Tween® 80 and TPGS were formulated within two type of gels: Lutrol® F127 and HEC. These two gelling agents are widely used in dermal and cosmetic applications as permeability enhancers. The main scope was therefore to reach a certain permeation level, where quercetin can exert its antioxidative effect on viable keratinocytes and at the same time can be associated to a formulation with suitable

viscosity for the topical application. As an example, Lutrol® F127 (reversible thermogel) showed 6.4, 7.5, and 19.5 fold higher permeation coefficients for 5-aminolevulinic acid (treatment of actinic keratosis in photodynamic therapy) on human stratum corneum compared to the German Pharmacopeia Dolgit®, Basisscreme DAC, and to water containing hydrophilic ointment [61]. It was also proved to give superior percutaneous absorption in rats for indomethacin (in 20% (w/w) Lutrol® F127 hydrogel) [42] as well as with other drug as the anti-cancer doxorubicin [62]. Advantageous topical application was also observed using HEC (nonionic water-soluble polymer that possesses thickening abilities) with the antibiotic vancomycin for wound treatment [41]. The introduction of propylene glycol to the HEC based formulation of cidofovir (anti-viral drug) increased its transdermal delivery form 0.2% to 2.1% [63].

In this study after their formulations, gels including smartCrystals® were diluted with milliQ water in order to control the size, polydispersity index and zeta potential of the formulated smartCrystals® using PCS (Fig. 9). PCS is not the most adapted method for the visualization of smartCrystals® behavior upon their association to gel, however, this should provide information to which extent incorporation into gels can cause smartCrystals® aggregation and affect the stabilizing charge. Here, smartCrystals® incorporated to HEC gels showed larger sizes with both stabilizers Tween® 80 (651 nm, PDI 0.33) and TPGS (666 nm, PDI 0.42) (Fig. 9, a) compared to Lutrol® F127 based gels: (378 nm, PDI 0.20) and (399 nm, PDI 0.30) for quercetin nanosuspensions stabilized with Tween® 80 and TPGS, respectively (Fig. 9, a). The increase in smartCrystals® particles size upon their association to gels compared to smartCrystals® alone can be linked to the presence of Lutrol® F127 and HEC molecules at the surface of stabilized smartCrystals®. Mun et al., described a retardation in the diffusion of PEGylated nanoparticles because of the presence of HEC polymers using NanoSight nanoparticle tracking analysis, and evidenced an interaction between PEG chains and HEC polymers [64]. This could be the case for quercetin smartCrystals® stabilized by Tween® 80 and TPGS (PEG containing stabilizers). The presence of HEC molecules interacting with PEG chains at the surface of smartCrystals® could led to the observed size increase. In the same way, hydrophilic interactions between PEG moieties (from the surfactant stabilized smartCrystals® and the Lutrol® F127 molecules) could happen and could be correlated to the previously evocated size and zeta measurement modifications with smartCrystals® after their association to Lutrol® F127 gel [65]. Indeed, we observed a decrease in the zeta potential values for smartCrystals® associated to gels compared to smartCrystals® alone (zeta potential: -27 mV vs. -4 mV for smartCrystals®

stabilized by Tween® 80 and -23 mV vs. -4 mV for smartCrystals® stabilized by TPGS). This decrease can be explained both by (i) the presence of gels molecules at smartCrystals® surface (leading to a shift of the plan of shear to a greater distance thus causing a reduction in the measured value). (ii) To a change in the dynamic electrophoretic mobility of the smartCrystals®. In contrast to smartCrystals® alone, zeta potential values in the gels were higher in 50 µS/cm water compared to original stabilizer solution. This can be due to the readsorption of the stabilizer molecules found in the original stabilizer solution on the diffuse layer of the polymers (HEC, Lutrol® F127), thus decreasing the measured zeta potential.

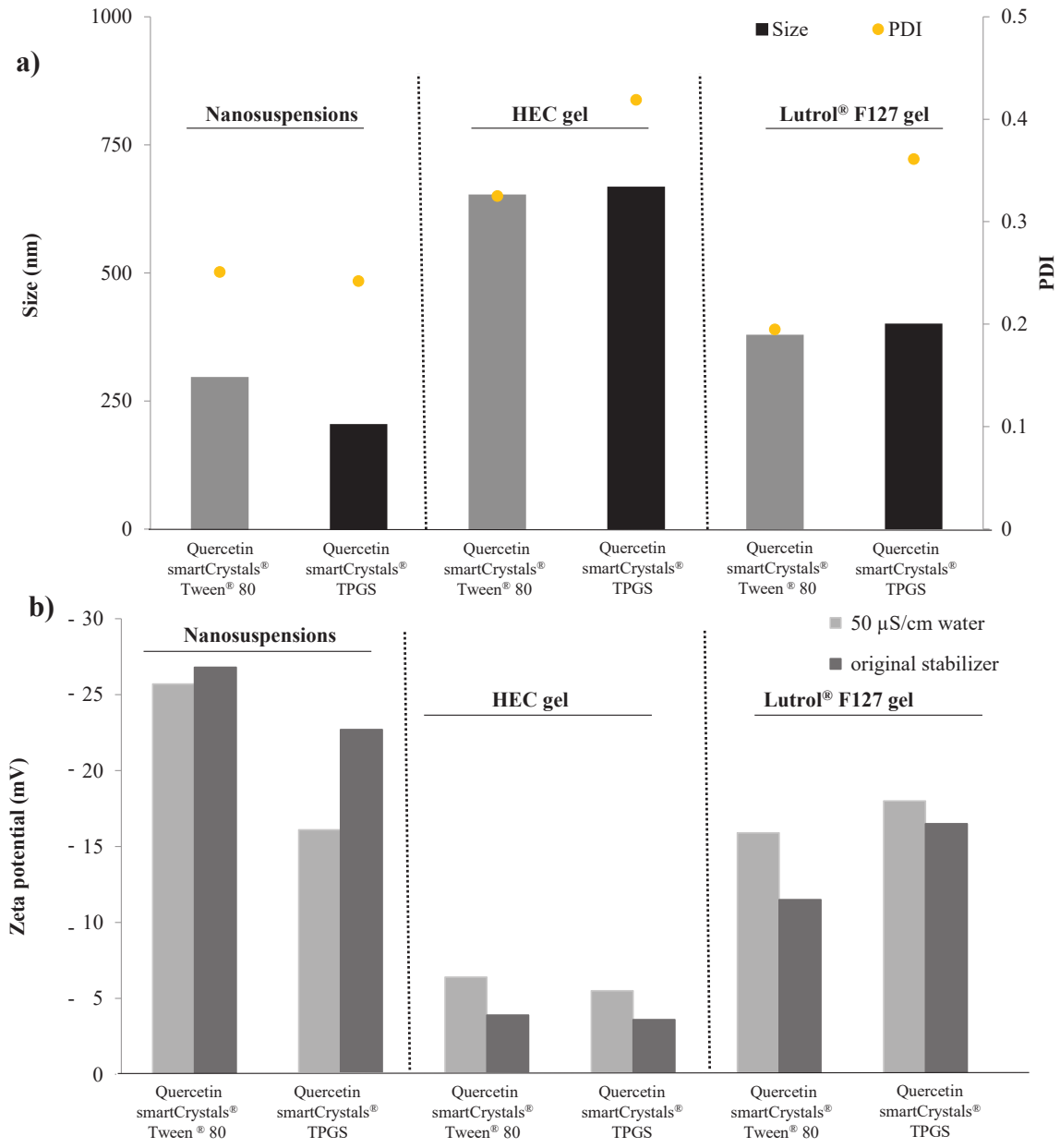

Fig. 9: Quercetin smartCrystals® associated to nonionic gels results PCS

Quercetin smartCrystals® formulated into HEC 1.7 w/w% gel and Lutrol® F127 16.7 w/w% gel, a) average particles size and polydispersity index (PDI) b) Zeta potential (absolute value).

Regarding the stability of quercetin nanosuspensions associated to gels (Fig. 10, a and b), at day 0, nanosuspensions associated to HEC gels showed higher size and PDI results compared to nanosuspensions associated to Lutrol® F127 gels. At day 90 at 40°C, nanosuspensions associated to both gels showed particle sizes above 400 nm and PDI above 0.31. Sizes were 568 nm and 469

nm for nanosuspension stabilized with Tween® 80 (Fig. 10, a) and 419 nm and 598 nm for nanosuspension stabilized with TPGS ((Fig. 9, b) with HEC and Lutrol® F127 respectively. Values were about 200 nm higher than that of nanosuspensions alone at the same temperature (Fig 5, a: 381 and 389 nm with Tween® 80 and TPGS), which indicates that 40°C is not a suitable storage temperature for both gels.

At day 90 at 25°C, quercetin nanosuspension stabilized with Tween® 80 presented higher size values than that of nanosuspension stabilized with TPGS (481 nm, PDI = 0.37 vs. 342 nm, PDI = 0.33) for both HEC gel and (474 nm, PDI = 0.34 vs. 352 nm, PDI = 0.33) Lutrol® F127 gel. By referring back to nanosuspension alone at the same temperature, the size increase with nanosuspension stabilized with Tween® 80 after the gel association is more pronounced (from 343 nm to 481 nm and 474 nm) compared to nanosuspension stabilized with TPGS (340 nm to 342 and 352 nm). This result indicates that nanosuspension stabilized with TPGS presented an increased stability in gels compared to nanosuspension stabilized with Tween® 80.

Lastly excluding values at 40°C, all gel formulations after 90 days, smartCrystals® size exposed after dilution were less than 500 nm and PDI values 0.4, which indicates acceptable homogeneity of the formulated gels (for dermal application). However, the preferred storage condition seems to be 25°C for gel formulations, and this seems adequate to a cosmetic use. To conclude, TPGS seems to allow an increased stabilization of quercetin nanosuspensions in the gel formulations compared to Tween® 80.

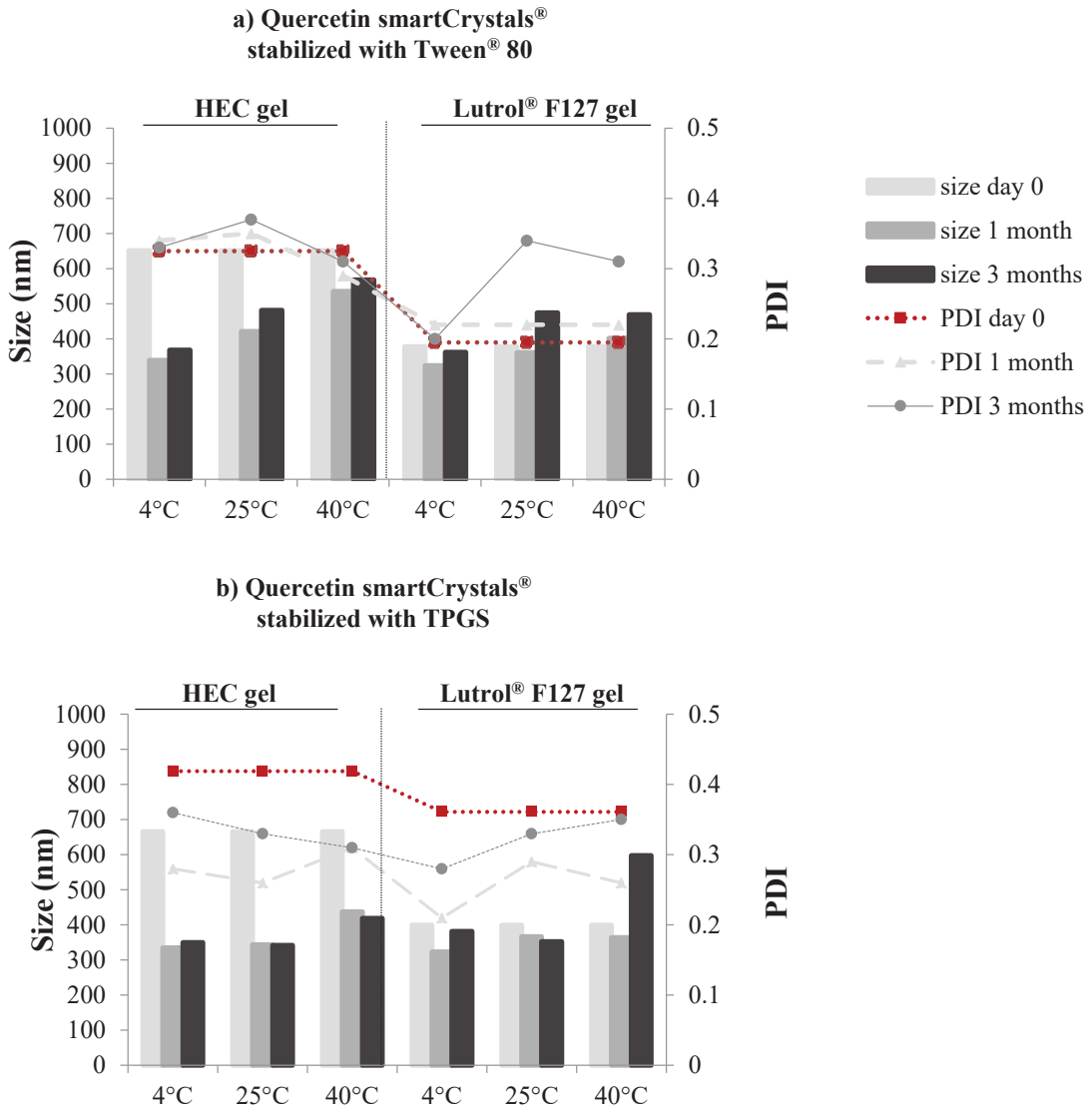

Fig. 10: Stability results of (a) quercetin smartCrystals® stabilized with Tween® 80 incorporated into nonionic gels, (b) quercetin smartCrystals® stabilized with TPGS incorporated into nonionic gels

PCS diameter and PDI of a) quercetin smartCrystals® stabilized with Tween® 80 incorporated into HEC and Lutrol® F127 nonionic gels. b) quercetin smartCrystals® stabilized with TPGS incorporated into HEC and Lutrol® F127 nonionic gels (storage at 4°C, 25°C, and 40°C.)

4. Conclusion

Quercetin second-generation nanocrystals (smartCrystals®) were successfully formulated allowing a decrease in both the stabilizer amount required (0.5%) as well as in time of preparation process compared to previous studies [34]. Among the five tested stabilizers, quercetin smartCrystals®

stabilized with Tween® 80 and TPGS had the smallest particle size with a short milling time (5 min). Produced quercetin smartCrystals® possessed higher kinetic solubility and dissolution velocity compared to crude drug (7 fold) and retained antioxidative activity. Moreover quercetin smartCrystals® proved physical stability over three months in nanosuspensions at 4°C, 25°C and 40°C. Interestingly, a higher antioxidative ability was observed with TPGS stabilized smartCrystals® on DPPH assay (3.14 µg/ml instead of 3.98 µg/ml with crude quercetin), in addition to a safe profile and protective activity on Vero cells at a concentration up to 50 µg/ml with retained activity against hydrogen peroxide toxicity. TPGS therefore proved to be superior stabilizer for quercetin smartCrystals®. These results are promising and propose TPGS as a novel stabilizer for nanocrystals, which, as a derivative of vitamin E, is well adapted for a topical application. With this objective in mind, quercetin nanosuspensions were incorporated into Lutrol® F127 and HEC gels. Quercetin dermal gels were stable at 25°C for 90 days which is coherent to a daily topical application and evidence the interest of our new formulation as a new antioxidant cosmetic product

Acknowledgments

Authors acknowledge the financial support of ERASMUS MUNDUS AVEMPACE 2 and L'Ecole Doctorale Sciences Chimiques Balard ED 459 associée à la Fondation Balard (Chaire Total) Montpellier. All the thanks for the technical support of Mme. Corinna Schmidt, Dr. Corine Tourne-Peteilh and Mr Pradial Peralta.

References

[1] J. Cheel, P.V. Antwerpen, L. Tůmová, G. Onofre, D. Vokurková, K. Zouaoui-Boudjeltia, M. Vanhaeverbeek, J. Nève, Free radical-scavenging, antioxidant and immunostimulating effects of a licorice infusion (Glycyrrhiza glabra L.), Food Chemistry, 122 (2010) 508-517.

[2] S.-Y. Lyu, J.-Y. Rhim, W.-B. Park, Antiherpetic activities of flavonoids against herpes simplex virus type 1 (HSV-1) and type 2 (HSV-2)in vitro, Archives of Pharmacal Research, 28 (2005) 1293-1301.

[3] M. Subramaneyaan, S. Rustagi, S.N. Bhattacharya, A.K. Tripathi, B.D. Banerjee, R.S. Ahmed, Effect of antioxidant supplementation on free radical scavenging system and immune response in lindane treated scabies patients, Pesticide Biochemistry and Physiology, 102 (2012) 91-94.

[4] R. Casagrande, S.R. Georgetti, W.A. Verri Jr, D.J. Dorta, A.C. dos Santos, M.J.V. Fonseca, Protective effect of topical formulations containing quercetin against UVB-induced oxidative stress in hairless mice, Journal of Photochemistry and Photobiology B: Biology, 84 (2006) 21-27.

[5] D. Liu, H. Hu, Z. Lin, D. Chen, Y. Zhu, S. Hou, X. Shi, Quercetin deformable liposome: Preparation and efficacy against ultraviolet B induced skin damages in vitro and in vivo, Journal of Photochemistry and Photobiology B: Biology, 127 (2013) 8-17.

[6] M.M. Heinen, M.C. Hughes, T.I. Ibiebele, G.C. Marks, A.C. Green, J.C. van der Pols, Intake of antioxidant nutrients and the risk of skin cancer, European Journal of Cancer, 43 (2007) 2707-2716.

[7] J.S. Reis, M.A. Corrêa, M.C. Chung, J.L. dos Santos, Synthesis, antioxidant and photoprotection activities of hybrid derivatives useful to prevent skin cancer, Bioorganic & Medicinal Chemistry, 22 (2014) 2733-2738.

[8] F.T.M.C. Vicentini, T.R.M. Simi, J.O. Del Ciampo, N.O. Wolga, D.L. Pitol, M.M. Iyomasa, M.V.L.B. Bentley, M.J.V. Fonseca, Quercetin in w/o microemulsion: In vitro and in vivo skin penetration and efficacy against UVB-induced skin damages evaluated in vivo, European Journal of Pharmaceutics and Biopharmaceutics, 69 (2008) 948-957.

[9] A. Schieber, P. Hilt, J. Conrad, U. Beifuss, R. Carle, Elution order of quercetin glycosides from apple pomace extracts on a new HPLC stationary phase with hydrophilic endcapping, Journal of Separation Science, 25 (2002) 361-364.

[10] G.A. Spanos, R.E. Wrolstad, Phenolics of apple, pear, and white grape juices and their changes with processing and storage. A review, Journal of Agricultural and Food Chemistry, 40 (1992) 1478-1487.

[11] M.-J. Ko, C.-I. Cheigh, S.-W. Cho, M.-S. Chung, Subcritical water extraction of flavonol quercetin from onion skin, Journal of Food Engineering, 102 (2011) 327-333.

[12] A. Kumar, A.K. Malik, D.K. Tewary, A new method for determination of myricetin and quercetin using solid phase microextraction–high performance liquid chromatography–ultra violet/visible system in grapes, vegetables and red wine samples, Analytica Chimica Acta, 631 (2009) 177-181.

[13] A. Saija, M. Scalese, M. Lanza, D. Marzullo, F. Bonina, F. Castelli, Flavonoids as antioxidant agents: Importance of their interaction with biomembranes, Free Radical Biology and Medicine, 19 (1995) 481-486.

[14] F. Bonina, M. Lanza, L. Montenegro, C. Puglisi, A. Tomaino, D. Trombetta, F. Castelli, A. Saija, Flavonoids as potential protective agents against photo-oxidative skin damage, International Journal of Pharmaceutics, 145 (1996) 87-94.

[15] M. Comalada, D. Camuesco, S. Sierra, I. Ballester, J. Xaus, J. Galvez, A. Zarzuelo, In vivo quercitrin anti-inflammatory effect involves release of quercetin, which inhibits inflammation through down-regulation of the NF-kappaB pathway, Eur J Immunol, 35 (2005) 584-592.

[16] C.F. Lin, Y.L. Leu, S.A. Al-Suwayeh, M.C. Ku, T.L. Hwang, J.Y. Fang, Anti-inflammatory activity and percutaneous absorption of quercetin and its polymethoxylated compound and glycosides: the relationships to chemical structures, Eur J Pharm Sci, 47 (2012) 857-864.

[17] C. Kandaswami, L.T. Lee, P.P. Lee, J.J. Hwang, F.C. Ke, Y.T. Huang, M.T. Lee, The antitumor activities of flavonoids, In Vivo, 19 (2005) 895-909.

[18] H. Zhang, M. Zhang, L. Yu, Y. Zhao, N. He, X. Yang, Antitumor activities of quercetin and quercetin-5′,8-disulfonate in human colon and breast cancer cell lines, Food and Chemical Toxicology, 50 (2012) 1589-1599.

[19] X. Qu, D. Qi, F. Dong, B. Wang, R. Guo, M. Luo, R. Yao, Quercetin improves hypoxia-ischemia induced cognitive deficits via promoting remyelination in neonatal rat, Brain Research, 1553 (2014) 31-40.

[20] C. Gupta, D.N. Tripathi, A. Vikram, P. Ramarao, G.B. Jena, Quercetin inhibits diethylnitrosamine-induced hepatic preneoplastic lesions in rats, Nutr Cancer, 63 (2011) 234-241.

[21] C.-M. Liu, Y.-Z. Sun, J.-M. Sun, J.-Q. Ma, C. Cheng, Protective role of quercetin against lead-induced inflammatory response in rat kidney through the ROS-mediated MAPKs and NF-κB pathway, Biochimica et Biophysica Acta (BBA) - General Subjects, 1820 (2012) 1693-1703.

[22] D. Dodda, R. Chhajed, J. Mishra, Protective effect of quercetin against acetic acid induced inflammatory bowel disease (IBD) like symptoms in rats: Possible morphological and biochemical alterations, Pharmacological Reports, 66 (2014) 169-173.

[23] K. Ioku, T. Tsushida, Y. Takei, N. Nakatani, J. Terao, Antioxidative activity of quercetin and quercetin monoglucosides in solution and phospholipid bilayers, Biochim Biophys Acta, 1234 (1995) 99-104.

[24] N. Chondrogianni, S. Kapeta, I. Chinou, K. Vassilatou, I. Papassideri, E.S. Gonos, Anti-ageing and rejuvenating effects of quercetin, Experimental Gerontology, 45 (2010) 763-771.

[25] R. Shegokar, R.H. Müller, Nanocrystals: Industrially feasible multifunctional formulation technology for poorly soluble actives, International Journal of Pharmaceutics, 399 (2010) 129-139.

[26] J. Junghanns, R.H. Müller, Nanocrystal technology, drug delivery and clinical applications, in: Int J Nanomedicine, 2008, pp. 295-310.

[27] G.G. Liversidge, K.C. Cundy, J.F. Bishop, D.A. Czekai, S.D. Inc., Dispersion, bioavailability, (1992).

[28] R.H. Muller, R. Becker, B. Kruss, K. Peters, Pharmaceutical nanosuspensions for medicament administration as systems with increased saturation solubility and rate of solution, in, Google Patents, 1999.

[29] J. Salazar, R.H. Müller, J.P. Möschwitzer, Combinative particle size reduction technologies for the production of drug nanocrystals, Journal of Pharmaceutics, 2014 (2014).

[30] R.H. Müller, C.M. Keck, Second generation of drug nanocrystals for delivery of poorly soluble drugs: smartCrystal technology, European Journal of Pharmaceutical Sciences, 34 (2008) S20-S21.

[31] R. Petersen, Nanocrystals for use in topical cosmetic formulations and method of production thereof, in: U.S. patent (Ed.), ABBOTT GMBH & CO. KG Wiesbaden DE, United States, 2006, pp. 2.

[32] L. Gao, G. Liu, X. Wang, F. Liu, Y. Xu, J. Ma, Preparation of a chemically stable quercetin formulation using nanosuspension technology, International Journal of Pharmaceutics, 404 (2011) 231-237.

[33] M. Kakran, R. Shegokar, N.G. Sahoo, S. Gohla, L. Li, R.H. Muller, Long-term stability of quercetin nanocrystals prepared by different methods, J Pharm Pharmacol, 64 (2012) 1394-1402.

[34] M. Kakran, R. Shegokar, N.G. Sahoo, L. Al Shaal, L. Li, R.H. MÃ¼ller, Fabrication of quercetin nanocrystals: Comparison of different methods, European Journal of Pharmaceutics and Biopharmaceutics, 80 (2012) 113-121.

[35] H. Li, X. Zhao, Y. Ma, G. Zhai, L. Li, H. Lou, Enhancement of gastrointestinal absorption of quercetin by solid lipid nanoparticles, J Control Release, 133 (2009) 238-244.

[36] L. Liu, Y. Tang, C. Gao, Y. Li, S. Chen, T. Xiong, J. Li, M. Du, Z. Gong, H. Chen, L. Liu, P. Yao, Characterization and biodistribution in vivo of quercetin-loaded cationic nanostructured lipid carriers, Colloids and Surfaces B: Biointerfaces, 115 (2014) 125-131.

[37] A.S.B. Goebel, U. Knie, C. Abels, J. Wohlrab, R.H.H. Neubert, Dermal targeting using colloidal carrier systems with linoleic acid, European Journal of Pharmaceutics and Biopharmaceutics, 75 (2010) 162-172.

[38] P.R. Mishra, L.A. Shaal, R.H. Müller, C.M. Keck, Production and characterization of Hesperetin nanosuspensions for dermal delivery, International Journal of Pharmaceutics, 371 (2009) 182-189.

[39] J.C. Schwarz, A. Weixelbaum, E. Pagitsch, M. Löw, G.P. Resch, C. Valenta, Nanocarriers for dermal drug delivery: Influence of preparation method, carrier type and rheological properties, International Journal of Pharmaceutics, 437 (2012) 83-88.

[40] C. Keck, S. Kobierski, R. Mauludin, H.R. Müller, Second generation of drug nanocrystals for delivery of poorly soluble drugs: smartCrystal technology, Dosis, Volume 24 (2008) pp. 124–128.

[41] G. Giandalia, V. De Caro, L. Cordone, L.I. Giannola, Trehalose–hydroxyethylcellulose microspheres containing vancomycin for topical drug delivery, European Journal of Pharmaceutics and Biopharmaceutics, 52 (2001) 83-89.

[42] S. Miyazaki, T. Tobiyama, M. Takada, D. Attwood, Percutaneous absorption of indomethacin from pluronic F127 gels in rats, J Pharm Pharmacol, 47 (1995) 455-457.

[43] R.H. Müller, C. Jacobs, Buparvaquone mucoadhesive nanosuspension: preparation, optimisation and long-term stability, International Journal of Pharmaceutics, 237 (2002) 151-161.

[44] L.J. Yang, P. Li, Y.J. Gao, H.F. Li, D.C. Wu, R.X. Li, [Time resolved UV-Vis absorption spectra of quercetin reacting with various concentrations of sodium hydroxide], Guang Pu Xue Yu Guang Pu Fen Xi, 29 (2009) 1632-1635.

[45] S.-J. Heo, S.-C. Ko, S.-M. Kang, H.-S. Kang, J.-P. Kim, S.-H. Kim, K.-W. Lee, M.-G. Cho, Y.-J. Jeon, Cytoprotective effect of fucoxanthin isolated from brown algae Sargassum siliquastrum against H2O2-induced cell damage, European Food Research and Technology, 228 (2008) 145-151.

[46] A.K. Nath, C. Jiten, K.C. Singh, Influence of ball milling parameters on the particle size of barium titanate nanocrystalline powders, Physica B: Condensed Matter, 405 (2010) 430-434.

[47] N. Sahoo, M. Kakran, L. Shaal, L. Li, R. Müller, M. Pal, L. Tan, Preparation and characterization of quercetin nanocrystals, Journal of pharmaceutical sciences, 100 (2011) 2379-2390.

[48] C.M. Keck, A. Kovačević, R.H. Müller, S. Savić, G. Vuleta, J. Milić, Formulation of solid lipid nanoparticles (SLN): The value of different alkyl polyglucoside surfactants, International Journal of Pharmaceutics, 474 (2014) 33-41.

[49] A. Vonarbourg, P. Saulnier, C. Passirani, J.P. Benoit, Electrokinetic properties of noncharged lipid nanocapsules: influence of the dipolar distribution at the interface, Electrophoresis, 26 (2005) 2066-2075.

[50] L. Wu, J. Zhang, W. Watanabe, Physical and chemical stability of drug nanoparticles, Advanced Drug Delivery Reviews, 63 (2011) 456-469.

[51] R.H. Müller, Colloidal carriers for controlled drug delivery and targeting: Modification, characterization and in vivo distribution, Taylor & Francis, 1991.

[52] K. Mitri, R. Shegokar, S. Gohla, C. Anselmi, R.H. Müller, Lipid nanocarriers for dermal delivery of lutein: Preparation, characterization, stability and performance, International Journal of Pharmaceutics, 414 (2011) 267-275.

[53] K. Peters, S. Leitzke, J.E. Diederichs, K. Borner, H. Hahn, R.H. Müller, S. Ehlers, Preparation of a clofazimine nanosuspension for intravenous use and evaluation of its therapeutic efficacy in murine Mycobacterium avium infection, Journal of Antimicrobial Chemotherapy, 45 (2000) 77-83.

[54] V. Teeranachaideekul, V.B. Junyaprasert, E.B. Souto, R.H. Müller, Development of ascorbyl palmitate nanocrystals applying the nanosuspension technology, International Journal of Pharmaceutics, 354 (2008) 227-234.

[55] G.S. Borghetti, I.M. Costa, P.R. Petrovick, V.P. Pereira, V.L. Bassani, Characterization of different samples of quercetin in solid-state: indication of polymorphism occurrence, Pharmazie, 61 (2006) 802-804.

[56] L. Hao, X. Wang, D. Zhang, Q. Xu, S. Song, F. Wang, C. Li, H. Guo, Y. Liu, D. Zheng, Q. Zhang, Studies on the preparation, characterization and pharmacokinetics of Amoitone B nanocrystals, International Journal of Pharmaceutics, 433 (2012) 157-164.

[57] G. Cevc, U. Vierl, Nanotechnology and the transdermal route: A state of the art review and critical appraisal, Journal of Controlled Release, 141 (2010) 277-299.

[58] K. Moser, K. Kriwet, A. Naik, Y.N. Kalia, R.H. Guy, Passive skin penetration enhancement and its quantification in vitro, European Journal of Pharmaceutics and Biopharmaceutics, 52 (2001) 103-112.

[59] M.S. Blois, Antioxidant Determinations by the Use of a Stable Free Radical, Nature, 181 (1958) 1199-1200.

[60] S.A.B.E. van Acker, L.M.H. Koymans, A. Bast, Molecular pharmacology of vitamin E: Structural aspects of antioxidant activity, Free Radical Biology and Medicine, 15 (1993) 311-328.

[61] N. Gruning, C.C. Muller-Goymann, Physicochemical characterisation of a novel thermogelling formulation for percutaneous penetration of 5-aminolevulinic acid, J Pharm Sci, 97 (2008) 2311-2323.

[62] V.Y. Erukova, O.O. Krylova, Y.N. Antonenko, N.S. Melik-Nubarov, Effect of ethylene oxide and propylene oxide block copolymers on the permeability of bilayer lipid membranes to small solutes including doxorubicin, Biochimica et Biophysica Acta (BBA) - Biomembranes, 1468 (2000) 73-86.

[63] K.C. Cundy, G. Lynch, W.A. Lee, Bioavailability and metabolism of cidofovir following topical administration to rabbits, Antiviral Research, 35 (1997) 113-122.

[64] E.A. Mun, C. Hannell, S.E. Rogers, P. Hole, A.C. Williams, V.V. Khutoryanskiy, On the Role of Specific Interactions in the Diffusion of Nanoparticles in Aqueous Polymer Solutions, Langmuir, 30 (2014) 308-317.

[65] S. Staufenbiel, C.M. Keck, R.H. Müller, The “Real Environment” Quantification of Surface Hydrophobicity of Differently Stabilized Nanocrystals as Key Parameter for Organ Distribution, Macromolecular Symposia, 345 (2014) 32-41.

Supplementary data

Step	Tween® 80		TPGS	
	Size	PDI	Size	PDI
Primary suspension	1765	0.56	811	0.95
Quercetin smartCrystals®	295	0.25	203	0.24
After lyophilisation	403	0.25	290	0.24
Quercetin smartCrystals® associated to HEC gel	651	0.33	666	0.42
Quercetin smartCrystals® associated to Lutrol® F127 gel	378	0.20	399	0.36

Supplementary Table 1: Summary of quercetin smartCrystals® with Tween® 80 and TPGS average particle size and PDI in the steps of preparation, lyophilisation and association to nonionic gel

Substance	Chemical name	Structure
Quercetin	3, 3', 4', 5, 7-pentahydroxy-2-phenylchromen-4-one	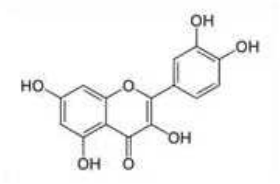
Tween® 80	polysorbate 80	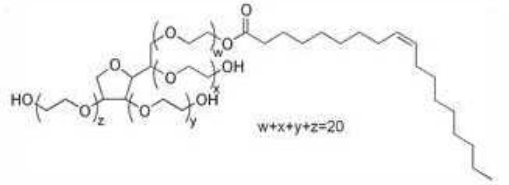
TPGS	α tocopheryl polyethylene glycol 1000 succinate	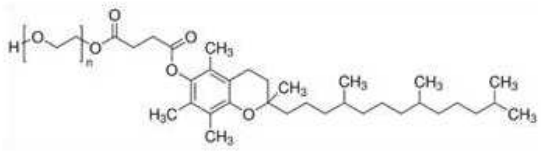
Lutrol® F68	Poly(ethylene glycol)-block-poly(propylene glycol)-block-poly(ethylene glycol)	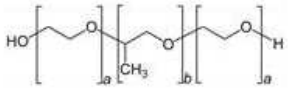 a = 79 and b = 28 approximately
Plantacare® 810	caprylyl/capryl glucoside	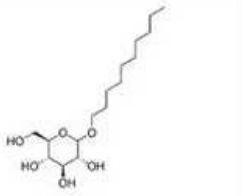
Plantacare® 1200	lauryl glycoside	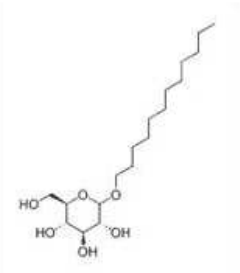

Supplementary Table 2: Chemical structure of quercetin and the stabilizers used for the preparation of quercetin smartCrystals®

Chapter two: Quercetin lipid nanocapsules

Goals:

Development of quercetin lipid nanocapsules

Physicochemical characterization

Quercetin loading and encapsulation efficiency

Quercetin *in vitro* release study

Cellular safety on THP-1 cells

Protection activity on THP-1 cells

Chapter two: Quercetin lipid nanocapsules

Preface

In this chapter, the second quercetin formulation approach is presented. Lipid nanocapsules is an interesting formulation with various particle size depending on excipient composition [1]. Moreover, adaptations of this formulation can be established to improve the encapsulated drug loading [2, 3]. The choice of this formulation is based on the fact that the drug is encapsulated within the nanocapsules, which is good for quercetin sensitivity to light. Even more, their lipidic nature and small size could confer good affinity to skin lipophilic character and enable an occlusive effect when applied that in turns can increase quercetin skin penetration [4, 5].

In this chapter, quercetin lipid nanocapsules were developed applying several medications in the preparation process and excipient composition for higher quercetin loading capacity. Then, physiochemical characterization in terms of particle size, PDI, particles morphology, physical stability of lipid nanocapsules were investigated. Also the quercetin loading, encapsulation efficiency, antioxidant activity *in vitro* using DPPH assay and *in vitro* release studies were performed. X ray analysis were also performed.

Finally, the cellular safety and protective activity of quercetin lipid nanocapsules were tested in THP-1 cells as a model for monocytes derived dendritic cells in inflammation conditions.

References

[1] B. Heurtault, P. Saulnier, B. Pech, M.C. Venier-Julienne, J.E. Proust, R. Phan-Tan-Luu, J.P. Benoit, The influence of lipid nanocapsule composition on their size distribution, European Journal of Pharmaceutical Sciences, 18 (2003) 55-61.

[2] M. Weyland, F. Manero, A. Paillard, D. GrÃ©e, G. Viault, D. Jarnet, P. Menei, P. Juin, I. Chourpa, J.P. Benoit, R. GrÃ©e, E. Garcion, Mitochondrial targeting by use of lipid nanocapsules loaded with SV30, an analogue of the small-molecule Bcl-2 inhibitor HA14-1, Journal of Controlled Release, 151 (2011) 74-82.

[3] C. Maupas, B. Moulari, A. BÃ©duneau, A. Lamprecht, Y. Pellequer, Surfactant dependent toxicity of lipid nanocapsules in HaCaT cells, International Journal of Pharmaceutics, 411 (2011) 136-141.

[4] B.a. Heurtault, P. Saulnier, B. Pech, J.-E. Proust, J.-P. Benoit, A Novel Phase Inversion-Based Process for the Preparation of Lipid Nanocarriers, Pharmaceutical Research, 19 (2002) 875-880.

[5] R.H. Müller, M. Radtke, S.A. Wissing, Solid lipid nanoparticles (SLN) and nanostructured lipid carriers (NLC) in cosmetic and dermatological preparations, Advanced Drug Delivery Reviews, 54, Supplement (2002) S131-S155

Dermal quercetin lipid nanocapsules: influence of the formulation on antioxidant activity and cellular protection against hydrogen peroxide

T. Hatahet[a*], M. Morille[a], A. Shamseddin[b], A. Aubert-Pouëssel[a], JM. Devoisselle [a], S. Bégu[a]

[a] Institut Charles Gerhardt Montpellier, UMR 5253 CNRS-ENSCM-UM, Equipe Matériaux Avancés pour la Catalyse et la Santé, 8 rue de l'Ecole Normale, 34296 Montpellier Cedex 5, France.

[b] Comparative Molecular Immuno-Physiopathology, IRD Laboratory, UMR-MD3, Faculty of Pharmacy, Montpellier University 15 Avenue Charles Flahault, 34093 Montpellier Cedex 5, France.

[*] Corresponding author.

Research article submitted to the

European Journal of Pharmaceutics and Biopharmaceutics

September 2016 (submitted article)

Abstract:

Quercetin is a plant flavonoid with strong antioxidant and antiinflammatory properties interesting for skin protection. However, its poor water solubility limits its penetration and so its efficiency on skin. For this purpose, quercetin lipid nanocapsules were formulated implementing phase inversion technique wherein several modifications were introduced to enhance quercetin loading. Quercetin lipid nanocapsules were formulated with two particle size range, (50 nm and 20 nm) allowing a drug loading of 18.6 and 32 mM respectively. The successful encapsulation of quercetin within lipid nanocapsules increased its apparent water solubility by more than 5,000 fold (from 0.5 µg/ml to about 5 mg/ml). The physicochemical properties of these formulations such as surface charge, stability and morphology were characterized. Lipid nanocapsules had spherical shape and were stable for 28 days at 25°C. Quercetin release from lipid nanocapsules was studied and revealed a prolonged release kinetics during 24 hours. Using DPPH assay, we demonstrated that the formulation process of lipid nanocapsules did not modify the antioxidant activity of quercetin *in vitro* (92.3 %). With the goal of a future dermal application, quercetin lipid nanocapsules were applied to THP-1 monocytes and proved the cellular safety of the formulation up to 2 µg/ml of quercetin. Finally, formulated quercetin was as efficient as the crude form in the protection of THP-1 cells from oxidative stress by exogenous hydrogen peroxide.With its lipophilic nature and occlusive effect on skin, lipid nanocapsules present a promising strategy to deliver quercetin to skin tissue and can be of value for other poorly water soluble drug candidates.

Key words:

Quercetin, flavonoid, lipid nanocapsules, DPPH assay, prolonged release, cellular protection, hydrogen peroxide.

Graphical abstract

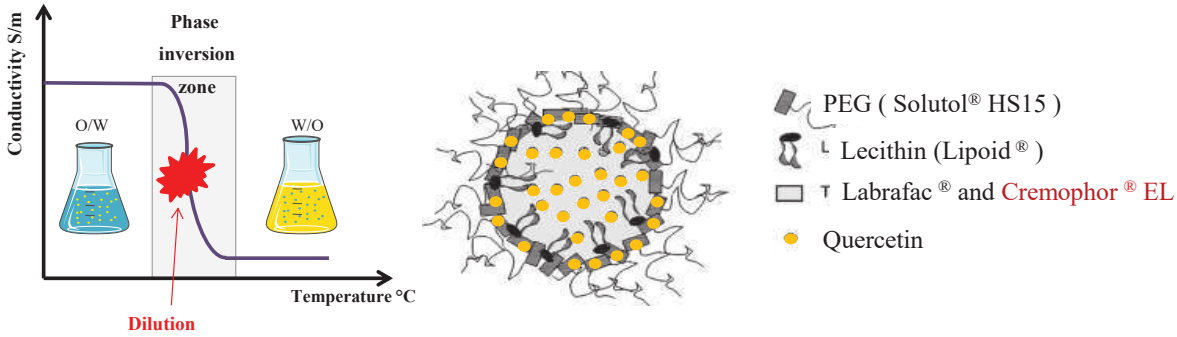

Que-LNC 20
- Size 26 nm and PDI 0.06
- Drug loading 32.0 mM

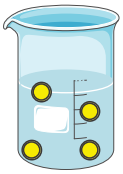

Que-LNC 50
- Size 54 nm and PDI 0.17
- Drug loading 18.6 mM

- Que-LNC stability: 28 days at 25°C
- LNC= sustained release for quercetin (during 24 hours)
- Retained antioxidant activity *in vitro* using DPPH
- Quercetin antioxidant properties not hindered by the process on THP-1 cells against H_2O_2

1. Introduction

Flavonoids are plant pigments which possess physiological activities. They are found in fruits and vegetables such as apples [1], onions [2], strawberries [3], spinach [4] and wine [5]. Their *2-phenyl-1, 4-benzopyrone C6-C3-C6* skeleton allows the classification of flavonoids into several groups of molecules regarding the presence of the *C4* ketone*, C3-C4* double bond, and the hydroxyl at *C3*. Because of an exceptional free radical scavenging [6], antiinflammatory [7] and immunomodulatory activities [8] flavonoid are believed to be very promising drug candidates. As a result, flavonoids were tested for various inflammatory disorders like osteoporosis [9], psoriasis [10], arthritis [7], and other cardiovascular diseases [5]. Their immunomodulatory functions were highlighted while investigating anti-cancer activity [11, 12]. The main reason for the diversity of flavonoids physiological actions is their very strong antioxidative properties and the capability to scavenge free radical species and inhibit lipid peroxidation *in vitro* [13].

Quercetin (3,3′,4′,5,7-pentahydroxyflavone) is one of the strongest antioxidants among flavonoids [14, 15]. In regards to systemic drug delivery, quercetin presented the highest inhibition of free radical-induced membrane lipid peroxidation, when compared to other flavonoids such as hesperetin, rutin, and naringenin [15]. Quercetin was also extensively tested in cancer therapy especially in trastuzumab-insensitive breast cancer [16, 17], prostate cancer [18], colon cancer [19], gastric carcinoma [20], squamous-cell carcinoma of head and neck origin [21] and chemosensitizing activity in multidrug resistance [22] with interesting results. This flavonol demonstrated metal chelating abilities [23] and protected mice hepatic tissue from sodium fluoride induced hepatotoxicity [24, 25], Quercetine also had positive effects on myocardial infracted rats by inhibiting mitochondrial lipid peroxidation and increasing mitochondrial marker enzymes and antioxidants [26].

Quercetin also holds great promise for topical application, as it shows strong protective effect against UV-induced lipid peroxidation [27] and proved to be effective on human keratinocytes with anti-ageing activity and skin rejuvenation capability [28]. Quercetin, dissolved in a mixture of ethanol, propylene glycol and water, was applied topically on hairless mice before the exposure to UV irradiation and showed wrinkle diminishing ability and an increase in collagen content with an increase in glutathione and a decrease in thiobarbituric acid reactive substances [29]. However, because quercetin possesses a poor water solubility, instability and very low skin permeability in its crude form [30], the development of adapted formulations should be investigated in order to deliver the effective dose of quercetin to skin tissue (epidermis). In this context, nanoformulations, such as nanostructured lipid carriers, nanoemulsions and liposomes have the potential to deliver poorly water-soluble drugs to skin tissue [31-34]. Among nanoformulations developed, lipid nanocapsules (LNC), prepared by a phase inversion dependent process, are spherical vesicles that can be formulated with selected size depending on excipients percentage with a high monodispersity [35, 36].

Many hydrophobic drugs (taxane, etoposide, docetaxel, paclitaxel, tamoxifen), but also hydrophilic (nucleic acids, insulin, peptides ...) and even amphiphilic compounds (amiodarone) were successfully incorporated into LNC [37-46]. The lipophilic composition of these particles along with their higher skin occlusive effect [47] highlight their applications for the improvement of topical delivery of drugs. In this way, quercetin lipid nanocapsules were previously prepared by Barras *et al* in 2009, but quercetin drug loading was limited, which is not sufficient for pharmacological application [48].

In this study, 20 nm and 50 nm LNC formulations were modified to improve quercetin drug loading by using novel excipient and a pre-solubilization step of quercetin in ethanol [44]. Physicochemical characterizations such as size, polydispersity index (PDI), surface charge, drug loading (DL), and encapsulation efficacy (EE) of quercetin were performed. This evidenced that 20 nm LNC efficiently encapsulated quercetin with a drug loading of 32.0 mM. X-ray diffractograms of crude quercetin and quercetin nanocapsules were recorded and compared to determine the influence of formulation on quercetin crystalline nature. Quercetin nanocapsules were then characterized to verify their size and spherical shape (TEM). Quercetin *in vitro* antioxidant activity was determined by DPPH assay to validate the preservation of quercetin activity after formulation. Finally, regarding a dermal application, the excessive immune response is a dominant feature of chronic inflammatory skin disorder such as psoriasis and in response to UV irradiation [49, 50]. As a consequence to chronic inflammation an additional group of dermal dendritic cells coming from monocytes and called monocytes-derived dendritic cells is activated [51, 52]. Therefore, quercetin interest against oxidative stress was tested on monocytic cell line (THP-1). First, the cellular toxicity of quercetin LNC formulations on THP-1 was determined via XTT assay. Second, the protective effect of these formulations against H_2O_2 induced oxidative stress was established on the same cellular model.

Lipid nanocapsules hold great promise for the topical delivery of quercetin as a UV sunscreen or even in the supportive treatment of inflammatory skin disorders such as psoriasis.

2. Materials and methods

Quercetin aglycone was purchased for Sigma-Aldrich (Sigma-Aldrich Chimie, France). Cremophor® EL (polyoxyl 35 castor oil) and Solutol® HS 15 (a mixture of free polyethylene glycol 660 and polyethylene glycol 660 hydroxystearate) were gift from BASF (Ludwigshafen, Germany). Lipophillic Labrafac® WL 1349 (caprylic acid triglycerides) and Lipoid® S75-3 (soybean lecithin at 69% of phosphatidylcholine) were kindly provided by Gattefosse® (Saint-Priest, France) and Lipoid® (Ludwigshafen, Germany) respectively. Because of the complex chemical composition of the mixtures, brand name will be used throughout the article and any amount indicated in the formulation model represents the whole mixture regardless of its

constituents. NaCl was provided from Prolabo® (Fontenay-sous-Bois, France), MilliQ water was obtained by the Milli® RO System (Millipore, Paris, France). 2,3-Bis-(2-methoxy-4-nitro-5-sulfophenyl)-2H-tetrazolium-5-carboxanilide salt (XTT) and 2',7' –dichlorofluorescin diacetate (DCFDA) were purchased for Sigma-Aldrich (Sigma-Aldrich Chimie, France). All HPLC chemicals and buffer components were purchased from Sigma-Aldrich (France).

2.1 Preparation of quercetin loaded lipid nanocapsules (que-LNC)

The phase inversion method reported by Heurtault *et al* in 2002 was improved for the preparation of quercetin lipid nanocapsules with the addition of Cremophor® EL to increase the solubility of quercetin within formulation [36] (Table 1). In brief, all the LNC excipients were mixed together along with quercetin. Magnetic agitation was kept at 300 rpm during the whole process. Temperature was recorded during the whole preparation process with HI98501 Checktemp® digital thermometer (Hanna Instruments, USA). A first homogenization step of the mixture was established by heating up to 85°C. At the end of this homogenization step, 500 µl of absolute ethanol was added to the mixture. After three heating and cooling cycles (65°C – 85°C), 5.5 ml of milliQ water at 4°C was added to the mixture at the transition phase. Lastly, quercetin lipid nanocapsules (que-LNC) were left to cool down to room temperature under agitation. Blank lipid nanocapsules (blank-LNC) were prepared by the same procedure without quercetin.

Composition (w/w%)	Solutol® HS 15	Cremophor® EL	Labrafac® WL 1349	NaCl	Lipoïd® S75-3	Quercetin	MilliQ water
Original formula for 50 nm LNC	16.92		20.56	1.78	1.50		59.24
Modified formula for 50 nm LNC	5.00	15.00	20.56	1.78	1.50	2.85	56.16
Original formula for 20 nm LNC	38.68		17.36	1.78	1.50		40.68
Modified formula for 20 nm LNC	14.50	29.00	16.60	1.70	1.40	3.23	36.80

Table 1: Chemical composition of original lipid nanocapsules (Heurtault *et al)* and quercetin modified lipid nanocapsules (w/w %).

2.2 Photon correlation spectroscopy and electrophoretic mobility measurements

20 µl of que-LNC were diluted to 1000 µl by milliQ water and characterized for hydrodynamic diameter and polydispersity index (PDI) using Zetasizer NanoZS (Malvern Instruments, UK). Zeta potential was measured by transferring 800 µl of diluted lipid nanocapsules suspension to Disposable Capillary Cell (Malvern Instruments, UK). All measurements were performed in triplicate.

Que-LNC and blank-LNC were divided into three groups immediately after preparation and stored at 4, 25, 37 °C respectively, samples are taken at day 0, 7, 14 and 28 and tested for average particle size, PDI, and zeta potential as described above.

2.3 Transmission electron microscopy

Transmission electron microscope (TEM) analysis was performed with TEM Jeol 1200EXII, (Jeol.Ltd, Tokyo, Japan) provided with a 4k/3 kelopixels quemesa Camera (Olympus, Japan) and uncoated carbon TEM grids Type CU formar carbon 3 MMM (Agar Scientific, UK). 5 µl of que-LNC were incubated 30 minutes at room temperature then images were taken using a measure IT software.

2.4 X ray analysis

X-ray diffractograms of crude quercetin and que-LNC were recorded using D8 Advance LA Cu 1.5406 Å Bruker axs (Burker, Karlsruhe, Germany) equipped with a parafocusing geometry circle of Bragg Brentano and generator (40kv 40mA). A solid detector lynx eyes 1D is used for the sample detection, the test was set from 2 to 70 θ angle at a fixed detection velocity,

2.5 HPLC analysis

The chromatographic analysis of quercetin was performed on LC6-2010HT (Shimadzu, Kyoto, Japan) using a C18 column Prontosil (120-5-C18 H5.0 µm, 250 ×4.0 mm) as stationary phase. The detection was carried out using a UV lamp (UV-VIS detector, Shimadzu, Kyoto, Japan) at 368 nm [53]. For the determination of quercetin encapsulation efficiency and drug loading within LNC (section 2.6), a mobile phase consisting of 10% methanol, 80% acetonitrile and 10% of phosphoric acid solution 0.2% at pH=1.9 was used. The flow rate was kept at 1 ml/min during the 15 min run time analysis. Serial dilutions of known concentrations of quercetin in methanol were used to make the calibration curve. The method showed linearity over a concentration range from 62.5 to 500 µg/ml (r^2 = 0.9998 and %RSD = 2.48). For the detection of quercetin *in vitro* release from que-LNC (section 2.8), another calibration curve of quercetin

was used from 0.2 to 4 µg/ml in PBS buffer pH 7.4 with Tween® 20 (2%) and a gradient flow rate according to Hatahet *et al* [54].

2.6 Encapsulation efficacy (EE) and drug loading capacity (DL)

Quercetin encapsulation efficacy (EE) was determined by filtering formulated que-LNC through 0.2 µm pore size filters (Sartorius Stedim Minisart®, Sartorius AG, Germany). Then, 50 µl of the filtered que-LNC were diluted with methanol and quercetin concentration was quantified by HPLC (section 2.5). Encapsulation efficiency and drug loading were calculated with the equations below:

Equation 1: $$Drug\ loading\ (\%) = \left[\frac{quercetin\ quantity}{lipid\ phase\ excipients\ quantity}\right] 100$$

For the comparison with previous reports [48], Quercetin loading within the lipid nanocapsules is expressed in mM and was calculated based on HPLC (section 2.5).

Equation 2: $$Encapsulation\ efficacy\ (\%) = \left[\frac{amount\ of\ encapsulated\ quercetin}{amount\ of\ quercetin\ initailly\ added}\right] 100$$

2.7 Hydrogen donating ability *in vitro* by *2, 2-diphenyl-1-picrylhydrazyl* (DPPH)

2, 2-diphenyl-1-picrylhydrazyl (DPPH) is a molecule with free radical at the hydrazine position where compounds possessing antioxidative activity can react with. DPPH in its radical form is known to have a strong absorption band at 517 nm. The absorbance at 517 nm diminishes when it reacts with an antioxidant [55]. The reaction ratio between quercetin and DPPH is 3.1 (V/ V). 400 µM DPPH solution was regarded as positive control and donated 100% free radical or 0% inhibition. Blank was methanol without neither DPPH nor quercetin. DPPH test was performed on que-LNC in order to determine the activity of encapsulated quercetin after formulation. DPPH percentage activity is then calculated according to the equation 3:

Equation 3: $$DPPH\ \%\ activity = \frac{quantity\ of\ active\ quercetin}{practically\ encapsulated\ quercetin} \times 100$$

2.8 *In vitro* release study

The concept of *in vitro* release study is attending a concentration gradient between que-LNC and a receptor medium when diffusion from quercetin formulation toward the receptor medium occurs. This diffusion is determined in function of quercetin concentration and the effect of formulation on quercetin movement through a nitrocellulose dialysis membrane. For this, a 12-14 MWCF Spectra/Pore® Dialysis Membrane (Spectrum laboratories INC, USA) was selected along with a receptor medium composed of 100 ml PBS at pH 7.4 with Tween® 20 (2%) that maintain sink conditions [56]. The experiment temperature was 37°C. In order to evaluate the effect of LNC particle size on the release of quercetin, que-LNC 20 and que-LNC 50 volumes were adjusted in order to contain the same concentration of quercetin. A solution of quercetin

containing the same quantity in propylene glycol was used as the positive release control. Samples were withdrawn at 5, 15, 30 minutes and then 1, 2, 3, 4, 5, 6 and 24 hours. Quercetin concentration was calculated by HPLC method (section 2.5).

2.9 Cell culture

Acute monocytic leukemia cell line (THP-1) was a kind gift from Professor Francisco Veas (IRD, Montpellier). Cells were cultured with Roswell Park Memorial Institute medium (RPMI) supplemented with 10% fetal bovine serum and 1% (v/v) penicillin/streptomycin by life technologies™ (Carlsbad, California, USA). Cells were seeded in Corning® 150 cm^2 at a density of 10^6 cell/mL in Canted Neck Flask with Vent Cap and incubated in humidified Heraeus® BB6220 incubator (Thermo Scientific™, Waltham, Massachusetts, USA) with at 5% CO_2 at 37°C. Cell replication was twice a week when cells attend confluence.

2.10 Cellular toxicity

For cellular toxicity study, THP-1 cells were seeded at cellular density of 300,000 cells/ml in flat bottom 24 well plate from Corning® Costar® cell culture plates (Corning incorporated, New York, USA). Following this, cells were directly treated with crude quercetin and que-LNC at a concentration of 0.5, 2 and 5 µg/ml for 72 hours. Crude quercetin and que-LNC were diluted with Dulbecco's phosphate-buffered saline (DPBS) from life technologies™ (Carlsbad, California, USA). Blank-LNC were used as a control to brighten up the cellular activity of quercetin. Control cells were treated with buffer and considered 100% viable cells. Afterwards, cellular viability was tested using 2,3-Bis-(2-methoxy-4-nitro-5-sulfophenyl)-2H-tetrazolium-5-carboxanilide salt (XTT) assay [57]. XTT assay differs from MTT assay that, it does not require a dissolving step for formazan crystals. 50 µl of XTT reagent were added to each well for 3 hours, and then absorbance was measured at 450 and 750 nm using Multiskan™ GO Microplate Spectrophotometer (Thermo Scientific™, Waltham, Massachusetts, USA). Cellular viability percentages were presented restively to control non-treated cells.

2.11 Quercetin protective effect on THP-1 cells against oxidative stress

THP-1 cells were seeded at 300,000 cells/ml in 24 well/plate and treated with crude quercetin or que-LNC for 24 hours. Then, cells were loaded with 2',7' –dichlorofluorescein diacetate (DCFDA reagent) (1 µM in RPMI without phenol red) for 60 minutes. DCFDA is a fluorogenic dye that is cell permeant. By internalization into cells, is DCFDA is deacetylated by cellular esterases to a non-fluorescent compound, which is later oxidized by ROS into 2', 7' –dichlorofluorescein (DCF), a highly fluorescent compound [58]. Next, oxidative stress was initiated using H_2O_2 (1 mM) for 120 minutes. After cellular exposure, cells were

collected with centrifugation and supernatant is discarded. Cells were then lysed with Tris cell lysis buffer (200 µl) for each well. After that, cell lysates were transferred to 96 wells black plate with clear bottom (Corning®, Massachusetts, USA). Finally, DCF is detected at maximum excitation and emission spectra of 485 nm and 525 nm using TriStar LB 941 from Berthold Technologies (Chollerstr, Switzerland).

2.12 Statistical analysis

Statistical analysis of the *in vitro* release study, cellular cytotoxicity and cellular protective activity was run using with Microsoft Excel 2013 tool Pack (Microsoft Corporation, USA). A Two-sample t-test with unequal variances was used to verify the significant difference between data. P expresses the significant value where * = $P < 0.05$, ** = $P < 0.01$ and *** = $P < 0.005$ respectively.

3. Results

3.1 Physicochemical characterizations of quercetin lipid nanocapsules

3.1.1 Average particle size and surface charge

Table 12 shows the average particle size and the zeta potential values for quercetin lipid nanocapsules 50 nm (que-LNC 50) and quercetin lipid nanocapsules 20 nm (que-LNC 20). The average particle size of que-LNC 50 was 54 ± 3 nm and 26 ± 3 nm for que-LNC 20. The particle size was similar in blank-LNC and que-LNC in both formulations: 46 nm vs. 54 nm for LNC 50 and 24 nm vs. 26 nm for LNC 20. Zeta potential values were -7.4 ± 4 mV for que-LNC 50 and -2.3 ± 0.8 mV for que-LNC 20. The introduction of Cremophor® EL and the use of ethanol in the preparation did not affect neither the particle size nor the zeta potential of the resulted formulations (data not shown) [36, 48].

Formulations	Crude quercetin	Blank LNC 50 nm	Quercetin LNC 50 nm	Blank LNC 20 nm	Quercetin LNC 20 nm
Size* (nm)	3976 ± 434	46 ± 2	54 ± 3	24 ± 2	26 ± 3
PDI	0.796 ± 0.186	0.09 ± 0.015	0.17 ± 0.002	0.06 ± 0.015	0.06 ± 0.001
Zeta potential (mV)		- 6.7 ± 3	-7.4 ± 4	- 1.9 ± 1.2	-2.3 ± 0.8
DL (%)			2.62 ± 0.1		2.79 ± 0.2
EE (%)			96.4 ± 1.2		90.9 ± 3.5
Total DL (mM)			18.6 ± 0.6		32.0 ± 2.4
DPPH activity (%)			92.3 ± 4.4		65.1 ± 5.7

Table 2: Physicochemical properties of formulated quercetin lipid nanocapsules.

PDI is the polydispersity index, DL is the drug loading within LNC formulations relative to lipid excipients, EE is the encapsulation efficacy and DPPH is antioxidant activity of encapsulated quercetin in reaction with DPPH (n=3). * Particle size and PDI was measured with photon correlation spectroscopy.

3.1.2 Formulations stability

Que-LNC stability was monitored over 28 days at three temperatures (4°C, 25°C and 37°C). Fig. 1 represents the average particle size and the PDI for que-LNC formulations at day 0, day 14 and day 28. Que-LNC 50 was stable over the three temperatures for the tested period as particle size was 58 ± 14 nm at day 28 (37°C) compared to 54 ± 3 nm at day 0. PDI stayed inferior to 0.2 during the whole period, whatever was the temperature. Que-LNC 20 was stable only at 4°C and 25°C, while at 37°C a dramatic increase in particle size to 75 ± 2 nm and PDI to 0.24 ± 0.02 that occurred at day 28 compared to 26 ± 3 nm and PDI 0.06 ± 0.001 at day 0.

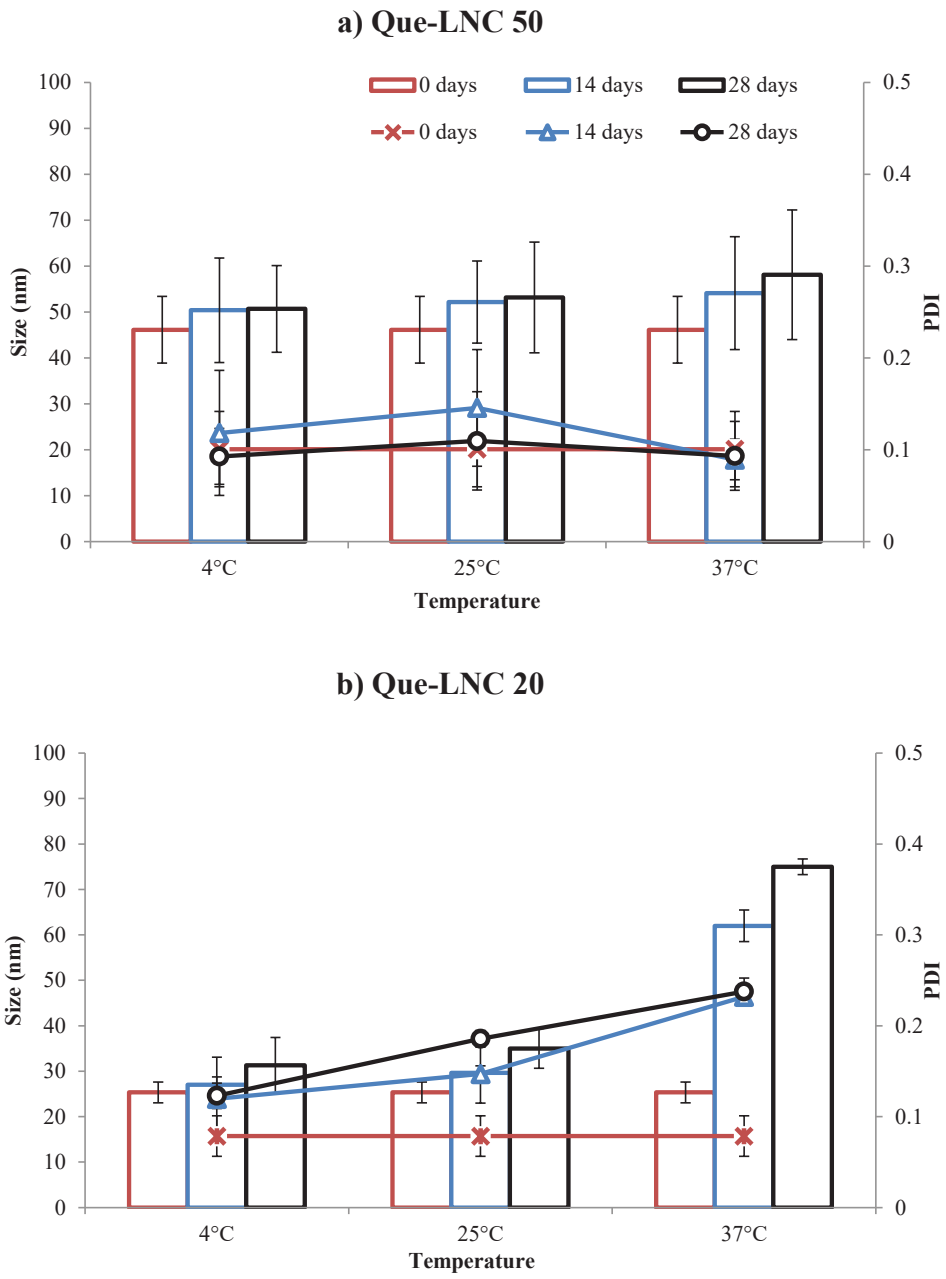

Fig. 1: Stability results for a) que-LNC 50 and b) que-LNC 20 for one month at 4°C, 25°C and 37°C (n=3). Stability is monitored with average particle size (columns) and PDI (x, △ and ○) changes upon storage.

3.1.3 Electron microscopic examination

TEM images were taken for both LNC formulations (Fig. 2). Particles were in spherical shape with no difference in morphology for que-LNC compared to blank-LNC. Particle size was in the same range of the

one recorded by photon correlation spectroscopy (Fig. 1). Particle size and shape are consistent with original LNC formulation [36].

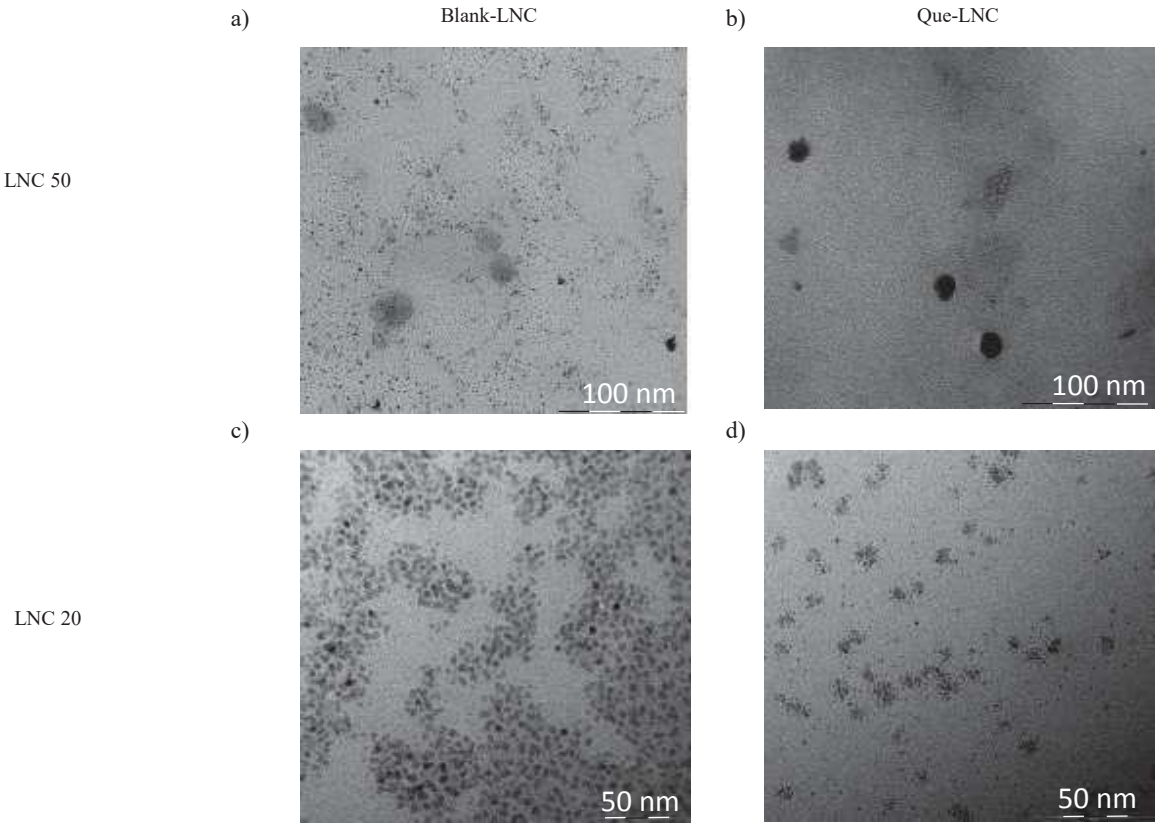

Fig. 2: TEM images for a) blank-LNC 50, b) que-LNC 50, c) blank-LNC 20 and d) que-LNC 20.

3.1.4 Crystallinity examination

X-ray diffractograms are presented in Fig. 3 for crude quercetin, que-LNC 50 and que-LNC 20 respectively. The X-ray diffractogram of crude quercetin revealed its crystalline nature (Fig. 3 left). The X-ray diffractogram of quercetin after ethanol evaporation reveals the interaction of quercetin with the ethanol and indicates changes in the diffractogram, which could highlight a possible polymorphic change. Both que-LNC formulations showed a broad peak centered at 20 θ, which indicates the disorder lattice of the capsules and the amorphous state of its composites (Fig. 3 middle and right). Blank-LNC had the same diffractogram as their quercetin loaded counterparts (data not shown).

3.2 Encapsulation efficacy (EE) and drug loading capacity (DL)

Table 2 presents the encapsulation efficiency and the drug loading for que-LNC 50 and que-LNC 20 respectively. DL and EE were calculated using equations 1 and 2 (section 2.6). DL is the amount of quercetin relative to total lipid excipients and was respectively 2.62 ± 0.1 % and 2.79 ± 0.2 % with que-

LNC 50 and que-LNC 20. EE is the measure of the experimentally encapsulated amount of quercetin relative to the added amount of quercetin. It was about 96.4 ± 1.2 % for que-LNC 50 and 90.9 ± 3.5 % for que-LNC 20. However, the DL of quercetin in que-LNC 20 was higher than the one obtained in que-LNC 50 (32.0 ± 2.4 vs. 18.6 ± 0.6 mM).

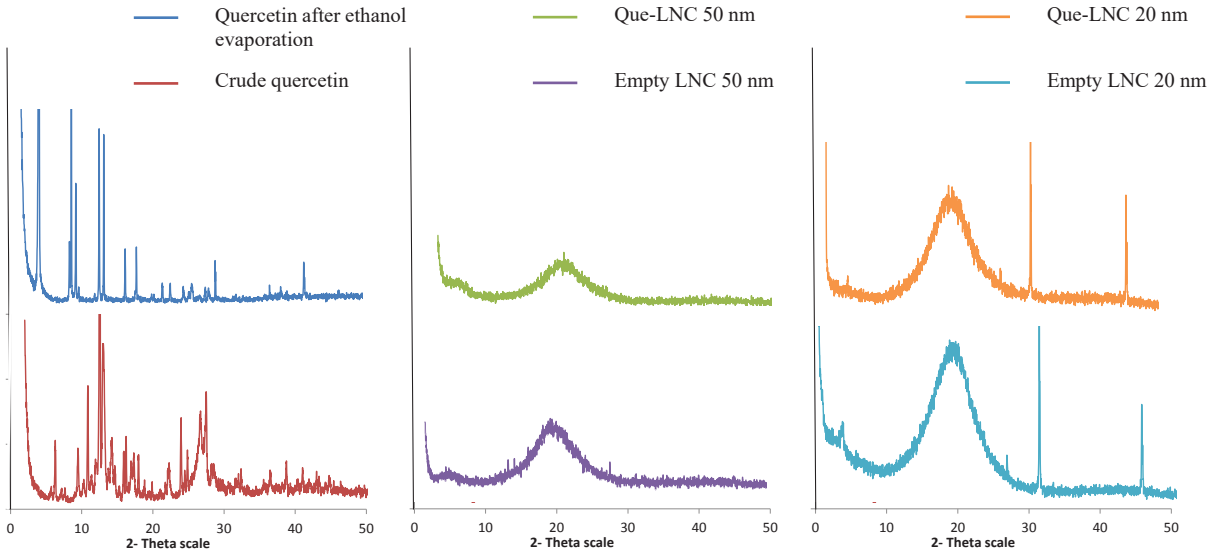

Fig. 3: X-ray diffractograms for crude quercetin (left), quercetin LNC 50 nm (middle) and quercetin LNC 20 nm (right).

3.3 Hydrogen donating ability *in vitro* by *2, 2-diphenyl-1-picrylhydrazyl* (DPPH)

The retained activity of encapsulated quercetin within LNC formulations was assessed *in vitro* using the reaction with DPPH radical. Table 2 shows the DPPH percentage activity of quercetin calculated with equation 3 (section 2.7). Active quercetin percentage of total encapsulated quercetin was 92.3 ± 4.4 % for que-LNC 50 and 65.1 ± 5.7 % for que-LNC 20.

3.4 *In vitro* release study

The release study of que-LNC formulations was done in dialysis bag for 24 hours in PBS 7.4 with Tween® 20 (2%). Fig. 4 presents the release profile of quercetin from lipid nanocapsules compared to quercetin solubized in propylene glycol. Both lipid nanocapsules formulation enabled a prolonged release profile of quercetin in comparison to the control. In contrast to the insignificant differences between que-LNC 50 and que-LNC 20 ($P > 0.05$), the released amount was significantly different from control ($P < 0.005$).After 24 hours, the released amount was 8.6 ± 2.3 % and 14.9 ± 4.4 % for que-LNC 50 and que-LNC 20 respectively, whereas 37.3 ± 1.8 % of quercetin was diffused form control solution.

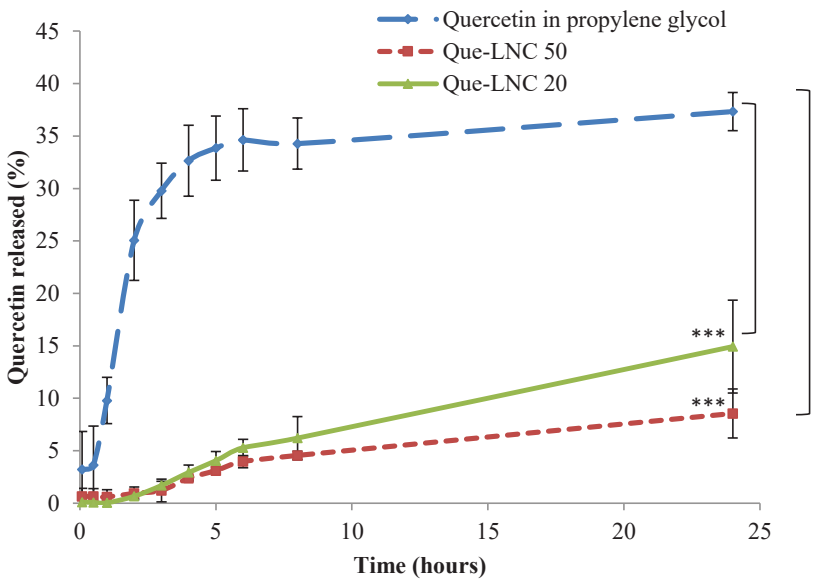

Fig. 4: *In vitro* quercetin release study with que-LNC 50, que-LNC 20 and quercetin in propylene glycol (n=3). *** indicates a $P < 0.005$ according to t-Test: two-sample assuming unequal variances relative to control.

3.5 Que-LNC toxicity on THP-1 cells

The study of quercetin toxicity profile from 0.5 to 5 µg/ml was examined on THP-1 cells for 72 hours. Fig. 5 shows the cellular viability results normalized to control (non-treated) cells for crude quercetin, blank-LNC 50 and 20 and que-LNC 20 and 50. Looking at blank-LNC formulations, no difference in cellular viability was observed between quercetin loaded and blank formulations, which indicates that encapsulated quercetin did not affect THP-1 cellular viability. Crude quercetin and que-LNC 20 were similar to control cells at the tested concentrations ($P > 0.5$). Que-LNC 50 was similar to control cells at 0.5 and 2 µg/ml of quercetin ($P > 0.5$).

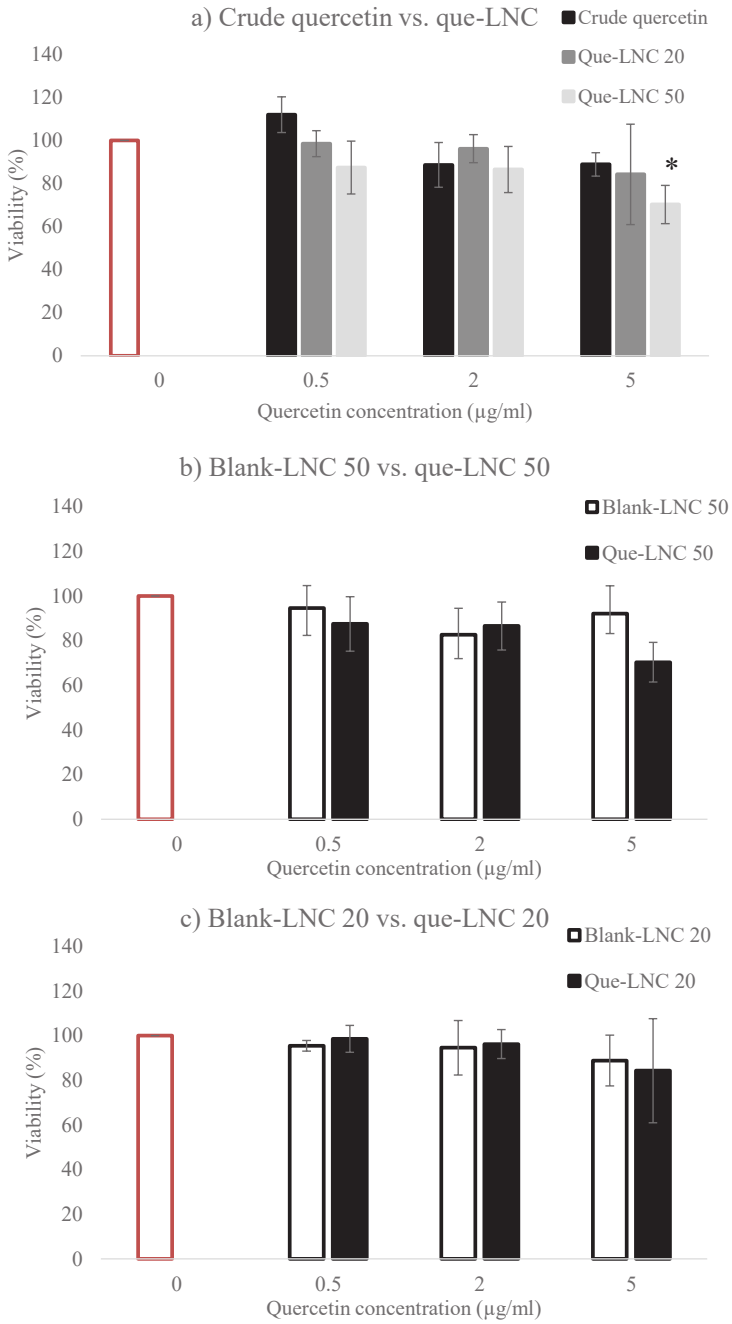

Fig. 5: *In vitro* toxicity on THP-1 cells of crude quercetin, blank-LNC formulations and que-LNC formulations for 72 hours (n=3).

a) Cellular toxicity comparison between crude quercetin and que-LNC formulations * indicates a $P < 0.05$ according to t-Test: two-sample assuming unequal variances relative to control (non-treated) cells.

b and c) Cellular toxicity for que-LNC formulations in comparison to blank-LNC, no statistical differences were observed between quercetin loaded LNC and blank ones.

3.6 Quercetin protective effect on THP-1 cells against oxidative stress

The ability of quercetin to support immune cells under oxidative stress conditions was studied via THP-1 cellular model *in vitro*. Cells were treated with either crude quercetin or que-LNC formulations at a concentration of 5 µg/ml then, labeled with DCFDA before the oxidative stress induction by H_2O_2. ROS were then quantified both in control (non-treated) cells (control negative) and in quercetin treated group (crude, LNC 50 and LNC 20). Results were compared to the ROS generated in H_2O_2 treated cells (control positive). H_2O_2 increased the ROS generated inside the cells (control positive) in comparison to non-treated cells (control negative) by 30 % ($P < 0.005$). Crude quercetin was able to reduce by 66 % the generated ROS in response to H_2O_2 oxidative attack ($P < 0.05$). Que-LNC 20 and que-LNC 50 also showed significant reduction in the generated ROS ($P < 0.005$), with a reduction of 65 % with both formulations. No significant difference in the ability to protect against oxidative stress between crude quercetin and the formulated one in the LNC was evidenced. It is worth to note that no cellular death was observed with crude quercetin and que-LNC under the tested experimental conditions (24 hours – data not shown).

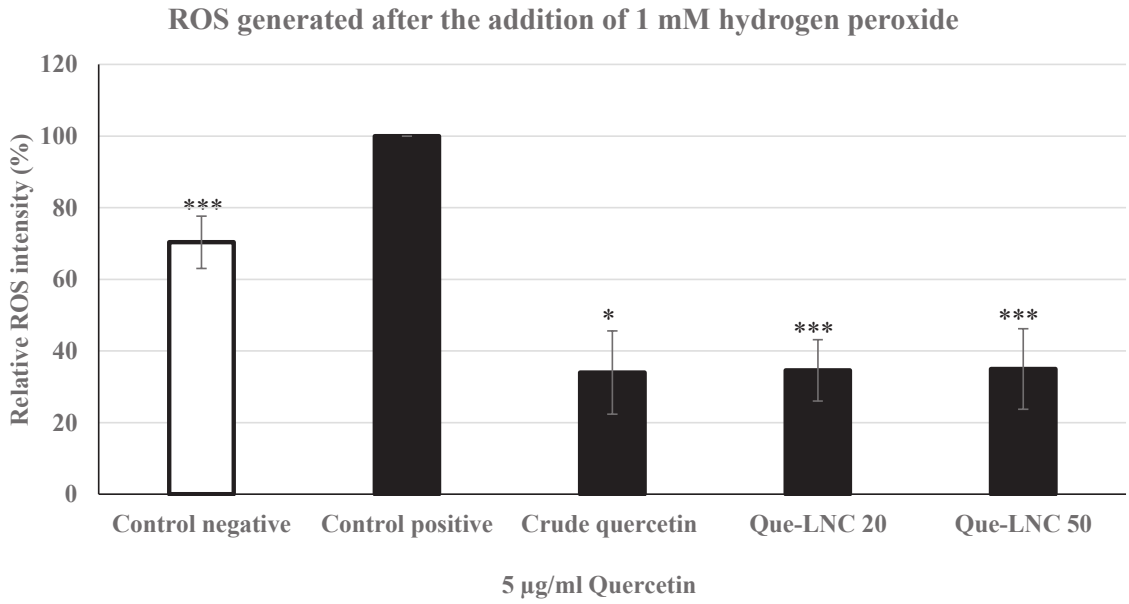

Fig. 6: *In vitro* antioxidant activity on THP-1 cells of crude quercetin and que-LNC formulations (n=3).
Control negative are cells without quercetin and H_2O_2 treatment. Control positive are cells treated with H_2O_2 without quercetin treatment. Fluorescent intensity was normalized to H_2O_2 treated group (control positive). The statistical analysis was comparing other conditions to the control positive (* = $P < 0.05$, ** = $P < 0.01$ and *** = $P < 0.005$ respectively).

4. Discussion

Quercetin is a promising drug candidate for topical applications as it possesses strong antioxidant [59-61] and broad antiinflammatory activities [62, 63]. These properties can be implemented in the treatment of skin inflammatory diseases like psoriasis [64] and in the support of skin in response to oxidative stress induced by UV irradiation [65]. However, crude (non-formulated) quercetin presents an essential drawback, which is its poor water solubility that hinders topical penetrating capacity and hence topical efficiency [30]. In this regard, formulation of suitable carrier systems increasing quercetin solubility is an important strategy to enhance its topical effectiveness. Among them, LNC presents the triple benefit of increasing the apparent water solubility of quercetin, protecting it from degradation [66] and enabling a higher occlusive effect on the skin [31]. In addition, the small size of LNC along with their lipid nature could facilitate the delivery of quercetin to skin epidermis.

Quercetin was previously formulated within LNC with limited drug loading [48]. In order to improve quercetin drug loading, several modifications were introduced to the LNC formulation process in order to attend higher affinity with LNC components and to increase quercetin slow dissolution observed with the original LNC excipients during the process [67]. Modifications were first the addition of Cremophor® EL to the formulation which allow an increase ability to encapsulate quercetin. It is worth to note also that Cremophor® EL has lower cellular toxicity to keratinocytes than Solutol® HS 15 conferring another advantage to the new formulation [68]. Then, to accelerate quercetin dissolution in the excipients matrix, ethanol was added at the end of homogenization step at 85°C. However, with the repetition of heating at 85°C in the next cycles, ethanol evaporates leading to quercetin precipitation into the matrix excipients. Nevertheless, the precipitated quercetin has very small particles size [69, 70], which enables its fast dissolution into the excipient matrix.

The particle size of que-LNC formulations and the subsequent TEM images are coherent and indicate that the applied modifications of the formulation and the preparation process did not alter the formation of LNC. Que-LNC 20 size distribution was 26 ± 3 nm, and que-LNC 50 one was 54 ± 3 nm (Table 2), and they both presented a spherical shape (TEM). The formulations were homogenous with a PDI inferior to 0.2 (Fig. 2). Quercetin loading within que-LNC 20 increased from 5.6 mM in the original formulation (Barras *et al* 2009) to 32 mM and from 3.72 to 18.6 mM in que-LNC 50 (Table 2) [48]. Consequently, quercetin water solubility apparently increased from 0.48 µg/ml to about 8 mg/ml in que-LNC 20 and to about 5 mg/ml in que-LNC 50 [54]. These results present LNC as an efficient system to overcome quercetin poor water solubility. In accordance with the study of Barras *et al* [48], the higher encapsulation within the LNC 20 (presenting higher lipid interface surface compared to LNC 50) highlights the quercetin deposition at the lipid/ water interface and not only inside the oily core of the capsule.

The stability of pharmaceutical dosage forms is an essential part of their successful design [71]. The stability of que-LNC 20 and que-LNC 50 was monitored for 28 days at 4°C, 25°C and 37°C. Both formulations were stable at 4°C and 25°C with insignificant increase in particles size and PDI less than 0.2 (Fig. 1). Only que-LNC 50 showed stability at 37°C. The instability of que-LNC 20 at 37°C may be attributed to the melting of the lipid excipients (Fig.1) and to the higher ratio of encapsulated quercetin (Table 2) compared to que-LNC 50 [72]. Nevertheless, this can be an advantage for topical application, as this formulation could start to melt and to release the encapsulated drug in contact to skin temperature (approximately 34°C) [73].

The X-ray diffractogram of crude quercetin reveals its crystalline organization (Fig. 3 lower) [74]. On the other hand, the X-ray diffractograms for que-LNC 20 and 50 are similar to each other and show one broad peak indicating the perturbed lattice of the lipid mixture forming the nanocapsules. This could come to the complex nature of these lipids and the presence of imperfections in the lattice linked to encapsulated quercetin [75]. Because of the small percentage of quercetin compared to other lipid excipients less than 3.5 %, for this reason the exact form of quercetin within lipid nanocapsules could not be identified (Table 1), quercetin specific peaks were not detected in LNC diffractograms [76].

Quercetin antioxidant activity was evaluated *in vitro* using DPPH assay, in order to ensure the retained antioxidant activity of quercetin after formulation. Quercetin retained its activity *in vitro* as percentage of active quercetin to total quercetin loaded into LNC was 92.3 % for LNC 50 and 65.1 % for LNC 20 (Table 2). This comes in accordance to previous reports where quercetin-loaded glycerosomes showed $\sim 95 \pm 1$ % DPPH activity in contrast to quercetin-loaded liposomes with $\sim 87 \pm 2$ % DPPH activity [77].LNC as a carrier system enabled a sustained release kinetic for encapsulated drugs such as ibuprofen in PBS (pH 7.4) at 37 °C for 24 hours [41] and amiodarone during 4 days study [42]. The sustained kinetic at 37°C was also observed with quercetin encapsulated in que-LNC 50 and 20, with less than 15 % released for both formulations after 24 hours at 37°C compared to more than 30 % for control (quercetin solubilized in propylene glycol) (Fig. 4). Indeed, LNC 20 showed a higher percentage release than LNC 50 after 24 hours (14.3 % vs. 8.6 %). This could be linked first, to the presence of greater amounts of quercetin at the interface of que-LNC 20 compared to que-LNC 50 (due to higher drug loading 32.0 mM vs. 18.6 mM). This could also be explained by the melting of LNC 20 lipids at 37°C (as already highlighted in stability results) and the subsequent release of encapsulated drug (Fig. 1). Finally, whatever the formulation, the sustained release of quercetin seems favorable for topical delivery. Penetrated LNC can be a reservoir for quercetin, allowing it slow diffusion to skin tissue. As a result, quercetin slow release at low concentrations could avoid side effects related to high concentrations of quercetin such as prooxidation effects [78, 79].

The main objective of these formulations is the enhancement of quercetin efficiency on skin benefiting from its antioxidant and antiinflammatory activates. These activates encourage the use of que-LNC in UV

sunscreen or in inflammatory skin diseases. UV exposure initiates inflammation cascade with an increase in the reactive oxygen species among them H_2O_2 in the skin tissue [80, 81]. Also, psoriasis is a chronic inflammatory pathology of the skin with an increase in inflammatory dendritic cells (monocytes derived dendritic cells) [82]. Excessive amounts of H_2O_2 are present during inflammation and are a major cause of T-cell impaired functions [83, 84], which is also observed in tumor heterogeneity and invasion [85, 86] For this, the protection of skin tissue and immune cells located in the skin from excessive oxidative stress is of high relevance. Quercetin, which is a strong antioxidant with antiinflammatory actions, is a potential candidate for skin supplementation. Therefore, THP-1 cells were used as a cellular model for immune cells to evaluate the ability of quercetin to counteract oxidative stress induced by H_2O_2.

The cellular viability after 72 hours treatment of crude quercetin and que-LNC 20 and 50 nm was determined (Fig. 5 a). The cellular viability were similar to control (non-treated) cells with crude quercetin and que-LNC 20 up to 5 µg/ml of quercetin, which indicates the safety of quercetin in the tested concentration (Fig. 5 a and c). Only the validity percentage with que-LNC 50 at 5 µg/ml of quercetin was significantly different from control group ($P < 0.05$) which a decrease to 70.3 % viability. However, by referring to blank-LNC 50 compared to quercetin loaded counterparts at the same excipients concentrations, no differences were observed in the viability percentage between blank-LNC 50 and que-LNC 50 (Fig. 5 b). This indicates that the main cause of toxicity is not quercetin by itself but rather the excipients, especially the surfactants used in LNC preparation, as an increase amounts of Solutol® HS 15 was used in LNC 50, such excipient known to be more toxic than Cremophor® EL [68].

Finally, the preserved activity of quercetin after its formulation within LNC was confirmed in comparison to crude form using H_2O_2. Exogenous H_2O_2 increased the endogenous ROS level in THP-1 cells by 1.4 fold ($P < 0.005$). Nevertheless, the pre-treatment with either crude quercetin or que-LNC 20 or que-LNC 50 reduced the endogenous ROS generated by H_2O_2 by 2.9 fold ($P < 0.05$ for crude quercetin and $P < 0.005$ for que-LNCs). Quercetin proved its free radical scavenging ability and protected THP-1 cells from the excessive amounts of ROS. This comes in accordance with previous reports about quercetin protective action against H_2O_2 on human peripheral blood lymphocytes [87] and human keratinocytes [77].

5. Conclusion

Quercetin, a natural antioxidant with poor water solubility and topical inactivity, was successfully formulated in optimized LNC 20 and 50. The modified formulations enabled six-fold increase in quercetin-loaded amount and more than 5,000 times increase in its apparent water solubility. Que-LNC 20 enabled a higher drug loading than que-LNC 50 indicating the presence of quercetin at the interface of the capsules

in accordance to previous reports. Both LNC formulations were homogenous with PDI values less than 0.2 and were stable for 28 days at 25°C. Furthermore, LNC formulations showed a prolonged release for encapsulated quercetin inducing no side effects. Encapsulated quercetin proved its antioxidant activity *in vitro* using DPPH assay. Interestingly, LNC formulations were shown to protect THP1 monocytes from oxidative stress induced by exogenous H_2O_2. The preserved antioxidant activity on cells holds great promise for skin supplementation with this natural molecule. With extremely small size distribution (26 and 54 nm), a lipophilic character for a better affinity to skin lipids and a strong occlusive effect to skin tissue, LNC as a carrier system could also hold a great interest for the dermal application of other poorly soluble molecules.

Acknowledgments

The authors acknowledge the financial support of ERASUMUS MUNDUS AVEMPACE 2 and the support of MACS research team. The authors have no conflict of interest to declare.

References

[1] M.A. Awad, A. de Jager, L.M. van Westing, Flavonoid and chlorogenic acid levels in apple fruit: characterisation of variation, Scientia Horticulturae, 83 (2000) 249-263.

[2] H. Zill e, M. Abert Vian, J.F. Maingonnat, F. Chemat, Clean recovery of antioxidant flavonoids from onions: Optimising solvent free microwave extraction method, Journal of Chromatography A, 1216 (2009) 7700-7707.

[3] Y. Shin, R.H. Liu, J.F. Nock, D. Holliday, C.B. Watkins, Temperature and relative humidity effects on quality, total ascorbic acid, phenolics and flavonoid concentrations, and antioxidant activity of strawberry, Postharvest Biology and Technology, 45 (2007) 349-357.

[4] M. Dehkharghanian, H. Adenier, M.A. Vijayalakshmi, Study of flavonoids in aqueous spinach extract using positive electrospray ionisation tandem quadrupole mass spectrometry, Food Chemistry, 121 (2010) 863-870.

[5] S. Arranz, G. Chiva-Blanch, R.M. Lamuela-Raventos, R. Estruch, Chapter 77 - Wine Polyphenols in the Management of Cardiovascular Risk Factors, in: R.R. Watson, V.R. Preedy, S. Zibadi (Eds.) Polyphenols in Human Health and Disease, Academic Press, San Diego, 2014, pp. 993-1006.

[6] P.G. Pietta, Flavonoids as antioxidants, J Nat Prod, 63 (2000) 1035-1042.

[7] T. Guardia, A.E. Rotelli, A.O. Juarez, L.E. Pelzer, Anti-inflammatory properties of plant flavonoids. Effects of rutin, quercetin and hesperidin on adjuvant arthritis in rat, Il Farmaco, 56 (2001) 683-687.

[8] Y. Kumazawa, K. Kawaguchi, H. Takimoto, Immunomodulating effects of flavonoids on acute and chronic inflammatory responses caused by tumor necrosis factor alpha, Curr Pharm Des, 12 (2006) 4271-4279.

[9] G. Zhang, L. Qin, W.Y. Hung, Y.Y. Shi, P.C. Leung, H.Y. Yeung, K.S. Leung, Flavonoids derived from herbal Epimedium Brevicornum Maxim prevent OVX-induced osteoporosis in rats independent of its enhancement in intestinal calcium absorption, Bone, 38 (2006) 818-825.

[10] A. Vijayalakshmi, G. Madhira, Anti-psoriatic activity of flavonoids from Cassia tora leaves using the rat ultraviolet B ray photodermatitis model, Revista Brasileira de Farmacognosia, 24 (2014) 322-329.

[11] C. Kandaswami, L.T. Lee, P.P. Lee, J.J. Hwang, F.C. Ke, Y.T. Huang, M.T. Lee, The antitumor activities of flavonoids, In Vivo, 19 (2005) 895-909.

[12] F.V. So, N. Guthrie, A.F. Chambers, M. Moussa, K.K. Carroll, Inhibition of human breast cancer cell proliferation and delay of mammary tumorigenesis by flavonoids and citrus juices, Nutr Cancer, 26 (1996) 167-181.

[13] E. Middleton, Jr., C. Kandaswami, T.C. Theoharides, The effects of plant flavonoids on mammalian cells: implications for inflammation, heart disease, and cancer, Pharmacol Rev, 52 (2000) 673-751.

[14] M.H. Gordon, A. Roedig-Penman, Antioxidant activity of quercetin and myricetin in liposomes, Chemistry and Physics of Lipids, 97 (1998) 79-85.

[15] A. Saija, M. Scalese, M. Lanza, D. Marzullo, F. Bonina, F. Castelli, Flavonoids as antioxidant agents: Importance of their interaction with biomembranes, Free Radical Biology and Medicine, 19 (1995) 481-486.

[16] M.-Y. Wong, G.N.C. Chiu, Liposome formulation of co-encapsulated vincristine and quercetin enhanced antitumor activity in a trastuzumab-insensitive breast tumor xenograft model, Nanomedicine: Nanotechnology, Biology and Medicine, 7 (2011) 834-840.

[17] A.K. Jain, K. Thanki, S. Jain, Novel self-nanoemulsifying formulation of quercetin: Implications of pro-oxidant activity on the anticancer efficacy, Nanomedicine: Nanotechnology, Biology and Medicine.

[18] G. Sharmila, F.A. Bhat, R. Arunkumar, P. Elumalai, P. Raja Singh, K. Senthilkumar, J. Arunakaran, Chemopreventive effect of quercetin, a natural dietary flavonoid on prostate cancer in in vivo model, Clinical Nutrition.

[19] H. Zhang, M. Zhang, L. Yu, Y. Zhao, N. He, X. Yang, Antitumor activities of quercetin and quercetin-5′,8-disulfonate in human colon and breast cancer cell lines, Food and Chemical Toxicology, 50 (2012) 1589-1599.

[20] S. Borska, M. Chmielewska, T. Wysocka, M. Drag-Zalesinska, M. Zabel, P. Dziegiel, In vitro effect of quercetin on human gastric carcinoma: Targeting cancer cells death and MDR, Food and Chemical Toxicology, 50 (2012) 3375-3383.

[21] M.H. Castillo, E. Perkins, J.H. Campbell, R. Doerr, J.M. Hassett, C. Kandaswami, E. Middleton, Jr., The effects of the bioflavonoid quercetin on squamous cell carcinoma of head and neck origin, Am J Surg, 158 (1989) 351-355.

[22] C. Chen, J. Zhou, C. Ji, Quercetin: A potential drug to reverse multidrug resistance, Life Sciences, 87 (2010) 333-338.

[23] P. Sestili, A. Guidarelli, M. Dachà, O. Cantoni, Quercetin Prevents DNA Single Strand Breakage and Cytotoxicity Caused By tert-Butylhydroperoxide: Free Radical Scavenging Versus Iron Chelating Mechanism, Free Radical Biology and Medicine, 25 (1998) 196-200.

[24] S.M. Nabavi, S.F. Nabavi, S. Eslami, A.H. Moghaddam, In vivo protective effects of quercetin against sodium fluoride-induced oxidative stress in the hepatic tissue, Food Chemistry, 132 (2012) 931-935.

[25] G.-N. Kim, Y.-I. Kwon, H.-D. Jang, Protective mechanism of quercetin and rutin on 2,2′-azobis(2-amidinopropane)dihydrochloride or Cu2+-induced oxidative stress in HepG2 cells, Toxicology in Vitro, 25 (2011) 138-144.

[26] P. Stanely Mainzen Prince, B. Sathya, Protective effects of quercetin on mitochondrial oxidative stress in isoproterenol induced myocardial infarcted rats: An in vivo and in vitro study, Food Research International, 49 (2012) 233-241.

[27] A. Saija, A. Tomaino, D. Trombetta, M. Luisa Pellegrino, B. Tita, C. Messina, F.P. Bonina, C. Rocco, G. Nicolosi, F. Castelli, ‘In vitro’ antioxidant and photoprotective properties and interaction with model membranes of three new quercetin esters, European Journal of Pharmaceutics and Biopharmaceutics, 56 (2003) 167-174.

[28] N. Chondrogianni, S. Kapeta, I. Chinou, K. Vassilatou, I. Papassideri, E.S. Gonos, Anti-ageing and rejuvenating effects of quercetin, Experimental Gerontology, 45 (2010) 763-771.

[29] D. Singh Joshan, S.K. Singh, Investigational study of Juglans regia extract and quercetin against photoaging, Biomedicine & Aging Pathology, 3 (2013) 193-200.

[30] F. Bonina, M. Lanza, L. Montenegro, C. Puglisi, A. Tomaino, D. Trombetta, F. Castelli, A. Saija, Flavonoids as potential protective agents against photo-oxidative skin damage, International Journal of Pharmaceutics, 145 (1996) 87-94.

[31] J. Pardeike, A. Hommoss, R.H. Müller, Lipid nanoparticles (SLN, NLC) in cosmetic and pharmaceutical dermal products, International Journal of Pharmaceutics, 366 (2009) 170-184.

[32] M. Schäfer-Korting, W. Mehnert, H.-C. Korting, Lipid nanoparticles for improved topical application of drugs for skin diseases, Advanced Drug Delivery Reviews, 59 (2007) 427-443.

[33] O. Sonneville-Aubrun, J.T. Simonnet, F. L'Alloret, Nanoemulsions: a new vehicle for skincare products, Adv Colloid Interface Sci, 108-109 (2004) 145-149.

[34] G.M. El Maghraby, B.W. Barry, A.C. Williams, Liposomes and skin: From drug delivery to model membranes, European Journal of Pharmaceutical Sciences, 34 (2008) 203-222.

[35] B. Heurtault, P. Saulnier, B. Pech, M.C. Venier-Julienne, J.E. Proust, R. Phan-Tan-Luu, J.P. Benoit, The influence of lipid nanocapsule composition on their size distribution, European Journal of Pharmaceutical Sciences, 18 (2003) 55-61.

[36] B.a. Heurtault, P. Saulnier, B. Pech, J.-E. Proust, J.-P. Benoit, A Novel Phase Inversion-Based Process for the Preparation of Lipid Nanocarriers, Pharmaceutical Research, 19 (2002) 875-880.

[37] A.-L. Lainé, E. Adriaenssens, A. Vessières, G. Jaouen, C. Corbet, E. Desruelles, P. Pigeon, R.-A. Toillon, C. Passirani, The in vivo performance of ferrocenyl tamoxifen lipid nanocapsules in xenografted triple negative breast cancer, Biomaterials, 34 (2013) 6949-6956.

[38] N.T. Huynh, C. Passirani, P. Saulnier, J.P. Benoit, Lipid nanocapsules: A new platform for nanomedicine, International Journal of Pharmaceutics, 379 (2009) 201-209.

[39] M. Morille, T. Montier, P. Legras, N. Carmoy, P. Brodin, B. Pitard, J.-P. Benoît, C. Passirani, Long-circulating DNA lipid nanocapsules as new vector for passive tumor targeting, Biomaterials, 31 (2010) 321-329.

[40] M. Morille, C. Passirani, S. Dufort, G. Bastiat, B. Pitard, J.-L. Coll, J.-P. Benoit, Tumor transfection after systemic injection of DNA lipid nanocapsules, Biomaterials, 32 (2011) 2327-2333.

[41] A. Lamprecht, J.-L. Saumet, J. Roux, J.-P. Benoit, Lipid nanocarriers as drug delivery system for ibuprofen in pain treatment, International Journal of Pharmaceutics, 278 (2004) 407-414.

[42] A. Lamprecht, Y. Bouligand, J.-P. Benoit, New lipid nanocapsules exhibit sustained release properties for amiodarone, Journal of Controlled Release, 84 (2002) 59-68.

[43] A.L. Laine, A. Clavreul, A. Rousseau, C. Tetaud, A. Vessieres, E. Garcion, G. Jaouen, L. Aubert, M. Guilbert, J.P. Benoit, R.A. Toillon, C. Passirani, Inhibition of ectopic glioma tumor growth by a potent ferrocenyl drug loaded into stealth lipid nanocapsules, Nanomedicine, 10 (2014) 1667-1677.

[44] M. Weyland, F. Manero, A. Paillard, D. Grée, G. Viault, D. Jarnet, P. Menei, P. Juin, I. Chourpa, J.P. Benoit, R. Grée, E. Garcion, Mitochondrial targeting by use of lipid nanocapsules loaded with SV30, an analogue of the small-molecule Bcl-2 inhibitor HA14-1, Journal of Controlled Release, 151 (2011) 74-82.

[45] S. David, C. Passirani, N. Carmoy, M. Morille, M. Mevel, B. Chatin, J.P. Benoit, T. Montier, B. Pitard, DNA nanocarriers for systemic administration: characterization and in vivo bioimaging in healthy mice, Mol Ther Nucleic Acids, 2 (2013) e64.

[46] S. Vrignaud, N. Anton, C. Passirani, J.P. Benoit, P. Saulnier, Aqueous core nanocapsules: a new solution for encapsulating doxorubicin hydrochloride, Drug Dev Ind Pharm, 39 (2013) 1706-1711.

[47] R.H. Müller, M. Radtke, S.A. Wissing, Solid lipid nanoparticles (SLN) and nanostructured lipid carriers (NLC) in cosmetic and dermatological preparations, Advanced Drug Delivery Reviews, 54, Supplement (2002) S131-S155.

[48] A. Barras, A. Mezzetti, A. Richard, S. Lazzaroni, S. Roux, P. Melnyk, D. Betbeder, N. Monfilliette-Dupont, Formulation and characterization of polyphenol-loaded lipid nanocapsules, International Journal of Pharmaceutics, 379 (2009) 270-277.

[49] F.O. Nestle, P. Di Meglio, J.-Z. Qin, B.J. Nickoloff, Skin immune sentinels in health and disease, Nature reviews. Immunology, 9 (2009) 679-691.

[50] L.L. Hruza, A.P. Pentland, Mechanisms of UV-induced inflammation, J Invest Dermatol, 100 (1993) 35s-41s.

[51] C. Auffray, M.H. Sieweke, F. Geissmann, Blood Monocytes: Development, Heterogeneity, and Relationship with Dendritic Cells, Annual Review of Immunology, 27 (2009) 669-692.

[52] K. Shortman, S.H. Naik, Steady-state and inflammatory dendritic-cell development, Nat Rev Immunol, 7 (2007) 19-30.

[53] L.J. Yang, P. Li, Y.J. Gao, H.F. Li, D.C. Wu, R.X. Li, [Time resolved UV-Vis absorption spectra of quercetin reacting with various concentrations of sodium hydroxide], Guang Pu Xue Yu Guang Pu Fen Xi, 29 (2009) 1632-1635.

[54] T. Hatahet, M. Morille, A. Hommoss, C. Dorandeu, R.H. Muller, S. Begu, Dermal quercetin smartCrystals(R): Formulation development, antioxidant activity and cellular safety, Eur J Pharm Biopharm, 102 (2016) 51-63.

[55] M.S. Blois, Antioxidant Determinations by the Use of a Stable Free Radical, Nature, 181 (1958) 1199-1200.

[56] S. Scalia, M. Mezzena, Incorporation of quercetin in lipid microparticles: Effect on photo- and chemical-stability, Journal of Pharmaceutical and Biomedical Analysis, 49 (2009) 90-94.

[57] D.A. Scudiero, R.H. Shoemaker, K.D. Paull, A. Monks, S. Tierney, T.H. Nofziger, M.J. Currens, D. Seniff, M.R. Boyd, Evaluation of a soluble tetrazolium/formazan assay for cell growth and drug sensitivity in culture using human and other tumor cell lines, Cancer Res, 48 (1988) 4827-4833.

[58] A. Aranda, L. Sequedo, L. Tolosa, G. Quintas, E. Burello, J.V. Castell, L. Gombau, Dichloro-dihydro-fluorescein diacetate (DCFH-DA) assay: A quantitative method for oxidative stress assessment of nanoparticle-treated cells, Toxicology in Vitro, 27 (2013) 954-963.

[59] I.B. Afanas'ev, A.I. Dcrozhko, A.V. Brodskii, V.A. Kostyuk, A.I. Potapovitch, Chelating and free radical scavenging mechanisms of inhibitory action of rutin and quercetin in lipid peroxidation, Biochemical Pharmacology, 38 (1989) 1763-1769.

[60] D. Liu, H. Hu, Z. Lin, D. Chen, Y. Zhu, S. Hou, X. Shi, Quercetin deformable liposome: Preparation and efficacy against ultraviolet B induced skin damages in vitro and in vivo, Journal of Photochemistry and Photobiology B: Biology, 127 (2013) 8-17.

[61] F.T.M.C. Vicentini, T.R.M. Simi, J.O. Del Ciampo, N.O. Wolga, D.L. Pitol, M.M. Iyomasa, M.V.L.B. Bentley, M.J.V. Fonseca, Quercetin in w/o microemulsion: In vitro and in vivo skin penetration and efficacy against UVB-induced skin damages evaluated in vivo, European Journal of Pharmaceutics and Biopharmaceutics, 69 (2008) 948-957.

[62] H. Kim, S. Namgoong, H. Kim, Antiinflammatory activity of flavonoids: Mouse ear edema inhibition, Archives of Pharmacal Research, 16 (1993) 18-24.

[63] F.T. Vicentini, T. He, Y. Shao, M.J. Fonseca, W.A. Verri, Jr., G.J. Fisher, Y. Xu, Quercetin inhibits UV irradiation-induced inflammatory cytokine production in primary human keratinocytes by suppressing NF-kappaB pathway, in: J Dermatol Sci, 2011 Japanese Society for Investigative Dermatology. Published by Elsevier Ireland Ltd, Netherlands, 2011, pp. 162-168.

[64] A. Vijayalakshmi, V. Ravichandiran, V. Malarkodi, S. Nirmala, S. Jayakumari, Screening of flavonoid “quercetin” from the rhizome of Smilax china Linn. for anti-psoriatic activity, in: Asian Pac J Trop Biomed, 2012, pp. 269-275.

[65] B. Choquenet, C. Couteau, E. Paparis, L.J.M. Coiffard, Quercetin and Rutin as Potential Sunscreen Agents: Determination of Efficacy by an in Vitro Method, Journal of Natural Products, 71 (2008) 1117-1118.

[66] J.B. Zvezdanović, J.S. Stanojević, D.Z. Marković, D.J. Cvetković, Irreversible UV-induced quercetin and rutin degradation in solution, studied by UV-spectrophotometry and HPLC chromatography, Journal of the Serbian Chemical Society, 77 (2012) 297-312.

[67] H. Pool, S. Mendoza, H. Xiao, D.J. McClements, Encapsulation and release of hydrophobic bioactive components in nanoemulsion-based delivery systems: impact of physical form on quercetin bioaccessibility, Food & function, 4 (2013) 162-174.

[68] C. Maupas, B. Moulari, A. BÃ©duneau, A. Lamprecht, Y. Pellequer, Surfactant dependent toxicity of lipid nanocapsules in HaCaT cells, International Journal of Pharmaceutics, 411 (2011) 136-141.

[69] M. Kakran, R. Shegokar, N.G. Sahoo, L. Al Shaal, L. Li, R.H. MÃ¼ller, Fabrication of quercetin nanocrystals: Comparison of different methods, European Journal of Pharmaceutics and Biopharmaceutics, 80 (2012) 113-121.

[70] A.A. Thorat, S.V. Dalvi, Liquid antisolvent precipitation and stabilization of nanoparticles of poorly water soluble drugs in aqueous suspensions: Recent developments and future perspective, Chemical Engineering Journal, 181–182 (2012) 1-34.

[71] M.E. Aulton, Pharmaceutics: The science of dosage form design, Churchill livingstone, 2002.

[72] B. Heurtault, P. Saulnier, B. Pech, J.-E. Proust, J.-P. Benoit, Physico-chemical stability of colloidal lipid particles, Biomaterials, 24 (2003) 4283-4300.

[73] Y. Liu, L. Wang, J. Liu, Y. Di, A study of human skin and surface temperatures in stable and unstable thermal environments, Journal of Thermal Biology, 38 (2013) 440-448.

[74] G.S. Borghetti, I.M. Costa, P.R. Petrovick, V.P. Pereira, V.L. Bassani, Characterization of different samples of quercetin in solid-state: indication of polymorphism occurrence, Pharmazie, 61 (2006) 802-804.

[75] K. Westesen, B. Siekmann, M.H.J. Koch, Investigations on the physical state of lipid nanoparticles by synchrotron radiation X-ray diffraction, International Journal of Pharmaceutics, 93 (1993) 189-199.

[76] H. Bunjes, T. Unruh, Characterization of lipid nanoparticles by differential scanning calorimetry, X-ray and neutron scattering, Advanced Drug Delivery Reviews, 59 (2007) 379-402.

[77] M.L. Manca, I. Castangia, C. Caddeo, D. Pando, E. Escribano, D. Valenti, S. Lampis, M. Zaru, A.M. Fadda, M. Manconi, Improvement of quercetin protective effect against oxidative stress skin damages by incorporation in nanovesicles, Colloids and Surfaces B: Biointerfaces, 123 (2014) 566-574.

[78] A. Robaszkiewicz, A. Balcerczyk, G. Bartosz, Antioxidative and prooxidative effects of quercetin on A549 cells, Cell Biology International, 31 (2007) 1245-1250.

[79] E.J. Choi, K.M. Chee, B.H. Lee, Anti- and prooxidant effects of chronic quercetin administration in rats, Eur J Pharmacol, 482 (2003) 281-285.

[80] J. D'Orazio, S. Jarrett, A. Amaro-Ortiz, T. Scott, UV Radiation and the Skin, in: Int J Mol Sci, 2013, pp. 12222-12248.

[81] A.B. Petersen, R. Gniadecki, J. Vicanova, T. Thorn, H.C. Wulf, Hydrogen peroxide is responsible for UVA-induced DNA damage measured by alkaline comet assay in HaCaT keratinocytes, Journal of Photochemistry and Photobiology B: Biology, 59 (2000) 123-131.

[82] F.O. Nestle, D.H. Kaplan, J. Barker, Psoriasis, N Engl J Med, 361 (2009) 496-509.

[83] J. Schmielau, O.J. Finn, Activated granulocytes and granulocyte-derived hydrogen peroxide are the underlying mechanism of suppression of t-cell function in advanced cancer patients, Cancer Res, 61 (2001) 4756-4760.

[84] C.W. Trenam, D.R. Blake, C.J. Morris, Skin Inflammation: Reactive Oxygen Species and the Role of Iron, Journal of Investigative Dermatology, 99 (1992) 675-682.

[85] T.P. Szatrowski, C.F. Nathan, Production of large amounts of hydrogen peroxide by human tumor cells, Cancer Res, 51 (1991) 794-798.

[86] C.S. Sander, F. Hamm, P. Elsner, J.J. Thiele, Oxidative stress in malignant melanoma and non-melanoma skin cancer, British Journal of Dermatology, 148 (2003) 913-922.

[87] S.J. Duthie, A.R. Collins, G.G. Duthie, V.L. Dobson, Quercetin and myricetin protect against hydrogen peroxide-induced DNA damage (strand breaks and oxidised pyrimidines) in

human lymphocytes, Mutation Research/Genetic Toxicology and Environmental Mutagenesis, 393 (1997) 223-231.

Chapter three: Quercetin liposomes and comparative study

Goals:

Development of quercetin liposomes

Physicochemical characterization

Quercetin loading and encapsulation efficiency

Quercetin in vitro release study

Comparative study on cellular safety on HaCaT cells

Comparative study on protection activity on HaCaT cells

Comparative study on cellular safety on THP-1 cells

Comparative study on protection activity on THP-1 cells

Comparative study on in vivo skin penetration

Chapter three: Quercetin liposomes and comparative study

Preface

In this chapter, the development of quercetin liposomes is presented. The use of liposomal formulation for quercetin is previously reported using different methods and compositions [1-4]. For this, we selected liposomal formulation because of its known usefulness in quercetin development and in order to be the reference for our comparative study with quercetin smartCrystals® and quercetin lipid nanocapsules.

In the first part of this chapter, the liposomal formulation process is optimized and liposomes are characterized in terms of particle size, PDI, physical stability, and quercetin loading, encapsulation efficiency *in vitro* DPPH activity and *in vitro* release kinetics.

In the second part, a comparative analysis of quercetin smartCrystals®, quercetin lipid nanocapsules and quercetin liposomes was established on two cell lines HaCaT (kératinocytes) and THP-1 (monocytes). The cellular safety of these formulations is evaluated and then the quercetin protective activity against hydrogen peroxide induced oxidative stress is done on both cellular models.

Finally on the basis of the *in vitro* cellular experiments, two formulations were selected and evaluated for quercetin *in vivo* skin penetration capacity: quercetin smartCrystals® stabilized with TPGS and quercetin lipid nanocapsules 20.

References

[1] S.N. Park, M.H. Lee, S.J. Kim, E.R. Yu, Preparation of quercetin and rutin-loaded ceramide liposomes and drug-releasing effect in liposome-in-hydrogel complex system, Biochemical and Biophysical Research Communications, 435 (2013) 361-366.

[2] C. Caddeo, O. Diez-Sales, R. Pons, X. Fernandez-Busquets, A.M. Fadda, M. Manconi, Topical anti-inflammatory potential of quercetin in lipid-based nanosystems: in vivo and in vitro evaluation, Pharm Res, 31 (2014) 959-968.

[3] P.G. Cadena, M.A. Pereira, R.B.S. Cordeiro, I.M.F. Cavalcanti, B. Barros Neto, M.d.C.C.B. Pimentel, J.L. Lima Filho, V.L. Silva, N.S. Santos-MagalhÃ£es, Nanoencapsulation of quercetin and resveratrol into elastic liposomes, Biochimica et Biophysica Acta (BBA) - Biomembranes, 1828 (2013) 309-316.

[4] D. Liu, H. Hu, Z. Lin, D. Chen, Y. Zhu, S. Hou, X. Shi, Quercetin deformable liposome: Preparation and efficacy against ultraviolet B induced skin damages in vitro and in vivo, Journal of Photochemistry and Photobiology B: Biology, 127 (2013) 8-17.

Liposomes, lipid nanocapsules and smartCrystals®: a comparative study for an effective quercetin delivery to skin

T. Hatahet[a], M. Morille[a], A. Hommoss[b], R. H. Müller[b], J.M. Devoisselle and S. Bégu[a*]

[a] Institut Charles Gerhardt Montpellier, UMR 5253 CNRS-ENSCM-UM, Equipe Matériaux Avancés pour la Catalyse et la Santé, 8 rue de l'Ecole Normale, 34296 Montpellier Cedex 5, France.

[b] Institute of Pharmacy, Department of Pharmaceutics, Biopharmaceutics and NutriCosmetics, Free University of Berlin, Kelchstr. 31, Berlin 12169, Germany.

[*] Corresponding author.

Research article will be submitted to the

European journal of pharmaceutics and biopharmaceutics

Abstract

Quercetin is a flavonoid with strong antioxidant and antiinflammatory activities considered as a potential drag candidate for skin exogenous supplementation. Nevertheless, crude quercetin suffers from poor water solubility and consequently topical inactivity. Therefore, quercetin formulation within a suitable system that overcomes its solubility limitation is a matter of investigation. Three approaches were tested to improve quercetin delivery to skin: liposomes, lipid nanocapsules and smartCrystals®. These nanoformulations were compared in terms of average particle size, homogeneity (PDI), quercetin loading and cellular interactions with HaCaT (keratinocytes) and TPH-1 (monocytes) cell lines. Finally, two formulations were selected for testing quercetin delivery to human skin *in vivo* using stripping test.

Quercetin nanoformulations presented different size distribution starting from 26 nm with quercetin lipid nanocapsules (que-LNC 20), 179 nm with liposomes to 295 nm with quercetin smartCrystals®. The drug loading also varied from 0.56 mg/ml with liposomes to10.8 mg/ml with nanocapsules and 14.4 mg/ml with smartCrystals®. No toxicity was observed on HaCaT cells with quercetin and free radical scavenging ability was established at 5 µg/ml. The safety of quercetin at 5 µg/ml was further confirmed on THP-1 cells with efficient free radical scavenging ability.

Finally, skin penetration with selected formulations: que-LNC 20 and quercetin smartCrystals® stabilized with TPGS was performed *in vivo*. Different behavior observed between the two formulations could led to different promising strategies for skin protection. On one side, quercetin smartCrystals® seems to enable the superficial deposition of quercetin on top of the skin, which presents a good strategy for a quercetin-based sunscreen product. On the other side, lipid nanocapsules seem to permit quercetin delivery to viable epidermis that holds the promise for skin inflammatory disorders such as psoriasis.

Key words

Quercetin, smartCrystals®, lipid nanocapsules, liposomes, HaCaT cells, THP-1 cells, *in vivo* skin penetration

Graphical abstract

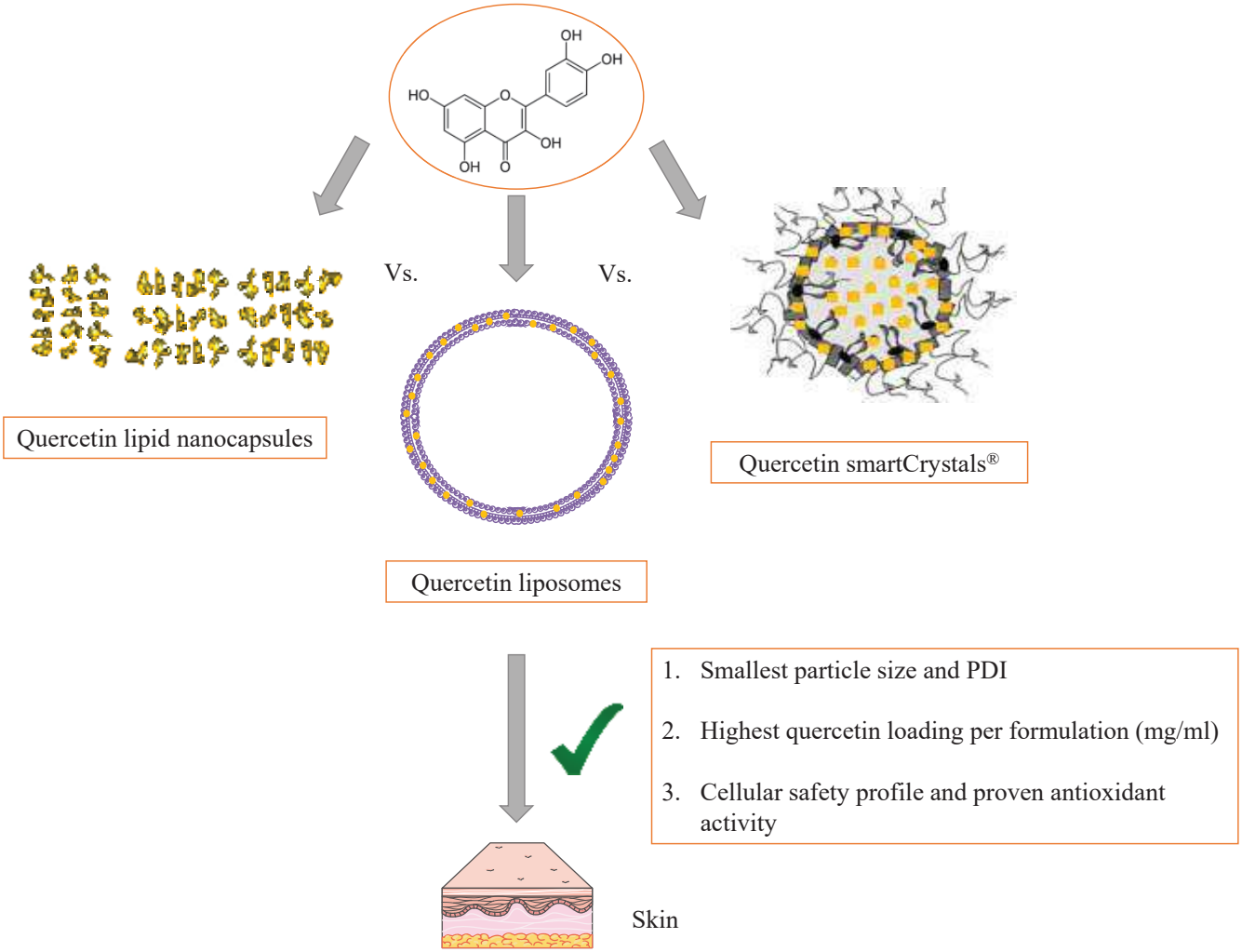

1. Introduction

Quercetin is a plant pigment that belongs to the flavonoids family and is considered as the most distributed flavonoid in nature [1]. Quercetin presents both antioxidant and antiinflammatory proprieties [2, 3]. Quercetin also presents interesting physiological activities starting from simple free radical scavenging abilities [4] to more complex modulation of proinflammatory cytokines release [5] and up-regulation and down-regulation of several pathways within the cellular system such as upregulation of hemeoxygenase-1 pathway [6] and down-regulation of the nuclear factor kappa B pathway [7]. Unfortunately, quercetin has limited bioavailability due to poor water solubility, which hinders its efficient delivery to its targets within the human body and this can explain the inactivity of quercetin in respect to the topical application [2]. To circumvent this issue, quercetin formulations were explored as very interesting delivery systems for the protection of the skin from oxidation, inflammation, photoageing and the support of immune system and during wound healing process [8-10]. Among the most promising approaches, liposomes appear as an attractive one.

Liposomes were first described by Bangham *et al,* 50 years ago as a simplified model for biological membranes [11]. In the beginnings of 70's, Gregoriadis and co-workers were the firsts to encapsulate drugs within liposomes [12]. Regarding topical application, liposomes are promising delivery system [13] as observed in different researches : liposomes increased the deposition of benzocaine by 2.5 fold on artificial membrane [14], vitamin E by seven fold on rat skin [15]. Capture® (Dior) was the first cosmetic formulation based on liposomes commercialized in 1986 and then Niosomes® (L'Oréal) were introduced in 1987. Interestingly, quercetin was already formulated in liposomes and proved promising protective actions against UV oxidative damage of skin [16]. In this study, quercetin liposomes (que-Lipo) were prepared with dipalmitoylphosphatidylcholine and Cremophor® EL.

We chose in this work to compare liposomes, with two others previously established nanoformulations. First, quercetin smartCrystals® (que-SC) were previously developed by implementing the second-generation smartCrystals® technology then stabilized with either Tween® 80 or TPGS. [17, 18]. Concerning the second formulation, quercetin lipid nanocapsules (que-LNC) were formulated using phase inversion method to obtain a distribution size of either 20 nm or 50 nm [19] (LNC article under review). These formulations enhanced quercetin water solubility.

In the first part of this article, particle size, charge, physical stability were studied and quercetin encapsulation efficiency, drug loading**,** *in vitro* antioxidant activity and *in vitro* quercetin release were determined for the liposomal formulation.

Afterwards in the second part, we compared quercetin smartCrystals® and quercetin lipid nanocapsules to quercetin liposomes in terms of particle size observed quercetin drug loading and quercetin safety /

efficiency on cells. Two cellular models were selected (i) keratinocytes cell lines HaCaT cells to evaluate the interaction between quercetin and its formulations with skin tissue [20] and (ii) monocytes THP-1 cell line to evaluate the impact of quercetin on monocytes derived dendritic cells found in inflamed skin [21, 22]. On each cellular model, the cellular viability upon the administration of crude quercetin or its formulations was determined. In parallel, quercetin free radical scavenging ability was assessed after the cellular exposure to hydrogen peroxide by the detection of reactive oxygen species (ROS) within cells. Finally, que-SC stabilized with TPGS and que-LNC 20 were selected to test quercetin *in vivo* skin penetration using stripping test. Indeed, que-SC seems to enable a superficial deposition for quercetin over skin highlighting its applicability in UV sunscreens. On the other side, que-LNC 20 could favor a deeper skin penetration highlighting their emphasizing its applicability in inflammatory skin disorders such as psoriasis, atopic dermatitis etc...

2. Materials and methods

Tween® 80 (polysorbate 80), TPGS (α tocopheryl polyethylene glycol 1000 succinate), Cremophor® EL (polyoxyl 35 castor oil) and Solutol® HS 15 (a mixture of free polyethylene glycol 660 and polyethylene glycol 660 hydroxystearate) were bought from BASF (Ludwigshafen, Germany). Lipophilic Labrafac® WL 1349 (caprylic acid triglycerides) and Lipoid® S75-3 (soybean lecithin at 69% of phosphatidylcholine) were kindly provided by Gattefosse® (Saint-Priest, France) and Lipoid® (Ludwigshafen, Germany) respectively. Because of the complex chemical composition of the mixtures, brand name will be used throughout the article, and any amount indicated in the formulation model represents the whole mixture regardless of its constituents. NaCl was provided from Prolabo® (Fontenay-sous-Bois, France), MilliQ water was obtained by the Milli® RO System (Millipore, Paris, France). Dipalmitoylphosphatidylcholine (DPPC) was purchased from Avanti® (Avanti Polar Lipids, Inc., USA). Quercetin aglycone (3, 3', 4', 5, 7-pentahydroxy-2-phenylchromen-4-one), 3-(4, 5-dimethylthiazol-2-yl)-2, 5-diphenyltetrazolium bromide (MTT), 2,3-Bis-(2-methoxy-4-nitro-5-sulfophenyl)-2H-tetrazolium-5-carboxanilide salt (XTT), 2',7' – dichlorofluorescein diacetate (DCFDA) and all HPLC organic solvents were purchased from Sigma (Sigma Aldrich, France). Hydrogen peroxide 3% (Eau oxygenée Gifrer 10 volumes) was purchased from Gifrer (Décines-Charpieu, France)

2.1 Preparation of quercetin nanoformulations

2.1.1 Preparation of quercetin liposomes (que-Lipo)

Quercetin liposomes (Que-Lipo) were prepared using the ethanol injection technique with several modifications [16]. Crude quercetin powder, DPPC and Cremophor® EL were accurately weighted in the following ratio 0.5:9:5 (w/w). The mixture was then dissolved in 2 ml of absolute ethanol and heated to about 40°C. Afterwards, ethanol solution was injected into 10 ml PBS buffer at 50°C using 2 ml borosilicate glass syringe (Fortuna® Optima, Poulten & Graf Ltd, UK) which was connected to needle with 0.5 mm diameter (gauge number 25). Ethanol was injected at a rate of 1 drop per second under stirring at 650 rpm using Eurostar power control-visc stirrer (IKA® Werke GmbH, Germany). At the end of injection, liposomal suspension is kept under stirring for 30 min at 50°C then left to cool down for 30 min without stirring. Blank liposomes (blank-Lipo) were prepared using the same process without quercetin. Que-Lipo were stored at 4°C for stability testing. Size and PDI were measured each month for three months (Section 2.2)

2.1.2 Preparation of quercetin lipid nanocapsules (que-LNC)

Que-LNC were prepared as described in (ref article LNC). Briefly, crude quercetin powder, lipophilic Labrafac®, Solutol® HS 15, Cremophor® EL, Lipoid® S75-3, NaCl and MilliQ water were homogenized under agitation and warmed to 85°C. At 85°C, a specified quantity of absolute ethanol was added to boost up the dissolution of quercetin within lipid excipients. Three cycles of cooling-heating were maintained under magnetic stirring and 5.5 ml of MilliQ water were then added to the mixture at the transition phase temperature to form lipid nanocapsules. Free quercetin was separated from encapsulated quercetin by filtering que-LNC through Sartorius Stedim Minisart® filters (0.2 µm pore size) [19]. Blank lipid nanocapsules blank-LNC were prepared using the same process without quercetin.

2.1.3 Preparation of quercetin smartCrystals® (que-SC)

Que-SC were prepared as described in Hatahet *et al* [18]. A primary suspension containing 0.5% of either Tween® 80 or TPGS and 5% of crude quercetin were subjected to five minutes of bead milling using pearl mill Bùhler PML 2 (Bùhler AG, Uzwil, Switzerland) with 0.2 mm zirconium oxide beads as milling medium. The resulted suspensions were then homogenized using a high-pressure homogenizer (HPH), Micron LAB 40 (APV Gaulin GmbH, Germany) for two cycles at 300 bar [18]. Blank formulations were 0.5% stabilizer solution.

2.2 Particle size measurement

The five nanoformulations were diluted according to quercetin final concentration (0.1 mg/ml) with MilliQ water for que-SC and que-LNC and with PBS 7.4 for que-Lipo. Size measurements were performed in triplicate using a Zetasizer NanoZS (Malvern Instruments, UK) at 25°C [18].

2.3 HPLC analysis

The chromatographic analysis of quercetin was performed on LC6-2010HT (Shimadzu, Kyoto, Japan) using a C-18 column Prontosil (120-5-C18 H5.0 µm, 250 ×4.0 mm) as stationary phase. The detection was carried out by a UV lamp (UV-VIS detector, Shimadzu, Kyoto, Japan) at 368 nm, which is a specific wavelength for quercetin detection [23]. For the purpose of determining quercetin encapsulation efficiency and drug loading within liposomes (section 2.4), a mobile phase consisting of 10% methanol 80% acetonitrile and 10% of phosphoric acid solution 0.2% at a pH=1.9 was used. The flow rate was kept at 1 ml/min during the 15 min run time analysis. Serial dilutions of known concentrations of quercetin in methanol were used to make the calibration curve. The method showed linearity over a concentration range from 3.9 to 62.5 µg/ml (r^2 = 0.999 and %RSD = 3.19). For the detection of quercetin *in vitro* release form que-Lipo (section 2.6), another calibration curve of quercetin from 0.2 to 4 µg/ml in a solution of PBS buffer pH 7.4 with Tween® 20 (2%) and a gradient flow rate were used according to previous studies [18]. Finally for the quantification of quercetin in the strips extract (section 2.10), an isocratic medium composed of 50/50 acetonitrile and buffer KH_2PO_4 (pH 2.3) at a flow rate of 0.5 ml/min at 37°C was selected as mobile phase. The stationary phase was a Eurospher 100-5 C18 column (250 × 4 mm, 5 µm) mounted on KromaSystem 2000 (Kontron Instruments GmbH, Germany) equipped with a solvent delivery with 20 µl loop and a rheodyne sample injector. Quercetin retention time was 6.3 min in a total of 13 min sample run. The injection volume was 20 µl and the detection wavelength was 370 nm using a diode array detector (DAD-Kontron Instrument HPLC 540). Method showed linearity for quercetin concentration range from 0.8 to 50 µg/ml of quercetin in ethanol (r^2 = 0.9988) [24].

2.4 Encapsulation efficiency (EE) and drug loading capacity (DL)

For que-Lipo, quercetin EE was determined directly by centrifuging formulated liposomes for 15 minutes at 21,000 gravitational force using a Sigma 2k 25 ultracentrifuge (sigma Zentrifugen, GmbH, Germany) to allow the aggregated quercetin to sediment. After that, 50 µl of the supernatant was collected and diluted to 1000 µl with methanol to dissolve liposomes membranes and quercetin. Then, quercetin concentration within liposomes were determined with HPLC, (section 2.3). DL and EE were calculated according to the equations below :

Equation 1: $$Drug\ loading = \left[\frac{quercetin\ quantity}{lipid\ phase\ excipients\ quantity}\right] 100$$

Equation 2: $$Encapsulation\ efficacy = \left[\frac{amount\ of\ encapsulated\ quercetin}{amount\ of\ quercetin\ added}\right] 100$$

2.5 Hydrogen donating ability in vitro by 2, 2-diphenyl-1-picrylhydrazyl (DPPH)

2,2-diphenyl-1-picrylhydrazyl (DPPH) is a molecule with a free radical at the hydrazine position where compounds possessing antioxidative effect can react with [25]. DPPH in its radical form is known to have a strong absorption band at 517 nm. However, DPPH absorption at 517 nm diminishes when reacting with an antioxidant. Quercetin showed linear inhibition from 1 µg/ml to 6 µg/ml where it reaches its plateau activity when reacted with a 400 µM DPPH methanolic solution (1.5 ml to 0.5 ml). The 400 µM DPPH solution was considered as positive control and showed 100% free radical or 0% inhibition. Blank was the methanol without neither DPPH nor quercetin. DPPH test was performed on que-Lipo in order to determine the activity of encapsulated quercetin. DPPH percentage activity is then calculated by the following equation:

Equation 3: $$DPPH\ \%\ activity = \frac{Quantity\ of\ active\ Quercetin}{Practically\ encapsulated\ Quercetin} \times 100$$

2.6 *In vitro* release study

A 12-14 molecular weight cut-off (MWCF) Spectra/Por® Dialysis Membrane (Spectrum laboratories INC, USA) was selected for the experiment. A receptor medium composed of 80 ml PBS at pH 7.4 at 37°C with Tween® 20 (2%) was used to maintain sink conditions [26]. 1 ml of Que-Lipo was placed at the inner side of the membrane. A propylene glycol solution of quercetin containing the same quantity was used as control. Samples (1 ml) were withdrawn at 5different times during 24 hours and replaced by fresh release medium. Quercetin concentration was calculated using HPLC method mentioned (section 2.3).

2.7 Cell culture

Human keratinocyte cell line (HaCaT) was purchased from CLS Cell Lines Service (GmbH, Germany). Cells were cultured with Dulbecco's Modified Eagle Medium (Gibco® DMEM) supplemented with 4.5 g/L glucose, 2 mM L-glutamine, 1% (v/v) penicillin/streptomycin (10,000 U/ml penicillin, 10,000 µg/ml streptomycin) and 10% fetal bovine serum provided by (Life technologies™ Carlsbad, California, USA). Cells were seeded at 10^6 cell/mL in Corning® 150 cm^2 Canted Neck Flask with Vent Cap from Corning incorporated (Corning®, Massachusetts, USA) and incubated in humidified Heraeus® BB6220 incubator (Thermo Scientific™, Massachusetts, USA) with 5% CO_2. Medium was changed twice a week and replication was set when cells attend sufficient confluence.

Acute monocytic leukemia cell line (THP-1) (kind gift from Professor Francisco Veas (IRD, Montpellier) were cultured with Roswell Park Memorial Institute medium (RPMI) supplemented with 10% fetal bovine serum and 1% (v/v) penicillin/streptomycin by life technologies™ (Carlsbad, California, USA). Cells were seeded at a density of 10^6 cell/mL in Corning® 150 cm^2 Canted Neck Flask with Vent Cap and incubated at 37°C and 5%CO_2. Cell replication was twice a week when cells attend confluence.

2.8 Cell viability

HaCaT cells were seeded at cellular density 200,000 cells/cm^2 in flat bottom 24 well plate (Corning incorporated, New York, USA) and kept overnight to adhere. Afterwards, cells were treated for another 24 hours with crude quercetin and quercetin formulations at a concentration range from 5 to 100 µg/ml. Crude quercetin and quercetin formulations were diluted with Dulbecco's phosphate-buffered saline (DPBS) (Life technologies™, Carlsbad, California, USA). Blank formulations were used as a control to highlight the cellular activity of the quercetin and allow the comparison between the formulations. Free cells were treated with DPBS buffer and considered as 100% viable cells. Cellular viability was performed using 3-(4,5-dimethylthiazol-2-yl)-2,5-diphenyltetrazolium bromide (MTT) assay. 20 µl of 5 mg/ml MTT were added to cells and incubated for 4 hours. Then, medium was withdrawn and 200 µl of 0.06N HCl isopropanol was added to each well to dissolve formazan crystals. Finally, absorbance was recorded at 570 nm and 750 nm using Multiskan™ GO Microplate Spectrophotometer (Thermo Scientific™, Waltham, Massachusetts, USA).

THP-1 cells were seeded at cellular density of 150,000 cells/ml in flat bottom well plate and directly treated with crude quercetin or formulations for 24 hours at a concentration of 5 µg/ml. Afterwards, cellular viability was tested using 2,3-Bis-(2-methoxy-4-nitro-5-sulfophenyl)-2H-tetrazolium-5-carboxanilide salt (XTT) assay. XTT assay differs from MTT assay as it does not require a dissolving step for formazan crystals. Consequently, it avoids to centrifuge cells before reading the absorbance. 50 µl of XTT reagent

were added to each well for 3 hours, and then absorbance was measured at 450 and 750 nm. 100 % viable cells were cells that were treated with DPBS buffer. Cellular viability percentage were presented relatively to control non-treated cells.

2.9 Crude quercetin and quercetin nanoformulations antioxidant activity

HaCaT cells were seeded at 200,000 cells/cm^2 in 24 well/plate and left overnight to adhere. Then, crude quercetin and quercetin formulations at 5 µg/ml were added for 24 hours. Cells were washed with PBS 200 µl and DCFDA reagent (1 µM in RPMI without phenol red) were added in each well for 60 minutes. Medium containing DCFA was discarded and cells were washed twice with PBS. Then, H_2O_2 (1 mM in PBS) was added for 120 minutes. After cellular exposure, cells were washed with PBS and 200 µl of Tris cell lysis buffer were added to each well. Cell lysates were transferred to 96 wells black plate with clear bottom (Corning®, Massachusetts, USA). Dichlorofluorescein (DCF) a highly fluorescent compound generated from the reaction with ROS was detected at maximum excitation and emission spectra of 485 nm and 525 nm using TriStar LB 941 from Berthold Technologies (Chollerstr, Switzerland).

THP-1 cells were seeded at 300,000 cells/ml in 24 well/plate and treated with crude quercetin or its formulations for 24 hours. Then, cells were loaded with DCFDA reagent (1 µM in RPMI without phenol red) for 60 minutes. Next, oxidative stress was initiated using H_2O_2 (1 mM) for 120 minutes. After cellular exposure, cells were collected by centrifugation and supernatant was discarded. Cells were then lysed with Tris cell lysis buffer (200 µl) for each well. After that, cell lysates were transferred to 96 wells black plate with clear bottom (Corning®, Massachusetts, USA). Finally, DCF is detected at maximum excitation and emission spectra of 485 nm and 525 nm using TriStar LB 941 from Berthold Technologies (Chollerstr, Switzerland).

2.10 *In vivo* skin penetration

Two formulations were selected for testing quercetin penetration enhancement *in vivo*. 8 healthy men with Caucasian skin aged between 25 and 29 participated in the study and signed consent for this investigation. The experiment was conducted according to declaration of Helsenki. In a controlled stripping room at 20 °C and 62% relative humidity, after wiping the skin with ethanol 96% and drying it, 50 µl of the formulations were applied to the forearm on an area of 2 × 3 cm^2. The formulations were applied with a pipette and were spread over skin with spatula for 1 hour. The loss in formulations by spatula was determined with 3 ml ethanol after spreading. After that, successive strips were applied to the skin with controlled pressure (1 kg rubber weight was rolled over it 10 times) [27]. Total stripped tapes were grouped in 7 groups as follows

(i) strip 1 (ii) strip 2 (iii) strip 3 (iv) strip 4 and 5 (v) strip 6 to 8 (vi) strip 9 to 11 and (vii) strip 12 to 15. Quercetin was extracted from the strips with 3 ml of ethanol on a shaker at 25°C at 125 rpm for 3 hours and then injected into HPLC (section 2.3).

2.11 Statistical analysis

Statistical analysis of the cellular cytotoxicity, cellular protective activity and the *in vivo* skin penetration study were made using Microsoft Excel 2013 tool Pack (Microsoft Corporation, USA). A two-sample t-test with unequal variances was used to verify the significant difference between the data in the release study. A two-sample t-test with equal variances was used for cellular data analysis. P expresses the significant value where * = $P < 0.05$, ** = $P < 0.01$ and *** = $P < 0.005$ respectively.

3 Results

3.1 Particle size measurement, encapsulation efficiency, drug loading and DPPH activity of que-Lipo

Table 1 presents the physicochemical characteristics of blank-Lipo and que-Lipo. Que-Lipo were 179 ± 15 nm with no statistical differences compared to blank-Lipo (188 ± 18 nm). Que-Lipo exhibited a PDI inferior to 0.1 indicating the homogenous dispersion of formulated liposomes. The DL was 2.58 ± 0.13 % (of total lipid excipients in the formulation) with an EE of quercetin of 68.2 ± 2.7 %. Quercetin retained the antioxidant activity *in vitro* with 55.1 ± 10.9 % of active quercetin using DPPH assay.

Blank liposomes	Physicochemical characterization	Quercetin liposomes
188 ± 16	Size (nm)	179 ± 15
0.10 ± 0.02	PDI	0.06 ± 0.02
--	DL (%)	2.58 ± 0.13
--	EE (%)	68.2 ± 2.7
--	DPPH activity (%)	55.1 ± 10.9

Table 1: Physicochemical characteristics of blank and quercetin liposomes (n=3).

Liposomes particle size, polydispersity index (PDI) were determined for both blank-que and que-Lipo. Encapsulation efficiency (EE), drug loading (DL) and 2,2-diphenyl-1-picrylhydrazyl (DPPH) activity were determined for que-Lipo using equations 1, 2 and 3 respectively.

3.2 Que-Lipo stability

Que-Lipo stability was monitored over three months at 4°C. Fig.1 shows the average particle size and the PDI during the stability study. Particle size was not increased significantly during the study, at day 0 particles were 179 nm and 181 nm at day 90. PDI remained under 0.2 during the whole period of storage. At day 90, PDI was 0.19.

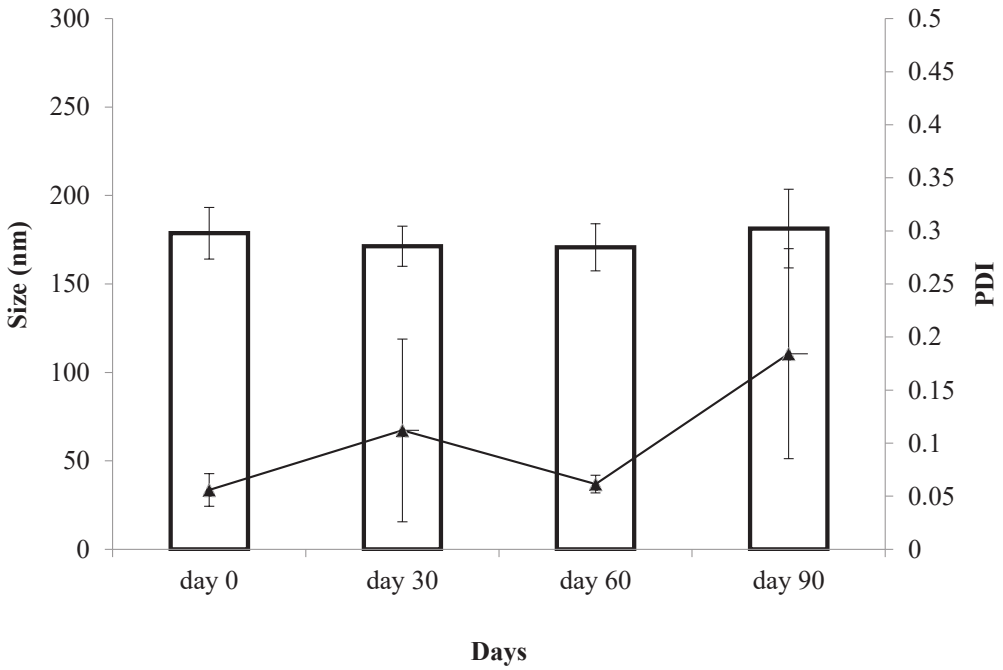

Fig. 1: Que-Lipo stability study at 4°C for 3 months (n=3).

Particle size (columns) and polydispersity index (PDI) (points) were recorded at day 0, day 30, day 60 and day 90.

3.3 *In vitro* quercetin release from que-Lipo

Quercetin release from liposomes was evaluated using dialysis bag method [26]. Fig. 2 presents the release profile of quercetin from liposomes compared to quercetin release for solution in propylene glycol. Liposomal formulation enabled a delayed release for quercetin as quercetin was detected after 2 hours and quercetin release from the control at 5 min. At 8 hours, 16.7 % of quercetin was released from liposomes, this was a significant difference compared to control (with 34.3 %) ($P < 0.005$). Finally, at 24 hours, quercetin from both liposomal formulation and propylene glycol solution achieved the similar released amounts (36.6 % vs. 37.4 %),

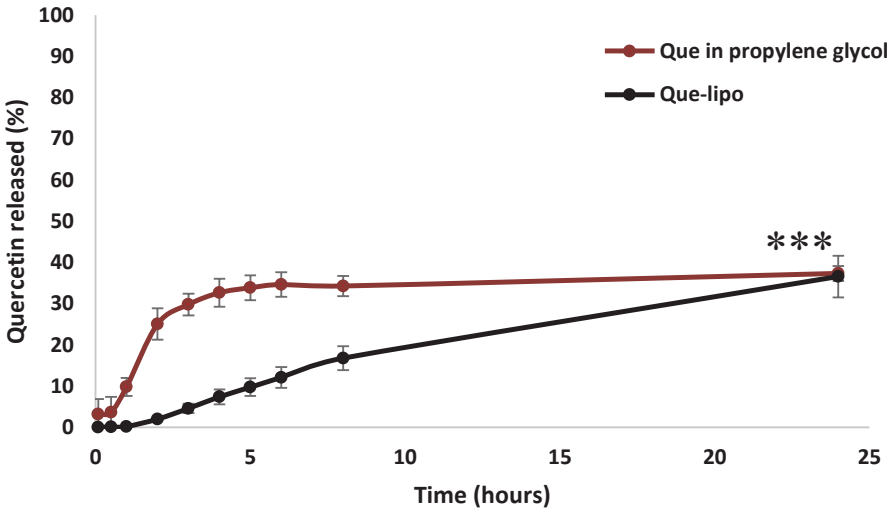

Fig. 2: *In vitro* quercetin release from que-Lipo during 24 hours (n=3).

Samples are withdrwon at 5, 30 min and 1, 2, 3, 4, 5, 5, 8 and 24 hours. P expresses the significant value where * = $P < 0.05$, ** = $P < 0.01$ and *** = $P < 0.005$ respectively.

3.4 Quercetin smartCrystals® and quercetin lipid nanocapsules

Que-SC and Que-LNC were formulated according to previous report [18]. Table 2 shows average particle size, PDI and the quercetin concentration per milliliter of formulation. The smallest particle size was observed with que-LNC 20 (26 nm) with a drug concentration up to 10 mg/ml but higher quercetin concentration was observed with que-SC stabilized with TPGS at 14.4 mg/ml (203 nm). Que-Lipo showed the lowest quercetin concentration with 0.56 mg/ml with higher particle size (179 nm).

Quercetin nanoformulation	Que-SC Tween® 80	Que-SC TPGS	Que-LNC 20	Que-LNC 50	Que-lipo
Size (nm)	295 ± 9	203 ± 3	27±3	54±3	179 ± 15
PDI	0.25 ± 0.03	0.24 ± 0.01	0.059±0.00	0.17±0.02	0.06 ± 0.02
Quercetin concentration (mg/ml)	14.10 ± 3.4	14.40 ± 0.027	10.80 ± 0.78	6.00 ± 0.70	0.56 ± 0.05

Table 2: Particle size, PDI and quercetin concentration per milliliter of smartCrystals® (SC stabilized with Tween® and TPGS), lipid nanocapsules (LNC 20 and LNC 50) and liposomes (n=3).

3.5 Cellular toxicity of crude quercetin and quercetin formulations on HaCaT cells.

In the scope of a topical application, the safety of quercetin formulations compared to crude quercetin was evaluated on HaCaT cells. Fig. 3 shows the cellular viability results of HaCaT cells after 24 hours exposure to either crude quercetin or quercetin nanoformulations. It is important to note that all these formulation were added to cells in the same amount of quercetin regardless of the amounts of carriers (excipient), as we chosen to fix the quercetine concentration (0, 5, 25, 50 and 100 µg/ml). Consequently, the number of nanocarriers in contact with the cells depends on the DL and EE of each nanoformulation. Starting by crude quercetin, no cellular toxicity was observed up to 100 µg/ml. Moreover, cellular proliferation increased with increasing quercetin dose from 25 µg/ml to 100 µg/ml. Que-SC with both stabilizers showed a significant difference in toxicity compared to control (stabilizers alone) from 5 µg/ml which was more pronounced with Tween® 80 than in TPGS ($P< 0.005$ vs. $P< 0.05$). Que-LNC 20 were similar to blank-LNC up to 50 µg/ml. Then at 100 µg/ml, que-LNC 20 showed a significant decrease in cellular viability to 60.5 ± 4.8 %, whereas que-LNC 50 was safe at this concentration. Finally, the viability results were 67.5 ± 7.2 % at 5 µg/ml and 77.3 ± 13.8 % at 25 µg/ml, which were not statistically different from blank-Lipo that showed a viability percentage of 84.8 ± 8.8 %. At 50 µg/ml and 100 µg/ml of quercetin, the cellular viability increased with que-Lipo similarly to crude quercetin ($P< 0.01$ at 100 µg/ml).

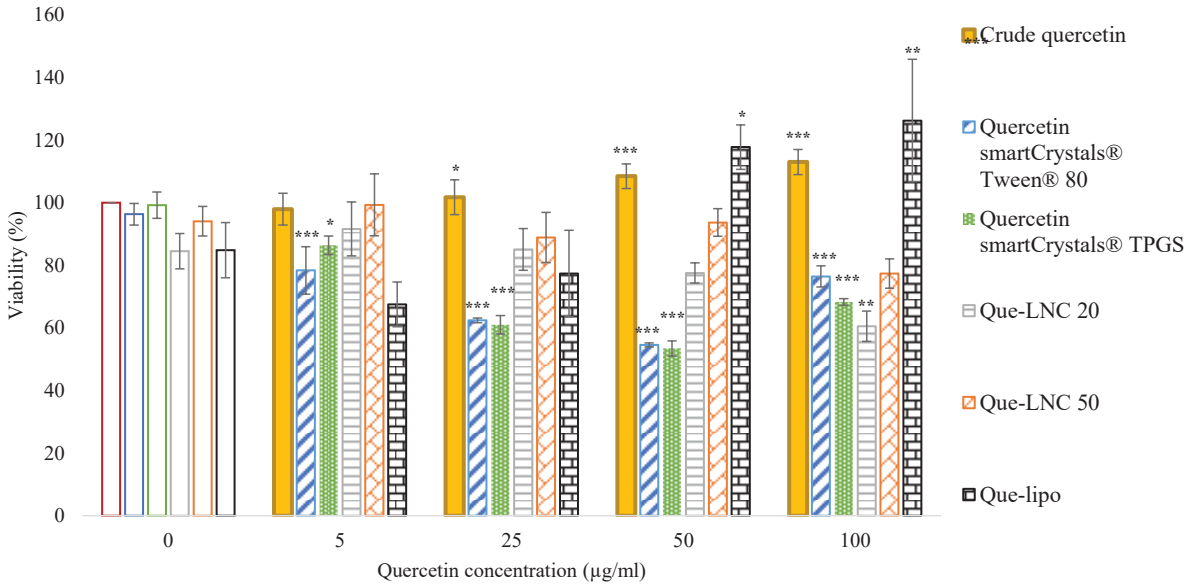

Fig. 3: HaCaT cellular viability using MTT assay after 24 hours of treatment with either crude quercetin or quercetin nanoformulations (n=3).

Cells were incubated with phosphate buffer as control (non-treated) cells and with crude quercetin as a control for the quercetin specific toxicity, with smartCrystals® stabilizers (Tween® 80 and TPGS), blank lipid nanocapsules and blank liposomes as a control for formulation specific toxicity and with quercetin smartCrystals®, quercetin lipid nanocapsules and quercetin liposomes for the safety of formulated quercetin. Letters indicates a significance difference relative to control formulation. P expresses the significant value where * = $P < 0.05$, ** = $P < 0.01$ and *** = $P < 0.005$ respectively.

3.6 Crude quercetin and quercetin nanoformulations free radical scavenging ability on HaCaT cells.

Based on toxicity study presented in Fig. 3, the concentration of 5 µg/ml of quercetin was selected to compare the quercetin free radical scavenging ability in crude form and nanoformulations. Fig. 4 presents the relative intensity of intracellular ROS generated upon the exposure to H_2O_2. H_2O_2 was used at a concentration of 1 mM. Control negative group is composed by the cells without treatment with quercetin and H_2O_2, while the control positive group is the cells treated only with H_2O_2. ROS were detected using the fluorescent DCFDA assay and results were expressed as relative intensity to control positive group the treatment of cells with H_2O_2 increased the intracellular ROS from 53.9 ± 15.1 % to 100 %.

The treatment of cells with crude quercetin reduced the intracellular ROS to control levels (56.8 ± 0.7 %) Quercetin loaded within LNC and liposomes enabled lower ROS intensities compared to que-SC. ROS relative intensities were 70.7 ± 14.7 % and 86.8 ± 6.5 % with que-SC stabilized with Tween® 80 and TPGS

respectively and 45.5 ± 17.2 %, 49.0 ± 19.6 % and 35.1 ± 16.3 % with que-LNC 20, 50 and que-Lipo respectively.

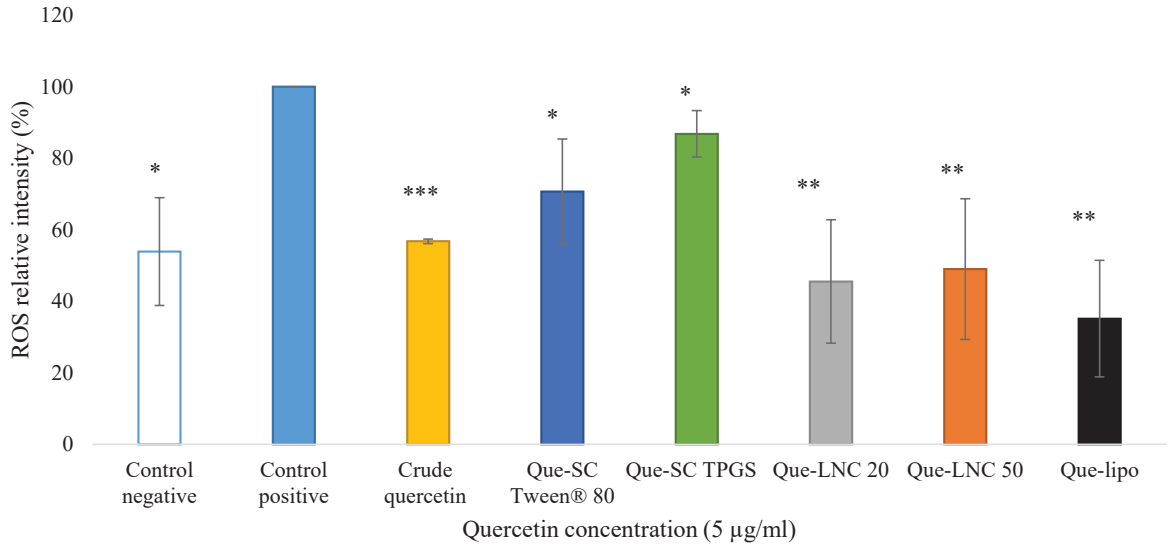

Fig. 4: HaCaT intracellular ROS generation using H_2O_2 after 24 hours of treatment with either crude quercetin or quercetin nanoformulations (n=3).

Cells were incubated with phosphate buffer as control negative (non-treated) cells and with H_2O_2 for control positive group. Cells treated with crude quercetin, quercetin smartCrystals®, quercetin lipid nanocapsules and quercetin liposomes were compared to control positive group (* = $P < 0.05$, ** = $P < 0.01$ and *** = $P < 0.005$ respectively).

3.7 Cellular toxicity of crude quercetin and quercetin nanoformulations on THP-1 cells.

To earn a wider understanding of quercetin potentials in topical application, crude quercetin and quercetin nanoformulations behavior on immune cells was tested using THP-1 cells as cellular model. Quercetin cellular toxicity at the concentration of 5 µg/ml selected from toxicity results on HaCaT cells was chosen for this assays. Fig. 5 shows the cellular viability percentage after the 24 hours treatment with crude quercetin and quercetin nanoformulations, where cellular viabilities were measured using XTT assay. No cellular toxicity was observed with crude quercetin and quercetin nanoformulations. In the case of que-SC stabilized with Tween® 80 and TPGS, the viability results were 102.0 ± 1.6 % and 102.2 ± 8.9 % respectively ($P > 0.05$). On the other hand, crude quercetin, que-LNC 20, que-LNC 50 and que-Lipo showed an increase of cellular viability compared to control non treated cells. The increase in viability was more

pronounced with que-LNC 50 and que-Lipo compared to crude quercetin and que-LNC 20 (P< 0.005 vs. P< 0.01).

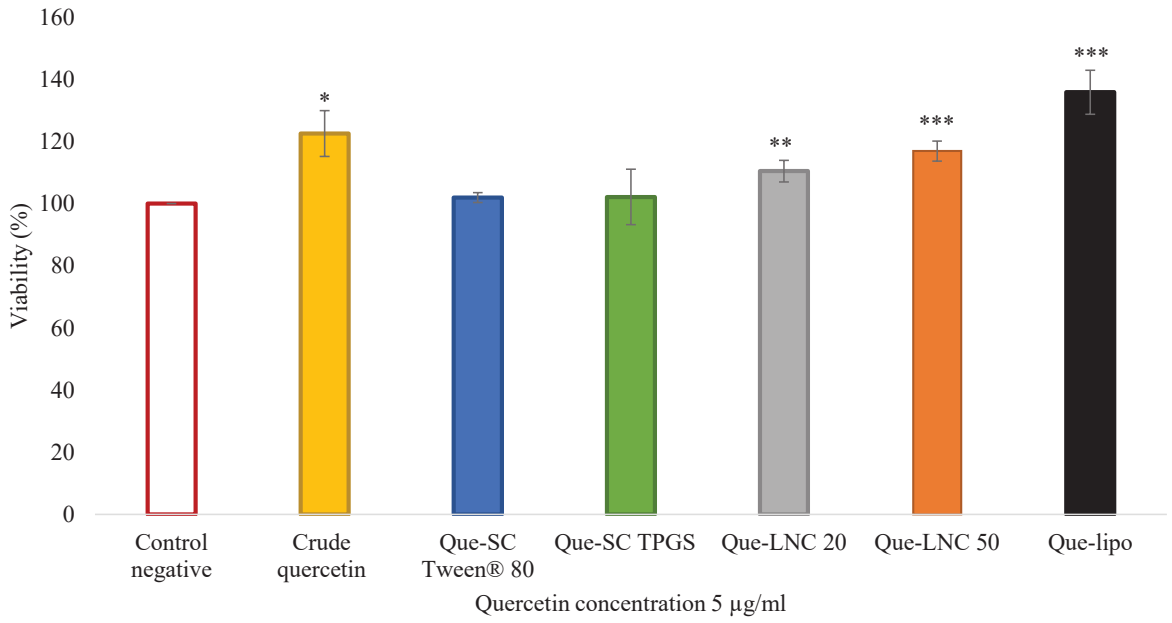

Fig. 5: THO-1 cellular viability using XTT assay after 24 hours of treatment with either crude quercetin or quercetin nanoformulations (5 µg/ml) (n=3).

Cells were incubated with phosphate buffer as control (non-treated) cells and with crude quercetin, quercetin smartCrystals®, quercetin lipid nanocapsules and quercetin liposomes for the safety of formulated quercetin. P expresses the significant value where * = P < 0.05, ** = P < 0.01 and *** = P < 0.005 respectively.

3.8 Crude quercetin and quercetin nanoformulations free radical scavenging ability on THP-1 cells.

Following the protocol used for HaCaT cells, 1 mM of H_2O_2 was used to induce oxidative stress within THP-1 cells and the subsequent increase in ROS generation. 5 µg/ml of quercetin, which previously showed to be a suitable concentration for comparison between formulations, was applied to cells prior to H_2O_2 exposure. ROS were detected using the fluorescent DCFDA assay and results were expressed as relative intensity to control positive group (Fig. 6).

The treatment of cells with H_2O_2 increased ROS generation within cells from 70.3 ± 7.3 % to 100 %. Crude quercetin and quercetin nanoformulations were significantly able to reduce ROS generation, relative ROS intensities was 34.0 ± 11.6 % with crude quercetin. ROS in que-SC treated group was 30.4 ± 11.4 % and

30.4 ± 6.2 % with Tween® 80 and TPGS (P< 0.005). Finally, ROS relative intensities were 34.6 ± 8.6 %, 35.5 ± 11.3 % and 34.2 ± 8.1 % with que-LNC 20, que-LNC 50 and que-lipo respectively (P< 0.005).

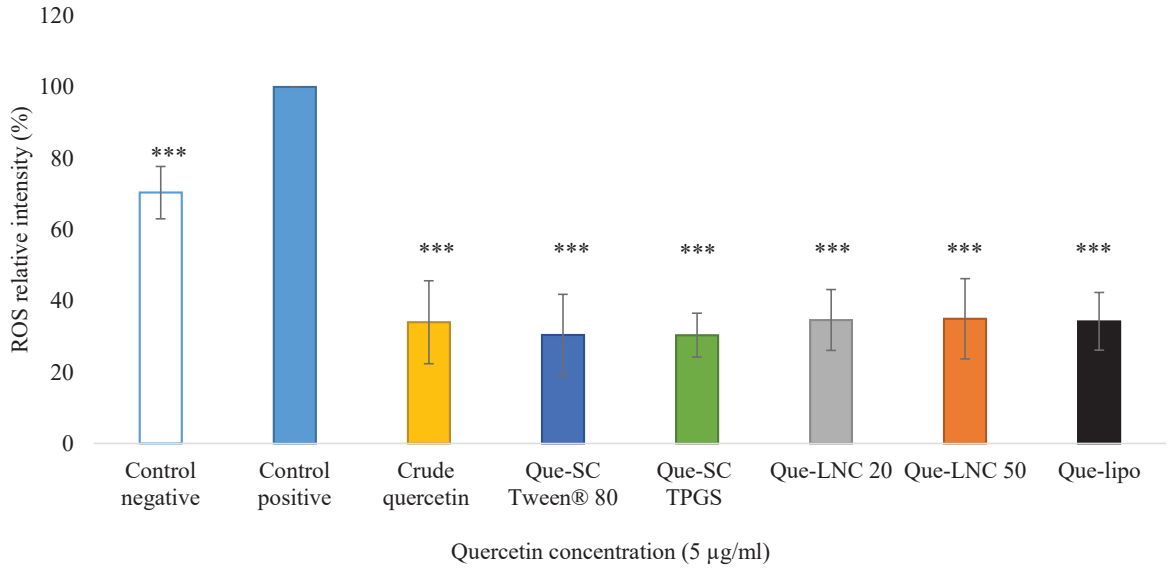

Fig. 6: THP-1 intracellular ROS generation using H_2O_2 after 24 hours of treatment with either crude quercetin or quercetin nanoformulations (n=3).

Cells were incubated with phosphate buffer as control negative (non-treated) cells and with H_2O_2 for control positive group. Cells treated with crude quercetin, quercetin smartCrystals®, quercetin lipid nanocapsules and quercetin liposomes were compared to control positive group (* = P < 0.05, ** = P < 0.01 and *** = P < 0.005 respectively).

3.9 *In vivo* skin penetration of quercetin smartCrystals® stabilized with TPGS and quercetin lipid nanocapsules 20

Based on physicochemical properties of nanoformulations and the cellular safety and free radical scavenging ability of formulated quercetin, que-SC stabilized with TPGS and que-LNC 20 formulations were selected for *in vivo* skin penetration test (stripping test). Fig. 7 presents penetrated amount of quercetin as percentage of applied dose. The amount of detect quercetin was decreasing with increasing strips number. 94.6 % of the applied dose of que-SC TPGS were detected in the 15 strips, which indicates that quercetin deposition was the upper region of the stratum corneum (around 75 µm) [28]. Whereas, 27.1 % of the applied dose were detected in case of que-LNC 20 indicating the penetration of quercetin beneath the stripped region of skin. In strip 3, the percentage of applied quercetin were 13.4 % and 3.4 % with que-SC and que-LNC respectively.

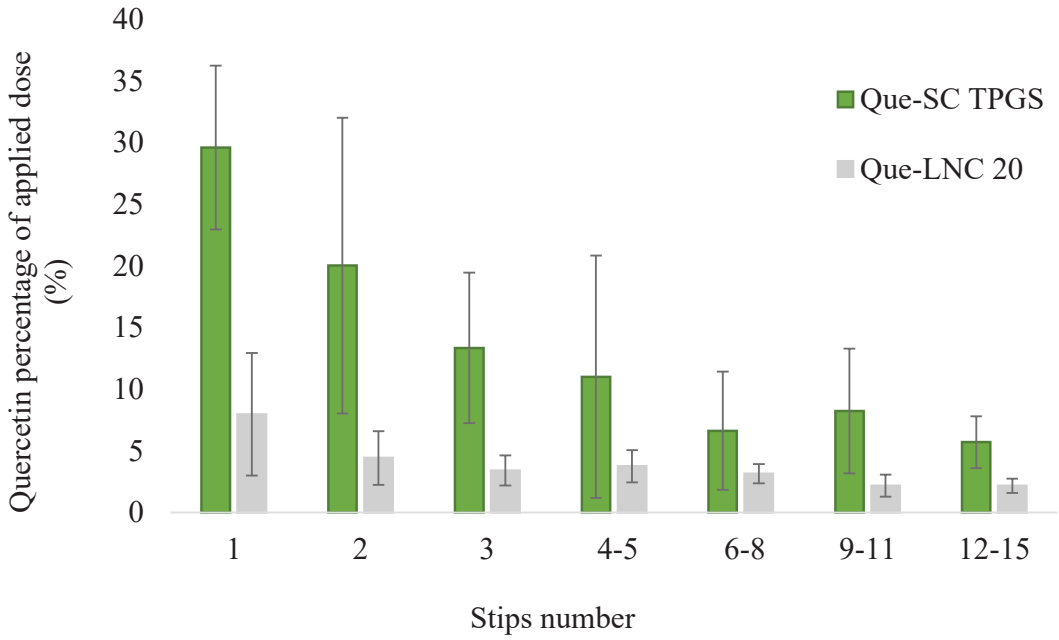

Fig. 7: *In vivo* skin penetration of quercetin smartCrystals® stabilized with TPGS (que-SC TPGS) and quercetin lipid nanocapsules 20 (Que-LNC 20) (n=8).

50 µl of que-SC TPGS and que-LNC 20 were applied to the forearm of 8 volunteers for 1 hour then, 15 strips were performed and collected in seven groups. Quercetin detected in each strip was normalized to total applied dose and presented as percentage of applied dose (%).

4 Discussion

Exogenous skin supplementation with antioxidants is a novel strategy to strengthen skin resistance to oxidative stress [29, 30]. Among interesting candidates, quercetin is a natural molecule with strong antioxidant and antiinflammatory properties [10, 31]. However, quercetin in its aglycone form (crude form) has very low water solubility (less than 0.5 µg/ml) [18] hindering its topical effectiveness [2]. In this context, nanotechnology provides an interesting tool for the formulation of poorly water-soluble drugs [32]. Therefore, three approaches in nanoformulations were investigated to overcome quercetin limited water solubility.

In this work, quercetin formulated within liposomes with the subsequent physicochemical characterization was compared to quercetin smartCrystals® and lipid nanocapsules formulation according to our previous publications [18] (LNC article under review). Indeed, the first approach was to prepare quercetin within liposomes used as reference of nanoformulations known from 70s [12]. The second approach was to increase quercetin water solubility with a formulation enabling a burst release implementing smartCrystals®

technology as described in our previous work [18]. The third approach was to increase quercetin apparent water solubility by encapsulation within a nanocarrier system enabling prolonged release kinetics for encapsulated drug (LNC article).

Que-Lipo prepared using ethanol injection method were 179 ± 15 nm (blank-Lipo 188 ± 16 nm) without any statistical differences ($P > 0.05$). The PDI less than 0.15 in blank-Lipo and que-Lipo indicates a homogenous size distribution without homogenization step like sonication or extrusion (Table 1) [33]. Liposomes size was shown to be dependent on the excipients as it increased from 127 nm (supplementary data) to 179 nm in the presence of Cremophor® EL. In parallel, Cremophor® EL increased the drug loading of quercetin from 1.55 % (data not shown) to 2.58 % (of the excipients).This can be explained by both the affinity of Cremophor® EL to quercetin and the size increase of liposomes that allows larger surface for quercetin entrapment within the phospholipid bilayer (Table 1).

Quercetin antioxidant activity was calculated as a percentage of the encapsulated quantity of quercetin. 55 ± 11 % of the encapsulated quercetin were able to reduce DPPH to DPPH-H in 30 minutes (Table 1). Despite that the percentage activity was lower compared to previous reports for que-Lipo [4], DPPH is a primary assay to confirm the preservation of the activity. As a result, the quantitative determination of the activity should be further explored with cellular assay for oxidation reducing capacity.

Que-Lipo stability was assessed at 4°C for three months with 181 ± 22 nm and PDI of 0.18 ± 0.10 (Fig. 2). The introduction of Cremophor® EL to the formulation conferred an enhanced stability for que-Lipo usually linked to the presence of cholesterol in the formulation but higher cholesterol concentration induces lower encapsulation of quercetin [16]. It is worth to note that the use of Cremophor® EL is approved in cosmetics and topically applied formulations [34].

Then, quercetin release from liposomal formulation was investigated using dialysis bag. Que-Lipo was compared to crude quercetin solution in propylene glycol. As expected quercetin control solution showed a burst release as the plateau had been reached after four hours (~33%). A delayed release profile with liposomes was established, as quercetin was not detected in the release medium until two hours. Finally, at 24 hours both quercetin control solution and que-Lipo released similar amounts (~36%) (Fig 3). The gradual release profile of quercetin from liposomes comes in accordance with previous reports [4, 16].

For the goal of topical application, HaCaT cells (human keratinocytes) were selected as a cellular model [20, 35]. The tested concentrations of quercetin were from 5 to 100 µg/ml. Crude quercetin did not show cellular toxicity even at 100 µg/ml. In contrast, it increased HaCaT cellular proliferation and this can be related to Que insolubility at these high concentrations in the culture medium (DMEM) that leads to lower cellular internalization (Fig. 3). This can be further supported with the que-SC toxicity values that were more pronounced with increased quercetin concentration as que-SC showed an increase quercetin solubility and dissolution velocity, which can lead to higher cellular internalization [18]. Que formulations efficiency

was compared on HaCaT cells. Que-SC and que-LNC were formulated according to our previous works [18] (LNC article). Que-LNC 20 and que-LNC 50 showed no significant differences in cellular viability compared to blank-LNC treated cells up to 50 µg/ml. While at 100 µg/ml, the cellular viability decreased by 40 % with que-LNC 20 ($P < 0.05$) and 23 % with que-LNC 50 ($P > 0.05$). The higher viability percentage observed with LNC 50 compared to LNC 20 (1.3 fold) can be linked to lower surfactant concentration used in the preparation of que-LNC 50 [36]. Cells treated with que-Lipo presented higher viability percentage with increasing quercetin concentration. As a possible explanation, it is worth to state that differences in cellular internalization of nanoparticles depending on cell cycle is already proven (ranking in the order G2/M > S > G0/G1) which could affect the cellular viability [37]. The same behavior of que-Lipo treated cells was observed with blank-Lipo when treating cells with increase liposomes concentration. This result gives a further support for the hypothesis that que-Lipo toxicity is linked to liposomes and not to encapsulated quercetin (supplementary data). Finally, 5 µg/ml of quercetin was the concentration of choice for HaCaT cells with cellular viability of 97.9 %, 91.6 % and 99.3 % with crude quercetin, que-LNC 20 and que-LNC 50 respectively ($P > 0.05$). In addition to be the concentration with the lowest toxicity with que-SC stabilized with Tween® 80 and TPGS (78.4 % and 86.4 %).

Based on the cellular safety results, 5 µg/ml of quercetin either in crude form or in nanoformulations was selected to test quercetin free radical scavenging ability (Fig. 4). Oxidative stress was induced in HaCaT cells using H_2O_2 (1mM) as H_2O_2 is to known to be responsible for UV induced damage [38]. H_2O_2 significantly increased ROS generation within cells compared to control (non-treated) cells ($P < 0.05$). Crude quercetin pretreatment was able to scavenge ROS and to return cells to control levels ($P < 0.05$). In the same way, quercetin in nanoformulations induced the same protective action with superior efficiency in que-LNC and que-Lipo compared to que-SC (Fig. 4). As a result, the concentration of 5 µg/ml of quercetin presented both safety and protective action on HaCaT cells, with a more pronounced effect with LNC and liposomes compared to smartCrystals®. This comes to support previous evidence about quercetin ability to scavenge ROS generated on HaCaT cells in response to UVA irradiation [39].

In order to explore quercetin activity on other cell types, THP-1 cells were selected as an example of dendritic cells derived from circulating monocytes in case of skin inflammation [22, 40, 41]. Referring back to primary results obtained from HaCaT keratinocytes cells, 5 µg/ml of quercetin was selected again on THP-1 cells. The cellular safety of crude quercetin and quercetin nanoformulations were determined (Fig. 5). The cellular viability results were similar to control group in case of que-SC ($P > 0.05$) and with higher viability results than control in case of crude quercetin, que-LNC 20, que-LNC 50 and que-Lipo. This higher viability percentage was previously observed with crude quercetin on A549 cells especially at low dose of quercetin [42]. Thus, quercetin was not toxic to THP-1 cells at 5 µg/ml in crude and formulated forms. Likewise, 5 µg/ml was tested for the protective action of quercetin against oxidative stress induced by H_2O_2

(1 mM) on THP-1 cells (Fig. 6). Similar to the case of HaCaT cells, H_2O_2 significantly increased the ROS generation in THP-1 cells ($P < 0.05$) (Fig. 6). Again, quercetin treated cells exhibited ROS intensities significantly lower than H_2O_2 treated cells and even lower than control (non-treated) cells, which indicates the efficient ROS scavenging ability of quercetin in THP-1 cells ($P < 0.05$).

Upon the successful reformulation of quercetin as SC and in LNC and the establishment of que-Lipo (Table 2), the comparison in order to select the best one in each case is evaluated taking into account three main parameters. First, the smallest particle size and PDI that can be achieved with each approach as the smaller particle size enables a prolonged retention and higher occlusion on skin [43]. Second, the total quercetin loading capacity expressed as mg of quercetin per ml of formulation can be further developed to other forms such as emulsions or gels. Third, the cellular safety of the formulation is observed along with preserved quercetin antioxidant activity, which is the essential target of these nanoformulations. Starting by the size and PDI, que-SC stabilized with TPGS and que-LNC 20 had the lowest particle size relative to que-SC stabilized with Tween® 80 and que-LNC 50. Particle size was 26 nm compared to 54 nm in LNC and 203 nm compared to 293 nm in case of SC. Likewise, que-SC stabilized with TPGS and que-LNC 20 had the highest quercetin concentration per ml of formulation (14.4 mg/ml with que-SC TPGS and 10.8 with que-LNC20). Lastly, the safety profile of que-SC TPGS vs. que-SC Tween® 80 and que-LNC 20 vs. que-LNC 50 were similar at 5 µg/ml of quercetin (78.3 % vs. 86.4 % for SC and 91.6 % vs. 99.3 % for LNC) and there was not a statistical differences in cellular viability between que-SC Tween® 80 and que-SC TPGS at the 5 µg/ml of quercetin. The safety and the activity of quercetin in nanoformulations were established at 5 µg/ml using both cellular models HaCaT and THP-1. Therefore, thanks to these results, the *in vivo* skin penetration (stripping test) was performed on que-SC TPGS and que-LNC 20 enabling to compare between the burst release approach for drug delivery and the sustained release profile. Que-Lipo presented a very low loading capacity (0.56 mg/ml) compared to other formulations and exhibited large particle size (179 nm), so que-Lipo was omitted form the *in vivo* skin penetration study.

Skin penetration tests involving quercetin formulations were mostly performed *in vitro* on pig [44] and rats [16] skin mounted on Franz diffusion cell, or *in vivo* on animals such as mice [8]. However, results from animals skin suffer from poor correlation with human skin results, as they are thinner and more permeable than human skin [45]. Only one study tested formulated quercetin in solid lipid nanoparticles *in vivo* on healthy volunteers [46], however, the tested formulation was not optimized and presented high particle size (527 nm) and high PDI (0.575) with missing information about quercetin loading with limited skin penetration capacity for formulated nanoparticles. For these reasons, the study of skin penetration of que-SC stabilized with TPGS and que-LNC 20 was done on human skin *in vivo* under the same procedure used by Scalia *et al* in 2013 [46]. 94.6% of the applied dose of que-SC were detected in the strips, which indicates the deposition of this formulation in the upper regions of the stratum corneum. As a result, less than 6% of

the applied dose were capable of penetrating into lower stratum corneum (around 75 µm) [28]. On the other side, only 27.1% of the applied dose of que-LNC 20 were detected in the strips, which could indicate that the deposition of this formulation is in the lower regions of the stratum corneum as more than 70% of quercetin was able to penetrate below strip 15. Both formulations (que-SC and que-LNC) enabled higher skin deposition of quercetin compared to Scalia *et al* formulation, as they stated that more than 50% of the applied dose were not absorbed and were detected in strip one compared to 29.6 % with que-SC and 8.0 % with que-LNC 20. About 10% of que-SC were detected in strip 15, this proves the enhancement of deeper skin penetration compared to about 5 % for quercetin nanoparticles prepared by Scalia *et al*. The higher skin penetration ability observed with que-LNC compared to que-SC may be attributed to the lipophilic character of LNC and the lower particle size (26 nm vs. 203 nm). The superficial deposition of quercetin from the smartCrystals® formulation favors its application in sunscreen and cosmetics [46]. The size of the lipid nanocapsules and their lipidic nature favors quercetin penetration into viable epidermis. This is very promising for quercetin applicability in pathologies such as inflammatory skin disorders (psoriasis) and the support of aged skin [27, 47, 48].

5 Conclusion

Quercetin is a strong antioxidant and free radical scavenger from natural origin regarded as a potential candidate for skin exogenous supplementation. The poor water solubility limits quercetin topical penetration and so efficiency. For this, quercetin was formulated in nanoformulations such as liposomes, LNC and smartCrystals®. The three approaches were compared in terms of particle size, quercetin loading per milliliter of formulation and the interaction with HaCaT and THP-1 cells. The highest cellular viability was observed at a concentration of 5 µg/ml of quercetin on HaCaT cells. Afterwards, this concentration was tested and proved efficient free radical scavenging ability against hydrogen peroxide induced oxidative stress on HaCaT cells. 5 µg/ml quercetin was also safe on THP-1 cells with strong free radical scavenging abilities. All quercetin nanoformulations showed similar activity results compared to crude quercetin indicating the preservation of quercetin antioxidant ability upon formulation. Finally, quercetin smartCrystals® stabilized with TPGS and quercetin LNC 20 were selected for *in vivo* skin penetration test (striping test).Quercetin smartCrystals® showed high skin deposition in the upper stratum corneum and gave a promise for a sunscreen product. Whereas quercetin LNC enabled deeper skin penetration for quercetin, thus presents an encouraging approach for the skin support in inflammatory disorders and psoriasis.

Acknowledgments

The authors acknowledge the financial support of ERASUMUS MUNDUS AVEMPACE 2 and the support of MACS research team. The authors have no conflict of interest to declare.

References

[1] M.G.L. Hertog, P.C.H. Hollman, M.B. Katan, Content of potentially anticarcinogenic flavonoids of 28 vegetables and 9 fruits commonly consumed in the Netherlands, Journal of Agricultural and Food Chemistry, 40 (1992) 2379-2383.

[2] F. Bonina, M. Lanza, L. Montenegro, C. Puglisi, A. Tomaino, D. Trombetta, F. Castelli, A. Saija, Flavonoids as potential protective agents against photo-oxidative skin damage, International Journal of Pharmaceutics, 145 (1996) 87-94.

[3] H. Kim, S. Namgoong, H. Kim, Antiinflammatory activity of flavonoids: Mouse ear edema inhibition, Archives of Pharmacal Research, 16 (1993) 18-24.

[4] M.L. Manca, I. Castangia, C. Caddeo, D. Pando, E. Escribano, D. Valenti, S. Lampis, M. Zaru, A.M. Fadda, M. Manconi, Improvement of quercetin protective effect against oxidative stress skin damages by incorporation in nanovesicles, Colloids and Surfaces B: Biointerfaces, 123 (2014) 566-574.

[5] T.L. Wadsworth, D.R. Koop, Effects of the wine polyphenolics quercetin and resveratrol on pro-inflammatory cytokine expression in RAW 264.7 macrophages, Biochemical Pharmacology, 57 (1999) 941-949.

[6] P. Yao, A. Nussler, L. Liu, L. Hao, F. Song, A. Schirmeier, N. Nussler, Quercetin protects human hepatocytes from ethanol-derived oxidative stress by inducing heme oxygenase-1 via the MAPK/Nrf2 pathways, Journal of Hepatology, 47 (2007) 253-261.

[7] V. García-Mediavilla, I. Crespo, P.S. Collado, A. Esteller, S. Sánchez-Campos, M.J. Tuñón, J. González-Gallego, The anti-inflammatory flavones quercetin and kaempferol cause inhibition of inducible nitric oxide synthase, cyclooxygenase-2 and reactive C-protein, and down-regulation of the nuclear factor kappaB pathway in Chang Liver cells, European Journal of Pharmacology, 557 (2007) 221-229.

[8] F.T.M.C. Vicentini, T.R.M. Simi, J.O. Del Ciampo, N.O. Wolga, D.L. Pitol, M.M. Iyomasa, M.V.L.B. Bentley, M.J.V. Fonseca, Quercetin in w/o microemulsion: In vitro and in vivo skin penetration and efficacy against UVB-induced skin damages evaluated in vivo, European Journal of Pharmaceutics and Biopharmaceutics, 69 (2008) 948-957.

[9] K. Gomathi, D. Gopinath, M. Rafiuddin Ahmed, R. Jayakumar, Quercetin incorporated collagen matrices for dermal wound healing processes in rat, Biomaterials, 24 (2003) 2767-2772.

[10] F.T. Vicentini, T. He, Y. Shao, M.J. Fonseca, W.A. Verri, Jr., G.J. Fisher, Y. Xu, Quercetin inhibits UV irradiation-induced inflammatory cytokine production in primary human keratinocytes by suppressing NF-kappaB pathway, in: J Dermatol Sci, 2011 Japanese Society for Investigative Dermatology. Published by Elsevier Ireland Ltd, Netherlands, 2011, pp. 162-168.

[11] A.D. Bangham, R.W. Horne, Negative staining of phospholipids and their structural modification by surface-active agents as observed in the electron microscope, Journal of Molecular Biology, 8 (1964) 660-IN610.

[12] G. Gregoriadis, P.D. Leathwood, B.E. Ryman, Enzyme entrapment in liposomes, FEBS Letters, 14 (1971) 95-99.

[13] G.M. El Maghraby, B.W. Barry, A.C. Williams, Liposomes and skin: From drug delivery to model membranes, European Journal of Pharmaceutical Sciences, 34 (2008) 203-222.

[14] P. Mura, F. Maestrelli, M.L. González-Rodríguez, I. Michelacci, C. Ghelardini, A.M. Rabasco, Development, characterization and in vivo evaluation of benzocaine-loaded liposomes, European Journal of Pharmaceutics and Biopharmaceutics, 67 (2007) 86-95.

[15] M.N. Padamwar, V.B. Pokharkar, Development of vitamin loaded topical liposomal formulation using factorial design approach: Drug deposition and stability, International Journal of Pharmaceutics, 320 (2006) 37-44.

[16] D. Liu, H. Hu, Z. Lin, D. Chen, Y. Zhu, S. Hou, X. Shi, Quercetin deformable liposome: Preparation and efficacy against ultraviolet B induced skin damages in vitro and in vivo, Journal of Photochemistry and Photobiology B: Biology, 127 (2013) 8-17.

[17] R.H. Müller, C.M. Keck, Second generation of drug nanocrystals for delivery of poorly soluble drugs: smartCrystal technology, European Journal of Pharmaceutical Sciences, 34 (2008) S20-S21.

[18] T. Hatahet, M. Morille, A. Hommoss, C. Dorandeu, R.H. Muller, S. Begu, Dermal quercetin smartCrystals(R): Formulation development, antioxidant activity and cellular safety, Eur J Pharm Biopharm, 102 (2016) 51-63.

[19] B.a. Heurtault, P. Saulnier, B. Pech, J.-E. Proust, J.-P. Benoit, A Novel Phase Inversion-Based Process for the Preparation of Lipid Nanocarriers, Pharmaceutical Research, 19 (2002) 875-880.

[20] P. Boukamp, R.T. Petrussevska, D. Breitkreutz, J. Hornung, A. Markham, N.E. Fusenig, Normal keratinization in a spontaneously immortalized aneuploid human keratinocyte cell line, J Cell Biol, 106 (1988) 761-771.

[21] S. Tsuchiya, M. Yamabe, Y. Yamaguchi, Y. Kobayashi, T. Konno, K. Tada, Establishment and characterization of a human acute monocytic leukemia cell line (THP-1), International Journal of Cancer, 26 (1980) 171-176.

[22] C. Auffray, M.H. Sieweke, F. Geissmann, Blood Monocytes: Development, Heterogeneity, and Relationship with Dendritic Cells, Annual Review of Immunology, 27 (2009) 669-692.

[23] L.J. Yang, P. Li, Y.J. Gao, H.F. Li, D.C. Wu, R.X. Li, [Time resolved UV-Vis absorption spectra of quercetin reacting with various concentrations of sodium hydroxide], Guang Pu Xue Yu Guang Pu Fen Xi, 29 (2009) 1632-1635.

[24] R. Chen, Tailor-made antioxidative nanocrystals: production and in vitro efficacy, (2013).

[25] M.S. Blois, Antioxidant Determinations by the Use of a Stable Free Radical, Nature, 181 (1958) 1199-1200.

[26] S. Scalia, M. Mezzena, Incorporation of quercetin in lipid microparticles: Effect on photo- and chemical-stability, Journal of Pharmaceutical and Biomedical Analysis, 49 (2009) 90-94.

[27] S.A. Wissing, R.H. Müller, Solid lipid nanoparticles as carrier for sunscreens: in vitro release and in vivo skin penetration, Journal of Controlled Release, 81 (2002) 225-233.

[28] D.A. Schwindt, K.P. Wilhelm, H.I. Maibach, Water diffusion characteristics of human stratum corneum at different anatomical sites in vivo, J Invest Dermatol, 111 (1998) 385-389.

[29] M. Podda, M. Grundmann-Kollmann, Low molecular weight antioxidants and their role in skin ageing, Clin Exp Dermatol, 26 (2001) 578-582.

[30] A. Godic, B. Poljšak, M. Adamic, R. Dahmane, The Role of Antioxidants in Skin Cancer Prevention and Treatment, Oxidative Medicine and Cellular Longevity, 2014 (2014) 860479.

[31] R. Casagrande, S.R. Georgetti, W.A. Verri Jr, M.F. Borin, R.F.V. Lopez, M.J.V. Fonseca, In vitro evaluation of quercetin cutaneous absorption from topical formulations and its functional stability by antioxidant activity, International Journal of Pharmaceutics, 328 (2007) 183-190.

[32] E. Merisko-Liversidge, G.G. Liversidge, E.R. Cooper, Nanosizing: a formulation approach for poorly-water-soluble compounds, European Journal of Pharmaceutical Sciences, 18 (2003) 113-120.

[33] C. Caddeo, O. Diez-Sales, R. Pons, X. Fernandez-Busquets, A.M. Fadda, M. Manconi, Topical anti-inflammatory potential of quercetin in lipid-based nanosystems: in vivo and in vitro evaluation, Pharm Res, 31 (2014) 959-968.

[34] C.L. Burnett, B. Heldreth, W.F. Bergfeld, D.V. Belsito, R.A. Hill, C.D. Klaassen, D.C. Liebler, J.G. Marks, Jr., R.C. Shank, T.J. Slaga, P.W. Snyder, F.A. Andersen, Safety Assessment of PEGylated oils as used in cosmetics, Int J Toxicol, 33 (2014) 13s-39s.

[35] B. Lehmann, HaCaT Cell Line as a Model System for Vitamin D3 Metabolism in Human Skin, Journal of Investigative Dermatology, 108 (1997) 78-82.

[36] C. Maupas, B. Moulari, A. BÃ©duneau, A. Lamprecht, Y. Pellequer, Surfactant dependent toxicity of lipid nanocapsules in HaCaT cells, International Journal of Pharmaceutics, 411 (2011) 136-141.

[37] J.A. Kim, C. Aberg, A. Salvati, K.A. Dawson, Role of cell cycle on the cellular uptake and dilution of nanoparticles in a cell population, Nat Nano, 7 (2012) 62-68.

[38] A.B. Petersen, R. Gniadecki, J. Vicanova, T. Thorn, H.C. Wulf, Hydrogen peroxide is responsible for UVA-induced DNA damage measured by alkaline comet assay in HaCaT keratinocytes, Journal of Photochemistry and Photobiology B: Biology, 59 (2000) 123-131.

[39] Kimura.S , Wqrqbi.E , Yanagawa.T , Ma.D , Ltch.K , Lshii.YKawachi.Y , Lshii.T, Essential role of Nrf2 in keratinocyte protection from UVA by quercetin, 387 (2009) 109–114.

[40] J. Auwerx, The human leukemia cell line, THP-1: a multifacetted model for the study of monocyte-macrophage differentiation, Experientia, 47 (1991) 22-31.

[41] F.O. Nestle, P. Di Meglio, J.-Z. Qin, B.J. Nickoloff, Skin immune sentinels in health and disease, Nature reviews. Immunology, 9 (2009) 679-691.

[42] A. Robaszkiewicz, A. Balcerczyk, G. Bartosz, Antioxidative and prooxidative effects of quercetin on A549 cells, Cell Biology International, 31 (2007) 1245-1250.

[43] J. Pardeike, A. Hommoss, R.H. Müller, Lipid nanoparticles (SLN, NLC) in cosmetic and pharmaceutical dermal products, International Journal of Pharmaceutics, 366 (2009) 170-184.

[44] M. Chessa, C. Caddeo, D. Valenti, M. Manconi, C. Sinico, A.M. Fadda, Effect of Penetration Enhancer Containing Vesicles on the Percutaneous Delivery of Quercetin through New Born Pig Skin, Pharmaceutics, 3 (2011) 497-509.

[45] Y. Liu, J.-y. Chen, H.-t. Shang, C.-e. Liu, Y. Wang, R. Niu, J. Wu, H. Wei, Light Microscopic, Electron Microscopic, and Immunohistochemical Comparison of Bama Minipig (Sus scrofa domestica) and Human Skin, Comparative Medicine, 60 (2010) 142-148.

[46] S. Scalia, E. Franceschinis, D. Bertelli, V. Iannuccelli, Comparative evaluation of the effect of permeation enhancers, lipid nanoparticles and colloidal silica on in vivo human skin penetration of quercetin, in: Skin Pharmacol Physiol, Basel., Switzerland, 2013, pp. 57-67.

[47] N. Chondrogianni, S. Kapeta, I. Chinou, K. Vassilatou, I. Papassideri, E.S. Gonos, Anti-ageing and rejuvenating effects of quercetin, Exp Gerontol, 45 (2010) 763-771.

[48] E.A. Hamminga, A.J. van der Lely, H.A.M. Neumann, H.B. Thio, Chronic inflammation in psoriasis and obesity: Implications for therapy, Medical Hypotheses, 67 (2006) 768-773.

Quercetin liposomes without Cremophor® EL	Physicochemical characterization	Quercetin liposomes with Cremophor® EL
127 ± 7	Size (nm)	179 ± 15
0.10 ± 0.01	PDI	0.06 ± 0.02
1.55 ± 0.36	DL (%)	2.58 ± 0.13
12.0 ± 1.0	EE (%)	68.2 ± 2.7

Supplementary Table 1: effect of Cremophor® EL on the physicochemical characterization of quercetin liposmoes.

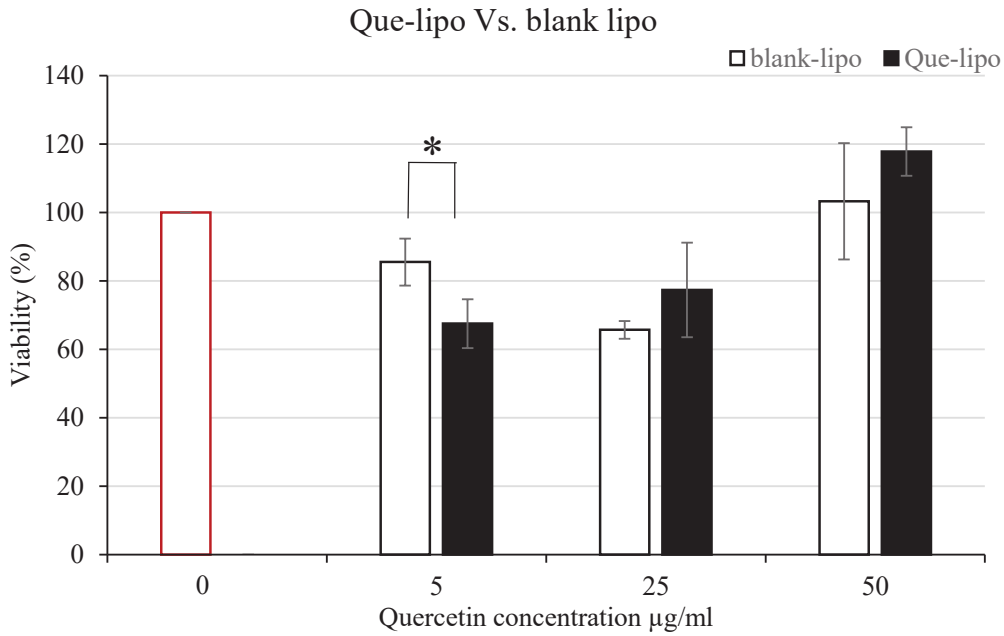

Supplementary Fig 1. HaCaT cellular viability upon the treatment with different concentrations of que-lipo and blank-lipo. The blank-lipo excipients are equal to que-lipo in for each concentration of quercetin.

Complementary results

Goals:

1. Selection of HaCaT cellular density

2. Selection of hydrogen peroxide molar concentration

3. SunTest CPS+ use for testing UV irradiation on cells

4. Quercetin inhibitory effect on MMP-9 release on THP-1 cells

5. *In vivo* animal skin penetration of quercetin lipid nanocapsules and quercetin liposomes

Complementary results

The development of experimental protocol used to establish the HaCaT cells culture methods, the condition of oxidative stress induction will be presented here to fully apprehend the model. In the scope of strengthen up our investigation on the activity of quercetin and its formulation for skin protection, we were exploring the use of SunTest CPS+ as a source of irradiation close to the solar spectrum.. At the same level, and in order to investigate quercetin protective action in relation to wound healing and skin cancer, quercetin inhibitory activity of MMP-9 is tested in collaboration with Comparative Molecular Immuno-Physiopathology, IRD Laboratory (Pr. Francisco Veas), UMR-MD3, Faculty of Pharmacy, Montpellier University. Finally, confocal imaging in 2 photon microscope, allowing fluorescence visualization in living tissues was performed in mice thanks to Dr. Muriel Golzio (Institut de Pharmacologie et de Biologie Struscturale UMR 5089). These are preliminary results and more investigation should be performed.

1. The selection of HaCaT cellular density

The determination of optimum cellular density is a critical point in cellular assays using keratinocytes, as the differentiation occurs only when cells attend confluence [1]. This process is the natural passage of keratinocytes from basal to superficial layers. For this, HaCaT cells were seeded at different cellular densities (i) 40,000 cells/cm^2, (ii) 80,000 cells/cm^2, (iii) 160,000 cells/cm^2 and (iv) 200,000 cells/cm^2 in 96 well plates. Then, cellular viability after the treatment with quercetin formulations was determined using MTT assay. Cellular toxicity due to both crude quercetin and quercetin formulations was decreased with the increase in cellular density (for example crude quercetin at 5 µg/ml, viability increased from 61.5% 40,000 cells/cm^2 at to 97.4 % at 200,000 cells/cm^2) (Fig. 1). This is in accordance with the well known fact that higher cellular density enables a cell to cell contact that in turns, strengthen the cellular resistance mechanisms [2]. Based on these findings, the cellular density of 200,000 cells/cm^2 was selected for our studies.

Complementary results

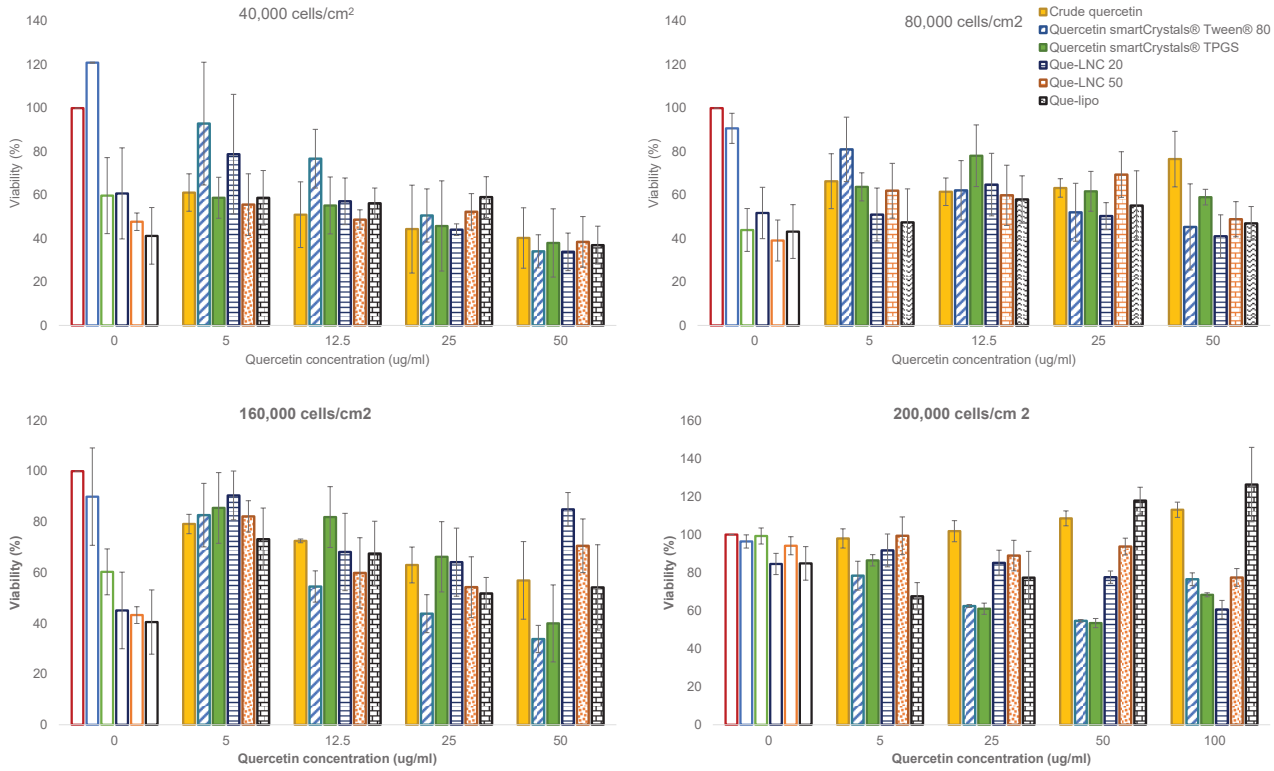

Fig. 1: HaCaT cellular viability percentage after 24 hours treatment with crude quercetin, quercetin smartCrystals® stabilized with Tween® 80 and TPGS, quercetin lipid nanocapsules 20 and 50 nm and quercetin liposomes at several cellular densities.

2. The selection of H_2O_2 molar concentration

The optimization of the oxidative stress induced by H_2O_2 was established by exposing HaCaT cells to several concentration of H_2O_2 from 25 µM to 1 mM. Fig. 2 presents the viability results of HaCaT cells upon 120 minutes exposure to H_2O_2. The cellular viability decreased with increasing H_2O_2 applied dose and this is related to the apoptotic activity of H_2O_2 on keratinocytes [3]. The cellular viability decreased to 20.5 % with 1 mM H_2O_2 compared to 61.0 % with the 0.5 mM. As a result, 1 mM H_2O_2 was selected for oxidative stress induction.

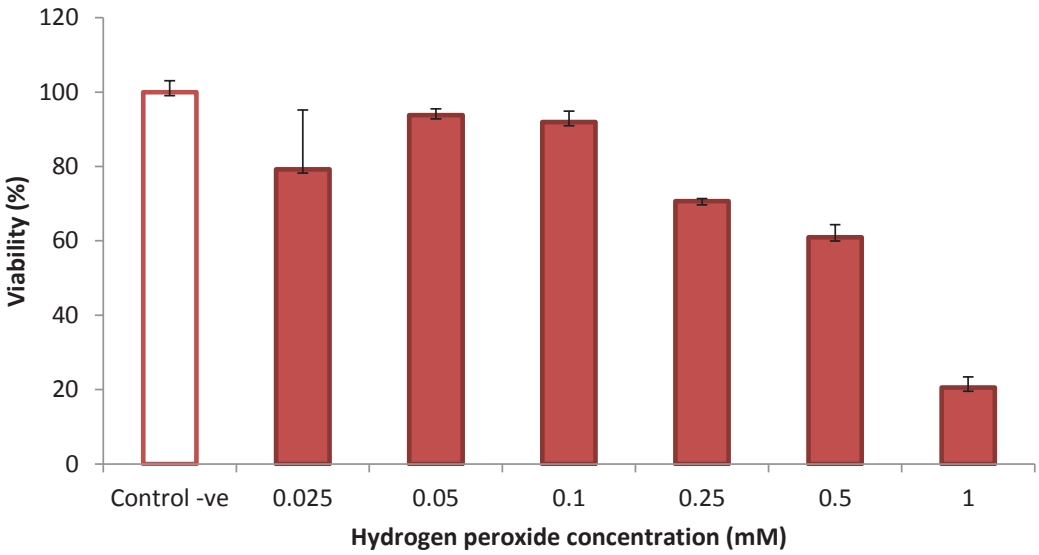

Fig. 2: HaCaT cellular viability percentage after 2 hours treatment with several concentration of H_2O_2 at 200,000 cells/cm^2 cellular density.

3. SunTest CPS+ for testing UV irradiation on cells

The SunTest CPS+ Atlas Material Testing Solutions (Linsengericht, Germany) (Fig. 3) is a light source used in pharmaceutical and cosmetics industry for the accelerated testing of cosmetics [4, 5]. The xenon lamp provides a spectrum of radiation as the solar spectrum. It is easy to use and the applied dose of irradiation can be adjusted.

Fig. 3: The Atlas SunTest CPS+

Complementary results

The use of SunTest CPS+ apparatus to mimic the solar radiation on cellular assays was not reported previously. As a result, the possibility of using SunTest CPS+ apparatus as a source of oxidation close to what happens under sunlight was investigated. Fig. 5 presents the procedure of cells treatment. The determination of the post-exposure period before MTT essay is based on the modulation of keratin 1, 10 and involucrin expression reported after the 6^{th} hours post-exposure to UV irradiation by a xenon solar UV-simulator equipped with a dichroic mirror and a 300±5 nm interference filter (Oriel Instruments, Stratford, CT, USA) [6].

The results for the optimization parameters of the experiment are showed in Fig. 4. Two main parameters were shown to have a crucial influence on cell viability: exposure time and presence of serum.

(a) The effect of **exposure time** to SunTest CPS+ irradiation on the cellular viability of HaCaT cells is evaluated. Cellular viability was reduced with increasing exposure time from 15 minutes to 30 minutes at 750 J/m^2. 56.6 ± 14.6 % of cells were viable after 15 minutes exposure to SunTest CPS+ when MTT assay was performed at 6 hours and 33.2 ± 13.7 % after 24 hours of exposure compared to 14.6 % after 6 hours and 3.7 % after 24 hours in 30 minutes exposure time (Fig. 5 a). This can be related to the higher energy input upon prolonged exposure time.

(b) The effect of presence of serum in the medium during the cells exposure to SunTest CPS+ test was also investigated. Surprisingly, we observed that cellular viability was higher when cells were covered with PBS instead of DMEM + serum (Fig. 5 b). We therefore hypothesized that serum proteins could be denatured during the exposure to SunTest CPS+ with subsequent cellular toxicity. As result, the 15 minutes exposure time in PBS was selected for the test of quercetin and its formulations protective action.

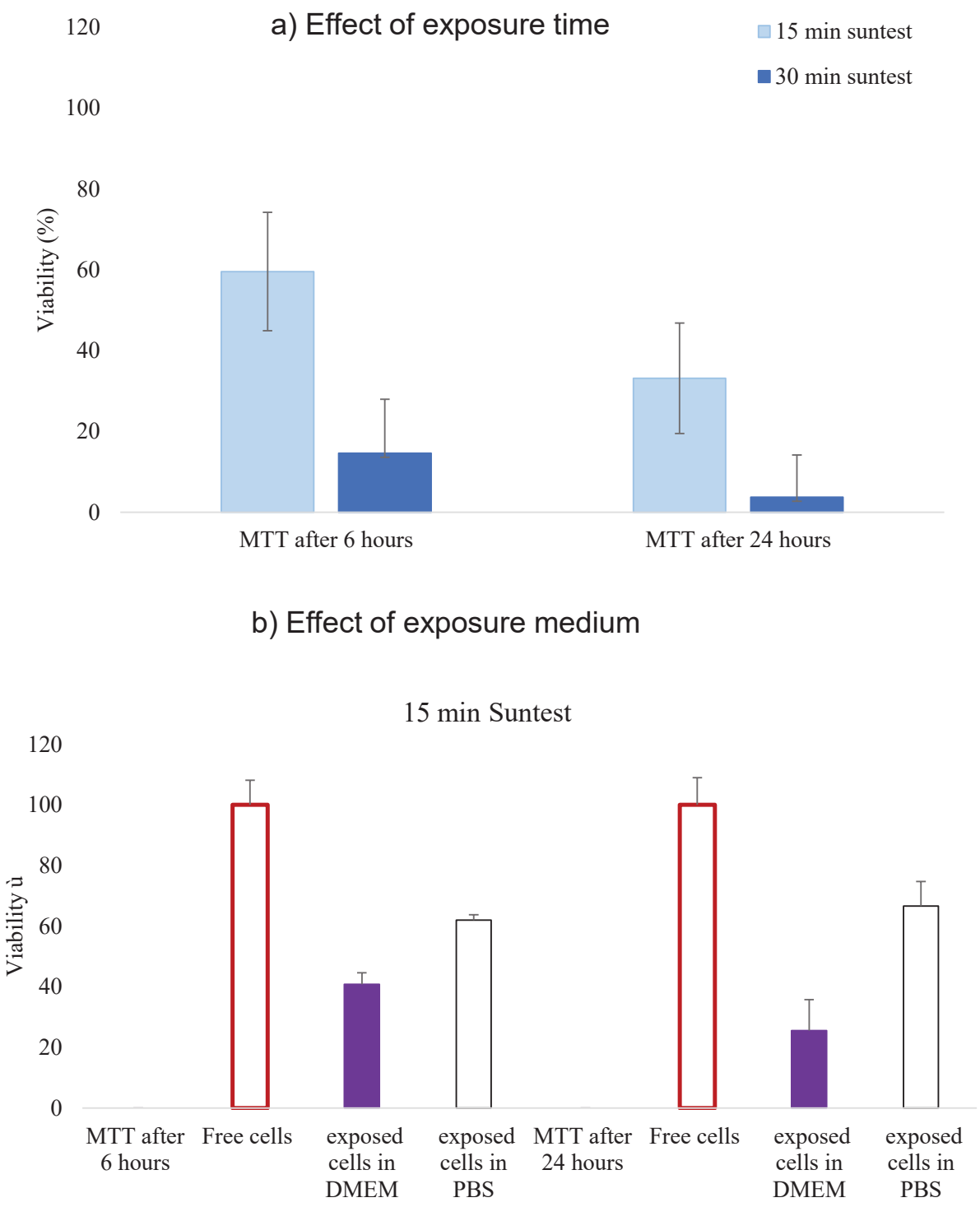

Fig. 4: Optimization parameters for SunTest CPS+ indication of oxidative stress on HaCaT cells. a) The effect of exposure time on cellular viability, b) The effect of medium composition on cellular viability.

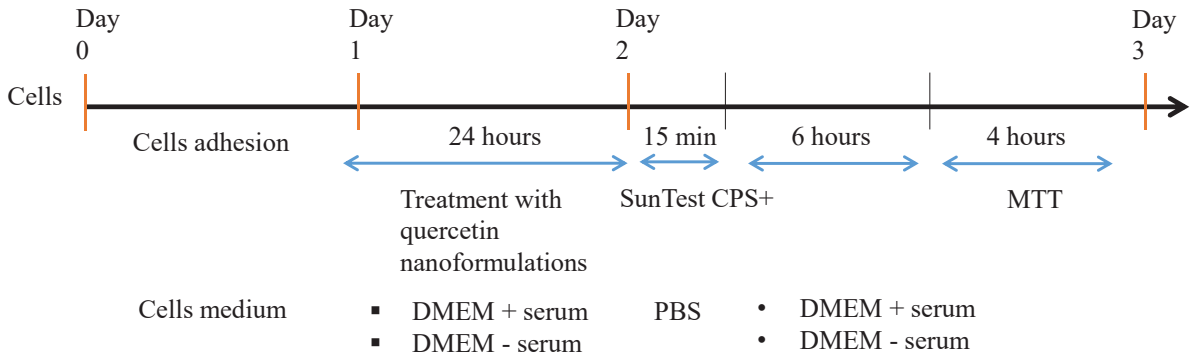

Fig. 5: Chronological presentation of SunTest CPS+ induction of cellular toxicity.

Based on these conditions, we tested the protective effect of 5 µg/ml concentration of crude quercetin and its formulations against SunTest CPS+. Vitamin C was used as a control of antioxidant molecules [7]. To determine the effect of the presence of serum during cells incubation pre-exposure and post-exposure on the results, cells were incubated with DMEM +/- serum (Fig. 6). We can notice that the control negative cells (cells non-treated with SunTest CPS+) were able to proliferate in serum positive conditions whereas the control positive cells (treated with SunTest CPS+) were not. This indicates that the SunTest CPS+ irradiation has potential to influence cell viability [8].

On the other side, in the serum free conditions the viability percentage of the control negative cells was similar to control positive one, thus supporting that the treatment of cells with SunTest CPS+ did not influence the viability but had rather a static effect on cell division. Consequently, we state that the use of MTT assay is an indicator of quercetin effect on cells in response to SunTest CPS+ exposure is not suitable.

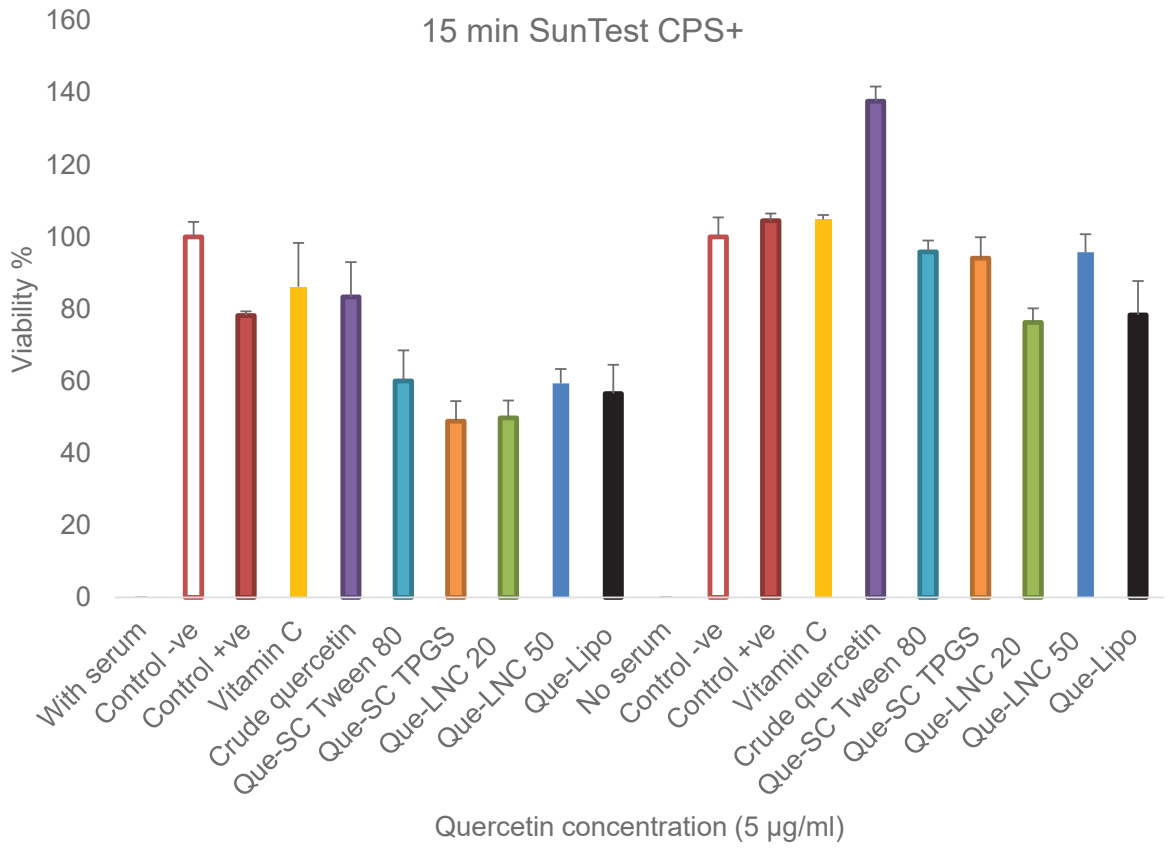

Fig. 6: HaCaT cellular viability percentage after 24 hours treatment with 5 µg/ml crude quercetin or its formulations followed by 15 minutes of SunTest CPS+ at 200,000 cells/cm^2 cellular density. MTT was performed 6 hours post exposure. Cells were incubated during quercetin treatment and 6 hours post exposure with either DMEM+ serum or DMEM only.

For this reason, we decided to look for ROS generation within SunTest CPS+ exposed cells using DCFDA assay. Cells were loaded with DCFDA after the treatment with quercetin or its formulations and before the exposure to SunTest CPS+. Fig. 7 presents the ROS generated expressed in terms of relative intensity compared to control negative cells (non-treated cells). Starting by the control positive cells, the cellular exposure to SunTest CPS+ initiated a strong oxidative stress inside cells (2.4 fold increase in ROS). However, neither Vitamin C nor crude quercetin was able to scavenge the ROS generated in response to SunTest CPS+ exposure (114.4 % with Vitamin C and 125.0 % with crude quercetin). This observation could indicate that the oxidative stress initiated by the exposure to SunTest CPS+ involves complex events and may involve the activation of heat shock proteins such as the expression of MMP-1 via calcium-

dependent protein kinase C α signaling as already observed in HaCaT cells [9]. This is supported by the fact that the SunTest CPS+ does not provide a consistent temperature in the exposure chamber. The results of quercetin and Vitamin C were both negative concerning cellular protection ability in response to SunTest CPS+. More investigations are required to certify the possibility to apply SunTest CPS+ in the UV irradiation involving the cells *in vitro* or not.

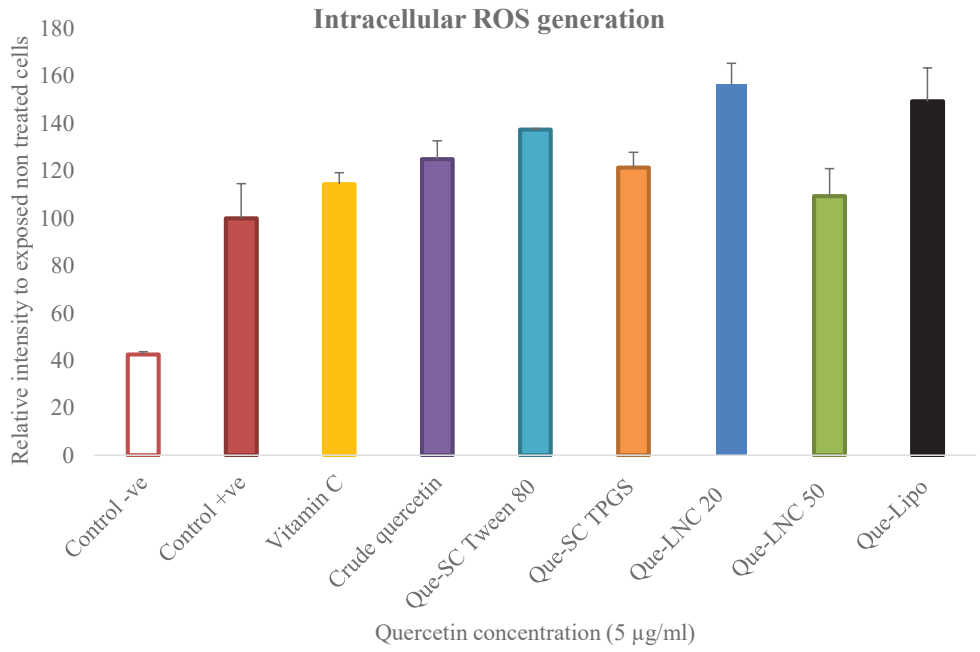

Fig. 7: ROS generation in HaCaT cells percentage after 24 hours treatment with 5 µg/ml crude quercetin or its formulations followed by 15 minutes of SunTest CPS+ at 200,000 cells/cm^2 cellular density. DCF quantification was performed directly post exposure.

4. Crude quercetin and its formulations effect on the MMP-9 release on THP-1 cells

The involvement of MMP-9 in the progression of tumors is well documented in literature such as in primary human breast cancer [10] and non-small cell lung cancer [11] and more importantly, it is known to be upregulated in aged skin and in progressive skin cancer [12]. Quercetin had previously been shown to inhibit MMP-9 directly by interaction with MMP-9 active sites [13] or its TNFαinduced expression [14].

Complementary results

For this, we wanted to evaluate crude quercetin and its formulations for potential inhibitory activity on MMP-9, which in turns could highlight the application of this polyphenol in the wound healing or even in protection against skin cancer.

THP-1 cells were induced with TNFα, which causes the induction of MMP-9 through intracellular signal-regulated kinase pathway 1/2 (ERK1/2). To explore quercetin activity against the release/activity of MMP-9, THP-1 cells were seeded at 300,000 cells/ml using RPMI medium without serum and stimulated with TNFα (12.5 ng/ml). Cells were treated with either crude quercetin or quercetin nanoformulations concurrently with TNFα stimulation. After 24 hours, cells were collected and centrifuged for 5 min at 1,500 RPM. Supernatants were collected and MMP-9 gelatinase activity was determined using 10% acrylamide separation gel and 4% acrylamide gel for stacking. 10 % glycerol solution was used for gel fixation. Gel preparation was according to Toth *et al* [15].

Fig. 8 presents the gelatin zymography of MMP-9 expressed in THP-1 cells in response to TNFα (12.5 ng/ml). The MMP-9 degradation of gelatin activity is presented by a denser band on the gel, as a result, the lighter the band, the higher the MMP-9 inhibition by quercetin. The control negative express the cells without stimulation by TNFα, whereas the control positive cells is the stimulation with TNFα without quercetin treatment. By a qualitative analysis, a weak inhibitory effect was observed for crude quercetin, que-SC and que-LNC formulations at 5 µg/ml. This may suggests the need for higher doses of quercetin in order to attend the inhibitory activity of MMP-9, as higher inhibitory activity was observed with crude quercetin at 10 µg/ml. Indeed in the other studies involving quercetin inhibition of MMP-9, quercetin applied dose was higher than what we tested, for example it was around 30 µg/ml on prostate cancer cells (PC-3) [16]. For this, further studies are requested applying higher doses of quercetin in order to explore quercetin efficient MMP-9 inhibitory activity

a)

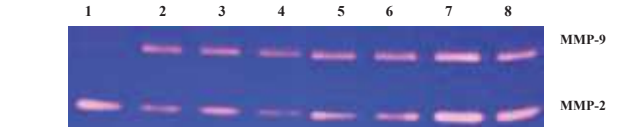

Lane	Sample
1	Negative Control
2	Positive Control
3	Crude quercetin 5 µg/ml
4	Crude quercetin 10 µg/ml
5	Que-SC Tween® 80 5 µg/ml
6	Control Tween® 80
7	Que-SC TPGS 5 µg/ml
8	Control TPGS

B)

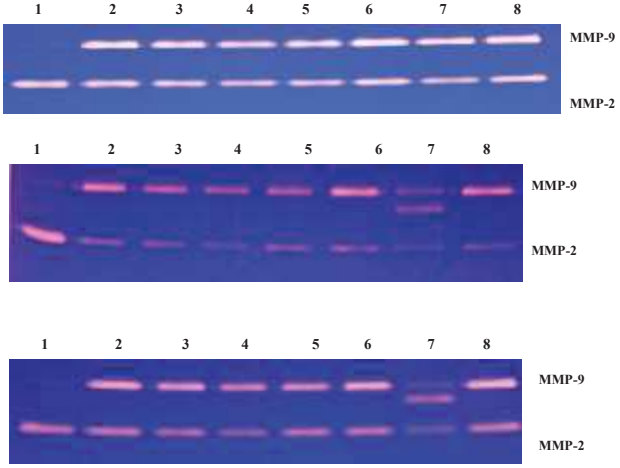

Lane	Sample
1	Negative Control
2	Positive Control
3	Crude quercetin 5 µg/ml
4	Crude quercetin 10 µg/ml
5	Que-LNC 20 5 µg/ml
6	Blank-LNC 20
7	Que-LNC 50 5 µg/ml
8	Blank-LNC50

Fig. 8: MMP-9 expression in THP-1 cells percentage after 24 hours treatment with 12.5 ng/ml of TNFα and several concentrations of crude quercetin or its formulations at 300,000 cells/ml cellular density.

5. *In vivo* animal skin penetration of quercetin lipid nanocapsules and quercetin liposomes

With the objective to compare the skin penetration capacity of lipid nanocapsules to liposomes, *in vivo* animal skin penetration studies were conducted by Dr. Muriel Golzio from the "Institut de Pharmacologie et de Biologie Struscturale" UMR 5089 of the "Centre National de la Recherche Scientifique" in Toulouse, France.

20 µl of que-LNC 20, que-LNC 50 and que-Lipo were applied for 24 hours on the ear of mice and confocal images were recorded using confocal microscope (Zeiss LSM710, Carl Zeiss, MicroImaging GmbH, Göttingen, Germany) equipped with the 40x Zeiss objective (1.3 numerical aperture, oil immersion). However, due to fluorescent interferences between quercetin and skin tissue using confocal microscopy, the three formulations were loaded with 1,1'-dioctadecyl-3,3,3',3'-tetramethylindocarbocyanine perchlorate (DiI, emission wavelength = 549 nm; excitation

wavelength = 565 nm). Dil purchased from (Invitrogen, Cergy Pontoise, France) was dissolved in acetone at 6 % (w/w) and the resulting stock solution was incorporated in Labrafac® (1:10 (w/w)) for LNC and in Cremophor® EL (1:10 (w/w)) for liposomes.

Fig. 9 presents the images of Dil loaded que-LNC 20, que-LNC 50 and que-Lipo. Due to different loading capacity of Dil within each formulation, the formulation were diluted in order to have the same Dil content prior to application to skin (6 µg/ml). The use of Dil for the labelling of LNC and Lipo was due to the interference between quercetin fluorescence and the skin auto-fluorescence, Consequently, Dil was selected as a marker for LNC and Lipo skin penetration. Images reveals that the Dil intensity was the highest with que-LNC 20 (Fig. 9, a) followed by que-LNC 50 (Fig. 9, b) and the lowest deposition was with que-Lipo (Fig. 9, c). This can be related to the differences in size between formulations and shows the superiority of LNC over liposomes for delivery to skin.

a) Que-LNC 20 b) Que-LNC 50 c) Que-Lipo

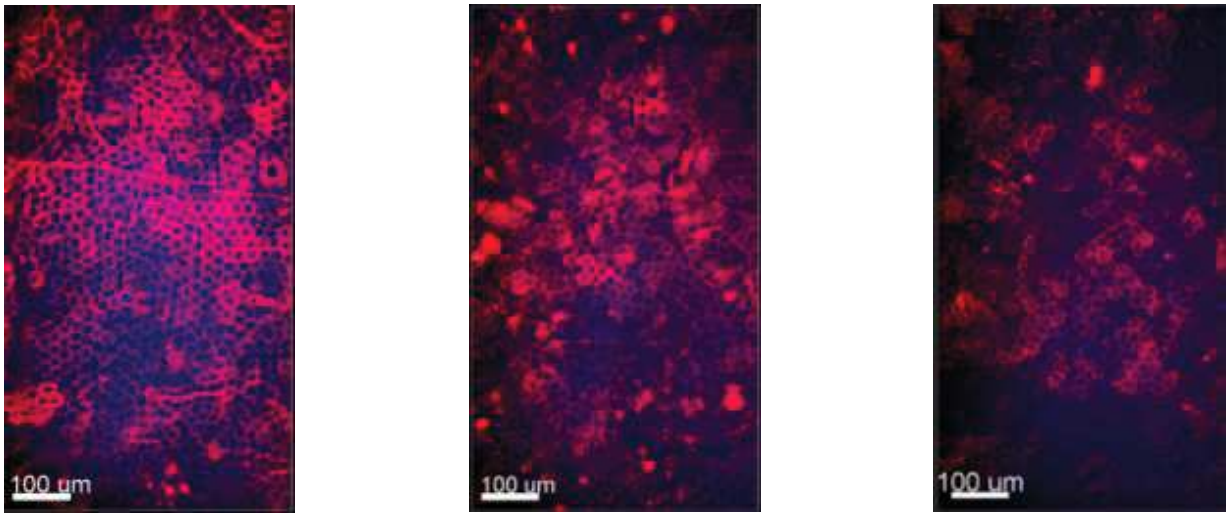

Fig. 9: Confocal images for Dil loaded que-LNC 20, que-LNC 50 and que-Lipo on the mice ear after application time of 24 hours. The images were captured with 500 ms exposure time.

References

[1] C.M. Ryle, D. Breitkreutz, H.-J. Stark, N.E. Fusening, I.M. Leigh, P.M. Stelnert, D. Roop, Density-dependent modulation of synthesis of keratins 1 and 10 in the human keratinocyte line HACAT and in ras-transfected tumorigenic clones, Differentiation, 40 (1989) 42-54.

[2] E. Bakondi, M. Gonczi, E. Szabo, P. Bai, P. Pacher, P. Gergely, L. Kovacs, J. Hunyadi, C. Szabo, L. Csernoch, L. Virag, Role of intracellular calcium mobilization and cell-density-dependent signaling in oxidative-stress-induced cytotoxicity in HaCaT keratinocytes, J Invest Dermatol, 121 (2003) 88-95.

[3] T. Zuliani, V. Denis, E. Noblesse, S. Schnebert, P. Andre, M. Dumas, M.-H. Ratinaud, Hydrogen peroxide-induced cell death in normal human keratinocytes is differentiation dependent, Free Radical Biology and Medicine, 38 (2005) 307-316.

[4] G. Berset, H. Gonzenbach, R. Christ, R. Martin, A. Deflandre, R.E. Mascotto, J.D.R. Jolley, W. Lowell, R. Pelzer, T. Stiehm, Proposed protocol for determination of photostability Part I: cosmetic UV filters, International Journal of Cosmetic Science, 18 (1996) 167-177.

[5] S.P. Huong, V. Andrieu, J.-P. Reynier, E. Rocher, J.-D. Fourneron, The photoisomerization of the sunscreen ethylhexyl p-methoxy cinnamate and its influence on the sun protection factor, Journal of Photochemistry and Photobiology A: Chemistry, 186 (2007) 65-70.

[6] M. Moravcova, A. Libra, J. Dvorakova, A. Viskova, T. Muthny, V. Velebny, L. Kubala, Modulation of keratin 1, 10 and involucrin expression as part of the complex response of the human keratinocyte cell line HaCaT to ultraviolet radiation, Interdiscip Toxicol, 6 (2013) 203-208.

[7] T. Doba, G.W. Burton, K.U. Ingold, Antioxidant and co-antioxidant activity of vitamin C. The effect of vitamin C, either alone or in the presence of vitamin E or a water-soluble vitamin E analogue, upon the peroxidation of aqueous multilamellar phospholipid liposomes, Biochimica et Biophysica Acta (BBA) - Lipids and Lipid Metabolism, 835 (1985) 298-303.

[8] T. Mosmann, Rapid colorimetric assay for cellular growth and survival: Application to proliferation and cytotoxicity assays, Journal of Immunological Methods, 65 (1983) 55-63.

[9] Y.M. Lee, W.H. Li, Y.K. Kim, K.H. Kim, J.H. Chung, Heat-induced MMP-1 expression is mediated by TRPV1 through PKCα signaling in HaCaT cells, Experimental Dermatology, 17 (2008) 864-870.

[10] A. Merdad, S. Karim, H.J. Schulten, A. Dallol, A. Buhmeida, F. Al-Thubaity, M.A. Gari, A.G. Chaudhary, A.M. Abuzenadah, M.H. Al-Qahtani, Expression of matrix metalloproteinases (MMPs) in primary human breast cancer: MMP-9 as a potential biomarker for cancer invasion and metastasis, Anticancer Res, 34 (2014) 1355-1366.

[11] D. Schveigert, S. Cicenas, S. Bruzas, N.E. Samalavicius, Z. Gudleviciene, J. Didziapetriene, The value of MMP-9 for breast and non-small cell lung cancer patients' survival, Adv Med Sci, 58 (2013) 73-82.

[12] N. Philips, S. Auler, R. Hugo, S. Gonzalez, Beneficial regulation of matrix metalloproteinases for skin health, Enzyme Res, 2011 (2011) 427285.

[13] A.C. Saragusti, M.G. Ortega, J.L. Cabrera, D.A. Estrin, M.A. Marti, G.A. Chiabrando, Inhibitory effect of quercetin on matrix metalloproteinase 9 activity molecular mechanism and structure-activity relationship of the flavonoid-enzyme interaction, Eur J Pharmacol, 644 (2010) 138-145.

[14] J. Majtan, J. Bohova, R. Garcia-Villalba, F. Tomas-Barberan, Z. Madakova, T. Majtan, V. Majtan, J. Klaudiny, Fir honeydew honey flavonoids inhibit TNF-α-induced MMP-9 expression in human keratinocytes: a new action of honey in wound healing, Archives of Dermatological Research, 305 (2013) 619-627.

[15] M. Toth, R. Fridman, Assessment of Gelatinases (MMP-2 and MMP-9) by Gelatin Zymography, Methods in molecular medicine, 57 (2001) 10.1385/1381-59259-59136-59251:59163.

[16] M.R. Vijayababu, A. Arunkumar, P. Kanagaraj, P. Venkataraman, G. Krishnamoorthy, J. Arunakaran, Quercetin downregulates matrix metalloproteinases 2 and 9 proteins expression in prostate cancer cells (PC-3), Mol Cell Biochem, 287 (2006) 109-116.

General discussion

Description of the preparation processes

Influence of excipients on quercetin loading

Influence of excipients on particle size

Influence of the formulation on quercetin crystallinity

Influence of the formulation on quercetin release profile

Scaling up of the process of preparation

Influence of the formulation on cellular behavior and antioxidant activity of quercetin

Influence of the formulation on quercetin in vivo skin penetration

General conclusion

Perspective

General discussion

Quercetin is a natural polyphenol with antioxidant and antiinflammatory properties and is the predominant among flavonoids in nature compared to apigenin, hesperetin etc… (More than 4 000 molecules). More than 20 000 articles related to quercetin or its activities were published between 1988 and 2015 making quercetin as one of the most investigated flavonoids and evidencing the growing interest of this molecule. Despite quercetin's promising activities in a long list of diseases such as Parkinson [1], Alzheimer [2], hypertension [3], diabetes [4], asthma [5] skin ageing [6] and UV skin sunscreen [7] etc.., its poor water solubility (less than 0.05 µg/ml) hinders its efficiency *in vivo*.

Quercetin physiological properties were a subject of research for more than 30 years. Nowadays, 44 studies involving quercetin are registered at the USA national institute of health (information retrieved in June 2016). Quercetin entered a phase one clinical trial in 1996 for its lymphocyte protein tyrosine phosphorylation inhibition via i.v. bolus (1400 mg/m^2), where this dose proved efficiency and safety [8] but quercetin has to be dissolved in DMSO prior to the formulation of i.v. bolus. Oral administration is not effective for treatment as the absolute oral bioavailability of crude quercetin is only 4 % [9] and topical application never led to topical activity for quercetin in its crude format [10]. As a result, to our knowledge, no product containing quercetin is neither in pharmaceutical dosage forms nor in cosmetics, is currently on the market. Quercetin containing products are mainly capsules intended for the food supplementation such as quercetin plus Vitamin C (250 mg / 700 mg) from Puritan's Pride, Inc (Oakdale, NY, USA).

Some recent research papers described the chemical modification of the crude form to allow a better quercetin absorption [6, 11]. However, the resulted molecules were less effective than the crude format. Consequently, the main solution to improve quercetin relies on the use of a suitable carrier system which could overcome its poor water solubility. It is towards this aspect, relying on quercetin formulation, to allow its use through topical administration, that was orientate this PhD work

In this project, we focused on the skin, as it represents the largest organ of the human body which is exposed to oxidative stress. In parallel, the already discussed powerful antioxidant and anti-inflammatory properties of quercetin, make it a choice molecule for skin supplementation. Three approaches, relying on quercetin nanoformulation, were developed for quercetin topical delivery and compared to each other's (smartCrystals®, lipid nanocapsules and liposomes). The selection

of smartCrystals® (drug nanocrystals) is based on their successfulness in overcoming the solubility limitation of several drugs such as: lutein [12], apigenin [13], fenofibrate [14], rutin [15] etc… and even more. By year 2008, 4 marketed drugs, which are Rapamune® sirolimus (Wyeth Pharmaceuticals, Madison, NJ) as oral suspensions and tablet, Emend® aprepitant Merck (Winehouse Station, NJ) as tablet, Tricor® fenofibrate (Abbott Laboratories) as tablet and Megace ES® megestrol acetate (Spring Valley, NY) as oral suspension.

In parallel, with the goal to both protect quercetin and increase its apparent water solubility and its bioavailability, we chose to focus on lipid based nanoparticles, as well as liposomes as a gold standard. We chose to develop quercetin within lipid nanocapsules benefiting from the ability to protect encapsulated drugs oxidation. In addition, lipid nanocapsules will confer better ability to bypass skin physical barriers [16].

Liposomal formulation was selected as a reference for nanometric delivery systems because it is recognized since the 70s as a successful approach for increasing the solubility and delivery of several drugs such as gemcitabine [17] sodium stibogluconate [18], fenofibrate [19], doxorubicin [20] etc... And these systems remain the first nanoparticles based product which was marketed in 1987 in cosmetics with Capture (Dior).

The description of the preparation process and the influence of the formulation excipients on (i) quercetin loading and (ii) particle size are discussed. Then, the effect of formulation on quercetin (i) crystallinity, (ii) release profile, (iii) interaction with cells and (iv) skin penetration are also presented. Finally, in the scope of large scale production of quercetin nanoformulations, the scale up process of these formulations is also discussed.

Description of the preparation processes

The simplicity and the ability to reproduce formulations within different settings and laboratories is one of the main objectives for industrially feasible methods. For this, the process of smartCrystals®, lipid nanocapsules and liposomes will be discussed at several levels (i) the principle of the utilized method, (ii) the instrumentation requested to perform the method, (iii) the production time and (iv) the yield of quercetin upon formulation.

SmartCrystals® technology is a top down process, where larger crystals are defragmented and disaggregated to smaller crystals eventually at the nanometric scale. This process, relying on the use of high energy level to obtain defragmentation and disaggregation, requires the use of one or

a mixture surfactant to thereafter stabilize the newly formed nanocrystals [21, 22]. Focusing on the laboratory scale production and keeping the industrial scale for later section, this method requires the use of special instrumentation such as wet bead miller, high pressure homogenizer (piston gap or microfluidizer) for processing larger crystals and transforming them to smaller ones. Thus, this limits their preparation in non-equipped laboratories. By contrast, lipid based nanoparticles do not need special instrumentation for their preparation. The lipid nanocapsules is made with the phase inversion method that produces nanocapsules by the aid of the thermic shock at the transition phase. This method requires only a heating-cooling system and this can be found in each laboratory. The only limit could be an issue is to control the temperature homogeneity in large volumes preparation. Liposome could be formulated with simple laboratory equipment, as the liposomes prepared by ethanol injection method are formed upon the natural evaporation of injected ethanol into the preheated aqueous phase. This method requires only a simple heating system and a syringe for the ethanol injection, but is maybe the more difficult to transpose at the industrial scale.

Looking at the preparation time, the second generation SmartCrystals® enables a vast decrease in the preparation time compared to quercetin nanocrystals prepared by first generation techniques from 60 minutes in bead milling to only 5 minutes and form 20 cycles in high pressure homogenizer to 2 cycles [23]. The total preparation time takes around 45 minutes starting from the weighing of quercetin to the collection of the SmartCrystals®.

Concerning the yield of quercetin due to the use of sieving and dilution after the bead milling for the separation of the SmartCrystals® from the beads, the yield of the process is around 30 % if we started with 5 % quercetin coarse suspension. Maybe by starting with a smaller percentage of quercetin like 2.5 % the yield of the process can be increased (Table 1). On the other side, the yield with lipid nanocapsules is more than 90 % and the total preparation time is between 45 minutes and 60 minutes depending on the heating-cooling speed used during the three cycles (Table 1). Finally, liposomes enabled a lower yield compared to lipid nanocapsules and higher than that of smartCrystals® with 68 %. The total preparation time for liposomes takes around 90 minutes (Table 1).

Formulations	Size (nm)	PDI	Drug loading (%)	Encapsulation efficiency (%)	Quercetin crystallinity	Solubility increase (apparent)	Dissolution / release profile	Preparation time
Crude quercetin 	3976 ± 434	0.80 ± 0.186	---	---	Crystals format pharmaceutical grade (QGPb)	0.48 ± 0.12 µg/ml	---	---
Quercetin smartCrystals® a) With Tween® 80 b) With TPGS 	295 ± 9 203 ± 3	0.25 ± 0.03 0.24 ± 0.01	--- ---	28.2 ± 6.8 28.8 ± 0.54	Crystals format pharmaceutical grade (QGPa)	14.1 ± 3.4 mg/ml 14.4 ± 0.027 mg/ml	Burst dissolution	45 minutes
Quercetin lipid nanocapsules a) 20 nm b) 50 nm 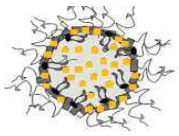	26 ± 3 54 ± 3	0.06 ± 0.001 0.17 ± 0.002	2.79 ± 0.2 2.62 ± 0.1	90.9 ± 3.5 96.4 ± 1.2	--- ---	10.80 ± 0.78 mg/ml 6.00 ± 0.70 mg/ml	Sustained release profile	45-60 minutes
Quercetin liposomes 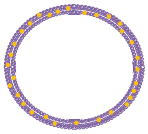	179 ± 15	0.06 ± 0.02	2.58 ± 0.13	68.2 ± 2.7	----	0.56 ± 0.05 mg/ml	Delayed release profile	90 minutes

Table 1: Summary table of the physicochemical characteristics of quercetin smartCrystals, quercetin lipid nanocapsules and quercetin liposomes

Influence of excipients on quercetin loading

We first focused on the selection of excipients to improve the solubility of quercetin. Primary solubility studies (data not shown) evidenced that Cremophor® EL (polyethoxylated castor oil) exposes good affinity to quercetin compared to other oils tested such as jojoba oil and olive oil and was therefore chosen to be introduced into lipid nanocapsules, leading to drug loading increase from 5.16 mM to 32.0 mM [24]. This excipient was also used in the liposomes preparation increasing the drug loading from 1.55 % to 2.58 %. The question that comes following the use of Cremophor® EL is, whether it is safe or not as previous articles report the discarding of Cremophor® EL from Taxol containing preparation leading to hypersensitivity reactions in oral route of administration [25-28]. Nevertheless, in another pathway, such as for topical

administration and use in cosmetics, Cremophor® EL is approved up to 22 % in hair products and it is safe in cosmetic products up to 50 % [29].

Influence of excipients on particle size

The choice of excipient may also improve the formulation process in the case of nanocrystals formulation. According to previous reports and based on our findings, the particle size of formulated nanoparticles is dependent on the preparation process and on the excipients used. Looking to smartCrystals®, the choice of the stabilizer was one of the most important parameter. In the preparations of smartCrystals®, two standard nonionic stabilizers: (i) Tween® 80) and (ii) Lutrol® F68 were selected for their known usefulness in the stabilization of drug nanocrystals [30-32]. In addition, two alkyl polyglucoside "green" stabilizers (iii) Plantacare® 810 and (iv) Plantacare® 1200, described as "skin friendly" stabilizers, were evaluated [33, 34]. Among tested stabilizers, TGPS (D-α-Tocopherol polyethylene glycol 1000 succinate) which is a derivative of Vitamin E with antioxidant capabilities [35], enabled lower particle size compared to Tween® 80, Lutrol® F68, Plantacare® 810 and Plantacare® 1200. Particle size was 203 nm with TPGS and 426 nm with Plantacare® 810 (Table 1). Concerning liposomes formulation by solvent injection, the introduction of Cremophor® EL to the formulation increased the particle size from 127 nm to 179 nm (Table 1)

Obviously, the process of preparation has also a strong influence on the particle size. Concerning smartCrystals® formulation, the pre-determination of the desired particle size is not possible as it is a top down technique [36]. On the other hand, the reproducibility of the same particle size for a drug applying the same preparation conditions is possible. The same is observed with liposomes using ethanol injection method, the particle size cannot be predicated exactly in the step of determining the formulation, and however, particle size is reproducible by standardization of protocol. By contrast, in the case of lipid nanocapsules, the size can be determined (thanks to the use of a tertiary diagram) by varying the percentage of the oily core relatively to the surfactant shell [37]. This confers the advantage for topical application by adapting the particle size for the desired targets within the skin. As an example, if targeting hair follicles, 120 nm particles the infundibutum section and the sebaceous glands could be targeted efficiently, whereas, the bulge can be targeted with particle with size around 300 nm [38].

Influence of the formulation on quercetin crystallinity

Quercetin crystalline nature was revealed by X ray studies on the crude quercetin borough from Sigma (Sigma Aldrich, France). However, with the nanonization process applied in the smartCrystals® production, quercetin changed its polymorphic form (Table 1), and this can affect quercetin physicochemical properties and its interaction with cells [39, 40]. On the other side, the detection of quercetin within lipid nanocapsules by X ray analysis was not possible due to its low percentage compared to other lipid excipients less than 3.5 %, (Table 1) [41]. Other suitable method should be selected for this purpose. We did not determine the crystalline nature of quercetin within liposomes due their inherent instability upon lyophilisation [42]. The use of cryoprotectant remains a solution for such issue. However, the low percentage of quercetin relative to other excipients in liposomes stays the major limitation for X ray studies (2.58 %) (Table 1).

Influence of the formulation on quercetin release profile

The selected formulations enabled different release profiles for quercetin *in vitro*. Quercetin first developed in the second-generation drug nanocrystals (smartCrystals® technology) showed a burst release profile (7.6 fold increase) in quercetin dissolution velocity with a total dissolution in 2 hours (Table 1). Quercetin within lipid nanocapsules showed then a sustained release profile with around 14 % released in 24 hours (Table 1). Finally, quercetin within liposomes showed a delayed release profile with no quercetin liberated in the first 2 hours compared to control solution (Table 1). It is worth to note that, we were obliged to stop *in vitro* release studies after 24 hours due to quercetin degradation in the PBS. Previous studies noted this degradation at pH 9, nonetheless we observed such degradation at pH 7.4 [43].

Scaling up of the process of preparation

The usefulness of these formulations should be extrapolated to industrial scale keeping in mind that quercetin was not marketed till the moment as an active ingredient. Consequently, the scaling up of the preparation process from lab scale to pilot scale and then to the industrial scale is discussed, the three approaches each owns advantages and disadvantages. The main characteristic of a good scale up design is by controlling the particle size, PDI and zeta potential of nanoparticles produced at the lab scale and at the pilot scale or industrial one [44, 45]. The drug loading can also

be monitored for formulations that encapsulate drug such as lipid nanocapsules and liposomes. The scale up of smartCrystals® is feasible and depends only on the size of the bead milling machine and high-pressure homogenizer [44]. The pearl mill Bùhler PML 2 used in the lab scale can be replaced with K-Serie in pilot scale then to SuperFlow™ for industrial scale (Bùhler AG, Uzwil, Switzerland). Similarly the Micron LAB 40 (APV Gaulin GmbH, Germany) with 40 ml batch volume to 600 ml batch volume in continuous mode with the Micron LAB 60 and then 60 000 litres/hour with High-pressure homogenizer Rannie 110T/125T (APV Gaulin GmbH, Germany). The major inconvenient for such process is that if quercetin nanosuspensions need to be further lyophilized, this could causes an increase in the preparation costs and adds more complexity to the process at the industrial scale. But this issues were already apprehended with the already marketed nanocrystals based products.

The scale up of lipid nanocapsules could also be feasible with previous reports about Ibuprofen [45]. The use of 20 ml flasks and plate heaters in the lab scale can be replaced by automatic reactor ARLA1, marketed by Algochem Company (Paris, France). These two double-jacketed reactors can hold the three cycles within the first reactor and the MilliQ water used for the dilution in the second reactor. Then, the reception of lipid nanocapsules can be within beaker. The volume of the reactors and the reception beaker determine the size of produced batches. Looking into quercetin liposomal formulation, the scale up of liposomes prepared by ethanol injection method seems to be the simplest [46]. The use of large reactors that are double-jacketed for the PBS buffer and the injection of phospholipid ethanolic solution can be performed through a syringe pump (model ST-670T, Samtronic) coupled to a stainless-steel needle (0.4 mm about 27 guage).

The expensive excipients used in liposomes preparation and the need to pass into an evaporation step may limit the scale up process. As liposomes do not offer advantages over smartCrystals® and lipid nanocapsules for quercetin topical delivery in terms of limited drug loading (0.56 mg/ml) and the preferred storage condition is 4°C.

Influence of the formulation on cellular behavior and antioxidant activity of quercetin

Quercetin smartCrystals® toxicity and protective activity were first tested on Vero cell line, because this was the first published work regarding drug nanocrystals interaction with cells [39]. As a result, the selection of Vero cells was done on the basis of their universal use in toxicological

studies and their presence in most of cell culture laboratories thus enabling the comparison of quercetin smartCrystals® to other formulations in the future.

In a second time, the cellular safety and quercetin protective activity with these formulations were tested mainly on two cell lines: HaCaT cells as immortalized keratinocytes [47] and THP-1 cells as monocytes in order to give insights of the quercetin and its formulations behavior in respect to immune cells and monocytes derived dendritic cells [48-50].Going back to HaCaT cells, the selection of the optimal cellular density was a critical point of the study, as the resistance of these cells to external stimuli is very dependent on cell to cell interactions in 2D culture [51]. Moreover, the 3D culture could also improve the cellular ability to survive against toxic agents [52]. On the basis of our studies, 200 000 cells /cm^2 were the optimal cellular density. The concentration of 5 µg/ml was safe and effective for crude quercetin and its formulations. This concentration comes in accordance with previous reports regarding quercetin protective activity against UVB radiation (20 mJ/cm^2) [53]. Interestingly, this concentration was twenty times lower than that of Manca *et al* for the efficiency against hydrogen peroxide induced oxidative stress [54]. Finally, quercetin showed anti-ageing and rejuvenating activities at 2 µg/ml HFL-1 human embryonic fibroblasts and whitening activity on mouse melanocytes (B16F10 cell line at 5 µg/ml [6]. The promising results on HaCaT encouraged us to test the 5 µg/ml of quercetin and its formulations on THP-1 cells, where this concentration was safe and proved protective activity against hydrogen peroxide induced oxidative stress. This comes to support that quercetin had previously showed an inhibition of superoxide anion and elastase release in neutrophils [55]. This study highlights the double benefit from quercetin topical administration for strong antioxidant and antiinflammatory activities.

The effective dose of 5 µg/ml is 2 880 fold and 2 160 fold lower than the prepared concentration of quercetin smartCrystals® (TPGS) and LNC 20 per one ml which indicates that the formulation gave a sufficient loading capacity for further formulation into gels or emulsions and kept quercetin concentration high enough for efficient delivery. On the other hand, liposomes that enabled a limited quercetin loading of 0.56 mg/ml meaning only 112 fold the effective concentration may struggle its incorporation into final products that require further dilution.

Influence of the formulation on quercetin *in vivo* skin penetration

Skin is an active organ that consists of the three main layers dermis (1-2 mm), epidermis (50-100 µm) and stratum corneum (5-8 µm) [56]. Dermis contains the blood vessels and sebaceous glands. The differentiation of keratinocytes starts from the basement membrane below the epidermis towards the terminal differentiation in the uppermost stratum lucidum where cells losses their nucleus to form the corneocytes [57].

Skin is a compact physiological barrier. This barrier function is mainly due to the superficial stratum corneum, where the bypass of stratum corneum is a great importance for transdermal delivery. The stratum corneum is composed of dead corneocytes that are filled with water and keratin. However, these dead cells are embedded in the continuous lipid environment, which consists of ceramides, cholesterol and free fatty acid. The lipid environment is responsible for the barrier function of the stratum corneum. These lipid environment is organized in the form of what is called lamellae [58]. In 1994, Forslind suggested the domain mosaic model of the skin barrier, which recognized the lipid bulks as segregated into crystalline / gel domain. These domains are surrounded by grain borders, where the lipids are in the fluid crystalline state [59]. The major flux of across skin can occur at the boundaries, where lipid chains can present packing defects due to the lyophobic / hydrophilic bilayer that composes the grain borders [60]. The electron microscopy examination of the skin shows that at the junction between neighbor corneocytes, there is a band of 13 nm width, this lamellar arrangement is due to the interaction of the lipid environment with the outer surface of nearby corneocytes [61].

After the discussion of the barrier function of the skin, the penetration of nanoparticles through the skin and the potential pathways that nanoparticles can follow is discussed. One potential pathway for skin penetration of nanoparticles is the follicular openings. Alvarez-Roman *et al* investigated polystyrene nanoparticles from 20 to 200 nm and observed that with longer exposure times the nanoparticles accumulate in the follicular openings more preferably with smaller nanoparticles [62]. The localization of nanoparticles within the hair follicles was further confirmed on titanium dioxide nanoparticles [63, 64]. Other studies revealed that gold nanoparticles below 10 nm where capable of penetrating the skin the lower layers of the stratum corneum via the lipidic matrix and the hair follicles [65]. This suggests that for the 13 nm lamellar bands present between neighboring corneocytes. Looking into lipid based nanoparticles such as liposomes, intact liposomes were not

able to pass the horny layer of the stratum corneum, and however, the penetration of encapsulated lipophilic drugs can be the fluidization of intercellular lipid domains [66].

The *in vivo* skin penetration test performed on quercetin smartCrystals® and quercetin lipid nanocapsules revealed higher skin penetration with lipid based nanoparticles. More than 90 % of quercetin applied dose with the smartCrystals® was detected in the 15 strips compared to less than 30 % with lipid nanocapsules. This observation can be linked to several differences in the formulation. Starting by the higher occlusive effect conferred by the lipid nanocapsules compared to the smartCrystals® besides to the lower particle size by about 8 fold (203 nm with smartCrystals® vs. 26 nm the lipid nanocapsules) (Table 1) [67]. The smaller size and the lipid nature generate higher occlusive effect in the skin reducing the packing of corneocytes and widening the intercellular gaps [56]. Furthermore, the lipid nanocapsules contains chains of triglycerides in the Labrafac® and castor oil in the Cremophor® EL that gather higher affinity for skin lipids (fatty acids and cholesterol) compared to the hydrophilic nature of smartCrystals®. Finally, the *in vivo* skin penetration performed cannot offer information on whether lipid nanocapsules were intact or destroyed, however, from the stability tests at 37 °C with the lipid nanocapsules, the disintegration of the capsules is more pronounced.

References

[1] S.S. Karuppagounder, S.K. Madathil, M. Pandey, R. Haobam, U. Rajamma, K.P. Mohanakumar, Quercetin up-regulates mitochondrial complex-I activity to protect against programmed cell death in rotenone model of Parkinson's disease in rats, Neuroscience, 236 (2013) 136-148.

[2] A.M. Sabogal-Guáqueta, J.I. Muñoz-Manco, J.R. Ramírez-Pineda, M. Lamprea-Rodriguez, E. Osorio, G.P. Cardona-Gómez, The flavonoid quercetin ameliorates Alzheimer's disease pathology and protects cognitive and emotional function in aged triple transgenic Alzheimer's disease model mice, Neuropharmacology, 93 (2015) 134-145.

[3] R.L. Edwards, T. Lyon, S.E. Litwin, A. Rabovsky, J.D. Symons, T. Jalili, Quercetin reduces blood pressure in hypertensive subjects, J Nutr, 137 (2007) 2405-2411.

[4] O. Coskun, M. Kanter, A. Korkmaz, S. Oter, Quercetin, a flavonoid antioxidant, prevents and protects streptozotocin-induced oxidative stress and β-cell damage in rat pancreas, Pharmacological Research, 51 (2005) 117-123.

[5] C.H. Jung, J.Y. Lee, C.H. Cho, C.J. Kim, Anti-asthmatic action of quercetin and rutin in conscious guinea-pigs challenged with aerosolized ovalbumin, Archives of Pharmacal Research, 30 (2007) 1599-1607.

[6] N. Chondrogianni, S. Kapeta, I. Chinou, K. Vassilatou, I. Papassideri, E.S. Gonos, Anti-ageing and rejuvenating effects of quercetin, Exp Gerontol, 45 (2010) 763-771.

[7] B. Choquenet, C. Couteau, E. Paparis, L.J.M. Coiffard, Quercetin and Rutin as Potential Sunscreen Agents: Determination of Efficacy by an in Vitro Method, Journal of Natural Products, 71 (2008) 1117-1118.

[8] D.R. Ferry, A. Smith, J. Malkhandi, D.W. Fyfe, P.G. deTakats, D. Anderson, J. Baker, D.J. Kerr, Phase I clinical trial of the flavonoid quercetin: pharmacokinetics and evidence for in vivo tyrosine kinase inhibition, Clin Cancer Res, 2 (1996) 659-668.

[9] M. Reinboth, S. Wolffram, G. Abraham, F.R. Ungemach, R. Cermak, Oral bioavailability of quercetin from different quercetin glycosides in dogs, Br J Nutr, 104 (2010) 198-203.

[10] F. Bonina, M. Lanza, L. Montenegro, C. Puglisi, A. Tomaino, D. Trombetta, F. Castelli, A. Saija, Flavonoids as potential protective agents against photo-oxidative skin damage, International Journal of Pharmaceutics, 145 (1996) 87-94.

[11] L. Montenegro, C. Carbone, C. Maniscalco, D. Lambusta, G. Nicolosi, C.A. Ventura, G. Puglisi, In vitro evaluation of quercetin-3-O-acyl esters as topical prodrugs, International Journal of Pharmaceutics, 336 (2007) 257-262.

[12] K. Mitri, R. Shegokar, S. Gohla, C. Anselmi, R.H. Müller, Lutein nanocrystals as antioxidant formulation for oral and dermal delivery, International Journal of Pharmaceutics, 420 (2011) 141-146.

[13] L. Al Shaal, R. Shegokar, R.H. Müller, Production and characterization of antioxidant apigenin nanocrystals as a novel UV skin protective formulation, International Journal of Pharmaceutics, 420 (2011) 133-140.

[14] P.P. Ige, R.K. Baria, S.G. Gattani, Fabrication of fenofibrate nanocrystals by probe sonication method for enhancement of dissolution rate and oral bioavailability, Colloids and Surfaces B: Biointerfaces, 108 (2013) 366-373.

[15] R. Mauludin, R.H. Müller, C.M. Keck, Development of an oral rutin nanocrystal formulation, International Journal of Pharmaceutics, 370 (2009) 202-209.

[16] M.M.A. Abdel-Mottaleb, D. Neumann, A. Lamprecht, Lipid nanocapsules for dermal application: A comparative study of lipid-based versus polymer-based nanocarriers, European Journal of Pharmaceutics and Biopharmaceutics, 79 (2011) 36-42.

[17] M.L. Immordino, P. Brusa, F. Rocco, S. Arpicco, M. Ceruti, L. Cattel, Preparation, characterization, cytotoxicity and pharmacokinetics of liposomes containing lipophilic gemcitabine prodrugs, Journal of Controlled Release, 100 (2004) 331-346.

[18] C.R. Alving, E.A. Steck, W.L. Chapman, V.B. Waits, L.D. Hendricks, G.M. Swartz, W.L. Hanson, Therapy of leishmaniasis: Superior efficacies of liposome-encapsulated drugs, Proceedings of the National Academy of Sciences, 75 (1978) 2959-2963.

[19] Y. Chen, Y. Lu, J. Chen, J. Lai, J. Sun, F. Hu, W. Wu, Enhanced bioavailability of the poorly water-soluble drug fenofibrate by using liposomes containing a bile salt, International Journal of Pharmaceutics, 376 (2009) 153-160.

[20] D.W. Northfelt, F.J. Martin, P. Working, P.A. Volberding, J. Russell, M. Newman, M.A. Amantea, L.D. Kaplan, Doxorubicin Encapsulated in Liposomes Containing Surface-Bound Polyethylene Glycol: Pharmacokinetics, Tumor Localization, and Safety in Patients with AIDS-Related Kaposi's Sarcoma, The Journal of Clinical Pharmacology, 36 (1996) 55-63.

[21] R. Shegokar, R.H. Müller, Nanocrystals: Industrially feasible multifunctional formulation technology for poorly soluble actives, International Journal of Pharmaceutics, 399 (2010) 129-139.

[22] A.R. Tao, S. Habas, P. Yang, Shape control of colloidal metal nanocrystals, small, 4 (2008) 310-325.

[23] M. Kakran, R. Shegokar, N.G. Sahoo, L. Al Shaal, L. Li, R.H. Müller, Fabrication of quercetin nanocrystals: Comparison of different methods, European Journal of Pharmaceutics and Biopharmaceutics, 80 (2012) 113-121.

[24] A. Barras, A. Mezzetti, A. Richard, S. Lazzaroni, S. Roux, P. Melnyk, D. Betbeder, N. Monfilliette-Dupont, Formulation and characterization of polyphenol-loaded lipid nanocapsules, International Journal of Pharmaceutics, 379 (2009) 270-277.

[25] P. Ma, R.J. Mumper, Paclitaxel Nano-Delivery Systems: A Comprehensive Review, Journal of nanomedicine & nanotechnology, 4 (2013) 1000164.

[26] Y. Liu, L. Huang, F. Liu, Paclitaxel Nanocrystals for Overcoming Multidrug Resistance in Cancer, Mol Pharm, 7 (2010) 863-869.

[27] S. Peltier, J.-M. Oger, F. Lagarce, W. Couet, J.-P. Benoît, Enhanced Oral Paclitaxel Bioavailability After Administration of Paclitaxel-Loaded Lipid Nanocapsules, Pharmaceutical Research, 23 (2006) 1243-1250.

[28] F. Lacoeuille, F. Hindre, F. Moal, J. Roux, C. Passirani, O. Couturier, P. Cales, J.J. Le Jeune, A. Lamprecht, J.P. Benoit, In vivo evaluation of lipid nanocapsules as a promising colloidal carrier for paclitaxel, International Journal of Pharmaceutics, 344 (2007) 143-149.

[29] C.L. Burnett, B. Heldreth, W.F. Bergfeld, D.V. Belsito, R.A. Hill, C.D. Klaassen, D.C. Liebler, J.G. Marks, Jr., R.C. Shank, T.J. Slaga, P.W. Snyder, F.A. Andersen, Safety Assessment of PEGylated oils as used in cosmetics, Int J Toxicol, 33 (2014) 13s-39s.

[30] A.S.B. Goebel, U. Knie, C. Abels, J. Wohlrab, R.H.H. Neubert, Dermal targeting using colloidal carrier systems with linoleic acid, European Journal of Pharmaceutics and Biopharmaceutics, 75 (2010) 162-172.

[31] P.R. Mishra, L.A. Shaal, R.H. Müller, C.M. Keck, Production and characterization of Hesperetin nanosuspensions for dermal delivery, International Journal of Pharmaceutics, 371 (2009) 182-189.

[32] J.C. Schwarz, A. Weixelbaum, E. Pagitsch, M. Löw, G.P. Resch, C. Valenta, Nanocarriers for dermal drug delivery: Influence of preparation method, carrier type and rheological properties, International Journal of Pharmaceutics, 437 (2012) 83-88.

[33] T.F. Tadros, Surfactants in Personal Care and Cosmetics, in: Applied Surfactants, Wiley-VCH Verlag, 2005, pp. 399-432.

[34] A. Mehling, M. Kleber, H. Hensen, Comparative studies on the ocular and dermal irritation potential of surfactants, Food and Chemical Toxicology, 45 (2007) 747-758.

[35] A. Yan, A. Von Dem Bussche, A.B. Kane, R.H. Hurt, Tocopheryl Polyethylene Glycol Succinate as a Safe, Antioxidant Surfactant for Processing Carbon Nanotubes and Fullerenes, Carbon, 45 (2007) 2463-2470.

[36] R.H. Müller, C.M. Keck, Second generation of drug nanocrystals for delivery of poorly soluble drugs: smartCrystal technology, European Journal of Pharmaceutical Sciences, 34 (2008) S20-S21.

[37] B. Heurtault, P. Saulnier, B. Pech, M.C. Venier-Julienne, J.E. Proust, R. Phan-Tan-Luu, J.P. Benoit, The influence of lipid nanocapsule composition on their size distribution, European Journal of Pharmaceutical Sciences, 18 (2003) 55-61.

[38] A. Patzelt, H. Richter, F. Knorr, U. Schäfer, C.-M. Lehr, L. Dähne, W. Sterry, J. Lademann, Selective follicular targeting by modification of the particle sizes, Journal of Controlled Release, 150 (2011) 45-48.

[39] T. Hatahet, M. Morille, A. Hommoss, C. Dorandeu, R.H. Muller, S. Begu, Dermal quercetin smartCrystals(R): Formulation development, antioxidant activity and cellular safety, Eur J Pharm Biopharm, 102 (2016) 51-63.

[40] G.S. Borghetti, I.M. Costa, P.R. Petrovick, V.P. Pereira, V.L. Bassani, Characterization of different samples of quercetin in solid-state: indication of polymorphism occurrence, Pharmazie, 61 (2006) 802-804.

[41] H. Bunjes, T. Unruh, Characterization of lipid nanoparticles by differential scanning calorimetry, X-ray and neutron scattering, Advanced Drug Delivery Reviews, 59 (2007) 379-402.

[42] M. Glavas-Dodov, E. Fredro-Kumbaradzi, K. Goracinova, M. Simonoska, S. Calis, S. Trajkovic-Jolevska, A.A. Hincal, The effects of lyophilization on the stability of liposomes containing 5-FU, International Journal of Pharmaceutics, 291 (2005) 79-86.

[43] Y. Zheng, I.S. Haworth, Z. Zuo, M.S.S. Chow, A.H.L. Chow, Physicochemical and structural characterization of Quercetin-β-Cyclodextrin Complexes, Journal of Pharmaceutical Sciences, 94 (2005) 1079-1089.

[44] L. Al Shaal, R.H. Müller, R. Shegokar, smartCrystal combination technology – scale up from lab to pilot scale and long term stability, Die Pharmazie - An International Journal of Pharmaceutical Sciences, 65 (2010) 877-884.

[45] O. Thomas, F. Lagarce, Lipid Nanocapsules: A Nanocarrier Suitable for Scale-Up Process, Journal of Drug Delivery Science and Technology, 23 (2013) 555-559.

[46] O.R. Justo, Â.M. Moraes, Analysis of process parameters on the characteristics of liposomes prepared by ethanol injection with a view to process scale-up: Effect of temperature and batch volume, Chemical Engineering Research and Design, 89 (2011) 785-792.

[47] P. Boukamp, R.T. Petrussevska, D. Breitkreutz, J. Hornung, A. Markham, N.E. Fusenig, Normal keratinization in a spontaneously immortalized aneuploid human keratinocyte cell line, J Cell Biol, 106 (1988) 761-771.

[48] J. Auwerx, The human leukemia cell line, THP-1: a multifacetted model for the study of monocyte-macrophage differentiation, Experientia, 47 (1991) 22-31.

[49] F.O. Nestle, P. Di Meglio, J.-Z. Qin, B.J. Nickoloff, Skin immune sentinels in health and disease, Nature reviews. Immunology, 9 (2009) 679-691.

[50] K. Shortman, S.H. Naik, Steady-state and inflammatory dendritic-cell development, Nat Rev Immunol, 7 (2007) 19-30.

[51] E. Bakondi, M. Gonczi, E. Szabo, P. Bai, P. Pacher, P. Gergely, L. Kovacs, J. Hunyadi, C. Szabo, L. Csernoch, L. Virag, Role of intracellular calcium mobilization and cell-density-dependent signaling in oxidative-stress-induced cytotoxicity in HaCaT keratinocytes, J Invest Dermatol, 121 (2003) 88-95.

[52] T. Sun, S. Jackson, J.W. Haycock, S. MacNeil, Culture of skin cells in 3D rather than 2D improves their ability to survive exposure to cytotoxic agents, Journal of Biotechnology, 122 (2006) 372-381.

[53] D. Liu, H. Hu, Z. Lin, D. Chen, Y. Zhu, S. Hou, X. Shi, Quercetin deformable liposome: Preparation and efficacy against ultraviolet B induced skin damages in vitro and in vivo, Journal of Photochemistry and Photobiology B: Biology, 127 (2013) 8-17.

[54] M.L. Manca, I. Castangia, C. Caddeo, D. Pando, E. Escribano, D. Valenti, S. Lampis, M. Zaru, A.M. Fadda, M. Manconi, Improvement of quercetin protective effect against oxidative stress skin damages by incorporation in nanovesicles, Colloids and Surfaces B: Biointerfaces, 123 (2014) 566-574.

[55] C.-F. Lin, Y.-L. Leu, S.A. Al-Suwayeh, M.-C. Ku, T.-L. Hwang, J.-Y. Fang, Anti-inflammatory activity and percutaneous absorption of quercetin and its polymethoxylated compound and glycosides: The relationships to chemical structures, European Journal of Pharmaceutical Sciences, 47 (2012) 857-864.

[56] M. Schäfer-Korting, W. Mehnert, H.-C. Korting, Lipid nanoparticles for improved topical application of drugs for skin diseases, Advanced Drug Delivery Reviews, 59 (2007) 427-443.

[57] C. Allombert-Blaise, S. Tamiji, L. Mortier, H. Fauvel, M. Tual, E. Delaporte, F. Piette, E.M. DeLassale, P. Formstecher, P. Marchetti, R. Polakowska, Terminal differentiation of human epidermal keratinocytes involves mitochondria- and caspase-dependent cell death pathway, Cell Death Differ, 10 (2003) 850-852.

[58] J.A. Bouwstra, G.S. Gooris, M. Ponec, Skin lipid organization, composition and barrier function, International Journal of Cosmetic Science, 30 (2008) 388-388.

[59] B. Forslind, A domain mosaic model of the skin barrier, Acta Derm Venereol, 74 (1994) 1-6.

[60] P.W. Wertz, Lipids and barrier function of the skin, Acta Derm Venereol Suppl (Stockh), 208 (2000) 7-11.

[61] K.C. Madison, D.C. Swartzendruber, P.W. Wertz, D.T. Downing, Presence of intact intercellular lipid lamellae in the upper layers of the stratum corneum, J Invest Dermatol, 88 (1987) 714-718.

[62] R. Alvarez-Román, A. Naik, Y.N. Kalia, R.H. Guy, H. Fessi, Skin penetration and distribution of polymeric nanoparticles, Journal of Controlled Release, 99 (2004) 53-62.

[63] J. Lademann, H. Weigmann, C. Rickmeyer, H. Barthelmes, H. Schaefer, G. Mueller, W. Sterry, Penetration of titanium dioxide microparticles in a sunscreen formulation into the horny layer and the follicular orifice, Skin Pharmacol Appl Skin Physiol, 12 (1999) 247-256.

[64] A. Mavon, C. Miquel, O. Lejeune, B. Payre, P. Moretto, In vitro percutaneous absorption and in vivo stratum corneum distribution of an organic and a mineral sunscreen, Skin Pharmacol Physiol, 20 (2007) 10-20.

[65] B. Baroli, M.G. Ennas, F. Loffredo, M. Isola, R. Pinna, M.A. Lopez-Quintela, Penetration of metallic nanoparticles in human full-thickness skin, J Invest Dermatol, 127 (2007) 1701-1712.

[66] J. Lasch, R. Laub, W. Wohlrab, How deep do intact liposomes penetrate into human skin?, Journal of Controlled Release, 18 (1992) 55-58.

[67] S.A. Wissing, R.H. Muller, Solid lipid nanoparticles (SLN)--a novel carrier for UV blockers, Pharmazie, 56 (2001) 783-786.

General conclusion

Quercetin is a natural plant pigment belonging to the flavonoids family. Despite of its interesting antioxidant and antiinflammatory activity, quercetin is poorly water soluble. Thus, the usefulness of this molecule is hindered by very low bioavailability and weak skin penetration capacity. In this project, three approaches were developed, optimized, tested and compared for the successful delivery of quercetin to skin tissue. The three approaches were smartCrystals®, lipid nanocapsules and liposomes, which are the top trend nanometric pharmaceutical formulations. These formulations showed their ability to enhance the physicochemical properties of several poorly water soluble molecules such apigenin with smartCrystals®, amiodarone with lipid nanocapsules and paclitaxel with liposomes.

The threes approaches were characterized in terms of size, PDI, quercetin loading capacity, *in vitro* antioxidant activity of quercetin using DPPH assay and *in vitro* release profile of quercetin. Particles size were 26 nm and 54 nm with lipid nanocapsules, 203 and 298 nm with quercetin smartCrystals® and 179 nm with the liposomal formulation. All formulations presented PDI values inferior to 0.3 that indicates the homogenous profile of formulated nanoparticles. Quercetin drug loading varied among formulation with less than 1 mg/ml in liposomes to around 10 mg/ml in lipid nanocapsules and to more than 13 mg/ml with smartCrystals®. DPPH assay proved the chemical stability of formulated quercetin and the retained antioxidant activity. Finally, each formulation exhibited a distinct effect on quercetin release profile *in vitro*, where the smartCrystals® enabled a burst release kinetics compared to sustained release with lipid nanocapsules and delayed release with liposomes.

Our main scope is addressing quercetin for topical application, starting from the fact that the skin is the largest organ of the human body and the organ the most exposed to oxidative stress. Consequently, the three approaches were compared on cellular level for their safety and quercetin protective activity on HaCaT cells (keratinocytes) and THP-1 cells (monocytes). On the basis of our findings, the concentration of 5 µg/ml quercetin was selected by showing the highest safety profile with all formulations and by proving the subsequent protective effect against hydrogen peroxide induced oxidative stress. This observation was confirmed on both cell lines, thus indicating the potentials of quercetin for supporting skin in both oxidation and inflammation. Finally, two formulations were selected (quercetin smartCrystals® stabilized with TPGS and quercetin lipid nanocapsules 20) for *in vivo* skin penetration, our findings suggest the higher

superficial deposition of quercetin in smartCrystals® highlighting its potential use in UV sunscreen. On the other hand, the penetration results of quercetin lipid nanocapsules suggest that lipid nanocapsules enabled quercetin penetration to deeper skin layers. As a result, quercetin lipid nanocapsules can be q promising approach for quercetin application in inflammatory skin disorders such psoriasis.

The preparation methods of both quercetin smartCrystals® and quercetin lipid nanocapsules are designed at a lab scale that can be transformed to a pilot scale and the subsequent industrial scale. Therefore, the extrapolation of this project to industrial preparation of such formulations is feasible. Moreover, the high quercetin loading enabled by these formulations facilitates their further processing to a final derma product such as gels and emulsions. This project is a starting point for market quercetin containing product and a model for the formulation of other poorly water soluble drugs.

Perspective

This project opens the doors for several applications at three levels. The first level is the continuity of the main findings of this project, where quercetin formulations can go further in respect to topical application. Quercetin smartCrystals®, which proved the protective activity of quercetin on HaCaT cells and THP-1 *in vitro* and enabled a superficial deposition of quercetin on skin *in vivo*, goes further with UV sunscreen investigation such as sun protection factor (SPF) for sunburn protection and the persistent pigment darkening (PPD) for protection against UVA irradiation at 370 nm according to European Union (Commission Recommendation 22 September 2006).

Quercetin lipid nanocapsules, which proved the protective activity of quercetin on HaCaT cells and THP-1 *in vitro* and enabled a deeper deposition of quercetin on skin *in vivo*, can be further investigated for inflammatory skin disorders such as psoriasis using models of inflamed skin and the *in vitro* detection of proinflammatory cytokines (IL-6, IL-8, IL-10 etc..), cyclooxygenase 2 and tumor necrosis factor alpha. This formulation could also be assayed for the possibility of supportive quercetin formulation in skin cancer building on their primary results of inhibition of MMP-9 *in vitro*.

The second level is the use of formulations evidenced in this project to other route of administration for quercetin. Quercetin smartCrystals® holds great promise for oral drug delivery and may increase quercetin oral bioavailability. This opens the scope for wider applications for quercetin mainly in diabetes, hypertension and other cardiovascular disease. Likewise, quercetin lipid nanocapsules due to their possible targeting and small particle size, which enable the passage through blood brain barrier, can providing a promising approach for quercetin delivery in neurodegenerative disease such as Parkinson and Alzheimer.

This project dealt with a flavonoid that share most of solubility problems similar to other flavonoids. Consequently, the third level of this project findings is the extrapolation that can be applicable for other flavonoids such as apigenin, hesperidin, Epigallocatechin… Even other poorly water soluble drugs could be investigated, keeping in mind that more that 40 % of drug molecules in the pipeline are poorly water soluble actives.

European Journal of Pharmaceutics and Biopharmaceutics 108 (2016) 41–53

Contents lists available at ScienceDirect

European Journal of Pharmaceutics and Biopharmaceutics

journal homepage: www.elsevier.com/locate/ejpb

Review Article

Quercetin topical application, from conventional dosage forms to nanodosage forms

T. Hatahet [a], M. Morille [a], A. Hommoss [b], J.M. Devoisselle [a], R.H. Müller [b], S. Bégu [a,*]

[a] Institut Charles Gerhardt Montpellier, UMR 5253 CNRS-ENSCM-UM, Equipe Matériaux Avancés Pour La Catalyse Et La Santé, 8 Rue de L'Ecole Normale, 34296 Montpellier Cedex 5, France
[b] Institute of Pharmacy, Department of Pharmaceutics, Biopharmaceutics and NutriCosmetics, Free University of Berlin, Kelchstr. 31, Berlin 12169, Germany

ARTICLE INFO

Article history:
Received 3 May 2016
Revised 19 August 2016
Accepted in revised form 22 August 2016
Available online 24 August 2016

Keywords:
Quercetin
Antioxidant activity
Antiinflammatory activity
Wound healing
Skin antiaging
In vitro skin penetration
In vivo skin penetration
Franz cells

ABSTRACT

Skin is a multifunctional organ with activities in protection, metabolism and regulation. Skin is in a continuous exposure to oxidizing agents and inflammogens from the sun and from the contact with the environment. These agents may overload the skin auto-defense capacity. To strengthen skin defense mechanisms against oxidation and inflammation, supplementation of exogenous antioxidants is a promising strategy. Quercetin is a flavonoid with very pronounced effective antioxidant and antiinflammatory activities, and thus a candidate of first choice for such skin supplementation. Quercetin showed interesting actions in cellular and animal based models, ranging from protecting cells from UV irradiation to support skin regeneration in wound healing. However, due to its poor solubility, quercetin has limited skin penetration ability, and various formulation approaches were taken to increase its dermal penetration. In this article, the quercetin antioxidant and antiinflammatory activities in wound healing and supporting skin against aging are discussed in detail. In addition, quercetin topical formulations from conventional emulsions to novel nanoformulations in terms of skin penetration enhancement are also presented. This article gives a comprehensive review of quercetin for topical application from biological effects to pharmaceutical formulation design for the last 25 years of research.

Contents

* Corresponding author.
E-mail address: sylvie.begu@enscm.fr (S. Bégu).

http://dx.doi.org/10.1016/j.ejpb.2016.08.011
0939-6411/

Table 1
Quercetin main physicochemical parameters.

Quercetin physicochemical properties	Values
Chemical structure	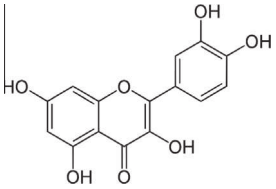
Molecular formula	$C_{15}H_{10}O_7$
Molecular weight	302.2 g/mol
Chemical name (IUPAC)	2-(3,4-dihydroxyphenyl)-3,5,7-trihydroxychromen-4-one
Solubility in MilliQ water	0.48 ± 0.1 μg/ml [16]
Solubility in PBS pH 3	0.44 ± 0.1 μg/ml [18]
Solubility in DMSO	30 mg/ml [17]
Solubility in ethanol	2 mg/ml [17]
Partition coefficient (log P)	1.82 ± 0.3 [19]
Polymorphism	Three polymorphic forms [25]

Quercetin partition coefficient is determined experimentally.

1. Introduction

Skin is the largest organ of the human body, which secures the internal homeostasis and regulates the temperature of the body. Besides that, skin has barrier function, and it prevents germs from passing into internal organs, and protects human body from exogenous pollutants and oxidizing agents such as radiation and corrosive materials. As a result, skin is continuously exposed to oxidants and inflammogens, even if skin possesses several antioxidative systems to withstand external oxidation sources. However, in case that oxidative stress is superior to the defense mechanism of skin, skin damage can occur [1,2].

Supporting skin defense mechanisms by exogenous antioxidants is a promising strategy. Antioxidants such as Coenzyme Q10 [3,4], vitamin C [5], β-carotene [6,7] and polyphenols [8,9] were tested to evaluate their benefits on skin. Among them, flavonoids, which are strong polyphenolic antioxidants, are potential good candidates. They are plant pigments found in several fruits and vegetables such as apples [10], onions [11] and peas [12]. With the presence of several hydroxyl groups on their structures, quercetin is the strongest antioxidant among flavonoids and the most common in nature [13]. At the same time, quercetin has the broadest antiinflammatory activity compared to apigenin, morin, (-)-epicatechin and biochanin A [14]. In spite of these promising activities, quercetin suffers from poor water solubility and inability to penetrate skin (Table 1) [15]. Quercetin shows water solubility less than 0.5 μg/ml and higher solubility in polar organic solvents (2 mg/ml in ethanol) [16–18]. Quercetin also has a partition coefficient of 1.82 ± 0.32 due to the presence of nonpolar groups in its structure [19]. But despite this log P, quercetin polar hydroxyl groups hinder its skin penetration capacity [13]. Focusing on topical delivery from formulation approach, the use of nanoformulations with therapeutic agents such as linoleic acid within ethosomes and transfersomes [20], paclitaxel-loaded within ethosomes [21] and asiaticoside in ultradeformable vesicles [22] showed to enhance their topical delivery. This is linked to nanoformulation characteristics such as their lipid nature and their small particle size along with their elasticity that facilitate their deep penetration. The presence of ethanol conferred higher skin penetration for encapsulated molecules compared to liposomes, and the rigid nature of liposomal bilayer is fluidized by the ethanol presence that facilities ethosomes penetration. Consequently, quercetin is also formulated within several nanoformulations in order to enhance topical drug delivery [23,24].

In this paper, recent studies on quercetin skin activities from *in vitro* models to *in vivo* animal studies will be presented. Then, formulation strategies followed to overcome quercetin limited water solubility and to increase its stability in formulation will be discussed. The effect of formulating quercetin in conventional dosage forms to enhance its skin penetration capacity will be explored. Finally, recent nanoformulations of quercetin and their potential as novel strategy for quercetin skin delivery will be discussed.

2. Quercetin physiological activities on skin

2.1. Quercetin antioxidant activity

Skin is the largest organ in the human body exposed to oxidizing agents from environment such as solar radiation (visible/UV) and chemicals (xenobiotic). These environmental pollutants can induce oxidative stress to skin tissue either directly or indirectly by the generation of reactive oxygen species (ROS). Skin tissue contains several defense mechanisms for the prevention or inception of oxidative stress and for the initiation of cellular repair afterward. Skin has many mechanisms to prevent the formation of free radicals. For example (i) metallothionein, present in cutaneous tissue, chelates metal ions, has a great importance in controlling free radical generating reactions; (ii) there was an increase in melanin production upon exposure to UV radiation. For the oxidative damage control, skin also has endogenous mechanisms based on two categories: nonenzymatic and enzymatic. Among nonenzymatic mechanisms, small molecular size antioxidants such as glutathione (GSH), α-tocopherol, carotenoids and oxycarotenoids found in skin cells, are molecules able of both neutralizing free radicals and relocalizing radical damaging functions from sensitive targets (as an example from lipid membrane to cytosol). Enzymatic activities depend on molecules such as superoxide dismutase, catalase and glutathione peroxidase. These enzymes serve as a backup for the regeneration of consumed antioxidants, like in the replenishment of GSH by glutathione disulfide (GSSG) reductase, as well as for the elimination of reactive compounds, such as the transfer system for glutathione S-conjugates [26].

Quercetin antioxidant activity will be explored in three parts. The first part will take into consideration all the chemical assays used to determine quercetin activity *in vitro*. Then, a second part will deal with quercetin activities tested at the cellular level, and the molecular mechanism underlining quercetin potentials. Finally, animal-based studies regarding quercetin protection to cutaneous tissue after its exposure to oxidative stress stimulators such as UV irradiation will be reviewed.

2.1.1. In vitro antioxidant activity (chemical tests)

In vitro tests for antioxidant activity provide information about the antioxidant activity of quercetin without the need for complex cellular based assays. They can ensure quercetin activity from batch to batch and can be set as routine analysis. Three aspects can be investigated *in vitro*. (i) Hydrogen donating activity can be measured with 2,2-diphenyl-1-picrylhydrazyl (DPPH assay) [27]. (ii) Superoxide anion formation inhibition and scavenging activity can both be quantified by means of xanthine oxidase and cytochrome C assays [28]. (iii) Metal chelating activity can be determined using metal specific methods [29]. Finally antioxidants can inhibit the peroxidation of unsaturated lipids, and thus antilipoperoxidative activity can be analyzed using the colorimetric detection of thiobarbituric acid reactive species (TBARS) by a reaction mediated by Fe^{2+}/Citrate [30]. In 2006 Casagrande et al. [31] evaluated iron-chelating activity of 4 μg/ml quercetin solution. Quercetin chelated 65% of total iron within 15 min contact

Table 2
Tests related to quercetin antioxidant activity.

Test type	*In vitro* chemical assay		*In vitro* cellular assay		*In vivo* animal assay	
	Method	Result	Method	Result	Method	Result
Antilipoperoxidative activity	Thiobarbituric acid reactive species (TBARS)	65.6% antilipoperoxidative activity [31] IC50 for quercetin 77.17 ± 9.98 g/ml [34]	N-methyl-2-phenylindole (HaCaT cells)	3-fold decrease in MDA concentration [23]	TBARS (mice)	1.6-fold decrease in MDA concentration [44]
Anti-superoxide formation	Xanthine oxidase	IC50 = 5.31 ± 0.12 g/ml [34]	N/A	N/A	N/A	N/A
Superoxide anion-scavenging activity	Cytochrome c	SC50 = 1.59 ± 0.6 g/ml [34]	Superoxide dismutase (SOD)-inhibitable reduction of ferricytochrome c (neutrophils	IC50 = 3.82 ± 0.45 μM [45]	O-phthalaldehyde fluorescent assay	3-fold increase in glutathione (mice) [42] 2.5-fold increase in glutathione (mice) [43]
					Superoxide dismutase	6-fold decrease in its concentration (rats) [46]
					Reduced glutathione	1.5-fold increase in concentration (mice) [44]
Hydrogen donating ability	DPPH	SC50 = 4.2 4 ± 0.48 g/ml [34]	Hydrogen peroxide (HaCaT)	2.5-fold increase in cell viability [38]	Catalase content	1,3-fold increase in catalase content (rats) [46]
			Buthionine sulfoximine (NHEK)	2.3-fold increase in cell viability [37]		
			UVB irradiation (HaCaT)	1.2–1.4-fold increase in cell viability [23]		

Three levels of assay can be performed to validate quercetin antioxidant activity:
(i) The *in vitro* chemical assays include thiobarbituric acid reactive species (TBARS) for antilipoperoxidative activity, xanthine oxidase for anti-superoxide formation activity, cytochrome C for superoxide anion-scavenging activity and di(phenyl)-(2,4,6-trinitrophenyl)iminoazanium (DPPH) for hydrogen donating activity.
(ii) The *in vitro* cellular assays include the detection of malondialdehyde (MDA) using n-methyl-2-phenylindole on HaCaT cells. The inhabitable reduction of ferricytochrome C by superoxide dismutase on neutrophils. Finally, the increase in cellular viability after the intoxication of keratinocytes by hydrogen peroxide.
(iii) The *in vivo* animal assays include the detection of TBARS, superoxide dismutase, glutathione, reduced glutathione and catalase content on mice or rats.

time. This is in agreement with the fact that quercetin presents two sites for chelating bivalents metals: 5-OH and 4-oxo group or between the 3′- and 4′-OH groups (Table 1) [32]. On the other hand, Casagrande et al. determined the functional stability of crude quercetin and formulated quercetin in emulsions for topical application. Antilipoperoxidative activity was tested during six months at four storage temperatures 4 °C, room temperature, 37 °C and 45 °C. Rat liver mitochondria were used as unsaturated lipid source for the lipid peroxidation assay. Initially crude quercetin presented 65.6% antilipoperoxidative activity, while 0.05% quercetin loaded within nonionic cream (high lipid content) and anionic gel cream (low lipid content) had 78%, and 70%, respectively. Upon storage, a higher loss of activity was observed in formulation with low lipid content especially at low temperatures. This may be attributed to precipitation of quercetin out from lipidic environment where lipids are in more packed conformation. Keeping in mind the lipophilic nature of quercetin rings, the more lipophilic the environment is for quercetin the better it is stabilized (Table 2). In 2007, the same group studied the antilipoperoxidative activity of quercetin in more detail [33]. The same nonionic cream and anionic gel cream formulations were compared to crude quercetin in terms of antioxidative stability during 6 months storage using DPPH test. Initial activity was 41.6%, 37.8%, and 38.5% for crude quercetin, nonionic cream and anionic gel cream, respectively. The activity was preserved during the whole storage period. Afterward skin retention of the formulated quercetin was monitored in terms of antilipoperoxidative activity on pig's skin mounted on Franz cell for 12 h. Anionic gel cream with lower lipid content showed higher drug release and consequently higher skin retention and antilipoperoxidative activity (25.0%) at 3 h interval. On the other hand nonionic cream with higher lipid content, showed a gradual release and with slight accumulation in skin and presented highest antilipoperoxidative activity (54.0%) after 12 h. This is in agreement with their previous report, that higher lipid content confers higher protection for quercetin activity, this time proven *in vitro* on pig's skin.

Wu et al. in 2008 [34] prepared quercetin in polymeric nanoparticles (Table 4). Quercetin was added to polyvinyl alcohol (PVA) and Eudragit® E at a ratio of 1:10:10 respectively. The nanoparticles, prepared by nanoprecipitation, presented a mean diameter of 82 nm with a polydispersity index (PDI) of 0.22; PDI shows how broad the particles size distribution is. Quercetin encapsulation efficiency was 99.9%. Quercetin nanoparticles were compared to quercetin-DMSO and quercetin-water in terms of DPPH activity, anti-superoxide formation, superoxide anion-scavenging activity and antilipoperoxidative activity. In all tests, quercetin nanoparticles showed scavenging concentration (SC50) and inhibitory concentration (IC50) (the concentration to cause 50% effect with respect to each test) close to quercetin-DMSO proving the preservation of quercetin activity after formulation (Table 2). Quercetin-water was hundred times less effective than quercetin nanoparticles and quercetin-DMSO. This may be explained by the fact that all the tests request the antioxidant molecules to be soluble in the reaction medium, and as a result suspended quercetin in water will be very weak compared to solubilized quercetin in DMSO or to nanoparticles. The second potential explanation may be due to the influence of the surface area of reacting quercetin, which is greater in the nanoparticles than in the larger suspended crude format. This confers higher reactivity for the nanoparticles compared to quercetin-water. Finally, the small

Table 3
Test performed for the determination of quercetin antiinflammatory activity.

	Method	Result
Edema	Ear thickness (mice) topical route Cotton oil Arachidonic acid	Control 0.25 mm, quercetin 0.19 mm Control 0.25 mm, quercetin 0.12 mm [14]
	Back skin weight (mice) 12-otetradecanoylphorbol 13-acetate	1.7-fold decrease in edema weight [58]
Elastase release	Degranulation of azurophilic granules in (neutrophils	IC50 = 6.25 ± 2.58 μM [45]
Myeloperoxidase release	Degranulation of azurophilic granules in (neutrophils) TPA-induced inflammation on mice back skin	3-fold decrease concentration [42] 4.7-fold decrease concentration [58]
Proinflammatory cytokines	Primary human keratinocytes were exposed to UV (0.05 J/cm^2)	
	Il-1β mRNA	2.5-fold decrease in release
	IL-6 mRNA	5-fold decrease in release
	IL-8 mRNA	3-fold decrease in release
	TNF-α mRNA	2-fold decrease in release
	NF-κB activation	80% inhibition of binding with DNA [54]

Edema was tested by either the thickness of mice ear or the weight of mice back skin. Elastase and myeloperoxidase release was determined by the degranulation of azurophilic granules in neutrophils. Western blot was used for the determination of proinflammatory cytokines and quantified using a chemifluorescent substrate.

size of formulated nanoparticles below 100 nm (82 nm) enabled to retain the activity of quercetin to values close to the solubilized form in DMSO.

2.1.2. In vitro antioxidant activity of quercetin (cellular evaluation)

Antioxidant actions are not limited to ROS scavenging abilities but also include the modulation of endogenous (antioxidant, detoxifying) enzymes. The evaluation of antioxidants at cellular level can be done by two different approaches. The first approach is a cellular antioxidant activity assay (CAA) used to evaluate the antioxidant activity of plant extracts and food supplements. It is based on the detection of ROS (such as hydrogen peroxide) inside the cell by reaction of these reactive species with the redox sensor dihydrodichlorofluorescein ($DCFH_2$). In this reaction, $DCFH_2$ oxidizes to fluorescent dichlorofluorescein (DCF). However, this method lacks the specificity to ROS generated in response to oxidative attacks [35]. The second approach is the evaluation of endogenous enzymes, like the upregulation of the expression of antioxidants enzymes, or the inhibition of prooxidant enzymes. As our main scope is quercetin and its skin penetration in formulation, we keep the more detailed review articles to give further information about antioxidants cellular tests for example in the publication by López-Alarcón et al. [36].

All biological investigations on formulated quercetin started from the concept that to test an antioxidative activity, a source of oxidation is required. As quercetin activity is of high interest in skin diseases related to phototoxicity, researchers tested quercetin activity to compensate for UV irradiation damage.

Quercetin cellular actions were evaluated as crude material on human fibroblasts and kératinocytes (NHEK) [37] and in formulations on normal human keratinocytes (HaCaT) [23,38]. The treatment with 50 μM of crude quercetin protected human keratinocytes and human fibroblast from intoxication by 500 μM buthionine sulfoximine. Keratinocytes viability increased by 2.3-fold (Table 2). However, this cytoprotective activity was not related to an increase in the intracellular glutathione (GSH), as quercetin was not able to reestablish the depleted GSH due to cellular intoxication [37]. Quercetin was formulated into liposomes by Liu et al. [23] and Manca et al. [38] with different excipients. Liu et al. [23] suggested formulation of quercetin deformable liposomes with Tween® 80 as edge activator (Table 4). Cells were irradiated with a UVB dose of 0.02 J/cm^2 and treated with 25 μg/ml quercetin liposomes 16 h before irradiation and 24 h or 48 h post irradiation. Then, cell viability was determined by MTT assay. UVB exposed cells without quercetin treatment decreased in viability from 65.7 ± 7.8% at 24 h to 42.5 ± 6.5% at 48 h. On the other hand quercetin in both control solution and liposomal formulation was capable of cells protection. Cell viability was 76.2 ± 4.3% at 24 h and 59.5 ± 3.8% at 48 h for quercetin in solution and 89.9 ± 4.5% at 24 h and 78.8 ± 3.2% at 48 h for liposomal quercetin (Table 2). Furthermore, Liu et al. proved that quercetin was able to attenuate ROS generation in cells exposed to UVB and showed the antilipoperoxidative activity of quercetin on cells. Quercetin also decreased the concentration of malondialdehyde from 10.98 nmol/mg protein in non-treated UVB exposed cells to 3.14 nmol/mg for treated UVB exposed cells (Table 2) [23]. Manca et al. [38] tested another quercetin liposomal formulation and compared it to glycerosomes (glycerol containing liposomes) (Table 4) on HaCaT cells with hydrogen peroxide. Quercetin liposomes and glycerosomes were also able to protect keratinocytes in culture from the damaging effect of hydrogen peroxide. Consequently, viable cells increased from 26.0 ± 9.0% in non-treated H_2O_2 exposed cells to 68.0 ± 4.0% and 67.0 ± 6.0% in the liposomes and glycerosomes group (Table 2). This result was explained by a better cellular uptake with both nanoformulations compared to crude quercetin. The enhanced cellular internalization with liposome may be due to the fusion with plasma membrane or pinocytosis [39]. The pinocytosis of liposomal formulation with the cell membrane enables the release of liposomes contents directly into the cytoplasm avoiding the potential passage by the lysosomal apparatus. In case of liposomal destabilization during the cell membrane fusion [40], the released drug can pass by micropinocytosis.

2.1.3. In vivo antioxidant activity assays of quercetin in animals

Referring back to cellular assays (Section 2.1.2), the concept of having a source of oxidation is presumed. Hairless mice were exposed to UV irradiation, and then skin health parameters such as Transepidermal water loss (TEWL) and erythema were assessed upon exposure to UV. For further details, Hung et al. defined the damaging effect of UV irradiation on mice stratum corneum [41].

Skin histological analysis was then performed and quercetin protective effect on skin was determined. Quercetin activity was demonstrated by quantification of endogenous antioxidant enzymes before and after exposure and without or with quercetin treatment. Two publications investigated the protective effect of quercetin *in vivo* on mice's skin [42,43]. Both applied UVB to dorsal skin of hairless mice from 20 cm above the table where mice were placed. Quercetin was formulated in emulsions in both publications and applied three times: 60 min and 5 min before irradiation and directly after irradiation.

In 2006, Casagrande et al. [42] compared quercetin nonionic emulsion (formulation 1 = high lipid content) and quercetin anionic emulsion (formulation 2 = low lipid content). In this study, reduced glutathione GSH (nmol) per mg of skin homogenate was detected after a dose of 2.46 J/cm^2 by fluorescence assay using o-phthalaldehyde. Quercetin containing formulations were applied topically at a dose of 5 mg. Quercetin showed higher activity in

Table 4
Formulated quercetin nanodosage forms for topical application.

Formulations	Preparation technique	Excipients	Particles size (nm)	PDI	Surface charge (mV)	Quercetin encapsulation efficiency %	Quercetin practical concentration (mg) per ml of formulation
Quercetin deformable liposomes [23]	Ethanol Injection method	Lecithin Cholesterol Tween 80	132 ± 14	N/A	21.1 ± 0.8	80.4 ± 4.22	N/A
Quercetin polymeric nanoparticles [34]	Nanoprecipitation technique	Polyvinyl alcohol (PVA) Eudragit® E	82 ± 0	0.22 ± 0.01	N/A	99.9 ± 0.59	4.995 ± 0.003 mg/mg powder
Quercetin loaded Liposomes and glycerosomes [38]	Thin film hydration method	Lecithin Glycerol	102 ± 3 80 ± 3	0.32 0.26	−78.0 ± 2.0 −67.0 ± 3.0	88.0 ± 3.00 81.0 ± 1.00	4.4 ± 0.15 4.1 ± 0.05
Quercetin in liposomes and PEVs (Penetration Enhancer-containing Vesicles) [58]	Thin film hydration method	Soybean lecithin with 70% phosphatidylcholine PEG 5% or 10%	116 ± 5 152 ± 3 148 ± 4	0.35 0.34 0.31	−9.0 ± 0.4 −10.0 ± 0.8 −10.0 ± 0.7	52.0 ± 4.40 75.0 ± 3.00 60.0 ± 0.80	5.2 ± 0.44 7.5 ± 0.30 6.0 ± 0.08
Quercetin nanoemulsion [74]	Spontaneous emulsification	Lecithin Octyldodecanol and cetyltrimethylammonium bromide	307 ± 19 188 ± 2	N/A	−27.4 ± 6.0 76.3 ± 2.1	99.5 ± 0,30 99.1 ± 0,60	1.00 ± 0.00 0.99 ± 0.01
Quercetin loaded penetration enhancer vesicles PEV [75]	Thin film hydration method	Lecithin and Transcutol® P or Labrasol® or Propylene glycol or PEG 400	226 ± 5 86 ± 5 83 ± 10 190 ± 4	0.28 0.29 0.35 0.31	–49.0 ± 5.0 –32.0 ± 3.0 –63.0 ± 4.0 –58.0 ± 2.0	59.0 ± 8.00 75.0 ± 9.00 57.0 ± 8.00 48.0 ± 7.00	1.18 ± 0.16 1.50 ± 0.18 1.14 ± 0.16 0.96 ± 0.14
Quercetin lipid nanoparticles [76]	Hot and cold high pressure homogenization	Tristearin Lecithin	527	0.58	N/A	46.5	N/A
Quercetin nanostructured lipid carrier (NLC) [77]	Probe ultrasonication	Compritol 888 Oleic acid	282 ± 3	0.31	−37.0 ± 3.0	0.025% drug loading	0.25 mg/ml
Quercetin aminopropyl functionalized mesoporous silica nanoparticles (NH2-MSN) [79]	Sol-gel method	N-cetyl-trimethylammonium bromide Tetraethyl orthosilicate	250 ± 50	N/A	+13.6 ± 0.2	8% mentioned as drug loading %	N/A
Quercetin-loaded lecithin-chitosan nanoparticles [24]	Ethanol Injection method	Lecithin Chitosan TPGS	95	0.44	10.9 ± 0.1	48.5	0.63 mg/ml

Comparative table of different nanoformulations with quercetin prepared for topical delivery. The comparison includes the type of nanoformulation, the preparation method, the used excipients and the physicochemical properties of each nanoformulation including the particle size, surface charge, quercetin encapsulation efficiency and quercetin concentration in mg per ml of formulation.

emulsion containing higher lipid content (formulation 1) than in anionic emulsion (formulation 2). Both formulations inhibited the UVB irradiation-induced depletion of GSH (50 nmol/mg skin in the UV group vs 140 nmol/mg formulation 1 and 60 nmol/mg formulation 2). However, only in the formulation 1 treated group the GSH activity returned to non-irradiated control levels (125 nmol/mg). Myeloperoxidase (MPO) activity in irradiated skin can be related to the presence of immune cells (neutrophils) and hence can be a good marker for skin inflammation. Hairless mice were exposed to a dose of 1.23 J/cm^2 and then the number of total leukocytes per mg of skin was determined. Again, both formulations inhibited the MPO activity increase and hence the neutrophil migration. However, only formulation 1 was able to reestablish control levels (Table 3). Lastly, qualitative analyses of skin proteinases by substrate-embedded enzymography showed that formulations containing quercetin were capable of inhibition of secretion/activity of proteinase in skin tissue. The results observed by Casagrande et al. were further supported by the work of Vicentini et al. in 2008 [43]. 3 mg of quercetin was applied topically on the dorsal skin from a water in oil (w/o) microemulsion and 2.87 J/cm^2 UVB dose was used for GSH depletion. Quercetin-loaded w/o microemulsion maintained GSH levels near to the ones in untreated–unexposed controls (90 nmol/mg vs. 100 nmol/mg control) (Table 2). Determination of skin proteinases by SDS–PAGE enzymography showed that quercetin-loaded w/o microemulsion regenerated the inhibition of proteinase secretion/activity increase induced by UVB irradiation. However, quercetin-loaded w/o microemulsion failed to confer protection against UV-induced skin reddening *in vivo*. These *in vivo* studies proved that is promising to apply quercetin topically to skin for antioxidative protective effects. Nonetheless, skin penetration and permeation should be carefully controlled to gain sufficient quercetin protective actions on skin tissue and to avoid its side effects in the systemic circulation.

2.2. Quercetin antiinflammatory activity

Inflammation is a protective response to localized injury. It can be due to physical causes such as trauma, chemical by a corrosive substance, and/or biological like stress. Inflammatory response may be also an effect of an autoimmune diseases such as psoriasis [47]. As evocated in the last section, inflammation is closely linked to oxidation and hence to UV irradiation. UV exposure causes the initiation and propagation of reactive oxygen species and hence induces oxidative stress damage. Oxidative stress activates several inflammatory associated signal transduction pathways in cells [48]. Among these pathways is nuclear factor-kappa B (NF-κB) [49], known for its ambiguous role in cytokine production and modulation of immune response [50]. Here comes the advantage of using quercetin as inhibitor on this pathway. Quercetin proved to inhibit (i) the recruitment of NF-κB transcription factor to proinflammatory gene promoters by tumor necrosis factor (TNF), and (ii) hydrogen peroxide (H_2O_2)-induced NF-κB DNA binding activity and consequently DNA damage [51,52]. Quercetin inhibitory

activity of NF-κB was detected on human hepatoma cells [53] and more recently on primary human keratinocytes [54].

Quercetin antiinflammatory activity was compared to several flavonoids, such as apigenin, morin, (-)-epicatechin and biochanin A and to a non-steroidal antiinflammatory drug (indomethacin). Indeed quercetin was the strongest antiinflammatory flavonoid against mice ear edema [14]. Quercetin was administered orally at a dose of 2 mg/mouse dissolved in 0.5% Tween® 80 one hour before the topical application of the inflammogens (2% cotton oil or 2% arachidonic acid) on the ear. For testing a possible activity via topical route 25 μl of 2 mg quercetin dissolved in acetone was applied to ear's skin and 30 min later, and the same inflammogens were applied. After five hours, ear thickness was measured (inhibition percent of ear's edema was calculated) and compared to the control group treated with vehicle and inflammogens only. For the oral route, control groups ear thicknesses were 0.22 and 0.27 mm with cotton oil and arachidonic acid, respectively, and 0.14 and 0.13 mm with indomethacin treatment. Quercetin was the flavonoid with highest ear edema inhibition capacity with 0.16 and 0.21 mm. The same was observed with topical administration of flavonoids. Quercetin diminished edema thickness from 0.25 mm with both inflammogens to 0.19 and 0.12 mm compared to indomethacin 0.14 and 0.05 mm with cotton oil and arachidonic acid, respectively. The skin penetration of crude quercetin here may be attributed to the destruction of barrier function with solvent (acetone). Quercetin proved to possess broad antiinflammatory activities [14]. Knowing that quercetin presents the lowest skin permeability compared to its polymethoxylated compounds and glycosides, it is the most powerful inhibitor of O_2 generation (by neutrophils) *in vitro* with an IC50 of 3.82 ± 0.45 μM compared to 5.34 ± 0.28 μM for rutin and 5.80 ± 0.67 μM for quercetin 3,5,7,30,40-pentamethylether (QM) (Table 2). This high antiinflammatory capacity was further confirmed by testing elastase release due to degranulation of azurophilic granules from neutrophils. Quercetin was five times more powerful than its glycoside (rutin) (Table 3). Even though rutin presented 2.5-fold increase in flux through nude mouse skin mounted on Franz cell, rutin showed a degree of skin irritation with higher erythema values over the control group [55].

Vicentini et al. investigated the mechanism underling quercetin antiinflammatory actions in 2011 [54]. Quercetin showed 80% inhibition of interleukin 1β mRNA (IL-1β mRNA) at a dose of 20 μg/ml in methanol when primary human keratinocytes were exposed to UVB (0.05 J/cm^2). Quercetin pretreatment also suppressed induction of IL-6, IL-8, and TNF-α in exposed cells measured by real-time quantitative RT-PCR. Furthermore, quercetin pretreatment inhibited UV irradiation-induced NF-kB DNA binding activity by approximately 80% (Table 3). This result presents the applicability of quercetin in protection against solar irradiation and the benefit effects of introducing it in novel sunscreens. However, quercetin also inhibited IL-1β activation of NF-kB and induction of cytokine expression. This indicates that quercetin inhibition of cytokine induction is not UV irradiation specific. Therefore, these results highlight other applicability of quercetin in other skin disease like psoriasis [54,56,57]. It is worth to note that quercetin activity on the inhibition of NF-kB is cell and stimulation specific for example quercetin did not inhibit TNF-α-induced NF-kB transcriptional activity on murine small intestinal epithelial cell (IEC) line Mode-K [51].

In 2014, Caddeo et al. formulated quercetin in liposomes and Penetration Enhancer-containing Vesicles (PEVs) (Table 4). Then, they tested quercetin antiinflammatory activity *in vivo* on the back skin of female mice. The inhibitory effect of vesicular quercetin on 12-ortho tetradecanoylphorbol 13-acetate (TPA)-induced inflammation was evaluated by two biomarkers: edema formation and myeloperoxidase (MPO) activity. Liposomes and PEVs were prepared by thin film hydration method and size homogenization was performed by sonication. In both formulations, soybean lecithin with 70% phosphatidylcholine (Lipoid® S75) was used as lipid phase. PEVs used either 5 or 10% PEG 400 in the aqueous phase (PEVs are liposomal formulation where PEG is added to PBS to boost skin penetration capacity of the formulation). Liposomes size was 116 ± 5.3 nm and PEVs 5% and 10% presented a size of 152 ± 2.4 nm and 148 ± 3.5 nm respectively. PDI results were ⩽0.35 with surface charge (−10 mV), due to the low charge carried by S75. Higher entrapment efficiency was achieved by PEVs than liposomes (52 ± 4.4% for liposomes vs. 75 ± 3.0% and 60 ± 0.8% for 5% PEG-PEVs and 10% PEG-PEVs respectively) (Table 4). Quercetin loaded liposomes reduced edema formation from 11.5 mg/g (biopsy/bodyweight) in TPA control group to 7 mg/g. Both quercetin loaded PEVs reduced biopsy weight to 6.2 mg/g (Table 3). MPO reduction was also validated for both liposomal formulation and PEVs. TPA positive control group increased MPO in the skin from 50 ng/ml supernatant in the negative control to 620 ng/ml. Quercetin liposomes reduced MPO concentration to 210 ng/ml and quercetin loaded PEVs to 110 ng/ml and 250 ng/ml for 5% and 10% PEG-PEVs, respectively (Table 3). Interestingly, in 2013, the same author tested diclofenac loaded 5% PEG-PEVs under the same conditions. This study provided evidence that topically applied quercetin, when delivered by 5% PEG-PEVs, was more effective than diclofenac at the same dose (10 mg/ml). Indeed, a 4.7-fold decrease was achieved by quercetin versus 2.7-fold with diclofenac [58,59].

2.3. Quercetin in wound healing

Potent antioxidant and free radical scavenger activities of quercetin along with its strong antiinflammatory activity highlighted the possible application of this flavonoid for wound healing. Wound healing is a complex physiological compensating mechanism [60]. The applicability of quercetin during wound healing is beneficial for suppressing the uncontrolled inflammation. Inflammation hinders the successful skin regeneration process and may transform an acute wound to a chronic one.

Quercetin ability to support the healing process was investigated in 2003 by Gomathi et al. *in vivo* on male albino Wistar rats. Quercetin was introduced to collagen films at a concentration of 1 mM. Wounds were generated by a mean of a scalp at day 0. Rats were separated in three groups: (i) control group, (ii) application of collagen films or and (iii) application of quercetin incorporated collagen films in the rat skin at the wound place. Wound contraction, hydroxyproline, uronic acid, total protein, superoxide dismutase and catalase were tested on the granulation tissue. Quercetin incorporated collagen films showed a significant wound contraction (80% reduction in wound surface) compared to collagen alone treated group (60%) and control group (57%). Quercetin incorporated with collagen increased hydroxproline concentration in the granulation tissue from 0.78 in the control group to 1.84 mg/mg tissue, which indicates that there was an enhanced production of collagen in the granulation tissue. Subsequent to collagen production, a decrease in hyaluronic acid is observed explaining the reduction of uronic acid content in quercetin treated groups. Considering superoxide dismutase, a 6-fold decrease in its concentration was observed with quercetin treated group, which might be related to quercetin antioxidant activity rather its antiinflammatory one. As free radicals are inducers of gene expression of superoxide dismutase, a more efficient free radical scavenging ability with the presence of quercetin resulted in the reduction of superoxide dismutase concentration in the granulation tissue. Quercetin converts the superoxide radical to hydrogen peroxide and hydrogen peroxide stimulates catalase release. This could be linked to an increase in catalase content from 1.91 in the control group to 2.55 unit/g tissue in quercetin treated rats [46]. In summary,

quercetin activity in wound healing is a matter of both its antioxidant and antiinflammatory actions. In contrast to skin protection against UV, fibroblasts are the main target for quercetin wound dressings to support the healing process.

2.4. Quercetin and skin aging

Retardation of skin aging and wrinkling is of major interest in cosmeceuticals. Skin aging is a complex process that involves both intrinsic (physiological changes on time) and extrinsic factors (photoaging, lifestyle, pollution). However the target of all antiaging products scopes on the extrinsic controllable ones. Skin aging is manifested by several physiological changes, for example defective barrier function, collagen atrophy, loss of skin elasticity, especially in the face. In addition, a generalized reduction in the vasculature of the dermis is observed, a factor more pronounced factor in smokers. Vitamin D production is also reduced in elderly people [61–63]. All these changes cooperate to induce skin aging and wrinkling.

Quercetin is useful in reducing photoaging because of its antioxidant activity. Quercetin protection against UV light and its application in sunscreen are discussed in detail in the quercetin antioxidant activity section (Section 2.1). It is also worth to note that quercetin antiinflammatory activity may also contribute to fighting skin aging. Skin elasticity is directly related to skin hydration state [64], which is linked to proper lipid biosynthesis and configuration. Quercetin as a lipid peroxidation inhibitor can protect skin from dehydration [65]. Quercetin inhibition of matrix metalloproteinase activity may also show a role in protection of skin collagen from destruction during inflammatory response to extrinsic aging factors [66,67]. In an *in vivo* study, Joshan et al. [44] tested quercetin protective activity against photoaging on female albino mice. Mice dorsal skin was exposed to an UV dose of 0.036–0.216 J/cm^2 over 12 weeks period, and then skin aging markers such as skin moisture, collagen content, thiobarbituric acid reacting substances (TBARS) and reduced glutathione were evaluated. Skin wrinkles and blood vessels were visually scaled and epidermal thickness was determined after the 12 weeks. 1% Quercetin was applied topically in mixture of ethanol, propylene glycol and water (0.5:1:1 (v/v/v). This application increased skin moisture content (43.0 ± 1.2%) compared to the UV exposed group (28.2 ± 0.9%) and reduced TBARS from 20 nM/mg (animal tissue) in the UV exposed group to 12.5 nM/mg in the quercetin group. Moreover, the concentration of reduced glutathione increased by 1.5-fold in quercetin treated group compared to UV exposed group (Table 2). The higher concentration of the reduced form indicates that quercetin was able to neutralize free radicals and to protect cellular antioxidants such as glutathione from depletion. As a last consequence after progressive UV exposure, skin wrinkles and superficial blood vessels appear, and epidermal thickness is also increased in photosensitivity [68]. Quercetin reduced wrinkles number and depth from several deep wrinkles overall the dorsal region of the UV exposed group to few shallow wrinkles along the back. Regarding epidermal thickness, the quercetin treated group was more similar to negative control group.

In another study, quercetin was studied on HFL-1 human embryonic fibroblasts and mouse melanocytes (B16F10 cell line) for its antiaging and rejuvenating actions. Chondrogianni et al. [69] treated young HFL-1 with 2 μg/ml quercetin in DMSO daily until senescence. β-galactosidase activity was regarded as a marker for senescence [70]. Cells treated with quercetin exhibited a lower percentage of β-galactosidase positive staining (13.7% for quercetin treated vs. 77% for DMSO group). On the other hand, quercetin-rejuvenating activity was tested on middle aged and terminally senescent HFL-1 cells. Quercetin (2 μg/ml) was added to middle aged cells for 5 days after senescence and 2 weeks for terminally senescent cells, and then proliferating cells were counted. Interestingly, quercetin increased the number of proliferating cells by 1.3-fold compared to DMSO group for both middle-aged cells and terminally senescent counterparts. After that, quercetin ability to protect HFL-1 from reactive oxygen species ROS was investigated. Cells were treated with 2 μg/ml quercetin and subjected to 300 μM H_2O_2 intoxication for 2.5 h and then a recovery period of 5 days was set. Viable cells were counted at the end of the experiment and the ROS was determined by 2′,7′-dichlorodihydrofluores cein diacetate H_2DCF-DA. Quercetin had no significant effect on cell survival number while showed a 40% decrease in ROS compared to the DMSO group. The mechanism underlying quercetin protective activity on HFL-1 was investigated. For this, proteasome that is the main secondary antioxidant system of the cell was studied. Young HFL-1 cells were treated with 2 μg/ml quercetin for 24 h and the CT-L proteasome (chymotrypsin-like proteasome) activity was measured. Quercetin increased both proteasome activity by 2.4-fold and enhanced protein expression levels of representative proteasome subunits.

Finally photoaging and exposure to UV light can induce skin pigmentation by anticipating several cellular pathways. For example, thymine dinucleotides enhance pigmentation of melanocytic cells and stimulate tyrosinase mRNA levels [71]. Tyrosinase is a copper-containing glycoprotein that catalyzes several steps in the melanin pigment biosynthesis and is mainly responsible for the age spots. Tyrosinase is regulated by proteasome activity as it is shown that tyrosinase is a proteasome substrate, and proteasome is responsible of the degradation of mutant or structurally aberrant tyrosinase [72]. Mouse melanocytes (B16F10 cell line) were treated with 5 μg/ml quercetin for 3 days, and afterward tyrosinase was extracted from cells and quantified along with proteasome activity. Quercetin was able to increase the proteasome activity by 1.5-fold and reduce tyrosinase by 30% compared to control cells [69]. These findings propose quercetin as a perfect candidate for a novel rejuvenating product. Quercetin is not only an antioxidant and skin cells protectant, but also presents interesting antiaging properties with whitening activities.

Quercetin presented potent antioxidant activity on three levels: *in vitro* chemical assays proved the increase in quercetin activity after its efficient formulation, on cellular level as quercetin showed cell protective actions on keratinocytes and *in vivo* on animal's skin. These antioxidative effects are also supported by the ability of quercetin to exert antiinflammatory actions such as inhibition of NF-κB and IL-6 induction by UV irradiation. The mixture between both antioxidant and antiinflammatory actions and their crosslinking mechanisms highlighted quercetin as a novel sunscreen. Furthermore, as quercetin possesses both antioxidant and antiinflammatory activities, it could be beneficial on wound healing, here; fibroblasts are the main targets in contrast to keratinocytes in sunscreen. In addition, quercetin showed promising rejuvenating actions on keratinocytes with supportive whitening effect. This makes quercetin highly suitable as a novel natural molecule for such actions.

Quercetin activities on cellular level that were proven for skin related disorders are presented in Fig. 1.

However, all these desired benefits necessitate quercetin topical application, and this application should be thoroughly studied according to the desired activity (Fig. 2). Ideally, quercetin should penetrate skin without reaching systemic circulation in case of cosmetic application for a possible sunscreen or anti-aging cream. At the same time, a satisfactory skin penetration to both stratum spinosum and stratum basale should be planned for quercetin to protect viable keratinocytes from UVA light, or to support in inflammatory skin disorders such as psoriasis. However, if the goal is to prolong fibroblasts survival and proliferation in burned skin and enhance the process of wound healing, a deeper penetration

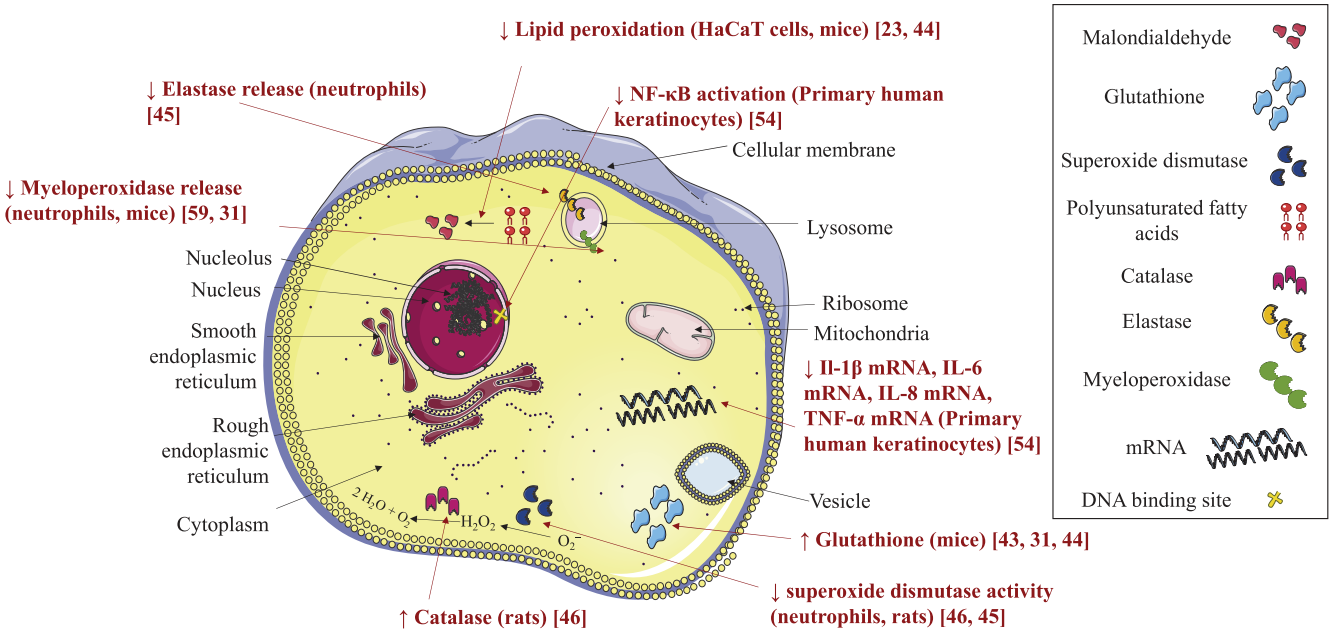

Fig. 1. Quercetin activities on cellular level. Quercetin decreased the release of myeloperoxidase and elastase, and also decreased the activity of superoxide dismutase on neutrophils. Quercetin decreased the lipid peroxidation on HaCaT cell line. Quercetin decreased the activation of NF-κB and inhibited the mRNA of IL-1β, IL-6, IL-8 and TNF-α on primary human keratinocytes.

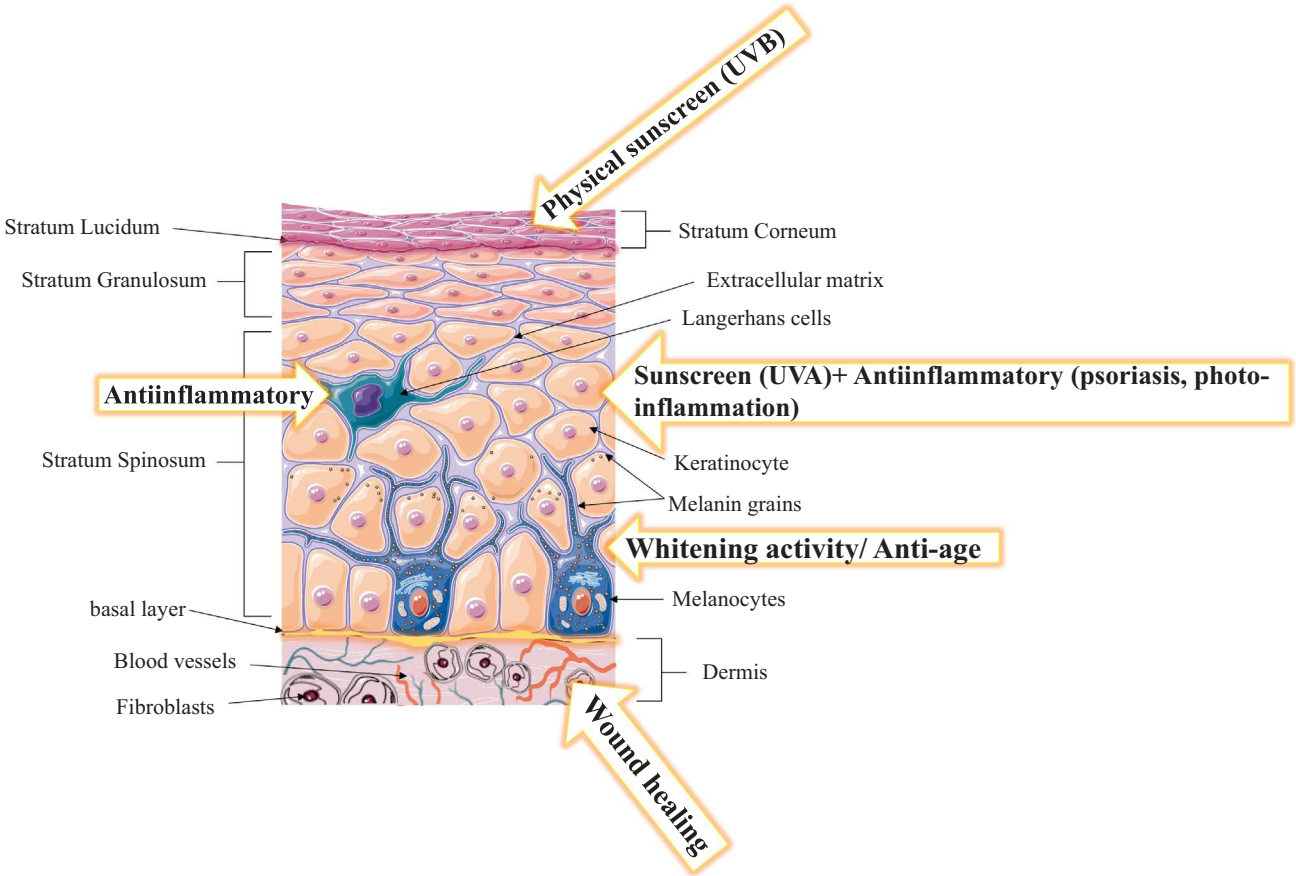

Fig. 2. Quercetin properties in function of site of action in different skin layers. Quercetin possesses a physical protection against UVB over stratum corneum. Within epidermis, quercetin shows a protective effect against UVA irradiation and in several inflammatory disorders like psoriasis. By targeting melanocytes, quercetin shows whitening and anti-aging effects by targeting fibroblasts. Finally, quercetin can support wound healing process in case of sufficient penetration into dermis.

is required, and this point is critical. The targeted fibroblasts are beyond the basement membrane, and then it is challenging to deliver the finite dose of quercetin to these cells without reaching systemic circulation i.e. avoiding the adverse effects by minimizing systemic uptake.

In order to transport quercetin, that is naturally of limited via topical route, to the desired site of action, a suitable delivery system is essential. Conventional dosage forms such as creams, emulsions and gels are the first way to formulate quercetin and to modulate its skin penetration profile. On the other hand, nanodosage forms are promising second way to formulate quercetin at the nanoscale range in order to enhance its dermal activity.

3. Conventional dosage to increase quercetin skin penetration

Conventional dosage forms for dermal application are either aqueous like gels, or oleic like hydrophobic ointments, or a mixture of both like creams and emulsions. The choice of the external phase of the formulation has a major effect on the drug release. Indeed aqueous gels are known to boost fast release, in contrast to oleic formulation that provides a reservoir for a prolonged release kinetics. Quercetin by itself has very limited skin penetration capacity. It is limited by both water insolubility and the lipophilic partition coefficient ($\log P = 1.82 \pm 0.32$) due to the nonpolar groups in its structure [73]. For this end, quercetin dermal delivery is very much dependent on the dosage form. The poor water solubility requires the presence of a lipid phase in order to enhance quercetin solubility in the formulation, On the other hand, quercetin polar heads favor water presence, so quercetin can localize at the interface. Furthermore, water-containing formulations are easier to apply, more friendly to the skin and preferred by patients over viscous lipid formulations and fluid watery ones. For these reasons, quercetin was formulated in emulsions.

Casagrande et al. in 2007 [33] formulated quercetin in two emulsions differing in their lipid content. The emulsion with high lipid content (formulation 1) contained 10% of self-emulsifying wax (Polawax®:cetostearyl alcohol and polyoxyethylene derived from a fatty acid ester of sorbitan 20E) and the emulsion with low lipid content contained 2% of Polawax® (formulation 2). Both emulsions contained the anionic hydrophilic colloid 0.18% (carboxypolymethylene, Carbopol® 940) as a stabilizer and triethanolamine 0.20% as neutralized. Macadamia nut oil 2.50% and squalene 1.00% were used emollients, and propylene glycol 6.00% as moisturizer and solubilizer. A mixture of phenoxyethanol and parabens 0.40% (Phenova®) was used as preservatives. High lipid content emulsion was superior in delivering quercetin to the skin, proven by higher quercetin antilipoperoxidative activity over the emulsion with low lipid content. However, the exact quantity of penetrated quercetin and its exact deposition within the skin were not determined.

In 2008, Vicentini et al. [43] prepared quercetin in w/o microemulsion. 0.3% of quercetin was dissolved in 38.25% of canola oil, 47.75% of Span® 80/Tween® 80 (3:1) and 15% water/propylene glycol mixture (3:1). The microemulsion formed spontaneously after vortexing. *In vitro* skin penetration study was performed on pig ear skin using Franz diffusion cell. In parallel, an *in vivo* penetration study was conducted using HRS/J mice. 100 mg of microemulsion (300 μg quercetin) was applied to 1.77 cm^2 Franz cell mounted with pig ear skin. 150 mM phosphate buffer (pH 7.2) containing Tween® 20 (0.5%) was selected as receptor medium. At the end of the study, the skin was stripped 15 times. The first strip was discarded and the rest was collected and considered as stratum corneum (SC), while the remaining skin portion was epidermis (E) and dermis (D). Quercetin microemulsion was compared to quercetin propylene glycol solution of same concentration. About 11% of the applied dose was detected in the SC and 5% in the E + D after 12 h of application. On contrary, quercetin from the control formulation was ~2 and 20 times lower than the microemulsion in the SC and E + D, respectively. No transdermal penetration was detected in the tested time. The *in vivo* study on mice was run for 6 h applying the same amount of formulation to about 2 cm^2 dorsal skin. Similarly, the microemulsion delivered about ~14% of the applied dose to the SC and ~8% to E + D, which was 1.5 and 2-fold greater than the delivered quercetin by the control formulation.

Conventional emulsions are a good strategy to improve the delivery of drugs to skin. Further studies are needed to explore more formulations with other lipids that possess better affinity to quercetin. However, quercetin may require a more advanced delivery system that ensures a high loading capacity of this drug and confers greater skin adhesiveness in order to prolong drug/skin contact time.

4. Nanodosage forms to increase quercetin skin penetration

The main objective of formulating quercetin in nanodosage forms was to overcome its topical limit penetration ability related to its poor water solubility and to increase its stability. Quercetin was formulated in several nanodosage forms for example nanoemulsions [74], liposomes [75], lipid nanoparticles [76] nanostructured lipid carriers NLC, solid lipid nanoparticles SLN [77,78] and mesoporous silica [79]. Quercetin showed no transdermal delivery with novel dosage forms such as lipid nanoparticles [76], nanostructured lipid carriers [78], aminopropyl functionalized mesoporous silica nanoparticles [79] and glycerosomes [38]. This phenomenon may be explained by quercetin poor water solubility [13,80] and selective lipophilicity to certain lipids [81] despite the barrier function of the stratum corneum (Table 4).

Extrapolation and comparison of skin penetration results are very difficult especially when skin from different sources is used for the tests. Besides this, the use of different methods of quantification of drug, different receptor mediums and variant durations of test make comparison difficult [82]. For this, skin penetration experiments will be divided into three groups. The first group will discuss about studies performed on mice [24] and SD rats [23] *ex vivo* on Franz diffusion cell. The second group will involve experiments performed on pig's skin [38,74,75,79] and the last group will explore tests on full thickness human skin *in vivo* [76] and *ex vivo* on Franz diffusion cell [78].

4.1. Rodent's skin based penetration tests

Rodent's skin is thinner and more permeable than human and pig skins [83]. However, they are less expensive and easier to handle in laboratory practice. Rodent's skin showed similar stratum corneum lipids composition [84]. Absorption profile of antiinflammatory (ammonium glycyrrhizinate in niosomes) [85] and short chain alcohols [86] was closed to human skin confirming the successful use of murine model for *in vitro*/*in vivo* correlation with human volunteers. Still hairy rodents have the disadvantage of extremely high density of hair follicles with higher appendage number [87,88]. For this, mice and rats are shaved prior to skin excision. The last studies with quercetin nanodosage forms were performed on skin of SD rats and kunming mice by Liu [23] and Tan [24], respectively.

Liu et al. [23] suggested deformable liposomes for effective skin delivery of quercetin. Tween® 80 was selected as edge activator, while cholesterol and phosphatidylcholine were chosen as lipid phase. Quercetin loaded deformable liposomes were prepared by ethanol injection technique and they presented a particle size of

132 nm and surface charge of −21.1 mV. Quercetin encapsulation efficiency was 80.4 ± 4.2% (Table 4). Skin penetration was analyzed with shaved skin excised from rats' abdomen using Franz diffusion cells. Experiments were run at 32 °C with physiological saline buffer as receptor fluid and a total time of 7 h before quercetin extraction from skin. About 3.5% of the applied dose was permeated through skin in case of deformable liposomes compared to less than 1% in case of quercetin suspension in water. Likewise, a higher quercetin settling in skin with nanodosage form was proven over the control. It is worth to note that the ability of quercetin to permeate the skin especially from the suspension (with keeping in mind the low affinity of quercetin to the receptor fluid is questionable). Indeed, it was previously proved using vasopressin that shaving of the skin before application increased flux 5 times over the control [89]. This result explains the presence of permeated portion.

In 2011, Tan et al. [24] studied lecithin-chitosan nanoparticles for the topical delivery of quercetin. These nanoparticles were also prepared by ethanol injection technique. Particles size was 95 nm (PDI 0.44); zeta potential was +10.9 mV (because of the presence of the polycationic polymer chitosan). Quercetin achieved 48.5% encapsulation efficiency and 2.5% drug loading within formulated nanoparticles (Table 4). Skin penetration tests were made both *in vitro* on mice excised skin and *in vivo* on viable animals. In both cases, no skin permeation was detected after 12 h, whereas quercetin deposition results were comparable between *in vitro* and *in vivo* experiments. Quercetin loaded lecithin-chitosan nanoparticles showed 2.3 and 1.2-fold increase in drug settling within epidermis and dermis respectively compared to quercetin control solution in propylene glycol.

4.2. Pig skin based penetration tests

The second group of research work covers studies with pig ear skin. Pig ear skin is a very close surrogate for human skin. It shares several anatomical and physiological similarities with human skin [90]. Moreover, pig ear skin is more available and less expensive [91].

In 2009, Fasolo et al. [74] developed quercetin containing nanoemulsions. Two types of nanoemulsions were prepared: one with negatively charged droplets composed of octyldodecanol and egg lecithin (surface charge −27.4 mV) and the second with positively charged droplets (surface charge +76.3 mV) by the addition of the cationic surfactant: cetyl trimethylammonium bromide (CTAB). Nanoemulsions were formulated by spontaneous emulsification that corresponds to the injection of organic solvent containing the oily materials into aqueous phase. Then, the evaporation of the organic phase is done under reduced pressure conditions. Nanoemulsions without CTAB possessed a larger particle size compared to nanoemulsions with CTAB (307 ± 19 nm vs. 188 ± 2 nm). Quercetin encapsulation efficacy was over 99% for both nanoemulsions (Table 4). Penetration assay on Franz cell was performed over 8 h using 50% v/v hydroethanol solution as receptor medium. To note, Fasolo et al. determined only quercetin permeated and did not provide data about quercetin skin deposition. Quercetin nanoemulsions were applied to skin at a dose of 1000 μg quercetin, and only 1.524 μg quercetin was permeated through pig ear skin in case of nanoemulsions without CTAB. In contrast, 4.064 μg quercetin permeated from quercetin nanoemulsions with CTAB. In terms of permeated drug percentage, both formulations showed less than 1% drug permeation. The higher drug permeation observed with positively charged nanoemulsions of quercetin is in agreement with other publications, where a higher drug permeation is observed with positively charged nanoemulsions having a higher affinity for negatively charged skin [92–94]. At the same time, cationic surfactants are known to be more skin destructive than anionic surfactants and cause higher drugs flux (drug diffusion through a surface unit of membrane per unit of time) [95]. The percentage of permeated quercetin could be potentially attributed to the fact that porcine skin is more permeable than human skin [96,97]. In addition, the use of a receptor medium that contains alcohol may also cause damage to the barrier function of the utilized skin [98].

In 2011 Chessa et al. [75] incorporated quercetin to liposomes using four different penetration enhancers: Transcutol® P (Trc), propylene glycol (PG), polyethylene glycol 400 (PEG) and Labrasol® (Lab). These penetration enhancer containing vesicles were prepared by thin the film hydration method followed by sonication. Particles size, PDI and zeta potential for Trc, PG, PEG and Lab were 226 nm (0.28 PDI, −49.0 mV), 83 nm (0.35 PDI, −63.0 mV), 190 nm (0.31 PDI, −58.0 mV) and 86 nm (0.29 PDI, −32.0 mV) respectively. Quercetin encapsulation efficiency ranged from 48% with PEG to 75% with Lab (Table 4). Following vesicles preparation, newborn pig's skin was mounted on Franz diffusion cells and skin penetration was assessed. After 8 h, the skin was subjected to 10 strips to separate the stratum corneum. Dermis was separated from epidermis using surgical sterile scalpel. PEG containing vesicles yielded the highest skin permeation with 30% of the applied dose detected in the receptor fluid, as well as the highest deposition in epidermis (55% of the applied dose). It is worth to note that PEG 400 was tested for its penetration enhancement with several drugs such as naloxone [99], estradiol [100], levonorgestrel [101] and zidovudine [102]. Nonetheless PEG 400 causes skin damage by alteration of skin structure and modulation of the mass flow of water [103].

Manca et al. [38] also developed quercetin loaded liposomes and glycerosomes. Similar to Chessa et al., they prepared quercetin nanovesicles using the thin film hydration method followed by sonication. However, instead of using a mixture of penetration enhancer/water to prepare PEVs, they prepared glycerosomes using a 50% mixture glycerol/water. They used lecithin as a lipid. Liposomes were 102 nm (PDI 0.32) with a surface charge −78.0 mV. The glycerosomes were 80 nm (PDI 0.26) with a surface charge −67.0 mV. Both formulations showed encapsulation efficiency over 80% (Table 4). Skin penetration tests were performed over 24 h at 37 °C using Franz cells with newborn pig's skin. At the end of the test, skin layers were separated in the same way as in the publication by Chessa et al. However, both liposomes and glycerosomes did not promote quercetin permeation, but glycerosomes were more efficient in delivering quercetin to the skin compared to liposomes (over 20% of the applied dose vs. 10–20% for liposomes). Quercetin deposition order was stratum corneum, epidermis and dermis respectively in both formulations. This seems to be in accordance with the fact that without the use of a strong penetration enhancer as in the example by Chessa et al., no skin permeation would be observed unless skin barrier function is damaged due to a wound or injury.

In 2015, Sapino et al. [79] investigated the formulation of quercetin within aminopropyl functionalized mesoporous silica nanoparticles (NH_2-MSN). CTAB was used as structure directing agent and tetraethyl orthosilicate as silica source. Quercetin was then loaded in NH_2-MSN at a concentration of 8% and incorporated into a w/o emulsion. At the end of the skin penetration studies no transdermal delivery of quercetin was detected (24 h), and this confirms other reports where quercetin showed no skin permeation in nanodosage forms [76,78]. However, association of quercetin to silica nanoparticles leads to 2-fold increase in skin deposition compared to free quercetin (10.98 μg/cm^2 vs. 4.77 μg/cm^2).

Respecting the fact that porcine skin is more permeable than human skin, quercetin loaded nanodosage forms showed no evidence for skin permeation except in case of the use of penetration enhancers such as CTAB or PEG 400.

4.3. Human skin based penetration tests

Ending by the third group, Scalia et al. in 2013 [76] reported *in vivo* skin penetration of quercetin from solid lipid nanoparticles (SLN). Quercetin was encapsulated in tristearin/phosphatidylcholine nanoparticles. For this, quercetin was dissolved in melted tristearin in the pre-emulsion step and then subjected to cold or hot high pressure homogenization. Quercetin encapsulation efficiency within lipid nanoparticles was 46.5%. Particles size was 527 nm with a PDI of 0.58 for nanoparticles prepared by hot high-pressure homogenization (Table 4). Afterward lipid nanoparticles were incorporated into an oil-in-water emulsion (0.3% w/w quercetin). Then the final emulsion was applied on the forearm of a group of 10 healthy volunteers (22–27 years old). Quercetin final emulsion was applied at a dose of 4 mg/cm^2 for 60 min, and quercetin non-encapsulated in lipid nanoparticles was incorporated in the same emulsion and regarded as control formulation. After the end of the application period, *in vivo* skin penetration assay was performed using 15 stripping tapes of scotch transparent adhesive tape. The first strip tape along with the cotton swab used to remove the remaining formulation was analyzed for unabsorbed quercetin. Then strips were separated into four groups (group 1: strips 2–4; group 2: strips 5–7; group 3: strips 8–11; and group 4: strips 12–15). 66.9 ± 11.1% of quercetin applied dose in the control formulation was recorded on the cotton swab and strip 1 while quercetin loaded lipid nanoparticles were 57.8 ± 11.0%. This very limited improvement by SLN may be attributed to the short duration of drug application, besides the intact barrier function of the stratum corneum (the volunteers were healthy and presented a healthy skin). 21.2 ± 2.9% of the applied dose was penetrated into the skin for quercetin lipid nanoparticles compared to only 18.1 ± 0.3% of the dose in the control. Penetration of quercetin from SLN in the strips was as follows: the highest drug portion was in strips 2–4 (approximately 14%) followed by 5–7 (3.5%), then 8–11 (3%) and finally strips 12–5 (1.5%). Quercetin in SLN showed higher drug deposition in the upper layers of the stratum corneum and lower percentage in the deeper layers. This observation is in accordance with that lipid nanoparticles generate an occlusive effect on the skin, thus increase skin hydration and promote drug delivery to upper skin layers [104]. Meanwhile their relatively large size above 500 nm favors deeper skin penetration via follicular route [105] rather than transepidermal penetration [106].

In 2013, Bose et al. [78] developed quercetin in both solid lipid nanoparticles (SLN) and nanostructured lipid carriers (NLC). Compritol® 888 was used as solid lipid for both nanosystems, whereas oleic acid was incorporated into nanostructured lipid carriers as liquid lipid. Both quercetin nanosystems were prepared by the probe ultrasonication method. Quercetin NLC were 282 nm, PDI of 0.31 and zeta potential of −37.0 mV (Table 4). Quercetin exhibited a better physical stability results for 14 weeks at 2–8 °C when loaded at 0.0125% than 0.025%. Skin penetration studies were performed on full thickness human skin *ex vivo* using 0.64 cm^2 Franz diffusion cell over 24 h. Bose et al. [78] reported the absence of transdermal delivery for quercetin from both nanosystems. This result is in accordance with Scalia et al. [76] who confirm that the majority of applied quercetin from nanoparticles was found in the top layers of the skin. This is very important for such antioxidant molecule, considering the main site of action is the skin cells in the upper layers. At the end of the penetration test, Bose et al. determined skin quercetin retention without detailing its distribution among skin layers. The percentage of drug skin retention was 19.2% with NLC according to Bose et al. and it falls in the same range that is in the *in vivo* work of Scalia et al. who detected 21.2 ± 2.9%.

In summary, quercetin even when formulated in a lipid nanoparticle vector shows no evidence for transdermal delivery on human skin. Keeping in mind that quercetin as a molecule is a paradigmatic model for a lipophilic drug (octanol–water partition coefficient log P = 1.82) [73] with 5 polar hydroxyl heads and very low water solubility [81], thus quercetin is not the perfect drug candidate for a transdermal delivery system. Quercetin local skin deposition is more valuable than performing a transdermal delivery through skin. Quercetin envisaged dermal applications described above (Section 2) are all of local interest and the absence of a systemic absorption is desirable. Nanodosage forms were able to increase quercetin skin retention via their occlusive effect and higher surface area. Transdermal delivery for quercetin nanodosage forms was not achieved without the help of penetration enhancers. The use of penetration enhancers should be taken with caution as these molecules affect skin barrier function and may cause skin damage. However, nanodosage forms are very promising drug delivery systems for targeting skin and upper layers of epidermis. This is desirable for quercetin to exert its activity in protecting skin tissue from oxidative stress, photoaging and uncontrolled skin inflammation.

Finally, one can compare *in vivo* skin permeation/penetration for quercetin between microemulsion [43] and lecithin-chitosan nanoparticles [24] as in both studies formulations were applied on dorsal skin of mice, quercetin applied quantity was the same (300 μg) and both studies detected quercetin levels in the skin after 6 h of application. Results are relatively close between nanoparticles and microemulsion. The larger portion of quercetin was detected in the upper skin layers at the SC level, and lower concentrations were detected in the dermis. Quercetin showed no transdermal delivery in both studies.

5. Conclusion

Quercetin proves to possess several interesting physiological actions on skin. It has a strong antioxidative activity. It protects keratinocytes for exogenous oxidizing agents and scavenges free radicals, prevents endogenous antioxidant depletion and inhibits lipid peroxidation upon exposure to UV. Quercetin also presents broad antiinflammatory actions. It is stronger than other flavonoids in inhibiting edema after contact with inflammogens. It presents inhibiting actions on NF-κB and on the release of several proinflammatory cytokines. These combined antioxidative/antiinflammatory actions highlight quercetin as a promising molecule for the treatment of chronic wounds. Additionally quercetin shows anti-aging actions on middle-aged keratinocytes and rejuvenating actions on terminally senescent cells. In parallel, quercetin inhibits tyrosinase in melanocytes and thus enables a whitening effect on skin. All these possible targets and applications for quercetin require a successful local delivery to skin. Due to quercetin poor water solubility and inability to penetrate skin, researches are conducted on the formulation of a potent delivery system. In this article, the last advances in delivery of quercetin to skin via conventional dosage forms and nanodosage forms were presented and discussed. The variation of formulations in terms of excipients used and the physicochemical characteristics, along with effect of particle size on skin penetration are discussed. Quercetin in both types of formulations presented no transdermal delivery except in case of the use of penetration enhancers. Conventional and nanodosage forms showed higher quercetin deposition in the upper skin layers of the epidermis. Despite achieving extremely small particle size with nanodosage forms, still the lipid content and the lipid type seem to be the main determinant of the extent of quercetin depth in skin layers. More studies should be performed to get more insight about the exact depth that a formulation containing quercetin can achieve. At the same time, more research should be made to investigate other possible applications for quercetin in other skin disorders such as psoriasis or atopic dermatitis.

References

[1] A.B. Wysocki, Skin anatomy, physiology, and pathophysiology, Nurs. Clin. North Am. 34 (1999) 777–797. v.
[2] C.S. Sander, H. Chang, S. Salzmann, C.S.L. Muller, S. Ekanayake-Mudiyanselage, P. Elsner, J.J. Thiele, Photoaging is associated with protein oxidation in human skin in vivo, J. Investigat. Dermatol. 118 (2002) 618–625.
[3] U. Hoppe, J. Bergemann, W. Diembeck, J. Ennen, S. Gohla, I. Harris, J. Jacob, J. Kielholz, W. Mei, D. Pollet, D. Schachtschabel, G. Sauermann, V. Schreiner, F. Stab, F. Steckel, Coenzyme Q10, a cutaneous antioxidant and energizer, BioFactors 9 (1999) 371–378.
[4] J. Pardeike, K. Schwabe, R.H. Müller, Influence of nanostructured lipid carriers (NLC) on the physical properties of the Cutanova Nanorepair Q10 cream and the in vivo skin hydration effect, Int. J. Pharm. 396 (2010) 166–173.
[5] S. Shibuya, H. Nojiri, D. Morikawa, H. Koyama, T. Shimizu, Chapter 14 - Protective Effects of Vitamin C on Age-Related Bone and Skin Phenotypes Caused by Intracellular Reactive Oxygen Species, in: V.R. Preedy (Ed.), Aging, Academic Press, San Diego, 2014, pp. 137–144.
[6] J.V. Freitas, N.P. Lopes, L.R. Gaspar, Photostability evaluation of five UV-filters, trans-resveratrol and beta-carotene in sunscreens, Eur. J. Pharm. Sci. 78 (2015) 79–89.
[7] E.A. Offord, J.-C. Gautier, O. Avanti, C. Scaletta, F. Runge, K. Krämer, L.A. Applegate, Photoprotective potential of lycopene, β-carotene, vitamin E, vitamin C and carnosic acid in UVA-irradiated human skin fibroblasts, Free Radical Biol. Med. 32 (2002) 1293–1303.
[8] P.K. Vayalil, A. Mittal, Y. Hara, C.A. Elmets, S.K. Katiyar, Green tea polyphenols prevent ultraviolet light-induced oxidative damage and matrix metalloproteinases expression in mouse skin, J. Investig. Dermatol. 122 (2004) 1480–1487.
[9] J. Nichols, S. Katiyar, Skin photoprotection by natural polyphenols: anti-inflammatory, antioxidant and DNA repair mechanisms, Arch. Dermatol. Res. 302 (2010) 71–83.
[10] S. Veeriah, T. Kautenburger, N. Habermann, J. Sauer, H. Dietrich, F. Will, B.L. Pool-Zobel, Apple flavonoids inhibit growth of HT29 human colon cancer cells and modulate expression of genes involved in the biotransformation of xenobiotics, Mol. Carcinog. 45 (2006) 164–174.
[11] R. Slimestad, T. Fossen, I.M. Vagen, Onions: a source of unique dietary flavonoids, J. Agric. Food Chem. 55 (2007) 10067–10080.
[12] C. Ewald, S. Fjelkner-Modig, K. Johansson, I. Sjöholm, B. Åkesson, Effect of processing on major flavonoids in processed onions, green beans, and peas, Food Chem. 64 (1999) 231–235.
[13] F. Bonina, M. Lanza, L. Montenegro, C. Puglisi, A. Tomaino, D. Trombetta, F. Castelli, A. Saija, Flavonoids as potential protective agents against photo-oxidative skin damage, Int. J. Pharm. 145 (1996) 87–94.
[14] H. Kim, S. Namgoong, H. Kim, Antiinflammatory activity of flavonoids: mouse ear edema inhibition, Arch. Pharmacal Res. 16 (1993) 18–24.
[15] A. Saija, A. Tomaino, D. Trombetta, M. Luisa Pellegrino, B. Tita, C. Messina, F.P. Bonina, C. Rocco, G. Nicolosi, F. Castelli, 'In vitro' antioxidant and photoprotective properties and interaction with model membranes of three new quercetin esters, Eur. J. Pharm. Biopharm. 56 (2003) 167–174.
[16] T. Hatahet, M. Morille, A. Hommoss, C. Dorandeu, R.H. Muller, S. Begu, Dermal quercetin smartCrystals(R): formulation development, antioxidant activity and cellular safety, Eur. J. Pharm. Biopharm. 102 (2016) 51–63.
[17] Lh, Quercetin, CAS 117–39-5, Santa Cruz Biotech, 2016.
[18] Y. Zheng, I.S. Haworth, Z. Zuo, M.S. Chow, A.H. Chow, Physicochemical and structural characterization of quercetin-beta-cyclodextrin complexes, J. Pharm. Sci. 94 (2005) 1079–1089.
[19] J.A. Rothwell, A.J. Day, M.R. Morgan, Experimental determination of octanol-water partition coefficients of quercetin and related flavonoids, J. Agric. Food Chem. 53 (2005) 4355–4360.
[20] C. Celia, F. Cilurzo, E. Trapasso, D. Cosco, M. Fresta, D. Paolino, Ethosomes(R) and transfersomes(R) containing linoleic acid: physicochemical and technological features of topical drug delivery carriers for the potential treatment of melasma disorders, Biomed. Microdevices 14 (2012) 119–130.
[21] D. Paolino, C. Celia, E. Trapasso, F. Cilurzo, M. Fresta, Paclitaxel-loaded ethosomes(R): potential treatment of squamous cell carcinoma, a malignant transformation of actinic keratoses, Eur. J. Pharm. Biopharm. 81 (2012) 102–112.
[22] D. Paolino, D. Cosco, F. Cilurzo, E. Trapasso, V.M. Morittu, C. Celia, M. Fresta, Improved in vitro and in vivo collagen biosynthesis by asiaticoside-loaded ultradeformable vesicles, J. Control. Release 162 (2012) 143–151.
[23] D. Liu, H. Hu, Z. Lin, D. Chen, Y. Zhu, S. Hou, X. Shi, Quercetin deformable liposome: preparation and efficacy against ultraviolet B induced skin damages in vitro and in vivo, J. Photochem. Photobiol., B 127 (2013) 8–17.
[24] Q. Tan, W. Liu, C. Guo, G. Zhai, Preparation and evaluation of quercetin-loaded lecithin-chitosan nanoparticles for topical delivery, Int. J. Nanomed. 6 (2011) 1621–1630.
[25] G.S. Borghetti, I.M. Costa, P.R. Petrovick, V.P. Pereira, V.L. Bassani, Characterization of different samples of quercetin in solid-state: indication of polymorphism occurrence, Pharmazie 61 (2006) 802–804.
[26] H. Sies, Strategies of antioxidant defense, Eur. J. Biochem. 215 (1993) 213–219.
[27] M.S. Blois, Antioxidant determinations by the use of a stable free radical, Nature 181 (1958) 1199–1200.
[28] I. Fridovich, Quantitative aspects of the production of superoxide anion radical by milk xanthine oxidase, J. Biol. Chem. 245 (1970) 4053–4057.
[29] N. Majkic-Singh, M. Koprivica, S. Spasic, M. Stojanov, I. Berkes, Evaluation of bathophenanthroline method for serum iron assay, Clin. Chem. 26 (1980) 1360.
[30] G. Lefevre, M. Beljean-Leymarie, F. Beyerle, D. Bonnefont-Rousselot, J.P. Cristol, P. Therond, J. Torreilles, Evaluation of lipid peroxidation by measuring thiobarbituric acid reactive substances, Ann. Biol. Clin. (Paris) 56 (1998) 305–319.
[31] R. Casagrande, S.R. Georgetti, W.A. Verri, J.R. Jabor, A.C. Santos, M.J.V. Fonseca, Evaluation of functional stability of quercetin as a raw material and in different topical formulations by its antilipoperoxidative activity, AAPS PharmSciTech (2006) E64–E71.
[32] K.E. Heim, A.R. Tagliaferro, D.J. Bobilya, Flavonoid antioxidants: chemistry, metabolism and structure-activity relationships, J. Nutr. Biochem. 13 (2002) 572–584.
[33] R. Casagrande, S.R. Georgetti, W.A. Verri Jr., M.F. Borin, R.F.V. Lopez, M.J.V. Fonseca, In vitro evaluation of quercetin cutaneous absorption from topical formulations and its functional stability by antioxidant activity, Int. J. Pharm. 328 (2007) 183–190.
[34] T.-H. Wu, F.-L. Yen, L.-T. Lin, T.-R. Tsai, C.-C. Lin, T.-M. Cham, Preparation, physicochemical characterization, and antioxidant effects of quercetin nanoparticles, Int. J. Pharm. 346 (2008) 160–168.
[35] K.L. Wolfe, R.H. Liu, Cellular antioxidant activity (CAA) assay for assessing antioxidants, foods, and dietary supplements, J. Agri. Food Chem. 55 (2007) 8896–8907.
[36] C. López-Alarcón, A. Denicola, Evaluating the antioxidant capacity of natural products: a review on chemical and cellular-based assays, Anal. Chim. Acta 763 (2013) 1–10.
[37] S.D. Skaper, M. Fabris, V. Ferrari, M. Dalle Carbonare, A. Leon, Quercetin protects cutaneous tissue-associated cell types including sensory neurons from oxidative stress induced by glutathione depletion: cooperative effects of ascorbic acid, Free Radic. Biol. Med. 22 (1997) 669–678.
[38] M.L. Manca, I. Castangia, C. Caddeo, D. Pando, E. Escribano, D. Valenti, S. Lampis, M. Zaru, A.M. Fadda, M. Manconi, Improvement of quercetin protective effect against oxidative stress skin damages by incorporation in nanovesicles, Colloids Surf. B 123 (2014) 566–574.
[39] N. Düzgüneş, S. Nir, Mechanisms and kinetics of liposome–cell interactions, Adv. Drug Deliv. Rev. 40 (1999) 3–18.
[40] V.P. Torchilin, Recent advances with liposomes as pharmaceutical carriers, Nat. Rev. Drug Discov. 4 (2005) 145–160.
[41] C.-F. Hung, C.-L. Fang, S.A. Al-Suwayeh, S.-Y. Yang, J.-Y. Fang, Evaluation of drug and sunscreen permeation via skin irradiated with UVA and UVB: comparisons of normal skin and chronologically aged skin, J. Dermatol. Sci. 68 (2012) 135–148.
[42] R. Casagrande, S.R. Georgetti, W.A. Verri Jr., D.J. Dorta, A.C. dos Santos, M.J.V. Fonseca, Protective effect of topical formulations containing quercetin against UVB-induced oxidative stress in hairless mice, J. Photochem. Photobiol., B 84 (2006) 21–27.
[43] F.T.M.C. Vicentini, T.R.M. Simi, J.O. Del Ciampo, N.O. Wolga, D.L. Pitol, M.M. Iyomasa, M.V.L.B. Bentley, M.J.V. Fonseca, Quercetin in w/o microemulsion: in vitro and in vivo skin penetration and efficacy against UVB-induced skin damages evaluated in vivo, Eur. J. Pharm. Biopharm. 69 (2008) 948–957.
[44] D. Singh Joshan, S.K. Singh, Investigational study of Juglans regia extract and quercetin against photoaging, Biomed. Ag. Pathol. 3 (2013) 193–200.
[45] C.F. Lin, Y.L. Leu, S.A. Al-Suwayeh, M.C. Ku, T.L. Hwang, J.Y. Fang, Anti-inflammatory activity and percutaneous absorption of quercetin and its polymethoxylated compound and glycosides: the relationships to chemical structures, Eur. J. Pharm. Sci. 47 (2012) 857–864.
[46] K. Gomathi, D. Gopinath, M. Rafiuddin Ahmed, R. Jayakumar, Quercetin incorporated collagen matrices for dermal wound healing processes in rat, Biomaterials 24 (2003) 2767–2772.
[47] E.A. Hamminga, A.J. van der Lely, H.A.M. Neumann, H.B. Thio, Chronic inflammation in psoriasis and obesity: implications for therapy, Med. Hypotheses 67 (2006) 768–773.
[48] D.R. Bickers, M. Athar, Oxidative stress in the pathogenesis of skin disease, J. Investigat. Dermatol. 126 (2006) 2565–2575.
[49] S.J. Cooper, G.T. Bowden, Ultraviolet B regulation of transcription factor families: roles of nuclear factor-kappa B (NF-kappaB) and activator protein-1 (AP-1) in UVB-induced skin carcinogenesis, Curr. Cancer Drug Targets 7 (2007) 325–334.
[50] P.P. Tak, G.S. Firestein, NF-κB: a key role in inflammatory diseases, J. Clin. Invest. (2001) 7–11.
[51] P.A. Ruiz, A. Braune, G. Holzlwimmer, L. Quintanilla-Fend, D. Haller, Quercetin inhibits TNF-induced NF-kappaB transcription factor recruitment to proinflammatory gene promoters in murine intestinal epithelial cells, J. Nutr. US (2007) 1208–1215.
[52] C.A. Musonda, J.K. Chipman, Quercetin inhibits hydrogen peroxide (H2O2)-induced NF-kappaB DNA binding activity and DNA damage in HepG2 cells, Carcinogenesis 19 (1998) 1583–1589.
[53] A.B. Granado-Serrano, M.A. Martin, L. Bravo, L. Goya, S. Ramos, Quercetin modulates NF-kappa B and AP-1/JNK pathways to induce cell death in human hepatoma cells, Nutr. Cancer, Engl. (2010) 390–401.
[54] F.T. Vicentini, T. He, Y. Shao, M.J. Fonseca, W.A. Verri Jr., G.J. Fisher, Y. Xu, Quercetin inhibits UV irradiation-induced inflammatory cytokine production

in primary human keratinocytes by suppressing NF-kappaB pathway, in: J Dermatol Sci, 2011 Japanese Society for Investigative Dermatology, Elsevier Ireland Ltd., Netherlands, 2011, pp. 162–168.
[55] C.-F. Lin, Y.-L. Leu, S.A. Al-Suwayeh, M.-C. Ku, T.-L. Hwang, J.-Y. Fang, Anti-inflammatory activity and percutaneous absorption of quercetin and its polymethoxylated compound and glycosides: the relationships to chemical structures, Eur. J. Pharm. Sci. 47 (2012) 857–864.
[56] B. Choquenet, C. Couteau, E. Paparis, L.J.M. Coiffard, Quercetin and rutin as potential sunscreen agents: determination of efficacy by an in vitro method, J. Nat. Prod. 71 (2008) 1117–1118.
[57] A. Vijayalakshmi, V. Ravichandiran, V. Malarkodi, S. Nirmala, S. Jayakumari, Screening of flavonoid "quercetin" from the rhizome of Smilax china Linn. for anti-psoriatic activity, Asian Pac. J. Trop. Biomed. (2012) 269–275.
[58] C. Caddeo, O. Diez-Sales, R. Pons, X. Fernandez-Busquets, A.M. Fadda, M. Manconi, Topical anti-inflammatory potential of quercetin in lipid-based nanosystems: in vivo and in vitro evaluation, Pharm. Res. 31 (2014) 959–968.
[59] C. Caddeo, O.D. Sales, D. Valenti, A.R. Sauri, A.M. Fadda, M. Manconi, Inhibition of skin inflammation in mice by diclofenac in vesicular carriers: liposomes, ethosomes and PEVs, Int. J. Pharm. 443 (2013) 128–136.
[60] T.K. Hunt, The physiology of wound healing, Ann. Emerg. Med. 17 (1988) 1265–1273.
[61] D. Cerimele, L. Celleno, F. Serri, Physiological changes in ageing skin, Br. J. Dermatol. 122 (1990) 13–20.
[62] J. Calleja-Agius, Y. Muscat-Baron, M.P. Brincat, Skin ageing, Menopause Int. 13 (2007) 60–64.
[63] M.A. Farage, K.W. Miller, P. Elsner, H.I. Maibach, Intrinsic and extrinsic factors in skin ageing: a review, Int. J. Cosmet. Sci. 30 (2008) 87–95.
[64] M. Hara, A.S. Verkman, Glycerol replacement corrects defective skin hydration, elasticity, and barrier function in aquaporin-3-deficient mice, Proc. Natl. Acad. Sci. 100 (2003) 7360–7365.
[65] J. Terao, M. Piskula, Q. Yao, Protective effect of epicatechin, epicatechin gallate, and quercetin on lipid peroxidation in phospholipid bilayers, Arch. Biochem. Biophys. 308 (1994) 278–284.
[66] J. Majtan, J. Bohova, R. Garcia-Villalba, F. Tomas-Barberan, Z. Madakova, T. Majtan, V. Majtan, J. Klaudiny, Fir honeydew honey flavonoids inhibit TNF-α-induced MMP-9 expression in human keratinocytes: a new action of honey in wound healing, Arch. Dermatol. Res. 305 (2013) 619–627.
[67] J.H. Chung, J.Y. Seo, H.R. Choi, M.K. Lee, C.S. Youn, G.-E. Rhie, K.H. Cho, K.H. Kim, K.C. Park, H.C. Eun, Modulation of skin collagen metabolism in aged and photoaged human skin in vivo, J. Investigat. Dermatol. 117 (2001) 1218–1224.
[68] J. Lock-Andersen, P. Therkildsen, F. de Fine Olivarius, M. Gniadecka, K. Dahlstrom, T. Poulsen, H.C. Wulf, Epidermal thickness, skin pigmentation and constitutive photosensitivity, Photodermatol. Photoimmunol. Photomed. 13 (1997) 153–158.
[69] N. Chondrogianni, S. Kapeta, I. Chinou, K. Vassilatou, I. Papassideri, E.S. Gonos, Anti-ageing and rejuvenating effects of quercetin, Exp. Gerontol. 45 (2010) 763–771.
[70] F. Debacq-Chainiaux, J.D. Erusalimsky, J. Campisi, O. Toussaint, Protocols to detect senescence-associated beta-galactosidase (SA-[beta]gal) activity, a biomarker of senescent cells in culture and in vivo, Nat. Prot. 4 (2009) 1798–1806.
[71] N. Agar, A.R. Young, Melanogenesis: a photoprotective response to DNA damage?, Mutat Res./Fund. Molec. Mech. Mutagen. 571 (2005) 121–132.
[72] H. Ando, H. Kondoh, M. Ichihashi, V.J. Hearing, Approaches to identify inhibitors of melanin biosynthesis via the quality control of tyrosinase, J. Investig. Dermatol. 127 (2007) 751–761.
[73] J.A. Rothwell, A.J. Day, M.R.A. Morgan, Experimental determination of octanol-water partition coefficients of quercetin and related flavonoids, J. Agri. Food Chem. 53 (2005) 4355–4360.
[74] D. Fasolo, V.L. Bassani, H.F. Teixeira, Development of topical nanoemulsions containing quercetin and 3-O-methylquercetin, Pharmazie 64 (2009) 726–730.
[75] M. Chessa, C. Caddeo, D. Valenti, M. Manconi, C. Sinico, A.M. Fadda, Effect of penetration enhancer containing vesicles on the percutaneous delivery of quercetin through new born pig skin, Pharmaceutics 3 (2011) 497–509.
[76] S. Scalia, E. Franceschinis, D. Bertelli, V. Iannuccelli, Comparative evaluation of the effect of permeation enhancers, lipid nanoparticles and colloidal silica on in vivo human skin penetration of quercetin, Skin Pharmacol. Physiol. (Basel., Switzerland) (2013) 57–67.
[77] S. Bose, Y. Du, P. Takhistov, B. Michniak-Kohn, Formulation optimization and topical delivery of quercetin from solid lipid based nanosystems, Int. J. Pharm. 441 (2012) 56–66.
[78] S. Bose, B. Michniak-Kohn, Preparation and characterization of lipid based nanosystems for topical delivery of quercetin, Eur. J. Pharm. Sci. 48 (2013) 442–452.
[79] S. Sapino, E. Ugazio, L. Gastaldi, I. Miletto, G. Berlier, D. Zonari, S. Oliaro-Bosso, Mesoporous silica as topical nanocarriers for quercetin: characterization and in vitro studies, Eur. J. Pharm. Biopharm. 89 (2015) 116–125.
[80] A. Saija, A. Tomaino, D. Trombetta, M. Giacchi, A.D. Pasquale, F. Bonina, Influence of different penetration enhancers on in vitro skin permeation and in vivo photoprotective effect of flavonoids, Int. J. Pharm. 175 (1998) 85–94.
[81] L. Montenegro, C. Carbone, C. Maniscalco, D. Lambusta, G. Nicolosi, C.A. Ventura, G. Puglisi, In vitro evaluation of quercetin-3-O-acyl esters as topical prodrugs, Int. J. Pharm. 336 (2007) 257–262.
[82] F.P. Schmook, J.G. Meingassner, A. Billich, Comparison of human skin or epidermis models with human and animal skin in in-vitro percutaneous absorption, Int. J. Pharm. 215 (2001) 51–56.
[83] R.L. Bronaugh, R.F. Stewart, E.R. Congdon, Methods for in vitro percutaneous absorption studies II. Animal models for human skin, Toxicol. Appl. Pharm. 62 (1982) 481–488.
[84] D. Chantasart, S.K. Li, N. He, K.S. Warner, S. Prakongpan, W.I. Higuchi, Mechanistic studies of branched-chain alkanols as skin permeation enhancers, J. Pharm. Sci. 93 (2004) 762–779.
[85] C. Marianecci, F. Rinaldi, M. Mastriota, S. Pieretti, E. Trapasso, D. Paolino, M. Carafa, Anti-inflammatory activity of novel ammonium glycyrrhizinate/niosomes delivery system: human and murine models, J. Control. Release 164 (2012) 17–25.
[86] H. Durrheim, G.L. Flynn, W.I. Higuchi, C.R. Behl, Permeation of hairless mouse skin I: Experimental methods and comparison with human epidermal permeation by alkanols, J. Pharm. Sci. 69 (1980) 781–786.
[87] E.C. Jung, H.I. Maibach, Animal models for percutaneous absorption, J. Appl. Toxicol. 35 (2015) 1–10.
[88] A. Capt, A.P. Luzy, D. Esdaile, O. Blanck, Comparison of the human skin grafted onto nude mouse model with in vivo and in vitro models in the prediction of percutaneous penetration of three lipophilic pesticides, Regul. Toxicol. Pharmacol. 47 (2007) 274–287.
[89] P.S. Banerjee, W.A. Ritschel, Transdermal permeation of vasopressin. I. Influence of pH, concentration, shaving and surfactant on in vitro permeation, Int. J. Pharm. 49 (1989) 189–197.
[90] I.P. Dick, R.C. Scott, Pig ear skin as an in-vitro model for human skin permeability, J. Pharm. Pharmacol. 44 (1992) 640–645.
[91] S. Singh, K. Zhao, J. Singh, In vitro permeability and binding of hydrocarbons in pig ear and human abdominal skin, Drug Chem. Toxicol. 25 (2002) 83–92.
[92] S. Hoeller, A. Sperger, C. Valenta, Lecithin based nanoemulsions: a comparative study of the influence of non-ionic surfactants and the cationic phytosphingosine on physicochemical behaviour and skin permeation, Int. J. Pharm. 370 (2009) 181–186.
[93] E. Yilmaz, H.-H. Borchert, Design of a phytosphingosine-containing, positively-charged nanoemulsion as a colloidal carrier system for dermal application of ceramides, Eur. J. Pharm. Biopharm. 60 (2005) 91–98.
[94] Y. Baspinar, H.-H. Borchert, Penetration and release studies of positively and negatively charged nanoemulsions—is there a benefit of the positive charge?, Int J. Pharm. 430 (2012) 247–252.
[95] E.W. Smith, H.I. Maibach, Percutaneous Penetration Enhancers, Taylor & Francis, 1995.
[96] M.J. Bartek, J.A. Labudde, H.I. Maibach, Skin permeability in vivo: comparison in rat, rabbit, pig and man, J. Investig. Dermatol. 58 (1972) 114–123.
[97] N.H.P. Cnubben, G.R. Elliott, B.C. Hakkert, W.J.A. Meuling, J.J.M. van de Sandt, Comparative in vitro–in vivo percutaneous penetration of the fungicide ortho-phenylphenol, Regul. Toxicol. Pharmacol. 35 (2002) 198–208.
[98] D.W. Lachenmeier, Safety evaluation of topical applications of ethanol on the skin and inside the oral cavity, J. Occupat. Med. Toxicol. (London, England) 3 (2008) 26.
[99] B.J. Aungst, N.J. Rogers, E. Shefter, Enhancement of naloxone penetration through human skin in vitro using fatty acids, fatty alcohols, surfactants, sulfoxides and amides, Int. J. Pharm. 33 (1986) 225–234.
[100] K.H. Valia, Y.W. Chien, E.C. Shinal, Long-term skin permeation kinetics of estradiol (I): Effect of drug solubilizer-polyethylene glycol 400, Drug Dev. Ind. Pharm. 10 (1984) 951–981.
[101] P. Catz, D.R. Friend, Transdermal delivery of levonorgestrel. VIII. Effect of enhancers on rat skin, hairless mouse skin, hairless guinea pig skin, and human skin, Int. J. Pharm. 58 (1990) 93–102.
[102] N. Suwanpidokkul, P. Thongnopnua, K. Umprayn, Transdermal delivery of zidovudine (AZT): the effects of vehicles, enhancers, and polymer membranes on permeation across cadaver pig skin, AAPS PharmSciTech 5 (2004) 82–89.
[103] P.P. Sarpotdar, J.L. Gaskill, R.P. Giannini, Effect of polyethylene glycol 400 on the penetration of drugs through human cadaver skin in vitro, J. Pharm. Sci. 75 (1986) 26–28.
[104] J. Pardeike, A. Hommoss, R.H. Müller, Lipid nanoparticles (SLN, NLC) in cosmetic and pharmaceutical dermal products, Int. J. Pharm. 366 (2009) 170–184.
[105] A. Patzelt, H. Richter, F. Knorr, U. Schäfer, C.-M. Lehr, L. Dähne, W. Sterry, J. Lademann, Selective follicular targeting by modification of the particle sizes, J. Control. Release 150 (2011) 45–48.
[106] B. Baroli, Penetration of nanoparticles and nanomaterials in the skin: fiction or reality?, J Pharm. Sci. 99 (2010) 21–50.

European Journal of Pharmaceutics and Biopharmaceutics 102 (2016) 51–63

Contents lists available at ScienceDirect

European Journal of Pharmaceutics and Biopharmaceutics

journal homepage: www.elsevier.com/locate/ejpb

Research paper

Dermal quercetin smartCrystals®: Formulation development, antioxidant activity and cellular safety

T. Hatahet [a], M. Morille [a], A. Hommoss [b], C. Dorandeu [a], R.H. Müller [b], S. Bégu [a,*]

[a] Institut Charles Gerhardt Montpellier, UMR 5253 CNRS-ENSCM-UM, Equipe Matériaux Avancés pour la Catalyse et la Santé, 8 rue de l'Ecole Normale, 34296 Montpellier Cedex 5, France
[b] Institute of Pharmacy, Department of Pharmaceutics, Biopharmaceutics and NutriCosmetics, Free University of Berlin, Kelchstr. 31, Berlin 12169, Germany

ARTICLE INFO

Article history:
Received 3 December 2015
Revised 25 February 2016
Accepted in revised form 2 March 2016
Available online 4 March 2016

Keywords:
Quercetin
SmartCrystals®
Nanocrystals
Nanosuspensions
Flavonoids
Antioxidative effect
Nonionic gel
Cellular toxicity
Hydrogen peroxide induced toxicity

ABSTRACT

Flavonoids are natural plant pigments, which possess high antioxidative and antiradical activities. However, their poor water solubility led to a limited bioavailability. To overcome this major hurdle, quercetin nanocrystals were produced implementing smartCrystals® technology. This process combines bead milling and subsequent high-pressure homogenization at relatively low pressure (300 bar). To test the possibility to develop a dermal formulation from quercetin smartCrystals®, quercetin nanosuspensions were admixed to Lutrol® F127 and hydroxythylcellulose nonionic gels.

The physicochemical properties (morphology, size and charge), saturation solubility, dissolution velocity and the antioxidant properties (DPPH assay) as well as the cellular interaction of the produced quercetin smartCrystals® were studied and compared to crude quercetin powder. Quercetin smartCrystals® showed a strong increase in the saturation solubility and the dissolution velocity (7.6 fold). SmartCrystals® loaded or not into gels proved to be physically stable over a period of three months at 25 °C. Interestingly, *in vitro* DPPH assay confirmed the preservation of quercetin antioxidative properties after nanonization. In parallel, the nanocrystalline form did not display cellular toxicity, even at high concentration (50 μg/ml), as assayed on an epithelial cell line (VERO cells). In addition, the nanocrystalline form confirmed a protective activity for VERO cells against hydrogen peroxide induced toxicity *in vitro*. This new formulation presents a promising approach to deliver quercetin efficiently to skin in well-tolerated formulations.

1. Introduction

Antioxidants are of high interest in the prevention of oxidative stress not only for oral administration but also for topical administration. In this context, antioxidants are used to support treatment for diseases that require a higher activity of the immune system (mosquito borne diseases or viral infections) [6,35,57]. In dermal preparations, products containing antioxidants are useful for protection against UV radiation damage [4,32] or for prevention of skin cancer [18,49,61]. Flavonoids are plant pigments found in a wide variety of fruits and vegetables such as apples [53], pears [56], onions [27], and red wine [28]. Many flavonoids such as quercetin, rutin, hesperidin and naringenin are potent antioxidants [51]. Quercetin was chosen as an active principle because it is considered as the most powerful antioxidant, and the most distributed in nature [2]. Moreover, it has already been used for its antiinflammatory [8,30] and anti-tumor activities [24,65], and also for cellular protective properties in brain [48], liver [16], kidney [31] and colon diseases [10]. In order to mimic the topical application, UV irradiation was used to introduce lipid peroxidation on phosphatidylcholine liposomes. Interestingly, in this model, quercetin showed the highest protective activity among various tested flavonoids [2,20]. This UV protective effect is of high relevance in skin aging and wrinkling [7] and indicates quercetin as potential active drug for skin protection against photoaging.

Nevertheless, its poor water solubility limits dermal bioavailability leading to a decrease in its potential for topical administration. In this context, nanocrystals proved to be a successful formulation strategy for the increase in dermal bioavailability of poorly soluble actives [55]. Nanocrystals have a simple but effective mechanism of bioavailability enhancement by increasing the kinetic saturation solubility (Cs) and thus increasing the concentration gradient between the application site (e.g. dermal formulation) and the acceptor medium (e.g. skin). In addition, a higher dissolution velocity due to the large surface area occurs. Finally,

* Corresponding author.
E-mail address: sylvie.begu@enscm.fr (S. Bégu).

http://dx.doi.org/10.1016/j.ejpb.2016.03.004
0939-6411/

nanocrystals show high adhesion and prolonged retention times, by adhering firmly to the skin [21]. Nanocrystals can be obtained by different industrial processes. The first-generation of nanocrystals is used to be produced by different processes, but generally in a one-step procedure: bottom-up such as "Nanomorph®", or top-down processes such as wet bead milling developed by Alkermes® [34] and high-pressure homogenization (HPH) developed by Müller et al. from the company DDS Germany [41]. The second-generation of nanocrystals is generally produced thanks to combinative process, such as association of microprecipitation followed by HPH (Nanoedge or H69 technologies), spray drying and HPH (H42 technology), freeze drying and HPH (H96) and wet bead milling associated with HPH (CT technology) [52]. SmartCrystals® were developed as second-generation technology [43] using combination processes as a "toolbox" for tailor-made nanocrystals specific for different demands. In this study, the combination technology of bead milling and subsequent HPH was performed (known as CT process®) [47]. This yields monodispersed nanocrystals, homogenous in size with increased physical stability [12].

Research groups mainly focused on the preparation of quercetin nanocrystals either by bead milling or by high-pressure homogenization [22,23]. Others focused on the application of nanotechnology (nanocrystals, solid lipid nanoparticles, etc.) for expected oral delivery [29,33]. Up until now, the advantages of formulating quercetin nanocrystals using the second-generation of smartCrystals® for dermal application have not been investigated.

To stabilize these smartCrystals®, five different stabilizers were tested. Two standard nonionic stabilizers: (i) polysorbate 80 (Tween® 80) and (ii) poloxamer 188 (Lutrol® F68), and two alkyl polyglucoside "green" stabilizers (iii) caprylyl/capryl glucoside (Plantacare® 810) and (iv) lauryl glucoside (Plantacare® 1200) were previously used in drug nanocrystal stabilizations [14,36,54]. Finally, (v) a vitamin E derived surfactant, α-tocopheryl polyethylene glycol 1000 succinate (TPGS) is used as a novel stabilizer for drug nanocrystals. The obtained quercetin smartCrystals® were characterized and compared to crude quercetin regarding physicochemical characteristics (size, charge, shape, saturation solubility and dissolution velocity) as well as antioxidative properties and cytotoxicity against an epithelial cell line (VERO cells). As a last step, quercetin nanosuspensions were admixed to two different nonionic gels Lutrol® F127 (poloxamer 407) and hydroxythylcellulose (HEC) and the stability of the smartCrystals® in suspension and in dermal non-ionic gels was assessed over a period of three months at three different temperatures (4 °C, 25 °C and 40 °C).

2. Materials and methods

2.1. Materials

Quercetin aglycone (3,3′,4′,5,7-pentahydroxy-2-phenylchromen-4-one), 3-(4,5-dimethylthiazol-2-yl)-2, 5-diphenyltetrazolium bromide (MTT) and hydroxythylcellulose (HEC) were purchased from Sigma (Sigma Aldrich, France). Tween® 80 (polysorbate 80), TPGS (α tocopheryl polyethylene glycol 1000 succinate), Plantacare® 810 (caprylyl/capryl glucoside), and Plantacare® 1200 (lauryl glycoside) were purchased from Cognis (Ludwigshafen, Germany). Lutrol® F68 (poloxamer188, 1800 g/mol) and Lutrol® F127 (poloxamer407) were kindly provided by BASF (Ludwigshafen, Germany).

2.2. Preparation of quercetin nanosuspensions

Crude quercetin (5%) was suspended in a 0.5% stabilizer solution (Tween® 80, TPGS, Lutrol® F68, Plantacare® 810 or Plantacare® 1200) in milliQ water. Quercetin nanosuspensions were then produced using the smartCrystals® technology [43]. Briefly, 120 ml of primary quercetin suspension was subjected to 30 min milling time using a pearl mill Bühler PML 2 (Bühler AG, Uzwil, Switzerland) with 0.2 mm zirconium oxide beads as milling medium. Samples were withdrawn every 5 min from the wet bead-milling machine to perform in-process size measurements (Sections 2.5 and 2.6). Optimal milling time was determined after analyzing the sizes. After milling, the suspension was separated from the beads using a sieve (mesh size 80). The beads were then washed with 120 ml of original 0.5% stabilizer solution to collect any quercetin crystals adhered to the beads. The resulted suspensions were then homogenized using a high-pressure homogenizer (HPH), Micron LAB 40 (APV Gaulin GmbH, Germany) for two cycles at 300 bar [25]. Finally, the selected stabilizers were used to prepare new batches using the concluded optimal milling time.

2.3. Nanosuspensions – gel formulation

Quercetin nanosuspensions were admixed to two different gel formulations: Lutrol® F127, which is a temperature dependent gelling agent or hydroxythylcellulose (HEC). First, 5% quercetin nanosuspensions were diluted with milliQ water by a mass ratio factor of 1:1.6 and then Lutrol® F127 or HEC was added to allow a final concentration of 16.7% and 1.7% respectively [13,38]. The resulted gels were tested for stability at 4 °C, 25 °C and 40 °C. Size, polydispersity index (PDI) and zeta potential of smartCrystals® were measured at day 0, day 30 and day 90, after a dilution step, to break the gel and allow measurement by photon correlation spectroscopy (see thereafter, Section 2.5 for precise sample preparation).

2.4. Lyophilization

Quercetin nanosuspensions were frozen to -80 °C using Cryonext freezer (Cryonext laboratories, France), and then freeze-dried by Heto lyophilizer (PowerDry Laboservices, France) for 24 h to obtain dry quercetin smartCrystals®.

2.5. Photon correlation spectroscopy and electrophoretic mobility measurements

10 µl of the quercetin nanosuspension was added to 10 ml of MilliQ water, vortexed for 10 s and then measured at 25 °C to obtain the average size (Z-average) and polydispersity index (PDI) by photon correlation spectroscopy using a Zetasizer Nano ZS (Malvern Instruments, UK). 10 µl of the quercetin nanosuspension was diluted with either 10 ml of 50 µS/cm water (calculated by the addition of NaCl solution to MilliQ water) or 10 ml of original stabilizer solution [42]. 1 ml of this mixture was transferred into a Disposable Capillary Cell (Malvern Instruments, UK) allowing the measurement of the electrophoretic velocity of particles in an electrical field and the determination of zeta potential thanks to Helmholtz–Smoluchowski equation.

For size measurements after gel formulation, 10 µl of the gel formulation was diluted with 10 ml MilliQ water and vortexed for 30 s, and then 2 ml was transferred to PCS analysis. For zeta potential measurements, 10 µl of the gel formulation was diluted with 10 ml of either 50 µS/cm water or original stabilizer solution, and vortexed for 1 min; then, 1 ml was transferred to PCS for measurement.

2.6. Laser diffraction (LD)

Size distribution was measured by laser diffraction (Mastersizer 2000 Malvern Instruments, UK) with an agitation speed of 1750 rpm. Sample volume was adjusted according to the

concentration indicated by the manufacturer using deionized water. All sizes were analyzed using the characterization mode of the Mie equation with optical parameters 0.01 for the imaginary refractive index (IRI) and 1.59 for the real refractive index (RI).

2.7. X-ray analysis

X-ray diffraction patterns of dry quercetin smartCrystals® were analyzed using a D8 Advance LA Cu 1.5406 Å Bruker axs (Bruker, Karlsruhe, Germany) equipped with a generator (40 kv 40 mA) and a parafocusing geometry circle of Bragg Brentano. The test was performed between angles of 2 and 70 θ at a fixed detection velocity, and a solid detector lynx eyes 1D was used for the sample detection.

2.8. Transmission electron microscopy

Transmission electron microscope (TEM) analysis was performed with a TEM Jeol 1200EXII (Jeol Ltd, Japan) with an accelerating voltage of 100 kV and equipped with a 4 k/3 kelopixels quemesa Camera (Olympus, Japan). 5 µl of the nanosuspension was left to dry for 30 min at 25 °C after being deposited on uncoated carbon TEM grids Type CU formar carbon 3 MMM (Agar Scientific, UK). Images were taken using MEASURE IT software at appropriate magnification.

2.9. HPLC analysis

HPLC was used for the determination of quercetin concentration in the nanosuspensions and the saturation solubility. The chromatographic analysis of the quercetin nanosuspensions was performed on a LC62010HT (Shimadzu, Kyoto, Japan) using a C18 column Prontosil (120-5-C18 H5.0 µm), NC-04 (250 × 4.0 mm) as stationary phase and a mobile phase solution composed of 10% methanol 80%, acetonitrile and 10% of phosphoric acid 0.2% at a pH = 1.9. The detection was carried by a UV lamp (UV–VIS detector, Shimadzu, Kyoto, Japan) at 368 nm, which is specific for quercetin [64].

Two experiments were developed for the determination of (i) quercetin concentration in the nanosuspension (experiment 1: quercetin is extracted by methanol and then quantified) and (ii) saturation solubility (experiment 2: quercetin concentration is determined in solution without extraction).

For experiment 1, a fixed flow rate of 1 ml/min during a run time of 15 min was set and applied to calculate the quercetin concentration in the final nanosuspension. Standard quercetin solutions prepared in methanol within a range 62.5–500 µg/ml were used as a calibration curve (calibration curve 1 r^2 = 0.999 and % RSD is 2.5). The quercetin retention time was 2.3 min. 10 µl of the quercetin nanosuspension was diluted to 1 ml with methanol and then injected (n = 3).

Secondly, for experiment 2 (quercetin saturation solubility measurements), a gradient flow rate was used in a 20 min run time by increasing the acetonitrile concentration from 40% to 80% while the acidified water concentration decreased from 50% to 10%. The gradient flow was performed in order to delay the elution of quercetin from that of Tween® 20. The quercetin retention time was 4.10 min. Serial dilutions of known concentrations of quercetin in 0.5% Tween® 20 PBS buffer pH = 7.4 were used to prepare a calibration curve from 0.2 to 4 µg/ml (calibration curve 2 r^2 = 0.996 and % RSD is 7.7). Quercetin quantification limit was 0.1 µg/ml. This was performed in order to mimic the situation in an aqueous medium. Then 1 ml of the quercetin nanosuspension, and the quercetin physical dispersion (crude quercetin suspended in milliQ water) were centrifuged at 21,000 gravitational force for 1 h using a Sigma 2k 25 ultracentrifuge (sigma Zentrifugen, GmbH, Germany), to separate the non-solubilized quercetin (bottom of the tube) to the solubilized one (in the supernatant). Centrifugation time is adjusted according to the *Stoke* equation for particle sedimentation. Supernatants were collected and 50 µl of each was injected into HPLC and the water saturation solubility was calculated according to the method mentioned.

2.10. Dissolution velocity (flow through cells)

Flow through cell USP apparatus 4 equipped with a piston pump Sotax (Sotax AG, Aesch, Switzerland) was used for testing the dissolution velocity. 5 mg of dry quercetin smartCrystals® or crude quercetin was accurately weighed using an OHAUS Discovery balance (OHAUS Corporation, New Jersey, USA) and was placed in the sample chamber. 100 ml of degassed MilliQ water was used as release medium to maintain sink conditions. The flow rate was maintained at 8 ml/min at 32 °C (n = 3) and 1 ml of the release medium was withdrawn at 5, 10, 15, 30, 60 and 120 min, and then replaced by 1 ml of fresh medium. Afterward, the quercetin concentration was determined: 50 µl of withdrawn samples was diluted with 950 µl milliQ water and analyzed using HPLC (Section 2.9, experiment 2).

2.11. Hydrogen donating ability in vitro by 2, 2-diphenyl-1-picrylhydrazyl (DPPH)

Quercetin showed linear DPPH inhibition in concentrations between 1 and 6 µg/ml. Quercetin nanosuspensions with selected stabilizers were diluted with methanol to fit into linearity concentrations of quercetin. DPPH concentration was adjusted to 400 µM. The volume of DPPH solution to quercetin solution was 1:3 (volume factor). DPPH with methanol was used as a positive control with methanol as a reference. The activity reaction was performed in the dark for 30 min; afterward the DPPH absorbance was measured at 517 nm using a UV/VIS spectrophotometer (Lambda 35, PerkinElmer, USA). Then the DPPH percentage activity was calculated as efficient concentration 50 (EC50) (the concentration of crude quercetin or quercetin smartCrystals® able to reduce 50% of the initial DPPH concentration).

2.12. Cell culture and cellular cytotoxicity on Vero cells

Vero cells (CCL81™) were purchased from American Type Culture Collection ATCC (Manassas, Virginia, USA). Cells were cultured using Dulbecco's Modified Eagle's medium (DMEM) (Gibco®) with 10% fetal bovine serum (FBS) purchased from Life technologies™ (Carlsbad, California, USA). To assess the potential cytotoxicity of the formulation, cells were cultured at a concentration of 1×10^5 cells/well in 24 well plates (Corning, New York, USA), and incubated for 24 h at 37 °C, 5% CO_2. Cells were then exposed to 5, 15, 25, 50 µg/ml of crude quercetin, or quercetin smartCrystals® (diluted nanosuspensions) suspended in classic cell culture medium (DMEM + 10% FBS). After 24 h exposure, cell viability was assessed by the 3-(4,5-dimethylthiazol-2-yl)-2, 5-diphenyltetrazolium bromide (MTT) assay. The MTT assay evaluates cellular mitochondrial activity by following the cleavage of tetrazolium salts to a soluble formazan dye by succinate–tetrazolium reductase, a mitochondrial enzyme active only in viable cells. MTT (5 mg/ml) was added to each well for 4 h. Culture media were then aspirated and replaced by 200 µl of acidified isopropanol (0.06 N HCl) to dissolve formazan crystals. Finally, 100 µl was transferred to 96 well plates and read at 570 nm and 750 nm using a Multiskan™ GO microplate spectrophotometer (Thermo Scientific™, Waltham, Massachusetts, USA). Non-treated cells were recognized as the positive control and represent the 100% viability.

2.13. Protection against hydrogen peroxide induced cellular toxicity

Cells were cultured at a concentration of 1×10^5 cells/well in 24 well plates and incubated at 37 °C, 5% CO_2 for 24 h. Cells were then exposed to 50 µg/ml of crude quercetin, or quercetin smartCrystals® (diluted nanosuspensions) suspended in classic cell culture medium (DMEM + 10% FBS) for 4 h. After that, 40 µl of 10 mM of hydrogen peroxide (H_2O_2) was added to each well and incubated for 2 h. Cells were then washed two times with PBS. Then, 360 µl of DMEM + 10% FBS and 40 µl of MTT were added and let incubated for another 4 h. Culture media were then aspirated and 200 µl of acidified isopropanol (0.06 N HCl) was added. Finally, 100 µl was transferred into 96 well plate and absorbance at 570 nm and 750 nm was determined using a Multiskan™ GO microplate spectrophotometer (Thermo Scientific™, Waltham, Massachusetts, USA) [19].

2.14. Statistical analysis

Statistical analysis of the dissolution velocity and cellular cytotoxicity was run using Stata software (StataCorp, College Station, Texas, USA). A two-sample *t*-test with unequal variances was used for the analysis of cellular toxicity results and a two-sample *t*-test with unequal variances supported with a two-sample Kolmogorov–Smirnov test for equality of distribution functions was used to verify the significant difference of the dissolution profiles. *P* expresses the significant value where $^{*} = P < 0.05$, $^{**} = P < 0.01$ and $^{***} = P < 0.005$ respectively.

3. Results & discussion

3.1. Optimization of smartCrystals® production process

Optimization of the preparation was performed in two steps: (i) assessing the optimal milling time and (ii) producing the smallest homogenous crystals with each stabilizer (Tween® 80, TPGS, Lutrol® F68, Plantacare® 810 or Plantacare® 1200).

In the first step, the milling time was set for 30 min and quercetin size profile was measured every 5 min using PCS (Fig. 1) and LD (Fig. 2). PCS allow the size measurement of particles from about 3 nm to 3 µm, and LD was therefore used to detect particles larger than 3 µm. LD size results are expressed in terms of the percentage distribution of sizes within the population. Volumes equivalent to the hydrodynamic sphere diameter LD50, LD90, and LD99 diameters are used throughout this article.

By observing the hydrodynamic diameters measured by PCS in Fig. 1, particle size reduction in the nanometer range can be noticed within the first 10 min for all the stabilizers. Within 5 min of milling, the sizes were reduced to 329 nm (PDI 0.21), and to 303 nm (PDI 0.24) for quercetin nanosuspensions stabilized with Tween® 80 and TPGS respectively and to 526 nm (PDI 0.3) for quercetin nanosuspensions stabilized with Plantacare® 810. After 10 min of milling, the size decreased to reach 502 nm (PDI 0.22) with Lutrol® F68 and 574 nm (PDI 0.22) with Plantacare® 1200 respectively. Nevertheless, after either 5 min (Tween® 80, TPGS and Plantacare® 810 stabilized nanosuspensions) or 10 min milling (Lutrol® F68 and Plantacare® 1200 stabilized nanosuspensions), particles began to agglomerate. Upon this prolonged milling time, the energy used for particle fragmentation is converted into kinetic energy increasing particle adhesion and agglomeration, which could explain this size increase [44].

Fig. 2 shows the LD complementary results for the milling process providing information on larger particles in the suspension. The difference between the value of LD50 and LD99 (which is a diameter sensitive to measure very large particles) gives an indication about particles' aggregation state that cannot be monitored by PCS. Results at time 0 represent the size distribution of quercetin in the coarse suspension with each stabilizer. Aggregates larger than 3 µm were not observed at 5 min milling time with Tween® 80 and Plantacare® 810, but still present with TPGS as LD50 and LD99 5 µm and 32 µm respectively. Looking at Lutrol® F68 and Plantacare® 1200 stabilized nanosuspensions, only Lutrol® F68 at 10 min showed aggregation with LD99 equals to 35 µm. Again, by LD upon prolonged milling, particle agglomeration was confirmed with all stabilizers except Tween® 80 and Lutrol® F68. Thus, the best milling time for Tween® 80, TPGS and Plantacare® 810 stabilized nanosuspensions seems to be of 5 min whereas for Lutrol® F68 and Plantacare® 1200 stabilized nanosuspensions 10 min seems better adapted.

After the milling step (30 min), quercetin nanosuspensions stabilized with the five stabilizers were subjected to the same HPH condition (300 bar, 2 cycles). Fig. 3 presents the PCS and LD size results of the final nanosuspensions. The use of HPH yielded smaller and more homogeneous quercetin nanosuspensions with an average size of 220 nm (PDI 0.19) with Tween® 80, 397 nm (PDI 0.16) with TPGS, 381 nm (PDI 0.24) with Lutrol® F68, 426 nm (PDI 0.38) with Plantacare® 810 and 243 nm (PDI 0.37) with Plantacare® 1200 (Fig. 3a). LD99 results were all less than 450 nm for all stabilizers confirming the successful disaggregation with HPH (Fig. 3b). This decrease in particle size and the disappearance of aggregation confirm the advantage of the combinative techniques over one-process techniques. Taking the example of quercetin nanocrystals with Tween® 80 prepared using only bead milling by Kakran's et al., quercetin nanocrystals were approximately 340 nm (PDI 0.21)) and the milling time was 60 min [23]. By applying the smartCrystals® combinative technique, quercetin smartCrystals® were 220 nm (PDI 019) using only 5 min milling followed by HPH.

Taking into account the final suspension size, the smallest average size was obtained with Tween® 80 (220 nm), Plantacare® 1200 (243 nm) and Lutrol® F68 (381 nm) (Fig. 3a). By analyzing PDI data, TPGS was the stabilizer which leads to the lowest polydispersity index of 0.16, followed by Tween® 80 with 0.19 and Lutrol® F68 with 0.24 (Fig. 3a).

From the size, PDI and milling time, it can be concluded that the best two stabilizers for 5% quercetin nanosuspensions prepared by smartCrystals® technology were Tween® 80 and TPGS. SmartCrystals® stabilized with these two stabilizers showed the smallest particles size with homogenous profile in the shortest milling time. As a result, optimized milling conditions with HPH were used to produce new batches of quercetin smartCrystals® stabilized with Tween® 80 and TPGS. The reproduced quercetin nanosuspension was 295 nm (PDI 0.25) with Tween® 80 and 203 nm (PDI 0.24) with TPGS.

Tween® 80 concentration for stabilization of quercetin nanocrystals varied in the literature, from 1 to 2% when 5% quercetin nanosuspensions were prepared by HPH or bead milling. Quercetin nanocrystals prepared only by HPH (20 cycles at 1500 bar) were around 700 nm (PDI 0.17) [50] and quercetin nanocrystals prepared by bead milling alone using 0.2 mm beads were 340 nm (PDI 0.21). By applying the smartCrystals® combination process, a nanometric size of 220 nm (PDI 0.19) was achieved, with twofold lower stabilizer concentration [23].

To resume, small and monodisperse quercetin smartCrystals® were formulated using 2 fold less stabilizer than previously formulated nanocrystals with a shorter production time. This confirms the interest in the use of smartCrystals® combinative technology that allows a reduced milling time, which is very important considering large scale production as long preparation time increases costs and decreases the number of produced batches per day.

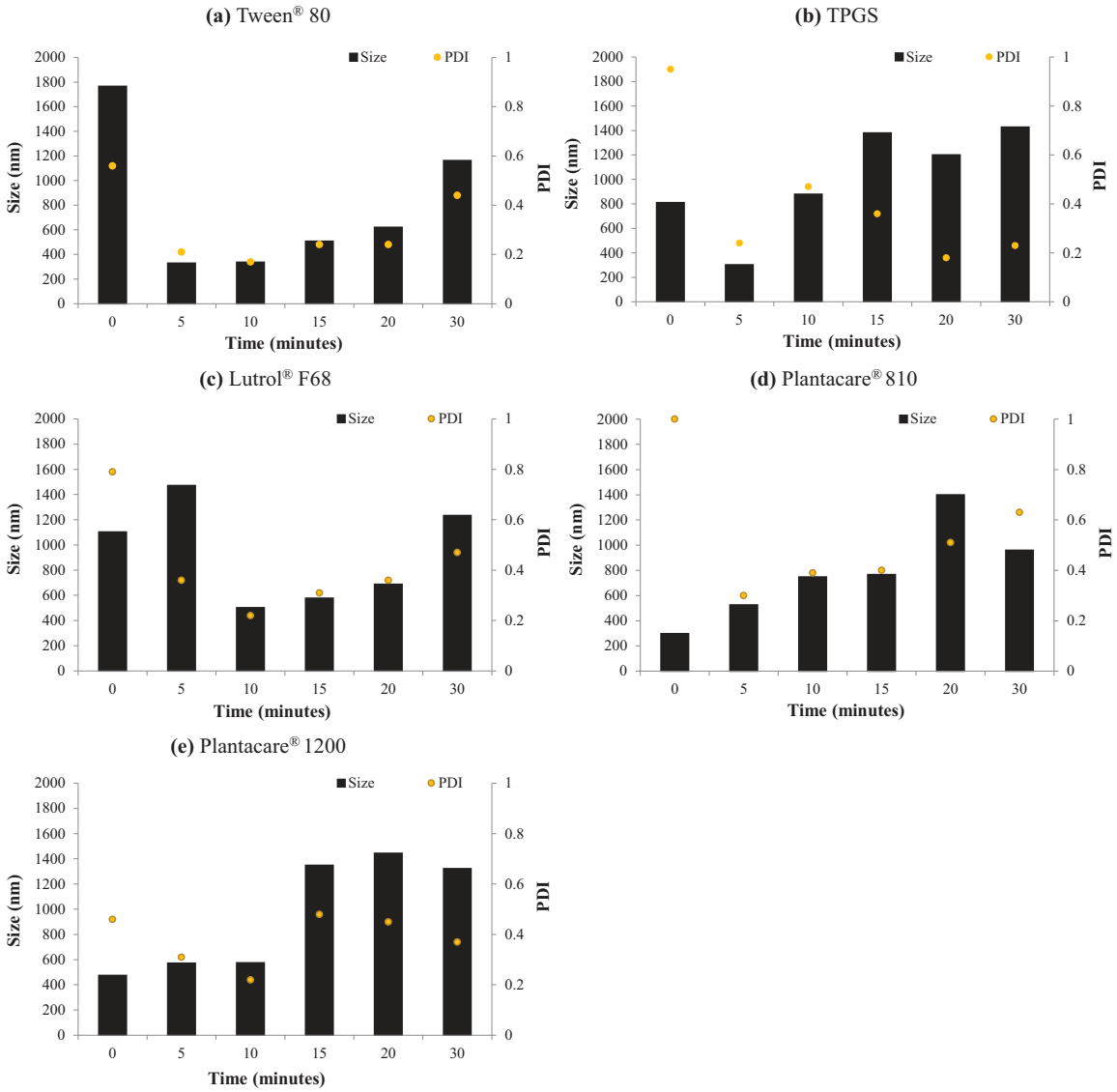

Fig. 1. Quercetin suspension size and PDI evaluation using PCS. PCS size and polydispersity index (PDI) as a function of milling time in the bead mill of suspensions stabilized with (a) Tween® 80, (b) TPGS, (c) Lutrol® F68, (d) Plantacare® 810 and (e) Plantacare® 1200.

3.2. Physicochemical characterizations of quercetin smartCrystals®

3.2.1. Surface charge

To predict the physical stability of quercetin smartCrystals®, zeta potential was measured. The higher the absolute values of the zeta potential, the more stable the particles are expected to be. Results are presented in Fig. 4. The difference between the measurements in the original stabilizer medium (0.5% Tween® 80 or TPGS) and the salted water (50 µS/cm water) provides an indication about the thickness of the diffuse layer, as the diffuse layer is eliminated in the salted water [26]. All zeta potentials of quercetin nanosuspensions were negative, as PEG chains present in the structure of Tween® 80 and TPGS can form negative dipoles that are able to decrease the surface charge proportionally to their concentration [62]. Nanosuspensions stabilized with Tween® 80 compared to TPGS stabilized ones expressed more negative zeta potential in both 50 µS/cm water (−25.7 compared to −16.1 mV) and original stabilizer solution (−26.8 mV compared to −22.7 mV) for nanosuspensions with Tween® 80 and TPGS respectively. Both stabilizers sterically stabilize the particles in addition to the electrical repulsive forces they could generate [63]. Indeed, it should be noted that the adsorbed steric stabilizer layer reduces the measured zeta potential, as it shifts the plan of shear to greater distance from the particle surface. Therefore, values around 25 mV observed with Tween® 80 seem sufficient to stabilize the system along with stearic stabilization [40]. Regarding TPGS, the difference between values at 50 µS/cm water and original stabilizer solution (−16.1 vs. −22.7 mV) may indicate a thicker adsorbed layer compared to Tween® 80 and hence an increased stability [36].

3.2.2. Quercetin nanosuspension stability

For all pharmaceutical and cosmetical products, a satisfactory stability profile is desired. Therefore, three month stability tests were performed on quercetin nanosuspensions. Stability tests were conducted at three different temperatures 4 °C, 25 °C and 40 °C. The average PCS size and PDI at day 0, day 30 and day 90 (Fig. 5a) were used to assess the stability.

The increase in quercetin nanosuspension size from day 0 to day 90 at 25 °C was 50 nm (from 295 to 343 nm) with Tween® 80, and 150 nm (from 203 to 340 nm) with TPGS. Interestingly, PDI remained under 0.30 for both formulations (Fig. 5a). This increase in size has already been observed with lutein nanocrystals

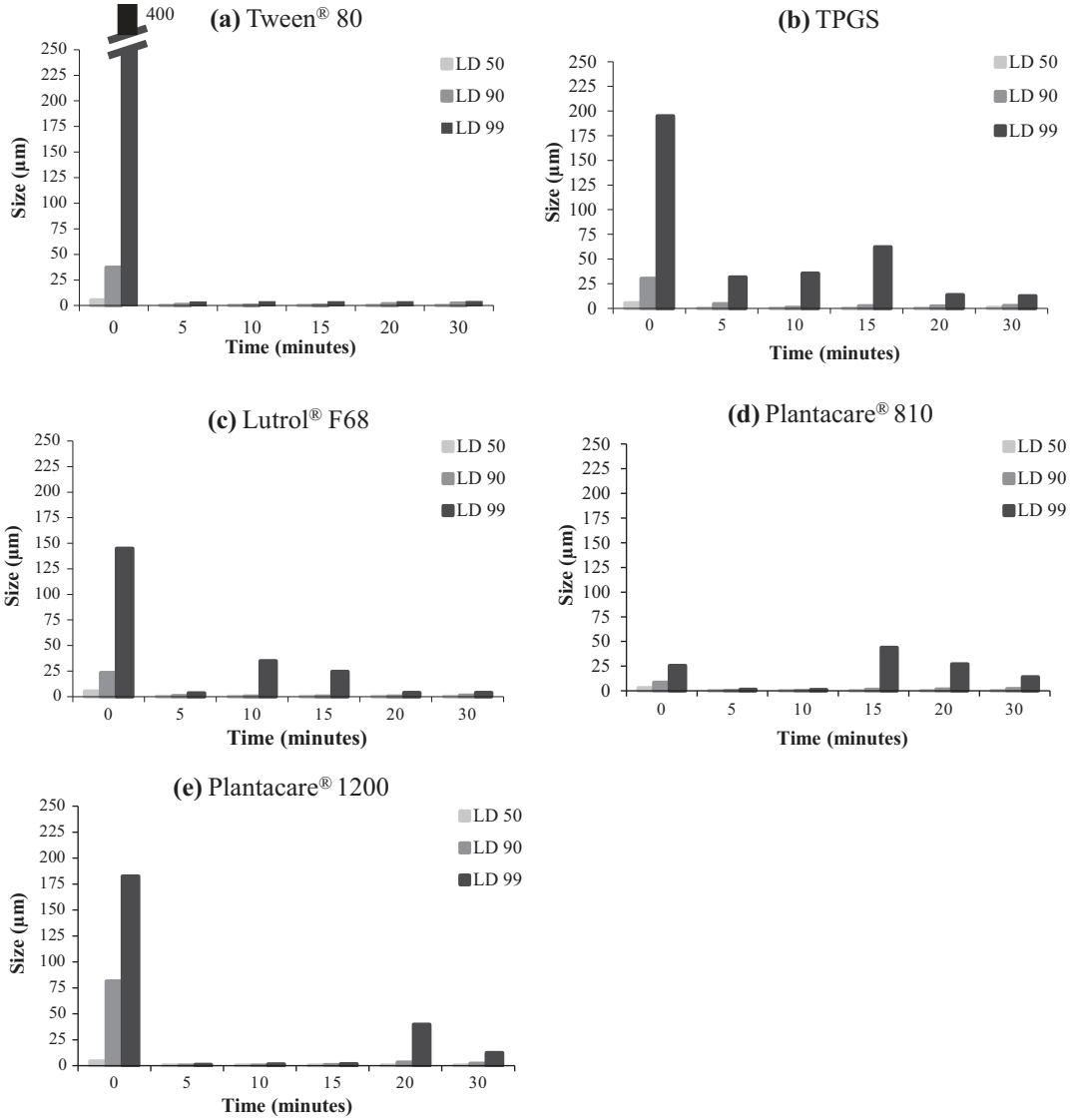

Fig. 2. Quercetin suspension size distribution evaluation using LD. LD size distribution as a function of milling time in the bead mill of suspensions stabilized with (a) Tween® 80, (b) TPGS, (c) Lutrol® F68, (d) Plantacare® 810 and (e) Plantacare® 1200.

when prepared by HPH [37]. In this study, after 90 days of storage at 40 °C, quercetin nanosuspension stabilized with Tween® 80 was 381 nm (PDI 0.19), and quercetin nanosuspensions stabilized with TPGS were 389 nm (PDI 0.16).

3.2.3. Lyophilization and crystallinity determination

To allow X-ray studies, the quercetin nanosuspensions were lyophilized [46]. Therefore, the effect of lyophilization on particles size was first evaluated. For this, dry quercetin smartCrystals® were rehydrated with the original stabilizer solution after lyophilization and the sizes and PDI of these nanosuspensions were measured (Fig. 5b). Before lyophilization, quercetin nanosuspensions stabilized with Tween® 80 were 366 ± 8 nm, and after reconstitution of the suspension the size increased to 403 ± 8 nm. The same increase by about 40 nm in particle size was observed with quercetin nanosuspensions stabilized with TPGS, where particle size increased from 239 ± 8 nm to 290 ± 3 nm. An increase in particles size upon lyophilization by 200 nm was reported with ascorbyl palmitate nanocrystals in the absence of cryoprotectant [59]. Cryoprotectant was not used in our case and the size increase was 5 times less. At the same time, in the case of the ascorbyl palmitate nanocrystals, the PDI increased from ~0.3 to ~0.4 while the PDI stayed the same (0.25 ± 0.03) before and after lyophilization for quercetin nanosuspensions stabilized with Tween® 80 and TPGS. Thus, smartCrystals® were lyophilized without cryoprotectant avoiding strong size increase while keeping a good dispersity.

The X-ray diffraction pattern of coarse quercetin, lyophilized quercetin smartCrystals® stabilized with Tween® 80 and TPGS are given in Fig. 6(a). Peaks at 2, 10.8, 12.5, 15.8, 27.4 θ observed on crude quercetin diffractogram were still present in both lyophilized smartCrystals® formulations, indicating that quercetin after nanonization process had kept its crystalline nature. However, the absence of some peaks on quercetin smartCrystals® stabilized with Tween® 80 and TPGS like the peaks at 9.5, 10.3, 11.4, 11.9 and the reduced extent of the peak at 10.8 and 12.5 compared to crude quercetin, clearly indicate a change in the polymorphic form of quercetin after the nanonization process. This comes in accordance with previous reports showing the presence of three polymorphic forms for quercetin. Crude quercetin powder was

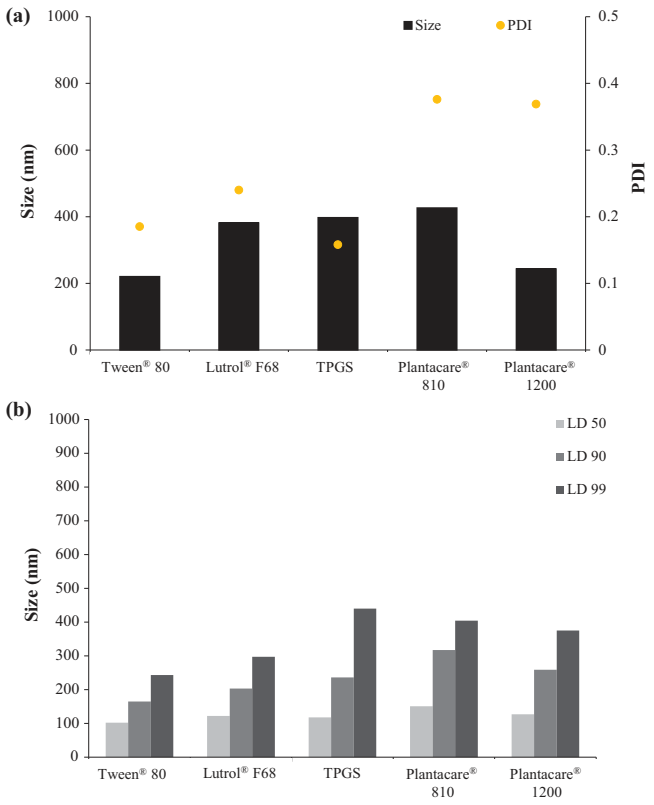

Fig. 3. Final quercetin nanosuspension size results (PCS/LD). Size results of the suspensions with 30 min bead milling with the subsequent HPH step (2 cycles at 300 bar). (a) PCS size and PDI. (b) LD50, LD90 and LD99 of suspensions stabilized with the five different stabilizers.

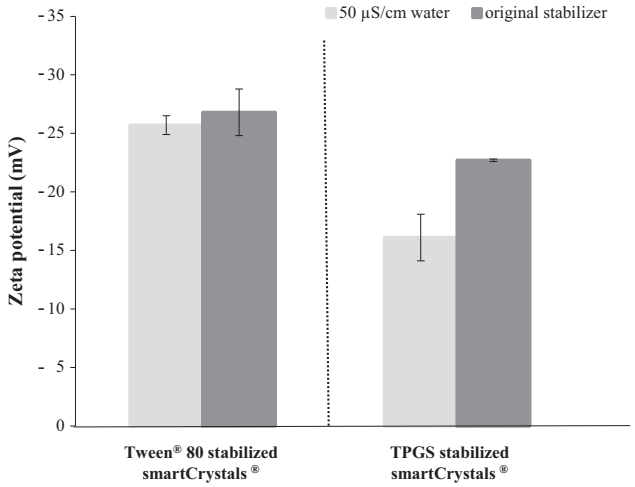

Fig. 4. Zeta potential of quercetin nanosuspensions. Zeta potential of quercetin nanosuspensions with Tween® 80 and TPGS produced by bead milling for 5 min followed by 2 cycles of high pressure homogenization at 300 bar. Reacting media 50 µS/cm water and original stabilizer solution.

pharmaceutical grade (QGPb), and then quercetin in its smartCrystals® form had the pharmaceutical grade (QGPa) [3]. This change in the polymorphic form could have its reflection on the behavior of quercetin in viable system and its interaction with cells.

3.2.4. Electron microscopic examination

5 µl of quercetin nanosuspensions was deposited and dried on TEM grids. Fig. 6(b) shows transmission electron microscopy images of quercetin smartCrystals® stabilized with Tween® 80 (Fig. 6b1 and b2) and TPGS (Fig. 6b3 and b4) diluted with original stabilizer solution (0.5% stabilizer). Images showed the absence of nanocrystals aggregates and liquid droplets around the crystals were hypothesized to be an excess of Tween® 80 (Fig. 6b1). SmartCrystals® in the presence of Tween® 80 were in a needle-like shape with a particle size of about 700 nm to about 2 µm (Fig. 6b2). By contrast, nanocrystals in the presence of TPGS behaved differently as a square shape (500 nm) was prevalent in the samples tested (Fig. 6b3). In addition, with this last stabilizer, a cubic shape, was observed in smaller numbers (Fig. 6b4), which could be linked to the fusion of several nanocrystals together. Particles size in the presence of TPGS was in the same range of PCS results observed between 200 and 500 nm. Square nanocrystal shape was already observed on particles stabilized by Lutrol® F68 (and lecithin) prepared by HPH [12] and also with other nanocrystals (Amoitone B, Nur77 receptor agonist) stabilized by Lutrol® F68 prepared by microfluidization [17]. This confirms that crystal shape is mainly determined by the stabilizers and not only by the process used to obtain nanocrystals.

3.3. Saturation solubility determination

A certain loss of quercetin during milling and in the course of the homogenization step cannot be avoided; thus, quercetin concentration was determined (Table 1). The saturation solubility was determined using HPLC (Section 2.9) for both crude quercetin and quercetin nanosuspensions. Nanosuspensions were centrifuged to separate nanocrystals from dissolved quercetin. Crude quercetin possessed a saturation solubility of 0.48 ± 0.12 µg/ml in MilliQ water, while quercetin smartCrystals® had a saturation solubility of 3.63 ± 0.67 µg/ml and 2.62 ± 0.26 µg/ml when stabilized with Tween® 80 and TPGS, respectively (Table 1). This allowed respectively a 7.56 fold and 5.46 fold increase in saturation solubility. This is in accordance with the fact that particle size in the nanometer range below 1000 nm leads to increase kinetic solubility [21].

3.4. Dissolution rate study

Topical application is also influenced by the dissolution profile of the applied drug. Indeed, with faster dissolution and higher saturation solubility, a higher concentration gradient is generated between dermal formulation and skin; hence, more dissolved drug will be absorbed (Fick law) [5]. The velocity of dissolution of such water insoluble molecule such as quercetin is a limiting step for its absorption. Decreasing particle size to the nanometer range proved to increase water solubility for quercetin nanosuspensions over crude quercetin, favoring an effect on their dissolution kinetics [12]. A faster dissolution profile is required in order to allow a rapid skin penetration of dissolved molecules. Quercetin molecules penetrating into skin should be immediately replaced in the dermal formulation by molecules fast dissolving from the nanocrystals (=depot) [39].

The quercetin smartCrystals® dissolution profile was determined using the flow cell USP apparatus 4 using MilliQ water as dissolution medium. To ensure a temperature near to the skin, dissolution kinetic was performed at 32 °C for 120 min.

Quercetin in its crude form required 30 min to get its highest dissolved amount of 13 ± 4.7% (Fig. 7). The quercetin nanosuspension stabilized with Tween® 80 showed approximately a 6 fold increase in the total dissolved amount compared to crude quercetin with faster dissolution profile with 56.4 ± 3.1% in 5 min and 79.1 ± 13.7% in 30 min ($P < 0.005$). Quercetin nanosuspension stabilized with TPGS showed a dissolution profile with 33.3 ± 2.3% in 5 min and provided its highest dissolved amount in 2 h with

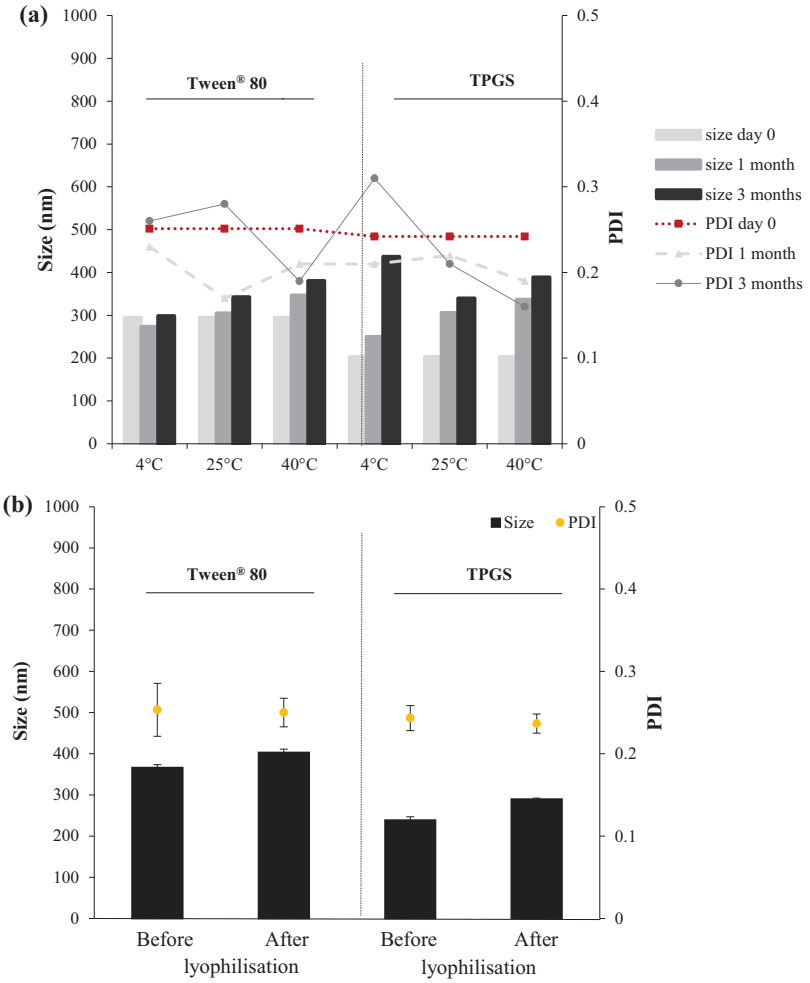

Fig. 5. (a) Quercetin nanosuspension stability at 4 °C, 25 °C and 40 °C. (b) Effect of lyophilisation on the PCS size and PDI of quercetin nanosuspensions. Results recorded before and after lyophilization ±SD ($n = 3$).

94.6 ± 12.6% (about 7.5 fold increase in dissolution compared to crude quercetin, $P < 0.005$). No significant difference was observed between quercetin nanosuspensions stabilized with Tween® 80 and quercetin nanosuspensions stabilized with TPGS dissolution profiles.

3.5. Hydrogen donating ability in vitro by 2,2-diphenyl-1-picrylhydrazyl (DPPH)

To evaluate the antioxidant activity of quercetin, the *in vitro* antioxidant assay with DPPH was used. This molecule, carrying a free radical on its hydrazine position, allows compounds exposing antioxidative effect to react with [1]. DPPH in its radical form has a strong absorption band at 517 nm. The absorbance at this wavelength will be diminished if the molecule reacts with an antioxidant. When quercetin in methanol was added to DPPH methanolic solution, a linear absorbance decrease was observed from 1 μg/ml to 6 μg/ml and then reached its plateau activity (data not shown). The DPPH test was performed on quercetin nanosuspensions in order to determine its activity and whether the formulation affected quercetin free radical activity. 400 μM DPPH solution was used as positive control representing 100% free radical activity or 0% inhibition. EC50 was compared between crude quercetin and quercetin smartCrystals® stabilized with Tween® 80 and TPGS.

Results of antioxidative activity of quercetin smartCrystals® stabilized with Tween® 80 and TPGS were 3.72 ± 0.08 and 3.41 ± 0.07 μg/ml respectively (Table 1). The EC50 values lower than 3.98 μg/ml (crude quercetin) may be attributed to the larger reacting surface of quercetin smartCrystals® compared to crude quercetin, hence providing a greater quantity of quercetin in the DPPH reaction. This can be also explained by a potentiating effect of quercetin with stabilizers, as controls with just stabilizers were not active [60].

3.6. Cellular cytotoxicity

To assess the safety of quercetin smartCrystals®, a cytotoxicity study on VERO cells was performed. Cells were incubated with quercetin smartCrystals® with increasing concentrations of quercetin (5, 15, 25 and 50 μg/ml). This concentration range was tested before on crude quercetin and proved to protect HaCaT cells from a UVB dose of 10 mJ/cm^2 [32].

After 24 h, a MTT assay was performed to determine the cell viability thanks to the evaluation of the mitochondrial succinate dehydrogenase activity. Interestingly, crude quercetin and quercetin smartCrystals® showed the same cell survival rates as the control of non-treated cells (representing the 100% of cell viability) (Fig. 8a). *T*-test was performed to compare the different formulations and no statistical difference was observed ($P > 0.05$), except in case of quercetin smartCrystals® stabilized with Tween® 80, where the lowest viability was observed (83 ± 15.5% viable cells at 50 μg/ml) ($P < 0.05$). To note, the influence of the stabilizers alone was evaluated and revealed no implication of such molecules

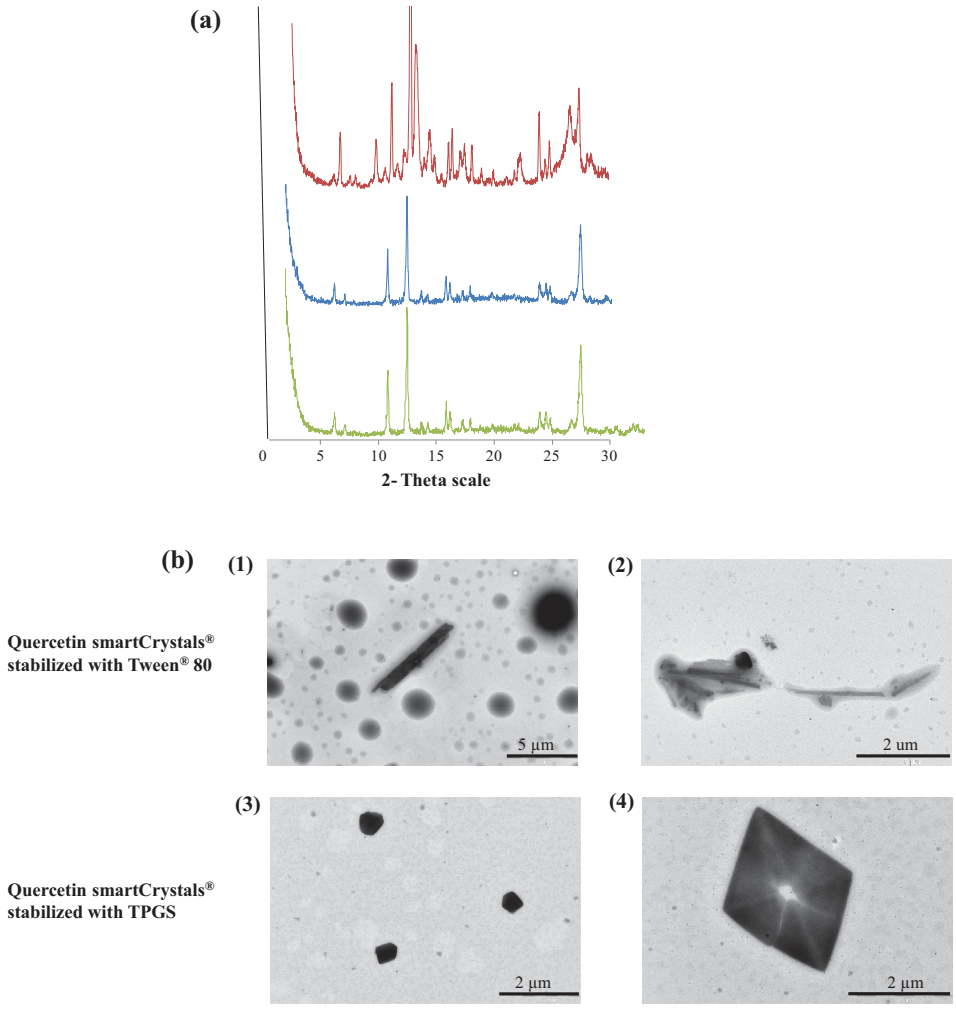

Fig. 6. X-ray diffraction pattern and TEM images of crude quercetin and quercetin nanosuspensions. (a) The X-ray diffraction pattern crude quercetin (upper), lyophilized quercetin smartCrystals® stabilized with Tween® 80 (middle) and TPGS (lower). (b) Images of transmission electron microscopy of quercetin smartCrystals® original stabilizer solution. (1 and 2) With Tween® 80, (3 and 4) with TPGS original stabilizer solution.

Table 1
Quercetin concentration in the nanosuspensions, their saturation solubilities and DPPH activities ±SD ($n = 3$) upon formulation.

	Theoretical concentration w/v%	Measured concentration w/v%	Saturation solubility µg/ml	Saturation solubility increasing factor	DPPH activity EC50 µg/ml
Crude quercetin in milliQ water		–	0.48 ± 0.12	1	3.98
Quercetin smartCrystals® stabilized with Tween® 80	5.00	1.41 ± 0.34	3.63 ± 0.67	7.56	3.72 ± 0.08
Quercetin smartCrystals® stabilized with TPGS	5.00	1.44 ± 0.027	2.62 ± 0.26	5.46	3.41 ± 0.07

on cellular viability. In the range of concentrations tested, no apparent toxicity for quercetin smartCrystals® stabilized with TPGS was observed (statistically indifferent from crude quercetin at the same concentration). Based on these results, quercetin smartCrystals® stabilized with TPGS were regarded safe up to 50 µg/ml concentration on Vero cells.

3.7. Protection against hydrogen peroxide induced cellular toxicity

After the determination of the safety of quercetin smartCrystals® stabilized with Tween® 80 and TPGS (Fig. 8a), the protective effect of quercetin against the cellular viability due to H_2O_2 intoxication was evaluated using MTT (Fig. 8b). 50 µg/ml of crude quercetin or quercetin smartCrystals® was added to cells 4 h before the exposure to H_2O_2. The increase in cellular viability with quercetin pretreatment reflects the antioxidant activity of quercetin. Interestingly, H_2O_2 exposure decreased the percentage of viable cells to 45 ± 9.5%, whereas the pretreatment with crude quercetin significantly protected the cells from H_2O_2 intoxication (96 ± 11%) (Fig. 8b) ($P < 0.005$). At the same level, quercetin smartCrystals® stabilized with Tween® 80 and TPGS were able to show cellular protective actions against H_2O_2 with viable cell percentage of 68 ± 6.8% and 65 ± 6.3% respectively (Fig. 8b). Both results were significantly different from H_2O_2 control cells ($P < 0.05$). The weaker protective ability observed with quercetin smartCrystals® in comparison with crude quercetin may be explained by the change in the polymorphic form of quercetin [3]. Nevertheless, it is important to note that the solubility improvement afforded by quercetin smartCrystals® stabilized allows to overcome this weaker activity.

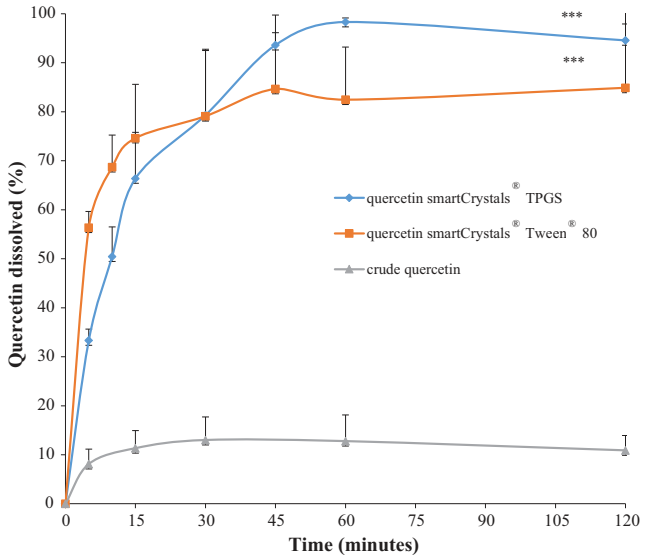

Fig. 7. Dissolution profiles of crude quercetin/quercetin smartCrystals® nanosuspensions stabilized with Tween® 80 and TPGS. Quercetin dissolved percentage normalized to total quercetin quantity ±SD ($n = 3$), *t*-test and Kolmogorov–Smirnov test showed significant difference between crude quercetin and quercetin smartCrystals®, * = $P < 0.05$, ** = $P < 0.01$ and *** = $P < 0.005$.

3.8. Quercetin smartCrystals® incorporation into nonionic gels and their stability in gel formulation

With the final goal of a topical application, Quercetin smartCrystals® stabilized with Tween® 80 and TPGS were formulated within two type of gels: Lutrol® F127 and HEC. These two gelling agents are widely used in dermal and cosmetic applications as permeability enhancers. The main scope was therefore to reach a certain permeation level, where quercetin can exert its antioxidative effect on viable keratinocytes and at the same time can be associated with a formulation with suitable viscosity for the topical application. As an example, Lutrol® F127 (reversible thermogel) showed 6.4, 7.5, and 19.5 fold higher permeation coefficients for 5-aminolevulinic acid (treatment of actinic keratosis in photodynamic therapy) on human stratum corneum compared to the German Pharmacopeia Dolgit®, Basiscreme DAC, and to water containing hydrophilic ointment [15]. It was also proved to give superior percutaneous absorption in rats for indomethacin (in 20% (w/w) Lutrol® F127 hydrogel) [38] as well as with other drug as the anticancer doxorubicin [11]. Advantageous topical application was also observed using HEC (nonionic water-soluble polymer that possesses thickening abilities) with the antibiotic vancomycin for wound treatment [13]. The introduction of propylene glycol to the HEC based formulation of cidofovir (anti-viral drug) increased its transdermal delivery form 0.2% to 2.1% [9].

In this study after their formulations, gels including smartCrystals® were diluted with milliQ water in order to control the size, polydispersity index and zeta potential of the formulated smartCrystals® using PCS (Fig. 9). PCS is not the most adapted method for the visualization of smartCrystals® behavior upon their association to gel; however, this should provide information to which extent incorporation into gels can cause smartCrystals® aggregation and affect the stabilizing charge. Here, smartCrystals® incorporated to HEC gels showed larger sizes with both stabilizers Tween® 80 (651 nm, PDI 0.33) and TPGS (666 nm, PDI 0.42) (Fig. 9a) compared to Lutrol® F127 based gels: (378 nm, PDI 0.20) and (399 nm, PDI 0.30) for quercetin nanosuspensions stabilized with Tween® 80 and TPGS, respectively (Fig. 9a). The increase in smartCrystals® particle size upon their association with gels compared to smartCrystals® alone can be linked to the presence of

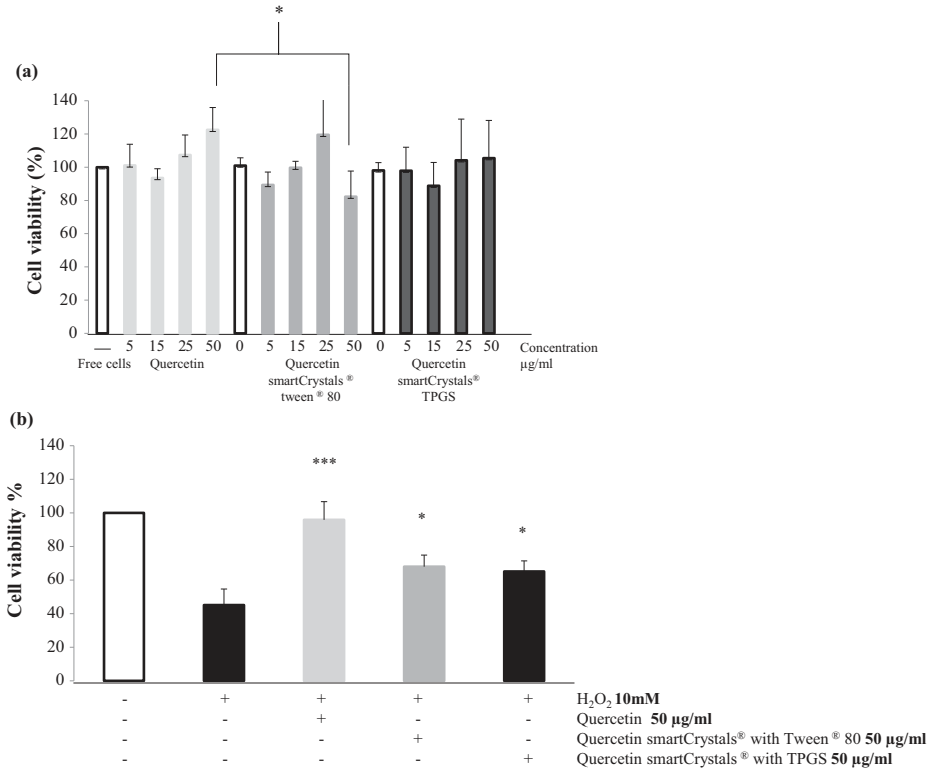

Fig. 8. Cellular toxicity (a) and cellular protective effect on H_2O_2 exposure (b) of quercetin and quercetin smartCrystals®. (a) Effect of crude quercetin and quercetin smartCrystals® stabilized with Tween® 80 and TPGS on viability of Vero cells. ±SD ($n = 3$) after 24 h treatment. (b) Protective effect of crude quercetin and quercetin smartCrystals® stabilized with Tween® 80 and TPGS on viability of Vero cells after the exposure to 10 mM of H_2O_2 (*T*-test *P* values > 0.05, no statistical difference between the data).

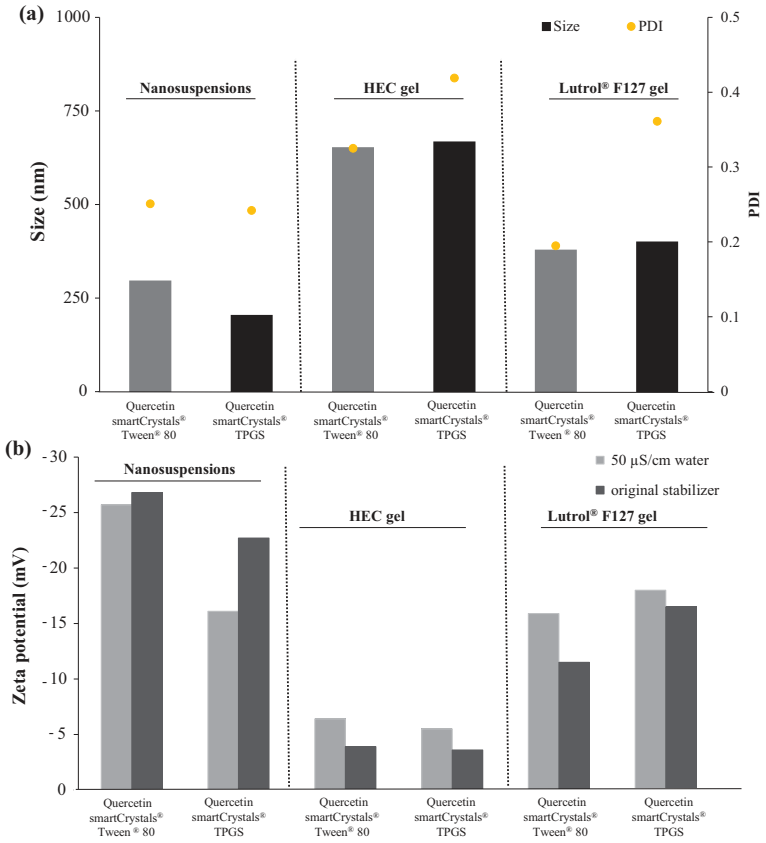

Fig. 9. Quercetin smartCrystals® associated with nonionic gels results PCS. Quercetin smartCrystals® formulated into HEC 1.7 w/w% gel and Lutrol® F127 16.7 w/w% gel, (a) average particles size and polydispersity index (PDI). (b) Zeta potential (absolute value).

Lutrol® F127 and HEC molecules at the surface of stabilized smartCrystals®. Mun et al., described a retardation in the diffusion of PEGylated nanoparticles because of the presence of HEC polymers using NanoSight nanoparticle tracking analysis, and evidenced an interaction between PEG chains and HEC polymers [45]. This could be the case for quercetin smartCrystals® stabilized by Tween® 80 and TPGS (PEG containing stabilizers). The presence of HEC molecules interacting with PEG chains at the surface of smartCrystals® could led to the observed size increase. In the same way, hydrophilic interactions between PEG moieties (from the surfactant stabilized smartCrystals® and the Lutrol® F127 molecules) could happen and could be correlated with the previously evocated size and zeta measurement modifications with smartCrystals® after their association with Lutrol® F127 gel. [58]. Indeed, we observed a decrease in the zeta potential values for smartCrystals® associated with gels compared to smartCrystals® alone (zeta potential: −27 mV vs. −4 mV for smartCrystals® stabilized by Tween® 80 and −23 mV vs. −4 mV for smartCrystals® stabilized by TPGS). This decrease can be explained both by (i) the presence of gels molecules at smartCrystals® surface (leading to a shift of the plan of shear to a greater distance thus causing a reduction in the measured value) and (ii) to a change in the dynamic electrophoretic mobility of the smartCrystals®. In contrast to smartCrystals® alone, zeta potential values in the gels were higher in 50 µS/cm water compared to original stabilizer solution. This can be due to the readsorption of the stabilizer molecules found in the original stabilizer solution on the diffuse layer of the polymers (HEC, Lutrol® F127), thus decreasing the measured zeta potential.

Regarding the stability of quercetin nanosuspensions associated with gels (Fig. 10a and b), at day 0, nanosuspensions associated with HEC gels showed higher size and PDI results compared to nanosuspensions associated with Lutrol® F127 gels. At day 90 at 40 °C, nanosuspensions associated with both gels showed particle sizes above 400 nm and PDI above 0.31. Sizes were 568 nm and 469 nm for nanosuspension stabilized with Tween® 80 (Fig. 10a) and 419 nm and 598 nm for nanosuspension stabilized with TPGS ((Fig. 9b) with HEC and Lutrol® F127 respectively. Values were about 200 nm higher than those of nanosuspensions alone at the same temperature (Fig. 5a: 381 and 389 nm with Tween® 80 and TPGS), which indicates that 40 °C is not a suitable storage temperature for both gels.

At day 90 at 25 °C, quercetin nanosuspension stabilized with Tween® 80 presented higher size values than that of nanosuspension stabilized with TPGS (481 nm, PDI = 0.37 vs. 342 nm, PDI = 0.33) for both HEC gel and (474 nm, PDI = 0.34 vs. 352 nm, PDI = 0.33) Lutrol® F127 gel. By referring back to nanosuspension alone at the same temperature, the size increase with nanosuspension stabilized with Tween® 80 after the gel association is more pronounced (from 343 nm to 481 nm and 474 nm) compared to nanosuspension stabilized with TPGS (340 nm to 342 and 352 nm). This result indicates that nanosuspension stabilized with TPGS presented an increased stability in gels compared to nanosuspension stabilized with Tween® 80.

Lastly excluding values at 40 °C, all gel formulations after 90 days, smartCrystals® size exposed after dilution was less than 500 nm and PDI values 0.4, which indicates acceptable homogeneity of the formulated gels (for dermal application). However, the preferred storage condition seems to be 25 °C for gel formulations, and this seems adequate to a cosmetic use. To conclude, TPGS seems to allow an increased stabilization of quercetin nanosuspensions in the gel formulations compared to Tween® 80.

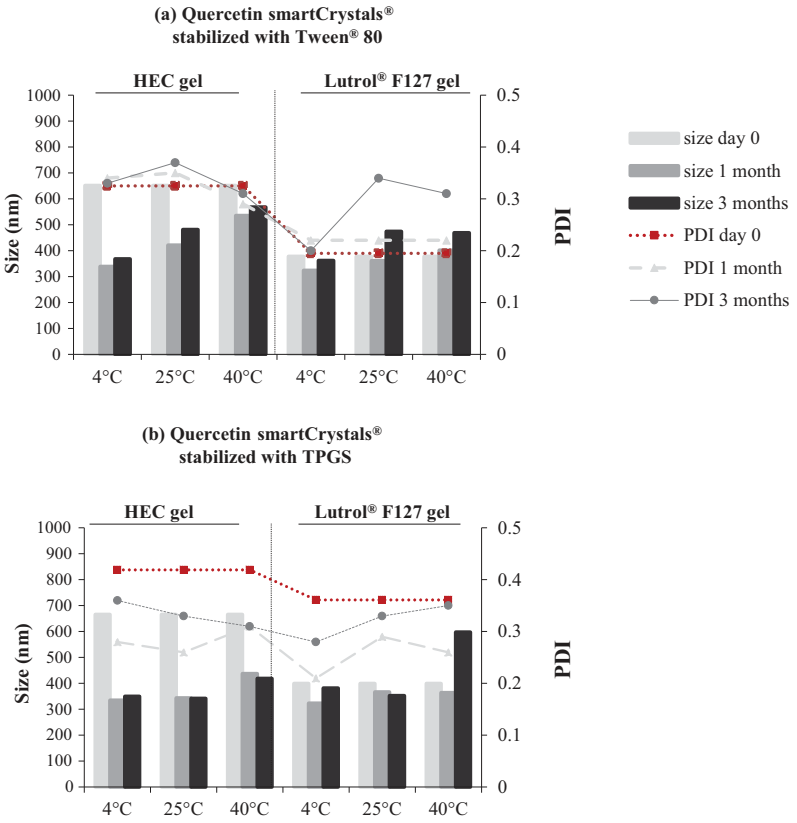

Fig. 10. Stability results of (a) quercetin smartCrystals® stabilized with Tween® 80 incorporated into nonionic gels, (b) quercetin smartCrystals® stabilized with TPGS incorporated into nonionic gels. PCS diameter and PDI of (a) quercetin smartCrystals® stabilized with Tween® 80 incorporated into HEC and Lutrol® F127 nonionic gels. (b) Quercetin smartCrystals® stabilized with TPGS incorporated into HEC and Lutrol® F127 nonionic gels (storage at 4 °C, 25 °C, and 40 °C).

4. Conclusion

Quercetin second-generation nanocrystals (smartCrystals®) were successfully formulated allowing a decrease in both the stabilizer amount required (0.5%) and time of preparation process compared to previous studies [22]. Among the five tested stabilizers, quercetin smartCrystals® stabilized with Tween® 80 and TPGS had the smallest particle size with a short milling time (5 min). Produced quercetin smartCrystals® possessed higher saturation solubility and dissolution velocity compared to crude drug (7 fold) and retained antioxidative activity. Moreover quercetin smartCrystals® proved physical stability over three months in nanosuspensions at 4 °C, 25 °C and 40 °C. Interestingly, a higher antioxidative ability was observed with TPGS stabilized smartCrystals® on DPPH assay (3.14 μg/ml instead of 3.98 μg/ml with crude quercetin), in addition to a safe profile and protective activity on Vero cells at a concentration up to 50 μg/ml with retained activity against hydrogen peroxide toxicity. TPGS therefore proved to be superior stabilizer for quercetin smartCrystals®. These results are promising and propose TPGS as a novel stabilizer for nanocrystals, which, as a derivative of vitamin E, is well adapted for a topical application. With this objective in mind, quercetin nanosuspensions were incorporated into Lutrol® F127 and HEC gels. Quercetin dermal gels were stable at 25 °C for 90 days which is coherent to a daily topical application and evidence the interest of our new formulation as a new antioxidant cosmetic product.

Acknowledgments

Authors acknowledge the financial support of ERASMUS MUNDUS AVEMPACE 2 and L'Ecole Doctorale Sciences Chimiques Balard ED 459 associée à la Fondation Balard (Chaire Total) Montpellier. All thanks go for the technical support of Mme. Corinna Schmidt, Dr. Corine Tourne-Peteilh and Mr. Pradial Peralta.

Appendix A. Supplementary material

Supplementary data associated with this article can be found, in the online version, at http://dx.doi.org/10.1016/j.ejpb.2016.03.004.

References

[1] M.S. Blois, Antioxidant determinations by the use of a stable free radical, Nature 181 (1958) 1199–1200.
[2] F. Bonina, M. Lanza, L. Montenegro, C. Puglisi, A. Tomaino, D. Trombetta, F. Castelli, A. Saija, Flavonoids as potential protective agents against photo-oxidative skin damage, Int. J. Pharm. 145 (1996) 87–94.
[3] G.S. Borghetti, I.M. Costa, P.R. Petrovick, V.P. Pereira, V.L. Bassani, Characterization of different samples of quercetin in solid-state: indication of polymorphism occurrence, Pharmazie 61 (9) (2006) 802–804.
[4] R. Casagrande, S.R. Georgetti, W.A. Verri Jr., D.J. Dorta, A.C. dos Santos, M.J.V. Fonseca, Protective effect of topical formulations containing quercetin against UVB-induced oxidative stress in hairless mice, J. Photochem. Photobiol., B 84 (2006) 21–27.
[5] G. Cevc, U. Vierl, Nanotechnology and the transdermal route: a state of the art review and critical appraisal, J. Control. Release 141 (2010) 277–299.
[6] J. Cheel, P.V. Antwerpen, L. Tůmová, G. Onofre, D. Vokurková, K. Zouaoui-Boudjeltia, M. Vanhaeverbeek, J. Nève, Free radical-scavenging, antioxidant and immunostimulating effects of a licorice infusion (*Glycyrrhiza glabra* L.), Food Chem. 122 (2010) 508–517.
[7] N. Chondrogianni, S. Kapeta, I. Chinou, K. Vassilatou, I. Papassideri, E.S. Gonos, Anti-ageing and rejuvenating effects of quercetin, Exp. Gerontol. 45 (2010) 763–771.
[8] M. Comalada, D. Camuesco, S. Sierra, I. Ballester, J. Xaus, J. Galvez, A. Zarzuelo, In vivo quercitrin anti-inflammatory effect involves release of quercetin, which inhibits inflammation through down-regulation of the NF-kappaB pathway, Eur. J. Immunol. 35 (2005) 584–592.
[9] K.C. Cundy, G. Lynch, W.A. Lee, Bioavailability and metabolism of cidofovir following topical administration to rabbits, Antivir. Res. 35 (1997) 113–122.

[10] D. Dodda, R. Chhajed, J. Mishra, Protective effect of quercetin against acetic acid induced inflammatory bowel disease (IBD) like symptoms in rats: possible morphological and biochemical alterations, Pharmacol. Rep. 66 (2014) 169–173.
[11] V.Y. Erukova, O.O. Krylova, Y.N. Antonenko, N.S. Melik-Nubarov, Effect of ethylene oxide and propylene oxide block copolymers on the permeability of bilayer lipid membranes to small solutes including doxorubicin, Biochim. et Biophys. Acta (BBA) – Biomembr. 1468 (2000) 73–86.
[12] L. Gao, G. Liu, X. Wang, F. Liu, Y. Xu, J. Ma, Preparation of a chemically stable quercetin formulation using nanosuspension technology, Int. J. Pharm. 404 (2011) 231–237.
[13] G. Giandalia, V. De Caro, L. Cordone, L.I. Giannola, Trehalose–hydroxyethylcellulose microspheres containing vancomycin for topical drug delivery, Eur. J. Pharm. Biopharm. 52 (2001) 83–89.
[14] A.S.B. Goebel, U. Knie, C. Abels, J. Wohlrab, R.H.H. Neubert, Dermal targeting using colloidal carrier systems with linoleic acid, Eur. J. Pharm. Biopharm. 75 (2010) 162–172.
[15] N. Gruning, C.C. Muller-Goymann, Physicochemical characterisation of a novel thermogelling formulation for percutaneous penetration of 5-aminolevulinic acid, J. Pharm. Sci. 97 (2008) 2311–2323.
[16] C. Gupta, D.N. Tripathi, A. Vikram, P. Ramarao, G.B. Jena, Quercetin inhibits diethylnitrosamine-induced hepatic preneoplastic lesions in rats, Nutr. Cancer 63 (2011) 234–241.
[17] L. Hao, X. Wang, D. Zhang, Q. Xu, S. Song, F. Wang, C. Li, H. Guo, Y. Liu, D. Zheng, Q. Zhang, Studies on the preparation, characterization and pharmacokinetics of Amoitone B nanocrystals, Int. J. Pharm. 433 (2012) 157–164.
[18] M.M. Heinen, M.C. Hughes, T.I. Ibiebele, G.C. Marks, A.C. Green, J.C. van der Pols, Intake of antioxidant nutrients and the risk of skin cancer, Eur. J. Cancer 43 (2007) 2707–2716.
[19] S.J. Heo, S.C. Ko, S.M. Kang, H.S. Kang, J.P. Kim, S.H. Kim, Y.J. Jeon, Cytoprotective effect of fucoxanthin isolated from brown algae sargassum siliquastrum against h2o2-induced cell damage, Eur. Food Res. Technol. 228 (1) (2008) 145–151.
[20] K. Ioku, T. Tsushida, Y. Takei, N. Nakatani, J. Terao, Antioxidative activity of quercetin and quercetin monoglucosides in solution and phospholipid bilayers, Biochim. Biophys. Acta 1234 (1995) 99–104.
[21] J.-U.A.H. Junghanns, R.H. Müller, Nanocrystal technology, drug delivery and clinical applications, Int. J. Nanomed. 3 (2008) 295–310.
[22] M. Kakran, N.G. Sahoo, L. Li, Z. Judeh, Fabrication of quercetin nanoparticles by anti-solvent precipitation method for enhanced dissolution, Powder Technol. 223 (2012) 59–64.
[23] M. Kakran, R. Shegokar, N.G. Sahoo, L. Al Shaal, L. Li, R.H. Müller, Fabrication of quercetin nanocrystals: comparison of different methods, Eur. J. Pharm. Biopharm. 80 (2012) 113–121.
[24] C. Kandaswami, L.T. Lee, P.P. Lee, J.J. Hwang, F.C. Ke, Y.T. Huang, M.T. Lee, The antitumor activities of flavonoids, In Vivo 19 (2005) 895–909.
[25] C. Keck, S. Kobierski, R. Mauludin, H.R. Müller, Second generation of drug nanocrystals for delivery of poorly soluble drugs: smartCrystal technology, Dosis 24 (2008) 124–128.
[26] C.M. Keck, A. Kovačević, R.H. Müller, S. Savić, G. Vuleta, J. Milić, Formulation of solid lipid nanoparticles (SLN): the value of different alkyl polyglucoside surfactants, Int. J. Pharm. 474 (2014) 33–41.
[27] M.J. Ko, C.I. Cheigh, S.W. Cho, M.S. Chung, Subcritical water extraction of flavonol quercetin from onion skin, J. Food Eng. 102 (2011) 327–333.
[28] A. Kumar, A.K. Malik, D.K. Tewary, A new method for determination of myricetin and quercetin using solid phase microextraction–high performance liquid chromatography–ultra violet/visible system in grapes, vegetables and red wine samples, Anal. Chim. Acta 631 (2009) 177–181.
[29] H. Li, X. Zhao, Y. Ma, G. Zhai, L. Li, H. Lou, Enhancement of gastrointestinal absorption of quercetin by solid lipid nanoparticles, J. Control. Release 133 (2009) 238–244.
[30] C.F. Lin, Y.L. Leu, S.A. Al-Suwayeh, M.C. Ku, T.-L. Hwang, J.-Y. Fang, Anti-inflammatory activity and percutaneous absorption of quercetin and its polymethoxylated compound and glycosides: the relationships to chemical structures, Eur. J. Pharm. Sci. 47 (2012) 857–864.
[31] C.M. Liu, Y.Z. Sun, J.M. Sun, J.Q. Ma, C. Cheng, Protective role of quercetin against lead-induced inflammatory response in rat kidney through the ROS-mediated MAPKs and NF-κB pathway, Biochim. et Biophys. Acta (BBA) – Gen. Sub. 1820 (2012) 1693–1703.
[32] D. Liu, H. Hu, Z. Lin, D. Chen, Y. Zhu, S. Hou, X. Shi, Quercetin deformable liposome: preparation and efficacy against ultraviolet B induced skin damages in vitro and in vivo, J. Photochem. Photobiol., B 127 (2013) 8–17.
[33] L. Liu, Y. Tang, C. Gao, Y. Li, S. Chen, T. Xiong, J. Li, M. Du, Z. Gong, H. Chen, L. Liu, P. Yao, Characterization and biodistribution in vivo of quercetin-loaded cationic nanostructured lipid carriers, Colloids Surf. B 115 (2014) 125–131.
[34] G.G. Liversidge, K.C. Cundy, J.F. Bishop, D.A. Czekai, S.D. Inc., Dispersion, Bioavailability, U.S. Patent No. 5,145,684. U.S. Patent and Trademark Office, Washington, DC, 1992.
[35] S.Y. Lyu, J.Y. Rhim, W.B. Park, Antiherpetic activities of flavonoids against herpes simplex virus type 1 (HSV-1) and type 2 (HSV-2) in vitro, Arch. Pharm. Res. 28 (2005) 1293–1301.
[36] P.R. Mishra, L.A. Shaal, R.H. Müller, C.M. Keck, Production and characterization of Hesperetin nanosuspensions for dermal delivery, Int. J. Pharm. 371 (2009) 182–189.
[37] K. Mitri, R. Shegokar, S. Gohla, C. Anselmi, R.H. Müller, Lipid nanocarriers for dermal delivery of lutein: preparation, characterization, stability and performance, Int. J. Pharm. 414 (2011) 267–275.
[38] S. Miyazaki, T. Tobiyama, M. Takada, D. Attwood, Percutaneous absorption of indomethacin from pluronic F127 gels in rats, J. Pharm. Pharmacol. 47 (1995) 455–457.
[39] K. Moser, K. Kriwet, A. Naik, Y.N. Kalia, R.H. Guy, Passive skin penetration enhancement and its quantification in vitro, Eur. J. Pharm. Biopharm. 52 (2001) 103–112.
[40] R.H. Müller, Colloidal Carriers for Controlled Drug Delivery and Targeting, Wissenschaftliche Verlagsgesellschaft, Stuttgart, Germany, 1991. and CRC Press, Boca Raton, FL.
[41] R.H. Müller, R. Becker, B. Kruss, K. Peters, Pharmaceutical Nanosuspensions for Medicament Administration as Systems With Increased Saturation Solubility and Rate of Solution, United States Patent 5,858,410, Medac Gesellschaft für Klinische Spezialpraparate mbH, 1999.
[42] R.H. Müller, C. Jacobs, Buparvaquone mucoadhesive nanosuspension: preparation, optimisation and long-term stability, Int. J. Pharm. 237 (2002) 151–161.
[43] R.H. Müller, C.M. Keck, Second generation of drug nanocrystals for delivery of poorly soluble drugs: smartCrystal technology, Eur. J. Pharm. Sci. 34 (2008) S20–S21.
[44] A.K. Nath, C. Jiten, K.C. Singh, Influence of ball milling parameters on the particle size of barium titanate nanocrystalline powders, Physica B 405 (2010) 430–434.
[45] E.A. Mun, C. Hannell, S.E. Rogers, P. Hole, A.C. Williams, V.V. Khutoryanskiy, On the role of specific interactions in the diffusion of nanoparticles in aqueous polymer solutions, Langmuir 30 (1) (2014) 308–317.
[46] K. Peters, S. Leitzke, J.E. Diederichs, K. Borner, H. Hahn, R.H. Müller, S. Ehlers, Preparation of a clofazimine nanosuspension for intravenous use and evaluation of its therapeutic efficacy in murine Mycobacterium avium infection, J. Antimicrob. Chemother. 45 (2000) 77–83.
[47] R. Petersen, Nanocrystals for Use in Topical Cosmetic Formulations and Method of Production Thereof, US Patent 60/8866233, 2006.
[48] X. Qu, D. Qi, F. Dong, B. Wang, R. Guo, M. Luo, R. Yao, Quercetin improves hypoxia–ischemia induced cognitive deficits via promoting remyelination in neonatal rat, Brain Res. 1553 (2014) 31–40.
[49] J.S. Reis, M.A. Corrêa, M.C. Chung, J.L. dos Santos, Synthesis, antioxidant and photoprotection activities of hybrid derivatives useful to prevent skin cancer, Bioorg. Med. Chem. 22 (2014) 2733–2738.
[50] N. Sahoo, M. Kakran, L. Shaal, L. Li, R. Müller, M. Pal, L. Tan, Preparation and characterization of quercetin nanocrystals, J. Pharm. Sci. 100 (2011) 2379–2390.
[51] A. Saija, M. Scalese, M. Lanza, D. Marzullo, F. Bonina, F. Castelli, Flavonoids as antioxidant agents: Importance of their interaction with biomembranes, Free Radical Biol. Med. 19 (1995) 481–486.
[52] J. Salazar, R.H. Müller, J.P. Möschwitzer, Combinative particle size reduction technologies for the production of drug nanocrystals, J. Pharm. 2014 (2014) 265–754.
[53] A. Schieber, P. Hilt, J. Conrad, U. Beifuss, R. Carle, Elution order of quercetin glycosides from apple pomace extracts on a new HPLC stationary phase with hydrophilic endcapping, J. Sep. Sci. 25 (2002) 361–364.
[54] J.C. Schwarz, A. Weixelbaum, E. Pagitsch, M. Löw, G.P. Resch, C. Valenta, Nanocarriers for dermal drug delivery: influence of preparation method, carrier type and rheological properties, Int. J. Pharm. 437 (2012) 83–88.
[55] R. Shegokar, R.H. Müller, Nanocrystals: industrially feasible multifunctional formulation technology for poorly soluble actives, Int. J. Pharm. 399 (2010) 129–139.
[56] G.A. Spanos, R.E. Wrolstad, Phenolics of apple, pear, and white grape juices and their changes with processing and storage. A review, J. Agric. Food Chem. 40 (1992) 1478–1487.
[57] M. Subramaneyaan, S. Rustagi, S.N. Bhattacharya, A.K. Tripathi, B.D. Banerjee, R.S. Ahmed, Effect of antioxidant supplementation on free radical scavenging system and immune response in lindane treated scabies patients, Pestic. Biochem. Physiol. 102 (2012) 91–94.
[58] S. Staufenbiel, C.M. Keck, R.H. Müller, The "real environment" quantification of surface hydrophobicity of differently stabilized nanocrystals as key parameter for organ distribution, Macromol. Sym. 345 (1) (2014) 32–41.
[59] V. Teeranachaideekul, V.B. Junyaprasert, E.B. Souto, R.H. Müller, Development of ascorbyl palmitate nanocrystals applying the nanosuspension technology, Int. J. Pharm. 354 (2008) 227–234.
[60] S.A.B.E. van Acker, L.M.H. Koymans, A. Bast, Molecular pharmacology of vitamin E: structural aspects of antioxidant activity, Free Rad. Biol. Med. 15 (1993) 311–328.
[61] F.T.M.C. Vicentini, T.R.M. Simi, J.O. Del Ciampo, N.O. Wolga, D.L. Pitol, M.M. Iyomasa, M.V.L.B. Bentley, M.J.V. Fonseca, Quercetin in w/o microemulsion: in vitro and in vivo skin penetration and efficacy against UVB-induced skin damages evaluated in vivo, Eur. J. Pharm. Biopharm. 69 (2008) 948–957.
[62] A. Vonarbourg, P. Saulnier, C. Passirani, J.P. Benoit, Electrokinetic properties of noncharged lipid nanocapsules: influence of the dipolar distribution at the interface, Electrophoresis 26 (11) (2005) 2066–2075.
[63] L. Wu, J. Zhang, W. Watanabe, Physical and chemical stability of drug nanoparticles, Adv. Drug Deliv. Rev. 63 (2011) 456–469.
[64] L.J. Yang, P. Li, Y.J. Gao, H.F. Li, D.C. Wu, R.X. Li, Time resolved UV–VIS absorption spectra of quercetin reacting with various concentrations of sodium hydroxide, Guang Pu Xue Yu Guang Pu Fen Xi 29 (6) (2009) 1632–1635.
[65] H. Zhang, M. Zhang, L. Yu, Y. Zhao, N. He, X. Yang, Antitumor activities of quercetin and quercetin-5′,8-disulfonate in human colon and breast cancer cell lines, Food Chem. Toxicol. 50 (2012) 1589–1599.

Résumé de thèse :

Les flavonoïdes sont des pigments d'origine naturelle conférant leurs couleurs aux fleurs et aux fruits, identifiés dans plus de quatre milles espèces. Les flavonoïdes sont classés selon leur structure chimique de base formée par deux cycles aromatiques reliés par trois carbones : C6-C3-C6, chaîne souvent fermée en un hétérocycle oxygéné hexa- ou pentagonal. Les flavonoïdes présentent des activités physiologiques qui leurs permettent d'être utilisés comme médicaments notamment pour leur pouvoir à piéger les radicaux libres. Les activités de flavonoïdes ont fait l'objet de nombreux articles de revue.

Parmi les flavonoïdes, la quercétine est la molécule la plus distribuée dans la nature qui présente la meilleure activité anti radicalaire et aussi antiinflammatoire comparativement aux autres molécules de la même famille. En général, les flavonoïdes et la quercétine en particulier présentent une solubilité très limitée dans l'eau, cette limitation réduit leur absorption/pénétration et donc leur efficacité.

En partant de l'idée que la peau est le l'organe le plus grand du corps humain et aussi l'organe le plus exposé au stress oxydant lié aux radiations UV et aux produits corrosifs et irritants, la quercétine est donc une molécule antioxydante de choix pour être appliquée sur la peau.

Le premier objectif de thèse a été de développer plusieurs formulations nanométriques de quercétine afin d'augmenter sa solubilité dans l'eau et améliorer ses propriétés physico chimiques. Le deuxième objectif sera de comparer ces formulations en termes de capacité de chargement de quercétine, de toxicité vis à vis des cellules HaCaT (kératinocytes) THP-1 (monocytes) et Vero (épithéliale), et enfin le maintien de l'activité de la quercétine sur les cellules *in vitro,* pour mettre *in fine* en évidence une augmentation de la pénétration cutanée la quercétine *in vivo.*

Dans ce projet, trois approches de formulations nanométriques (smartCrystals®, nanocapsules lipidiques et liposomes) ont été testées pour améliorer la solubilité de la quercétine. Les formulations sont optimisées en termes de procédé de préparation (transposition industrielle) et de composition des excipients pour augmenter la quantité de quercétine formulée. Les formulations ont été caractérisées sur plusieurs paramètres : taille, PDI, taux de chargement en quercétine, état cristallin et cinétique de libération de quercétine *in vitro*. Ensuite, les formulations ont été comparées entre elles sur les cellules HaCaT et THP-1 avec détermination de leur toxicité et activité protectrice. Enfin, deux formulations (quercétine smartCrystals® avec le TPGS et quercétine LNC 20) ont été sélectionnées et comparées *in vivo* pour évaluer l'amélioration de la pénétration cutanée de quercétine.

Ce projet propose une solution pour formuler la quercétine d'une façon pertinente et efficace qui pourra être extrapolée au niveau industriel pour des applications cutanées de molécules peu solubles dont l'efficacité est limitée par leur faible pénétration cutanée.

Mots-clés : flavonoïdes, quercétine, liposomes, nanocapsules lipidiques, smartCrystals®, la peau, antioxydant, HaCaT.